AD-A185 150 TECHNICAL PAPERS PRESENTED AT THE DEFENSE NUCLEAR AGENCY GLOBAL EFFECTS R..(U) DOD NUCLEAR INFORMATION AND ANALYSIS CENTER SANTA BARBARA CA. 15 MAY 86 — 1/4

UNCLASSIFIED DASIAC-TN-86-29-VOL-2 DNA001-82-C-0274 F/G 15/6.4 NL

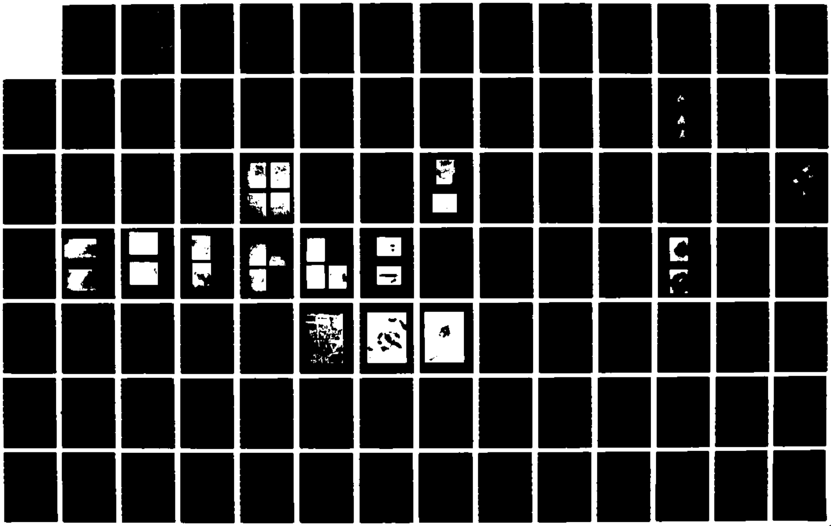

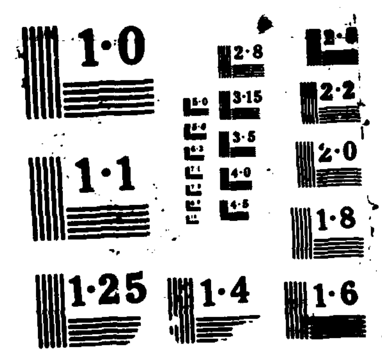
1·0
2·8
1·1
3·15
3·5
2·2
2·0
4·0
4·5
1·8
1·25
1·4
1·6

(10)

AD-A185 150

DASIAC-TN-86-29-V2

DTIC FILE COPY

TECHNICAL PAPERS PRESENTED AT THE DEFENSE NUCLEAR AGENCY GLOBAL EFFECTS REVIEW

Volume II

Kaman Tempo
Alexandria Office
Huntington Building
2560 Huntington Avenue
Alexandria, VA 22303-1410

15 May 1986

Technical Report

CONTRACT No. DNA 001-82-C-0274

Approved for public release; distribution is unlimited.

THIS WORK WAS SPONSORED BY THE DEFENSE NUCLEAR AGENCY UNDER RDT&E RMSS CODE B331086466 P99QMXDC00003 H2590D.

Prepared for
Director
DEFENSE NUCLEAR AGENCY
Washington, DC 20305-1000

CUT HERE AND RETURN

DISTRIBUTION LIST UPDATE

This mailer is provided to enable DNA to maintain current distribution lists for reports. We would appreciate your providing the requested information.

- ☐ Add the individual listed to your distribution list.
- ☐ Delete the cited organization/individual.
- ☐ Change of address.

NAME: ______________________

ORGANIZATION: ______________________

OLD ADDRESS	**CURRENT ADDRESS**

TELEPHONE NUMBER: ( ) ______________________

SUBJECT AREA(s) OF INTEREST:

DNA OR OTHER GOVERNMENT CONTRACT NUMBER: ______________________

CERTIFICATION OF NEED-TO-KNOW BY GOVERNMENT SPONSOR (if other than DNA):

SPONSORING ORGANIZATION: ______________________

CONTRACTING OFFICER OR REPRESENTATIVE: ______________________

SIGNATURE: ______________________

Director
Defense Nuclear Agency
ATTN: [redacted] TITL
Washington, DC 20305-1000

Director
Defense Nuclear Agency
ATTN: [redacted] TITL
Washington, DC 20305-1000

UNCLASSIFIED

SECURITY CLASSIFICATION OF THIS PAGE

AD-A185 150

REPORT DOCUMENTATION PAGE

1a REPORT SECURITY CLASSIFICATION: UNCLASSIFIED	1b RESTRICTIVE MARKINGS
2a SECURITY CLASSIFICATION AUTHORITY: N/A since Unclassified	3 DISTRIBUTION/AVAILABILITY OF REPORT: Approved for public release; distribution is unlimited.
2b DECLASSIFICATION/DOWNGRADING SCHEDULE: N/A since Unclassified	
4 PERFORMING ORGANIZATION REPORT NUMBER(S)	5 MONITORING ORGANIZATION REPORT NUMBER(S): DASIAC-TN-86-29-V2
6a NAME OF PERFORMING ORGANIZATION: Kaman Tempo; 6b OFFICE SYMBOL (If applicable)	7a NAME OF MONITORING ORGANIZATION: Director, Defense Nuclear Agency
6c ADDRESS (City, State, and ZIP Code): Alexandria Office, Huntington Building, 2560 Huntington Avenue, Alexandria, VA 22303-1410	7b ADDRESS (City, State, and ZIP Code): Washington, DC 20305-1000
8a NAME OF FUNDING/SPONSORING ORGANIZATION; 8b OFFICE SYMBOL (If applicable)	9 PROCUREMENT INSTRUMENT IDENTIFICATION NUMBER: DNA 001-82-C-0274
8c ADDRESS (City, State, and ZIP Code)	10 SOURCE OF FUNDING NUMBERS

PROGRAM ELEMENT NO	PROJECT NO	TASK NO	WORK UNIT ACCESSION NO
62715H	P99QMXD	C	DH008684

11 TITLE (Include Security Classification)
TECHNICAL PAPERS PRESENTED AT THE DEFENSE NUCLEAR AGENCY GLOBAL EFFECTS REVIEW
Volume II

12 PERSONAL AUTHOR(S)
Various

13a TYPE OF REPORT	13b TIME COVERED	14 DATE OF REPORT (Year, Month, Day)	15 PAGE COUNT
Technical Report	FROM 860225 TO 860512	860515	342

16 SUPPLEMENTARY NOTATION
This work was sponsored by the Defense Nuclear Agency under RDT&E RMSS Code B331086466 P99QMXDC00003 H2590D.

17 COSATI CODES			18 SUBJECT TERMS (Continue on reverse if necessary and identify by block number)
FIELD	GROUP	SUB-GROUP	Nuclear War,
04	01		Global Climate Effects.
15	06		

19 ABSTRACT (Continue on reverse if necessary and identify by block number)

This document contains technical papers presented at the Defense Nuclear Agency Review of Global Effects held at NASA Ames Research Center 25-27 February 1986. Keywords:

20 DISTRIBUTION/AVAILABILITY OF ABSTRACT: ☐ UNCLASSIFIED/UNLIMITED ☒ SAME AS RPT ☐ DTIC USERS	21 ABSTRACT SECURITY CLASSIFICATION: UNCLASSIFIED	
22a NAME OF RESPONSIBLE INDIVIDUAL: Sandra E. Young	22b TELEPHONE (Include Area Code): (202) 325-7042	22c OFFICE SYMBOL: DNA/CSTI

DD FORM 1473, 84 MAR

83 APR edition may be used until exhausted
All other editions are obsolete

SECURITY CLASSIFICATION OF THIS PAGE
UNCLASSIFIED

PREFACE

The Defense Nuclear Agency has collected and printed the attached papers from the February 25-27 1986 Global Effects review as a service to the community. The Defense Nuclear Agency takes this opportunity to express its gratitude to the numerous participants in the Global Effects review.

The technical papers enclosed include all those which were received by DNA prior to the closing date of 28 April 1986. Where papers are missing their place is occupied by the abstract received prior to the meeting.

The inclusion of a paper in this proceeding does not necessarily imply endorsement of the results of the research reported or conclusions which might be drawn from that research. It is the opinion of the Defense Nuclear Agency that, while good progress is being made in improving our understanding of Global Effects, the results to date are tentative and preliminary and should not be used for planning beyond the planning of future research.

TABLE OF CONTENTS

TABLE OF CONTENTS (Continued)

SECTION 1

CHEMISTRY AND MICROPHYSICS

LABORATORY STUDY OF WET COAGULATION

GLOBAL EFFECTS PROGRAM TECHNICAL MEETING

FEBRUARY 26, 1986

GEORGE CARRIER*
FRANK FENDELL
DAN KWOH
BRUCE LAKE

*Harvard University, Cambridge, Massachusetts 02138

TRW SPACE AND TECHNOLOGY GROUP
ONE SPACE PARK
REDONDO BEACH, CALIFORNIA 90278

OBJECTIVE

Do laboratory experiment:

(1) To see if light extinction by soot particles changes after confinement in a cloud

(2) To measure size distribution and number density of soot particles before and after confinement in a cloud

APPROACH

(1) Introduce soot particles and moist air into cloud chamber

(2) Measure extinction, number density and size distribution of soot particles

(3) Expand cloud chamber adiabetically to form cloud

(4) Sit for sometime for scavenging, wet coagulation to take place

(5) Compress cloud chamber to evaporate cloud

(6) Measure extinction, number density and size distribution of soot particles again

PROBLEMS TO BE SOLVED

(1) <u>Cloud Chamber</u>

Wall temperature must closely match gas temperature to prevent condensation, convection

(2) <u>Extinction Measurement</u>

Low number density of soot particles ⇒ low extinction which is hard to measure

(3) <u>Soot Particles' Number and Size Measurements</u>

Submicron particle size and number measurements are non-trivial

CLOUD CHAMBER: SCHEMATICS

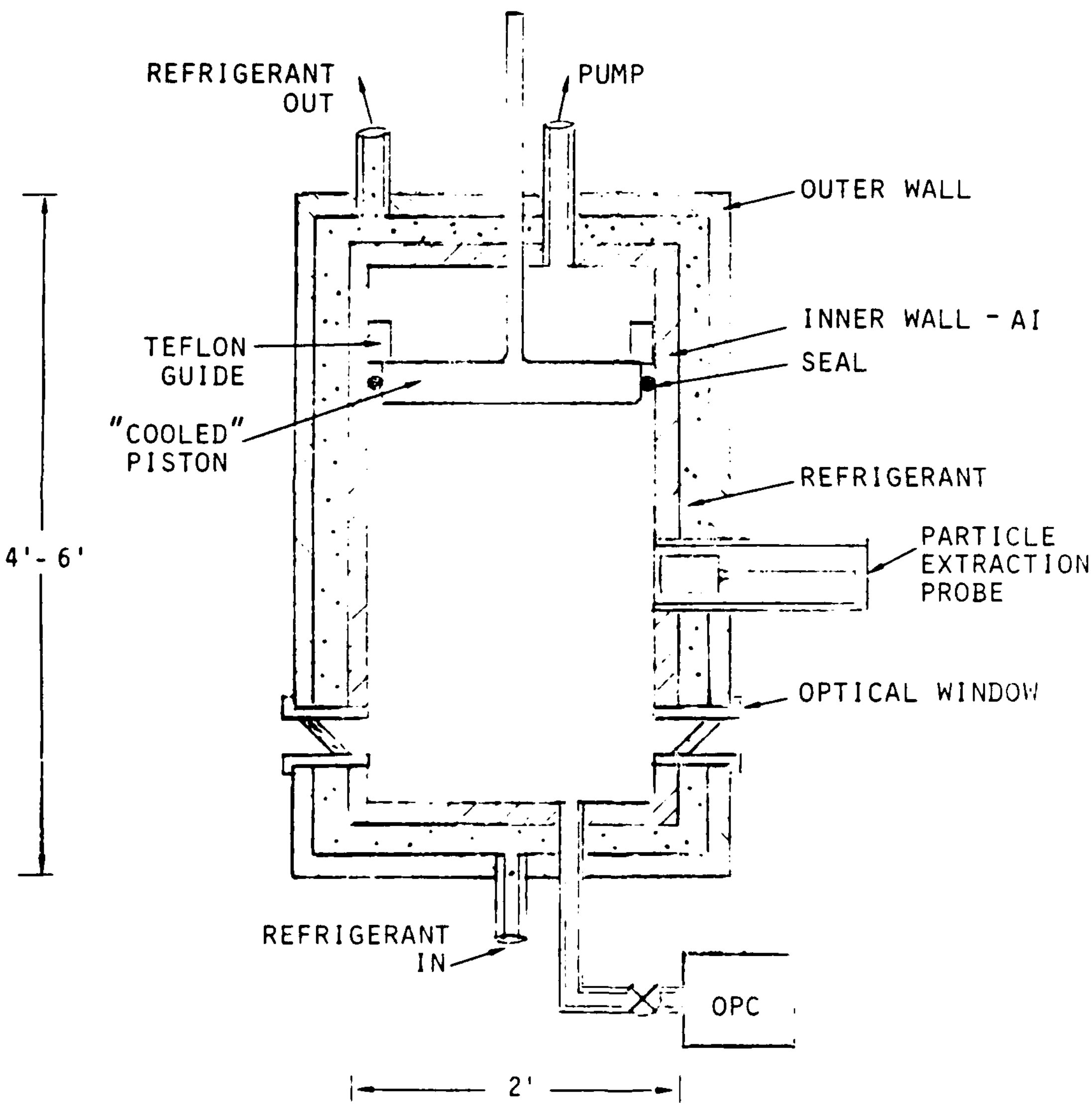

CLOUD CHAMBER: APPROACH

- Wall cooling by simply passing refrigerant through at controlled cold temperature and flow rate. Cool from R.T. to ~ -60°C in 1/2 hour.
- Gas cooling by adiabetic expansion using piston. Expansion ratio ~ 1:3
- Minimize leakage by piston by evacuating and equalizing pressure on back side of piston
- Monitor wall and gas temperature by thermocouple or transistor thermometer
- Make gas temperature to follow wall's
- Aim for wall 0.1-0.3°C warmer than gas to prevent condensation
- Make top of chamber warmer than bottom to suppress convection

EXTINCTION MEASUREMENT: SCHEMATICS

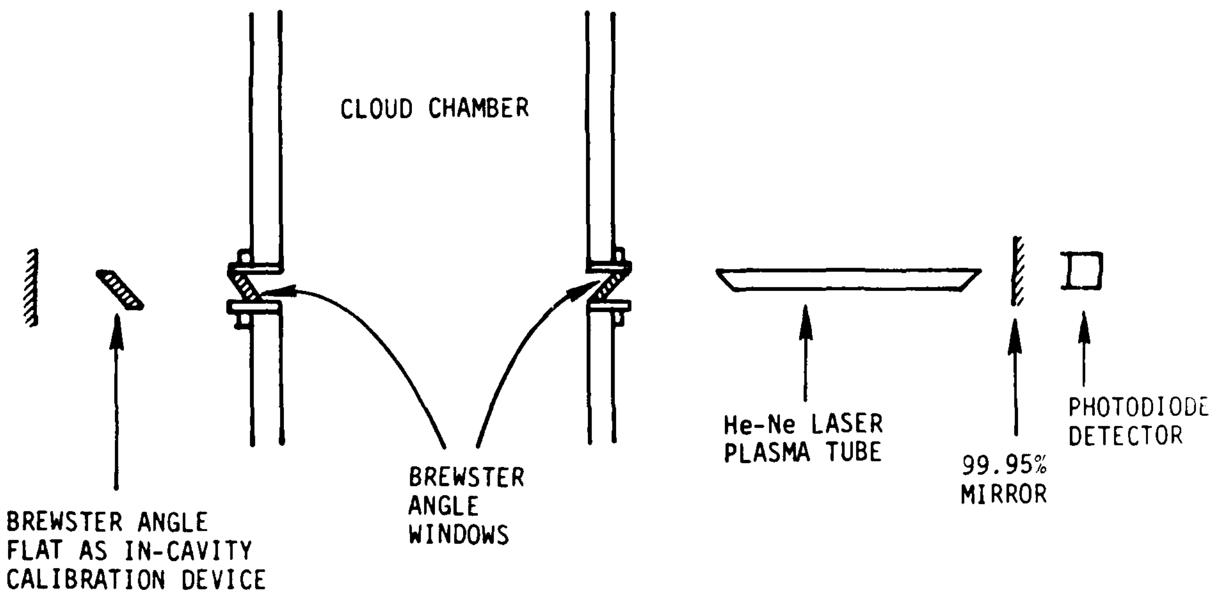

EXTINCTION MEASUREMENT: APPROACH

- 10^4-10^5 0.1 μ particles/c.c. $\Longrightarrow$ 10^{-4}-10^{-3}/m extinction coefficient
- Use "laser-cavity extinction" method:
  - make soot-laser air part of laser cavity
  - laser output highly non-linear function of cavity loss
  - equivalent measurement pathlength ~ kilometers
  - use variable Brewster angle flat as in-cavity calibration device
  - evacuate chamber either before or after dust measurement for calibration

LASER OUTPUT VS. CAVITY LOSS

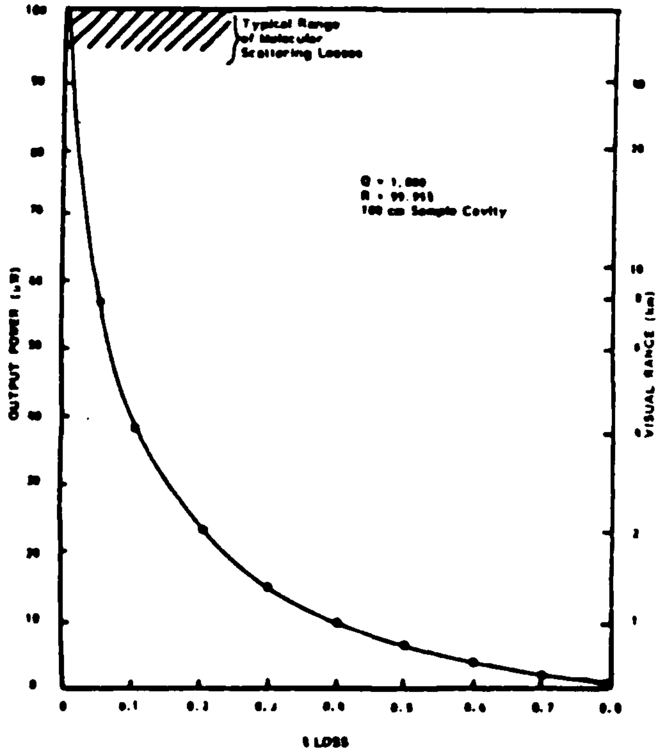

FIGURE 2. Visual range and output power versus percent cavity loss. The prototype uses a 100-cm sample cavity length. With current state-of-the-art high reflectivity mirrors, the sample cavity length can be reduced to less than 30 cm with a Q of 2,000 to 5,000.

BREWSTER ANGLE FLAT AS IN-CAVITY CALIBRATION STANDARD

Incident Angle	Loss
56.0	4×10^{-7}
56.5	6.4×10^{-5}
57.0	2.4×10^{-4}
57.5	5.3×10^{-4}
58.0	9.7×10^{-4}
58.5	1.53×10^{-3}
59.0	2.25×10^{-3}
60.0	4.18×10^{-3}

SOOT PARTICLE NUMBER AND SIZE MEASUREMENTS

Primary Measurement —— Extraction + electron microscopy

Secondary Measurement —— Optical scattering methods

EXTRACTION AND ELECTRON MICROSCOPY

Methods of Extraction:

(1) Impaction — many lose small particles X

(2) Suctioning and filtration — agglomeration may occur in suctioning probe or filter? X

(3) "Grabbing" and gravity settling — disturb particles the least. 0.1 μ particles settle in 3 hours √

Methods of Electron Microscopy:

(1) Scanning electron microscopy (SEM) — 0.1 μ resolution may be difficult, need to coat particles with 100-300 Å gold layer?

(2) Transmission electron microscopy (TEM) — sample preparation more involved but well developed. Mount Collidian film on screen or slide.

OPTICAL METHODS AVAILABLE FOR MEASURING NUMBER DENSITY AND SIZE

Ensemble Measurement (beam measurement)	Scattering extinction ratio
	2 angle intensity ratio
	diffusion broadening spectroscopy
	2 wavelength extinction ratio
	polarization ratio
Particle Measurement (focused measurement)	2 angle intensity ratio
	2 beam interferometry
	white light integrated forward scattering

COMMON SOURCES OF ERROR FOR ALL OPTICAL TECHNIQUES

1. Non-sphericity

   maximum error ~ 40%

2. Index of Refraction Uncertainty

   for highly absorptive particles like soot, a few percent

3. Depth of Field (for focused measurements)

   broadens size distribution, < 30%

TWO-ANGLE INTENSITY RATIO - PARTICLE MEASUREMENT
COMPARISON WITH SEM

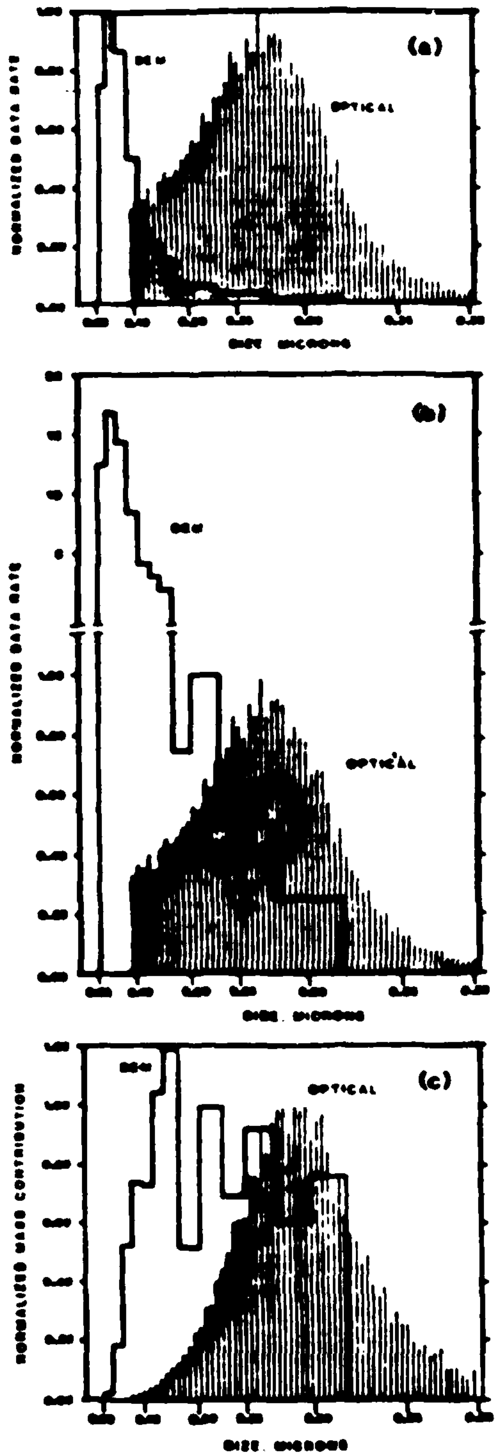

OPTICAL METHODS SELECTED

For small particles (< 0.1 μ) — extinction/scattering ratio or 2 angle intensity ratio (large angle pair)

For large particles (> several μ) — 2 angle intensity ratio (small angle pair)

MIE SCATTERING

Scattering/Extinction Ratio

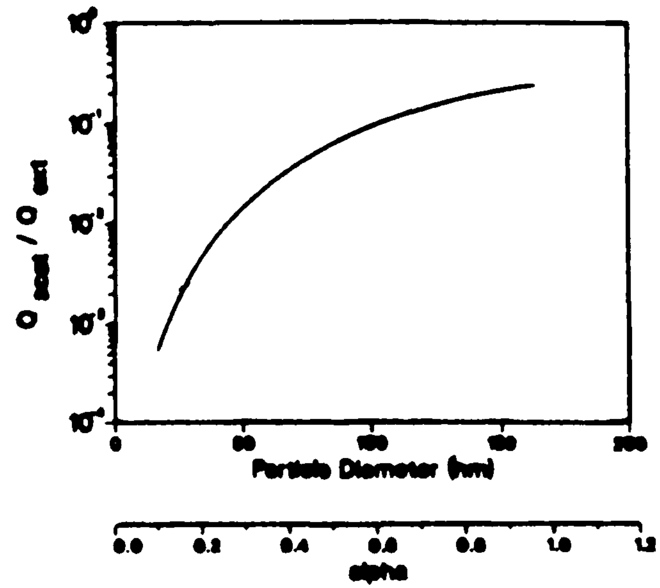

MIE SCATTERING

Two-Angle Intensity Ratio

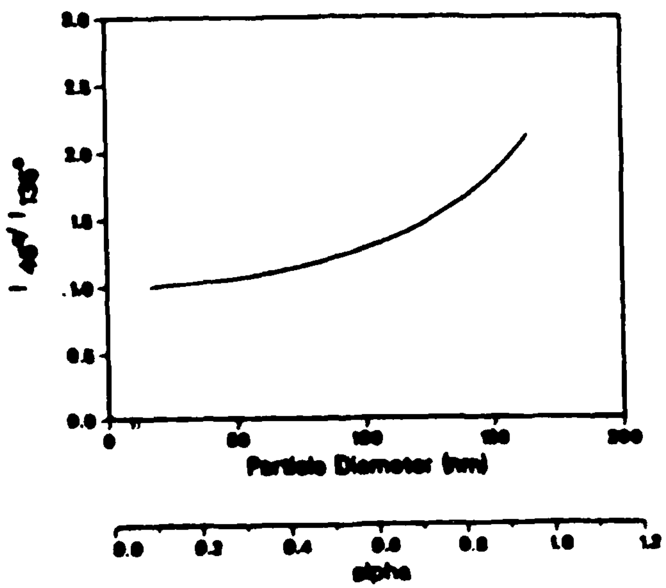

SUMMARY OF WHAT WE PROPOSE TO DO

(1) Measure extinction accurately

(2) Measure particle size distribution and number density accurately by extraction and TEM

(3) Use other optical techniques for real time monitoring and as secondary measurements

MICROPHYSICAL PROPERTIES AND REMOVAL PROCESSES OF SOOT

John Hallett, Barry Gardiner, Dennis Lamb,
Fred Rogers, Richard Pitter, Jim Hudson

Desert Research Institute
Reno, Nevada 89506

Viewgraphs - February 1986

NASA AMES DNA Meeting

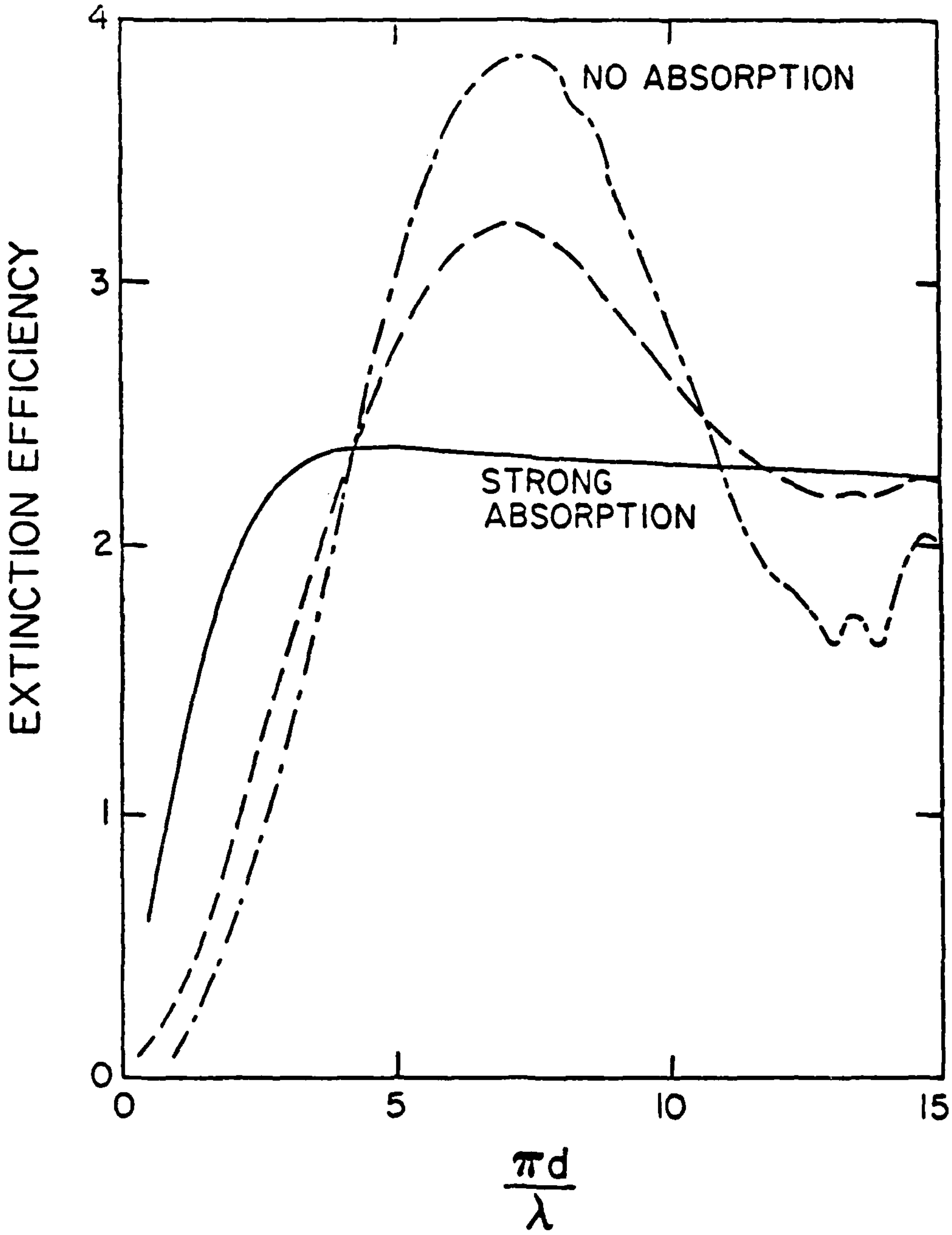

Fig. 1: Extinction efficiency for water spheres with different absorption.

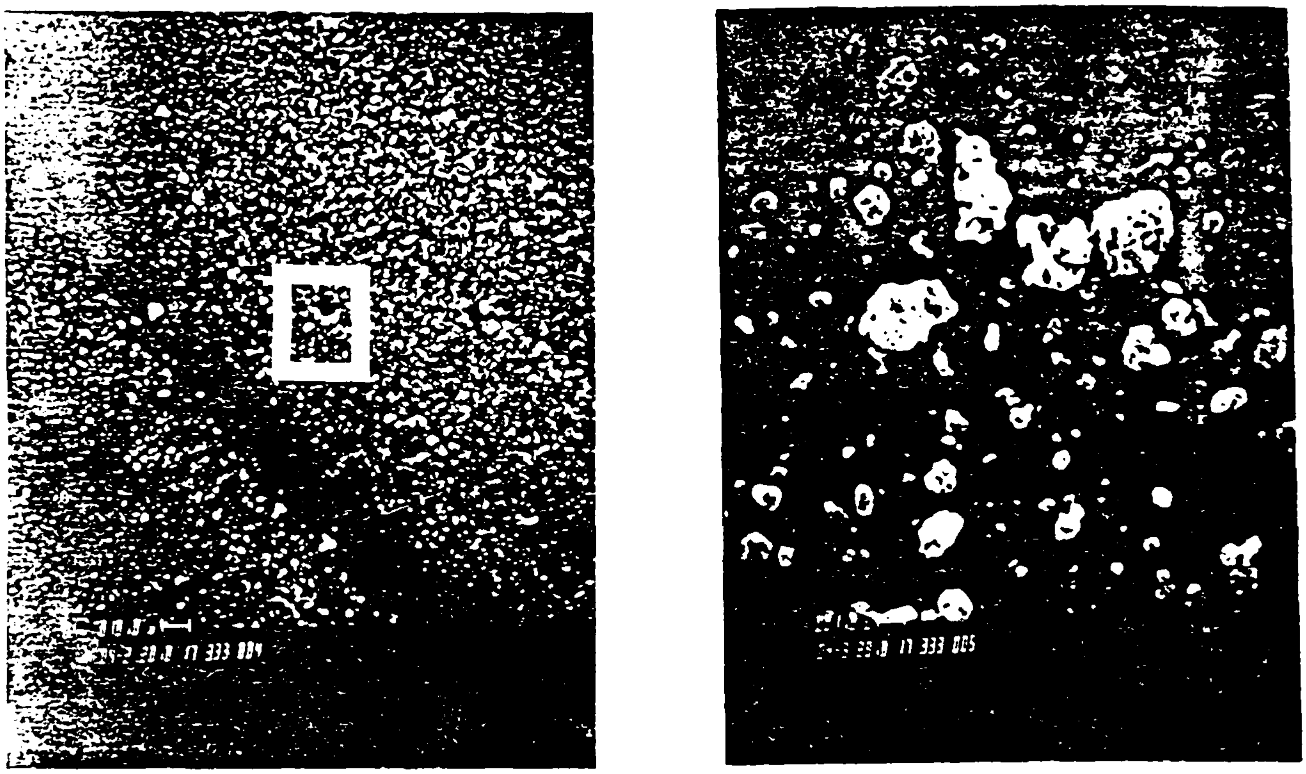

(a) (b)

Figure 2

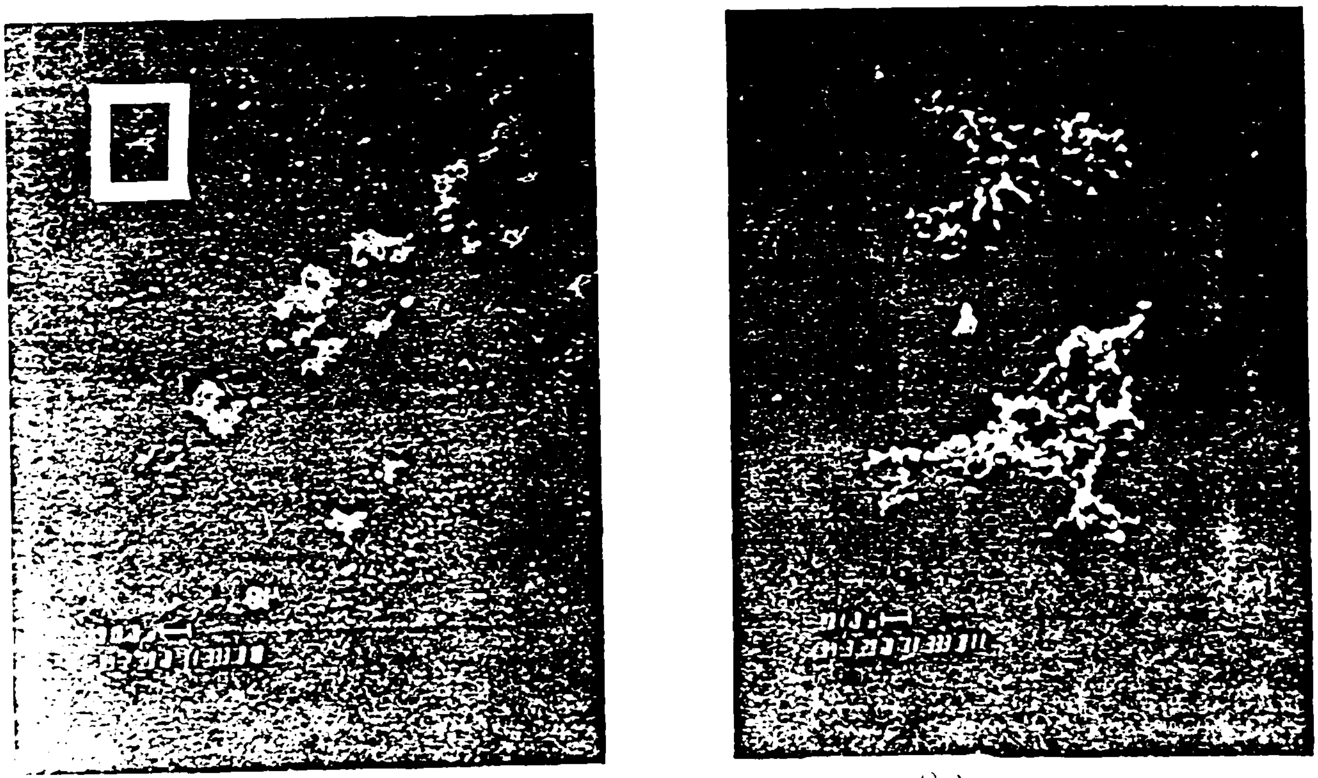

(c) (d)

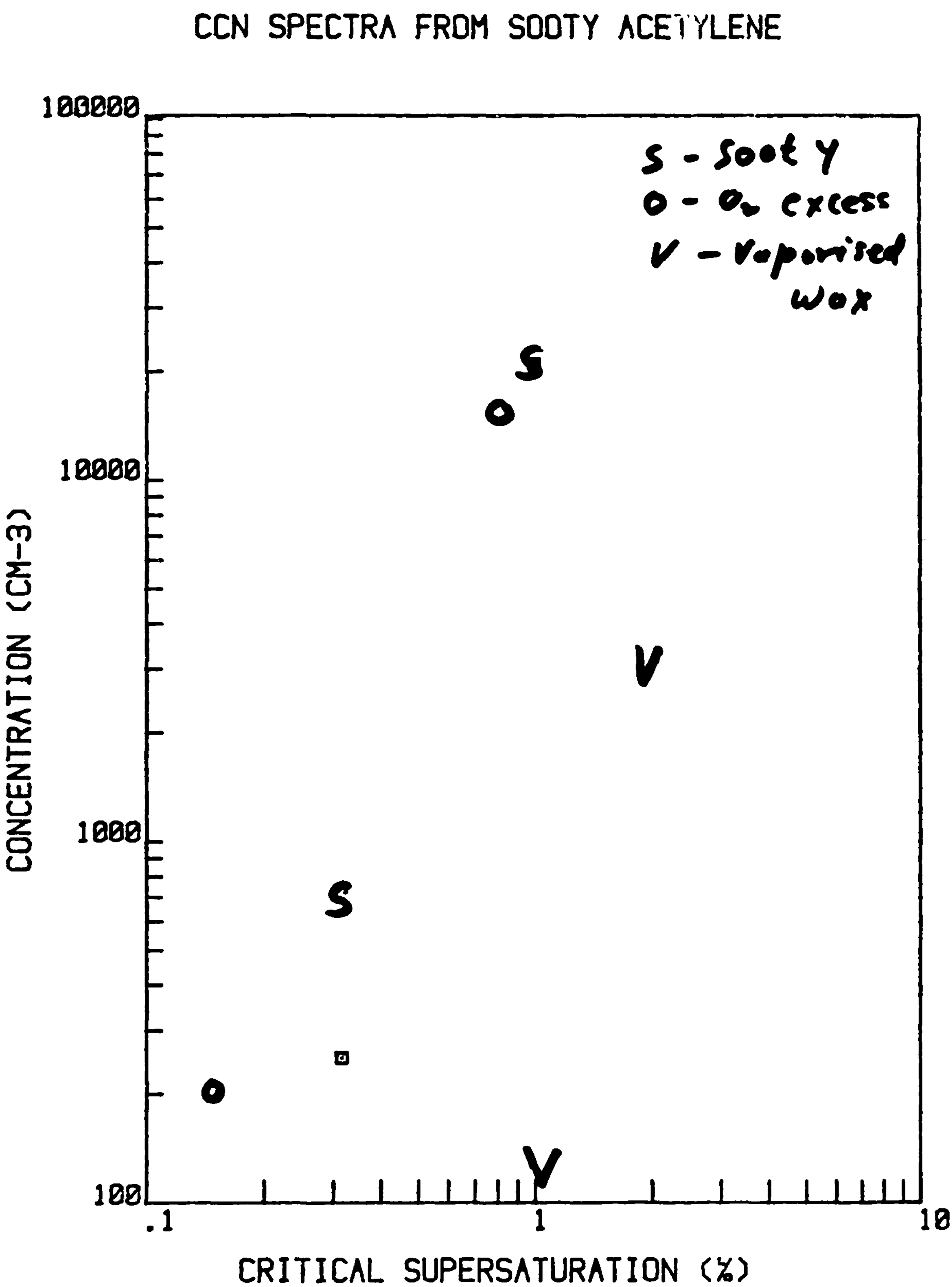

Figure 3 CCN spectra with immediate dilution.

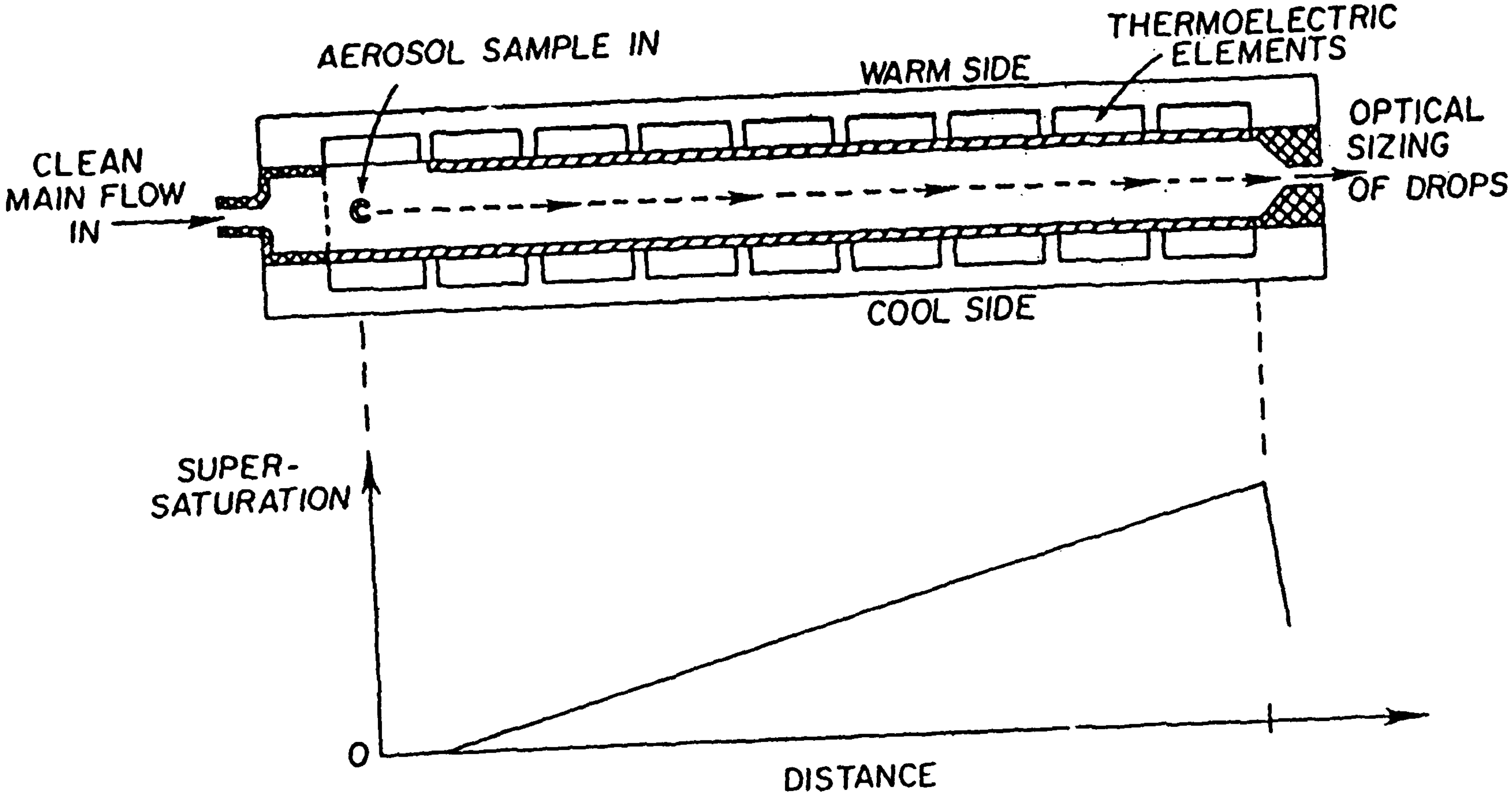

Figure 4 Diagram of the CCN thermal gradient spectrometer.

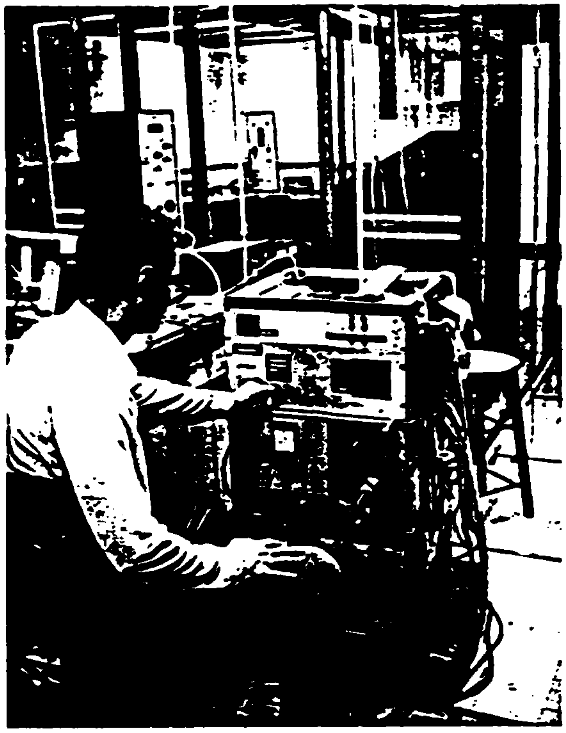

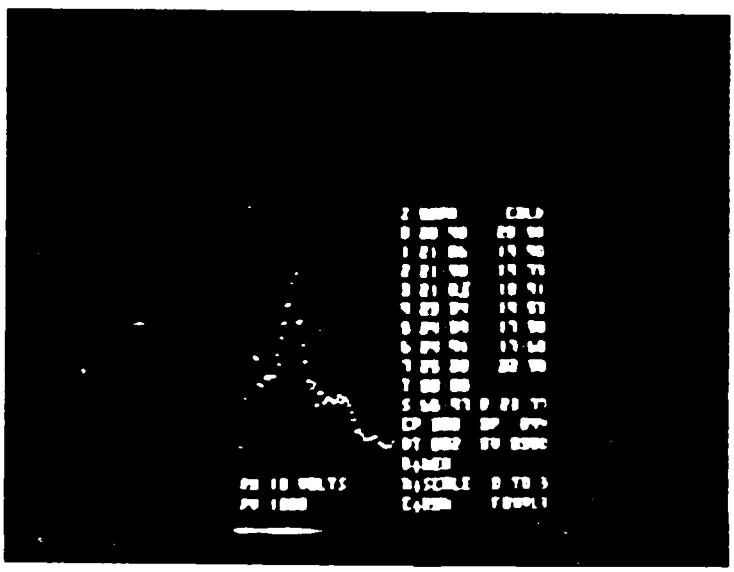

FIG 5: CCN CHAMBER AND SPECTRA

```
RECNUM =       353          -          358
TIME = 02 15 02 56 36.0
REC   TIME   PRES   SF   DUR   CP  P0   P1   P2   P3   P4   P5   P6   P7  MED
MEAN  SD %ISD   TOTAL C30  C40  C50  C60  C70  C80  C90 C100 C110 C120
     259:20.0  821 62.21 579.5 288 0.12 0.92 1.83 3.01 2.95 5.47 6.35 7.84  40
40    9  82     105   94   57   6   1   1   1   1   0   6   0
TIME = 02 15 02 59 50.5
```

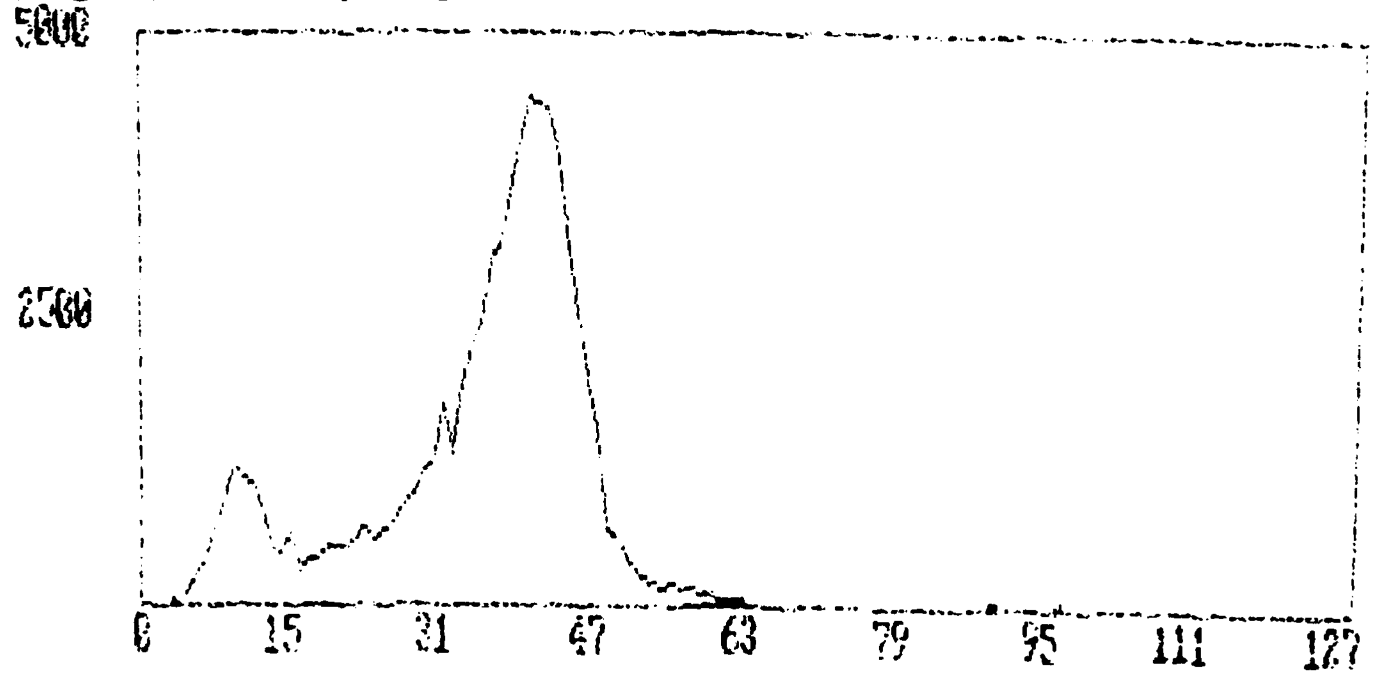

MIN CH 0   max ch 70   MEDIAN CH 39 MEAN CH 36   SD 11

FIG. 6:

CALIBRATION AEROSOL

NaCl 0.80 % S.

RECNUM = 382 - 387
TIME = 02 15 03 12 28.5
REC TIME PRES SF DUR CF P0 P1 P2 P3 P4 P5 P6 P7 MED
MEAN SD %SD TOTAL C30 C40 C50 C60 C70 C80 C90 C100 C110 C120
315.7 2.5 821 67.10 365.0 288 0.04 0.93 1.83 2.98 3.52 5.58 6.30 7.83 96
93 15 81 157 156 156 155 150 143 134 116 54 8 2
TIME = 02 15 03 15 40.5

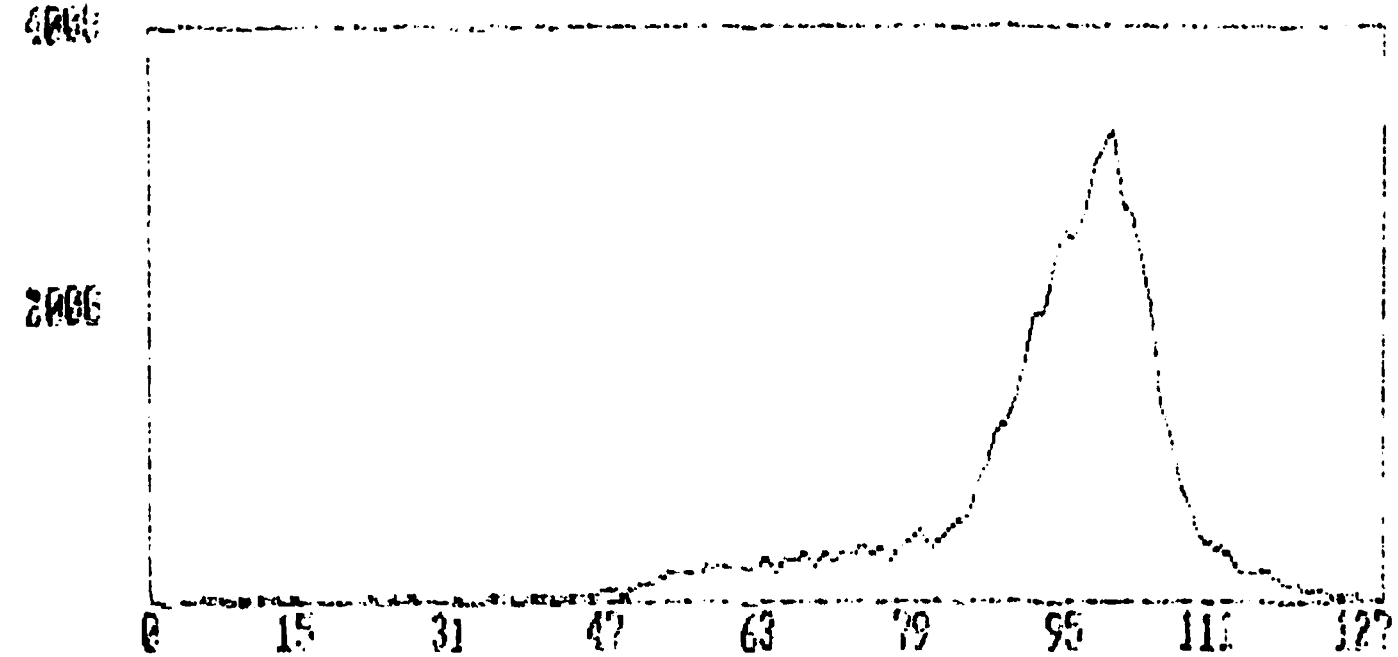

MIN CH 40 max ch 120 MEDIAN CH 96 MEAN CH 93 SD 13

FIG. 7:

CALIBRATION AEROSOL

NaCl 0.04% Sc

```
RECNUM =      299
TIME = 02 15 12 20 24.0
 REC   TIME    PRES   SF    DUR   CP  P0   P1   P2   P3   P4   P5   P6   P7  MED
MEAN  SD %1SD   TOTAL C30   C40  C50  C60  C70  C80  C90 C100 C110 C120
     220:24.0  824 63.82  30.5 289 0.06 1.03 1.67 3.11 3.98 6.40 7.20 8.77  60
64   25  69     101   96    84   65   52   40   31   16    6    4    4
TIME = 02 15 12 20 54.5
```

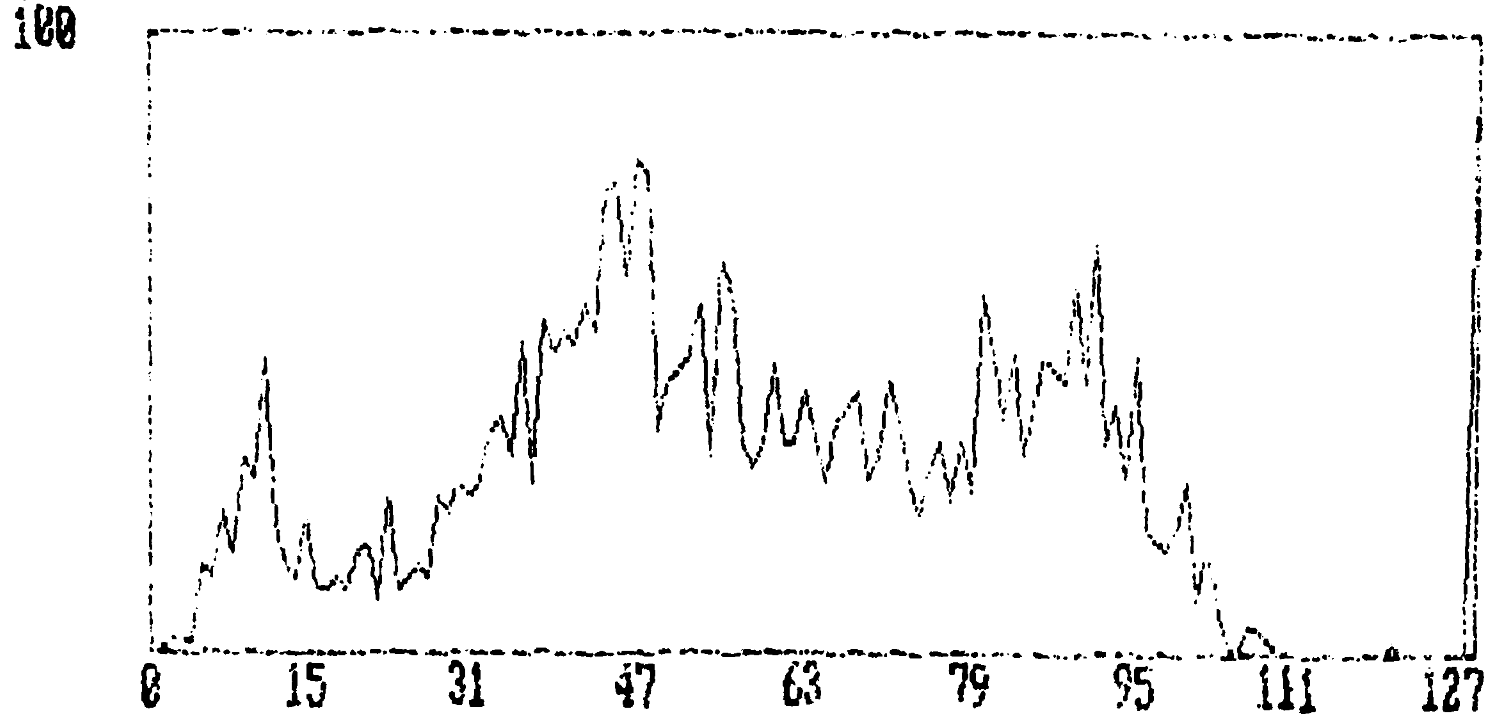

MIN CH 1   MEDIAN CH 56 MEAN CH 60

FIG. 8: background

```
RECNUM =      502
TIME = 02 24 15 56 20.5
 REC   TIME   FRES   SF   DUR   CP  P0   P1   P2   P3   P4   P5   P6   P7  MED
MEAN  SD %SD   TOTAL C30  C40  C50  C60  C70  C80  C90 C100 C110 C120
   556 20.5  844 43.07  23.6 364 0.33-0.32 4.73 5.60 4.02 5.40 5.17 5.39  53
64   35  63    6604 5451 4469 3556 2889 2414 2031 1697 1404 1133  894
TIME = 02 24 15 56 43.5
```

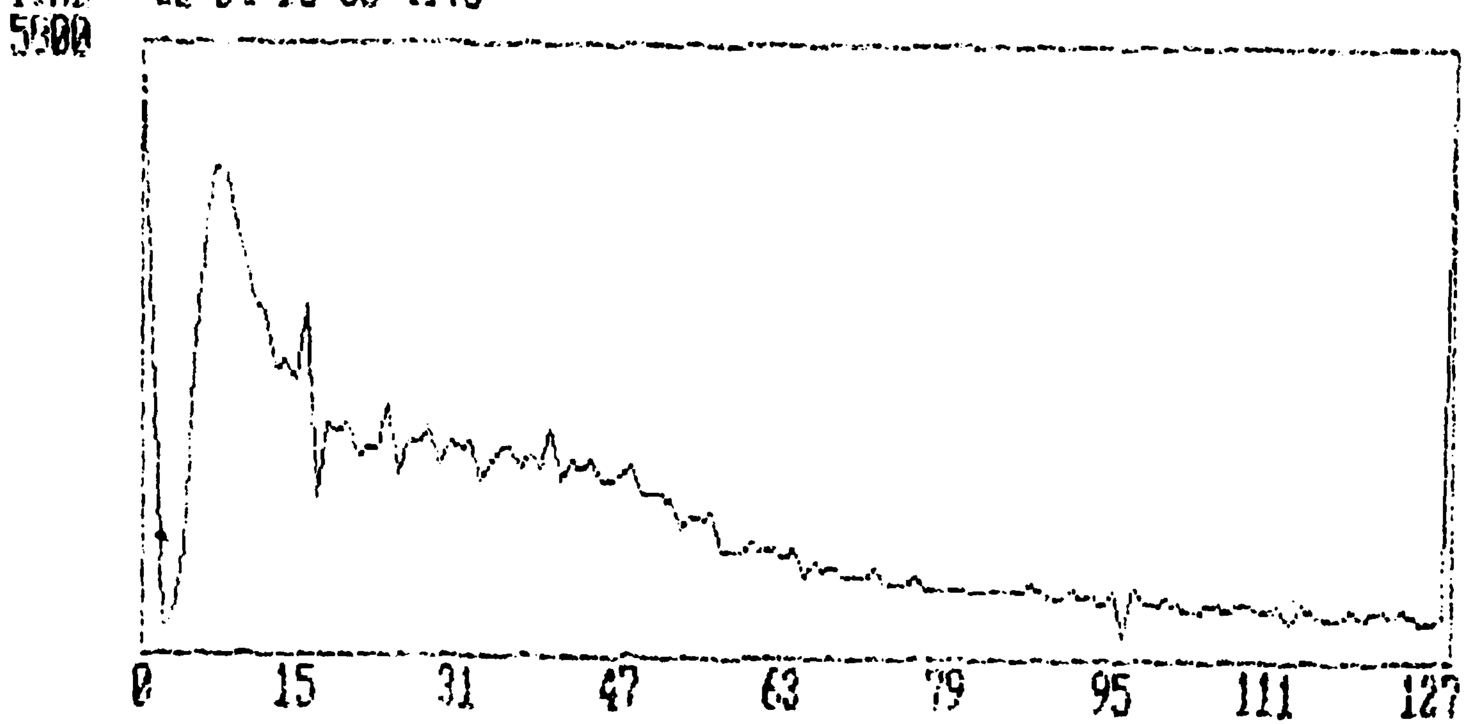

MIN CH 1   MEDIAN CH 39 MEAN CH 49

FIG. 9:

Acetylene Soot

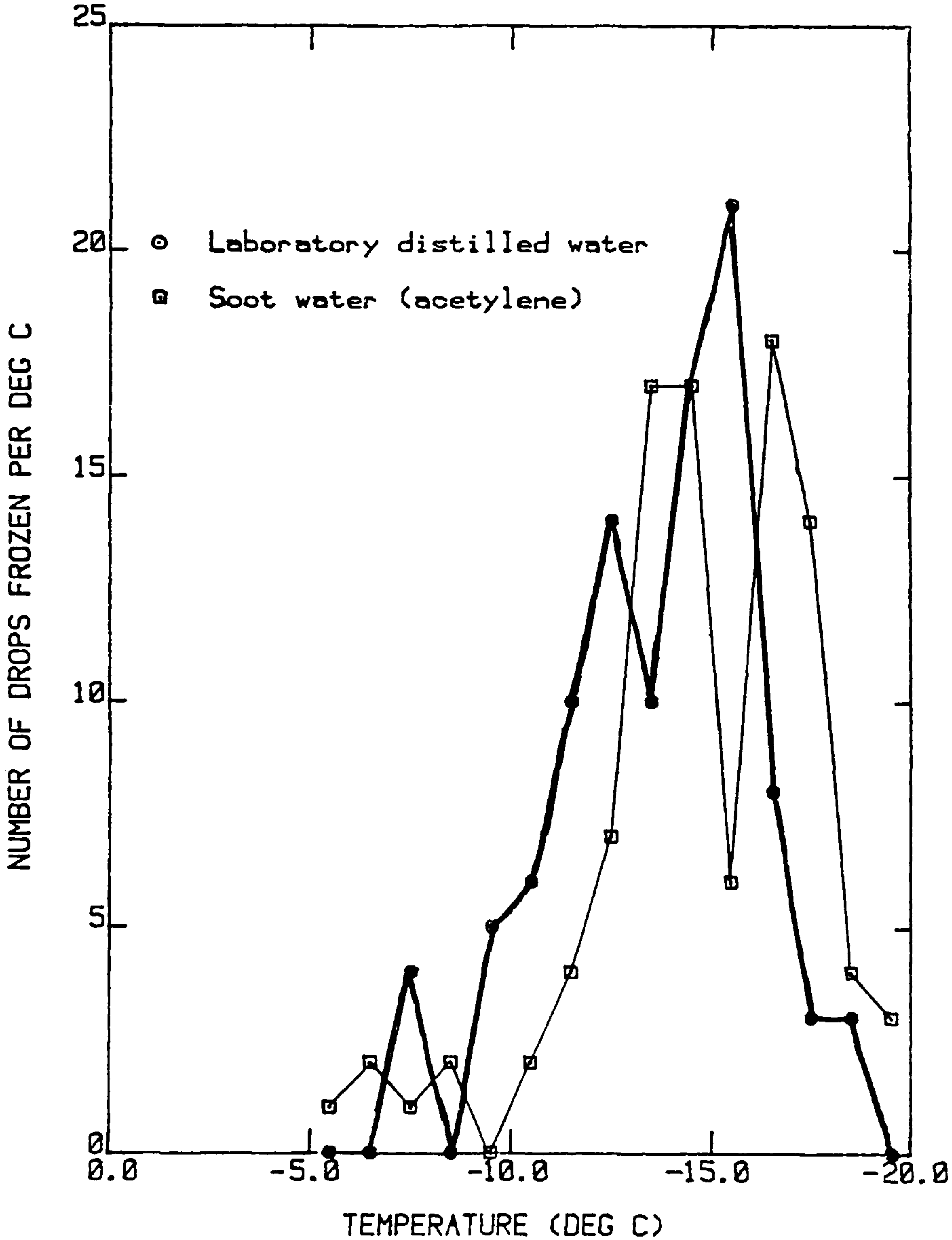

Figure 10. Number of drops frozen per degree temperature change as a function of temperature.

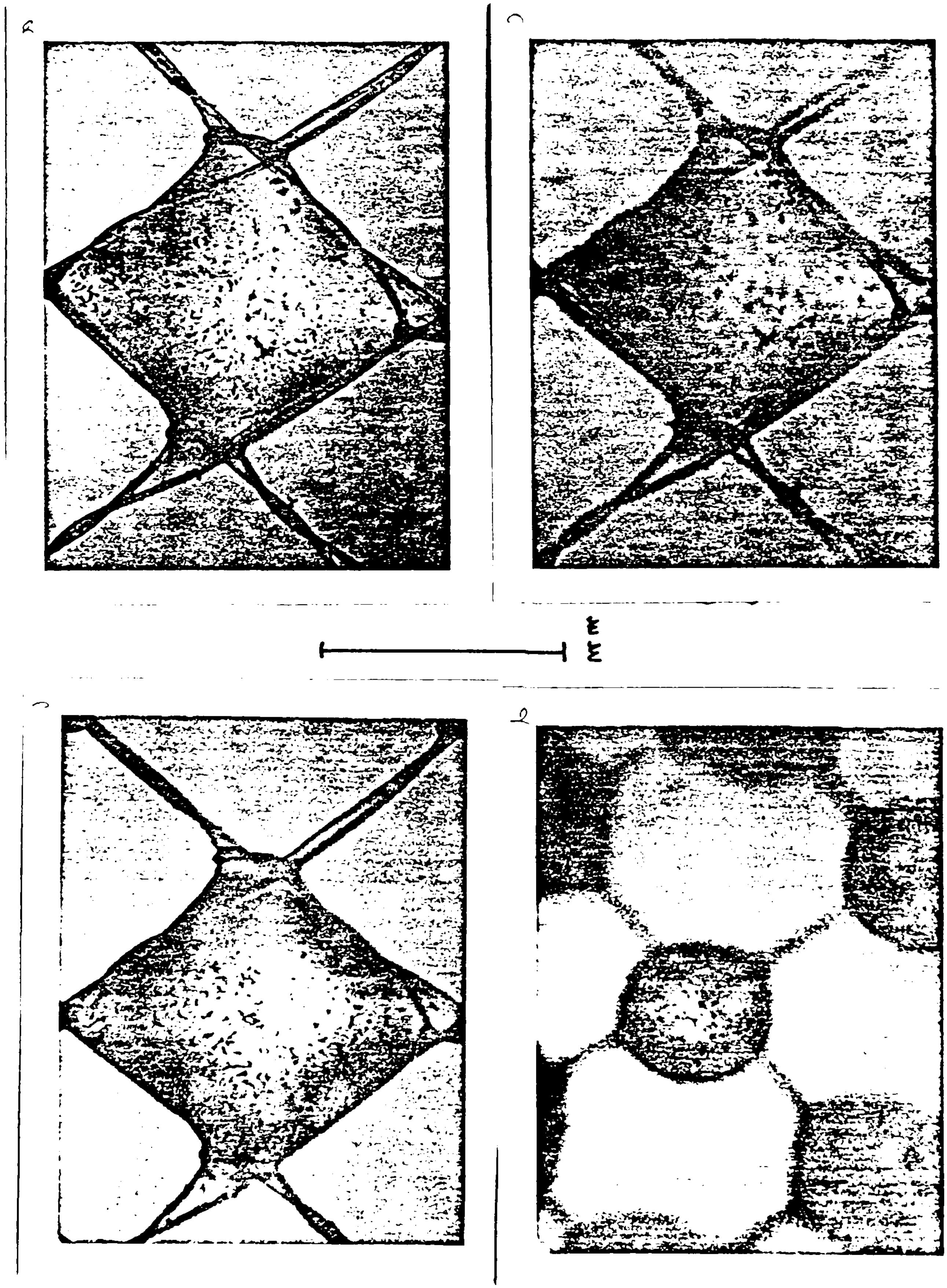

FIG. 11: ACETYLENE SOOT ON WATER DROP SURFACE

FIG. 12: COAGULATION RATE OF AEROSOL WITH CLOUD DROPLETS, TIME CONSTANT ~1000S

$$\frac{dn}{n} = \frac{dt}{\frac{3\eta r^2}{kT\lambda N} \cdot \frac{1}{F}}$$

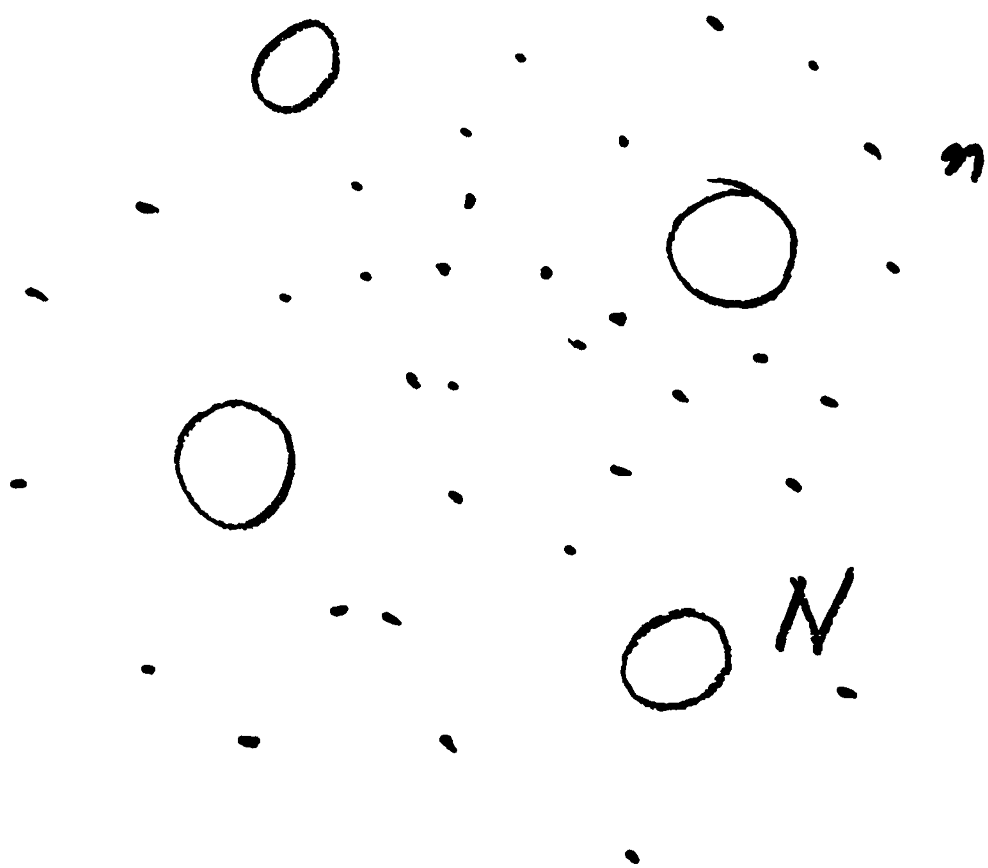

FIG. 13: SAMPLING OF RENO POOL FIRE

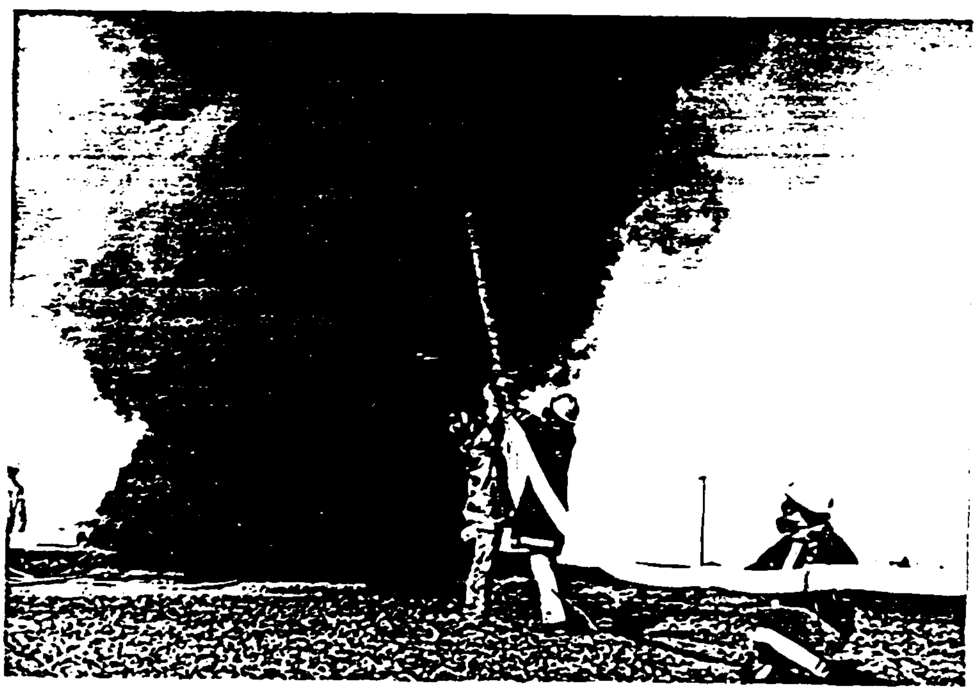

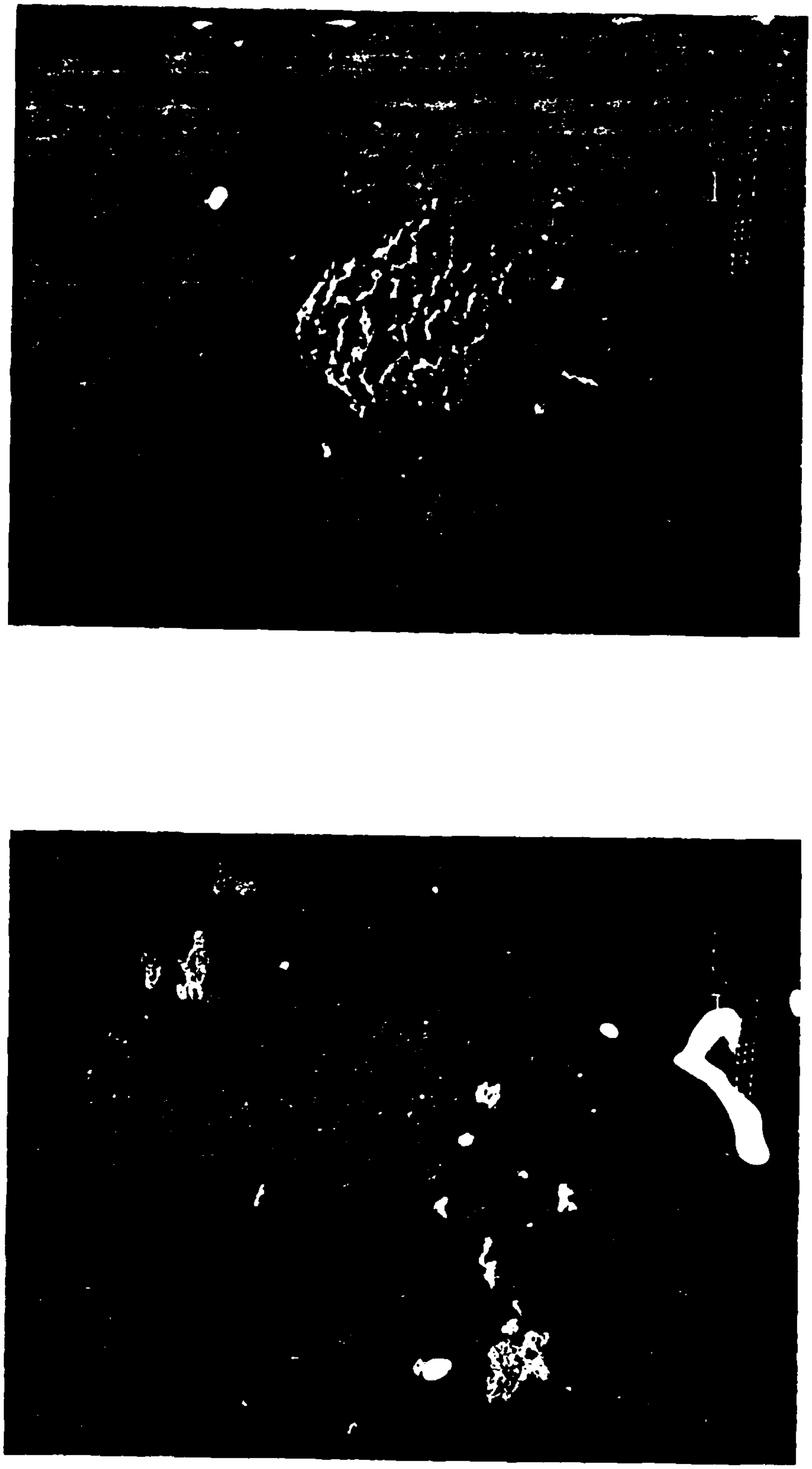

FIG. 14: SEM PICTURE OF FORMVAR REPLICATED SOOT FLAKE

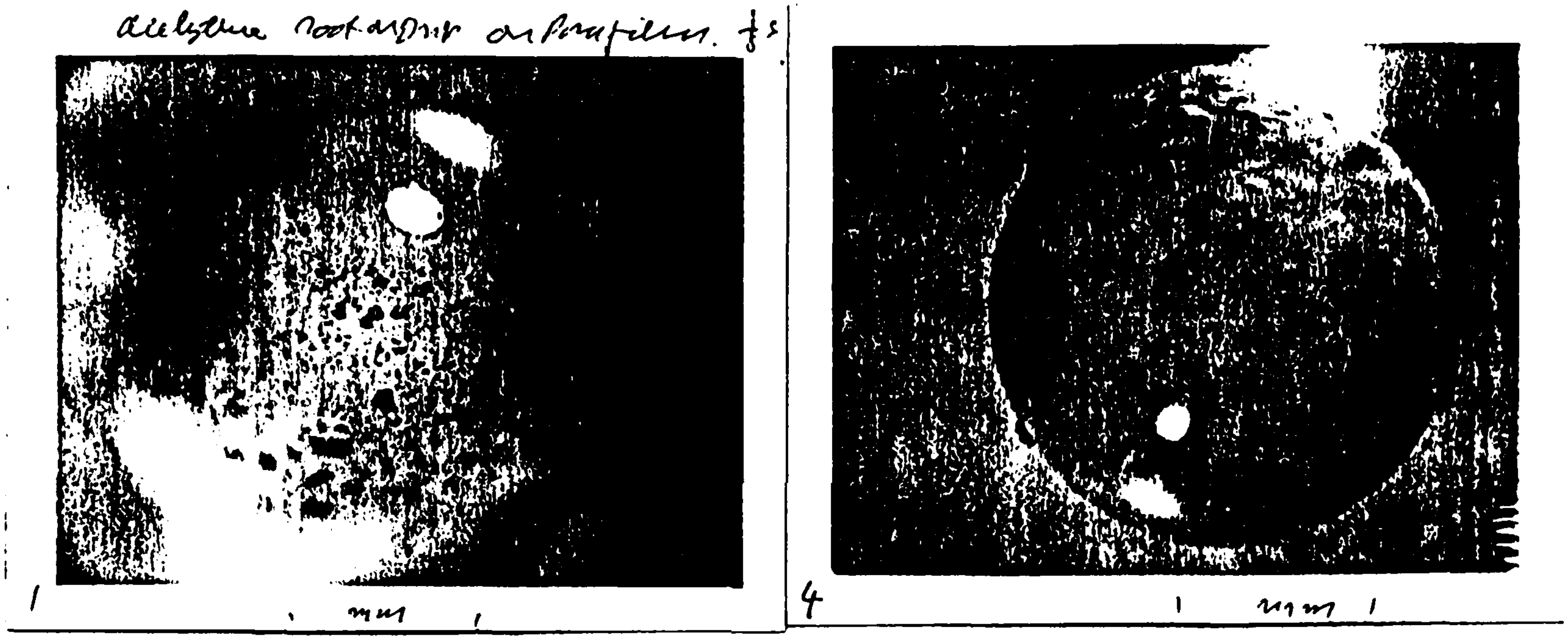

FIGURE 15:

Soot particles from acetylene on the surface; (a) and protruding from the periphery; (b) of a 2 mm waterdrop.

FIGURE 16:

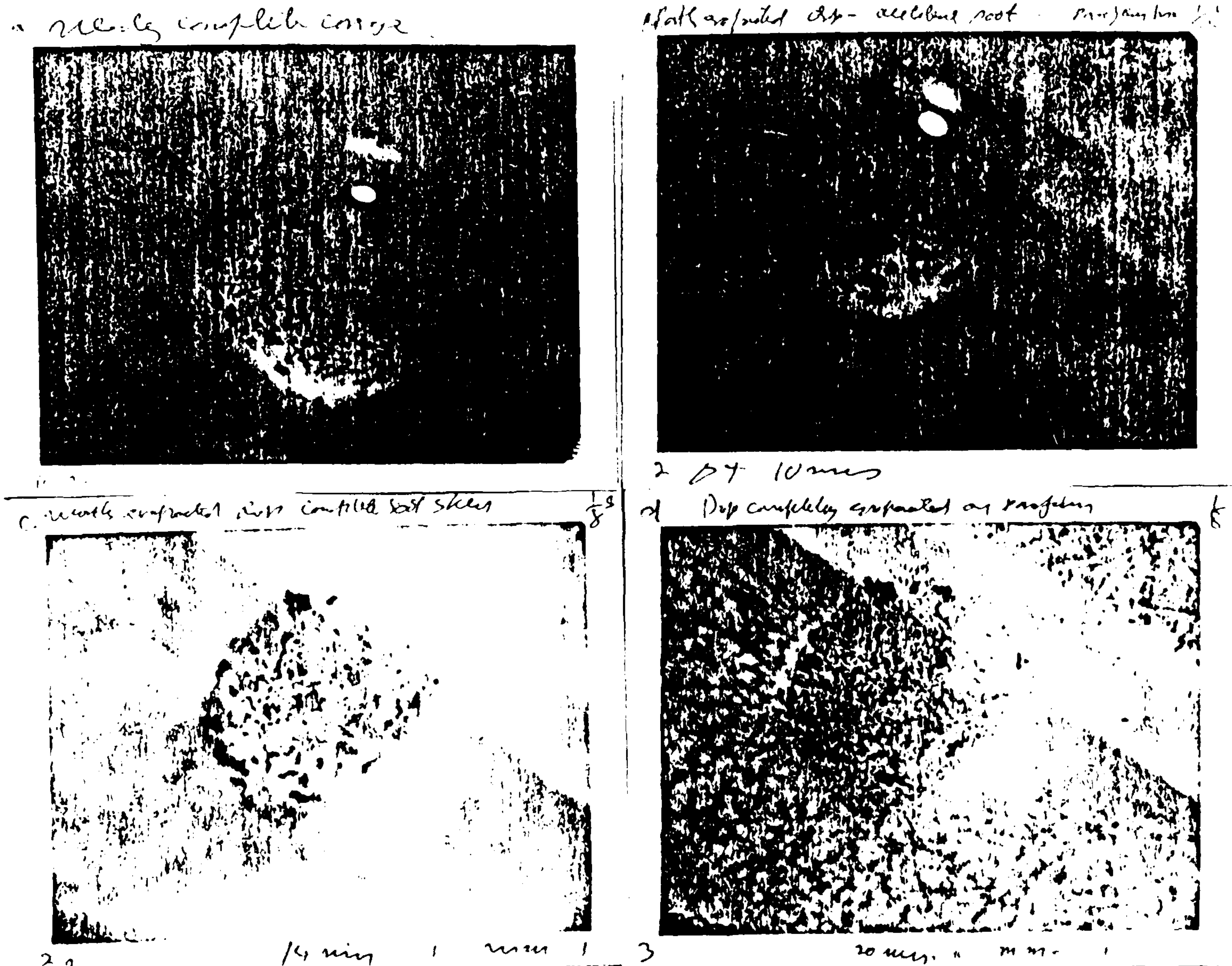

Evaporation sequence of a 2 mm soot covered waterdrop. (a) Shows an open water area (center); (b) is completely covered; (c) is beginning to shrink; (d) the shell has collapsed on the parafilm substrate.

FIGURE 17:

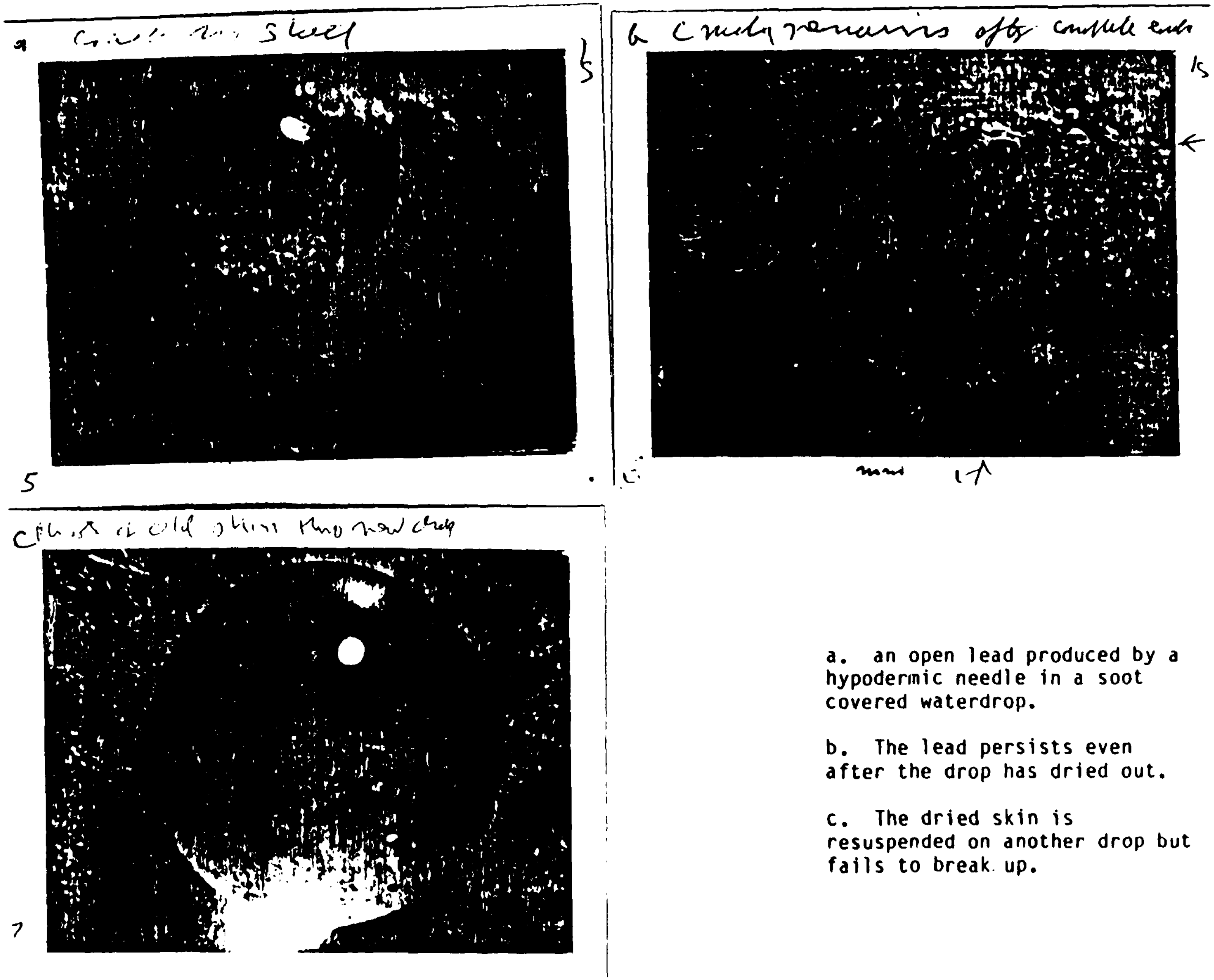

a. an open lead produced by a hypodermic needle in a soot covered waterdrop.

b. The lead persists even after the drop has dried out.

c. The dried skin is resuspended on another drop but fails to break up.

a

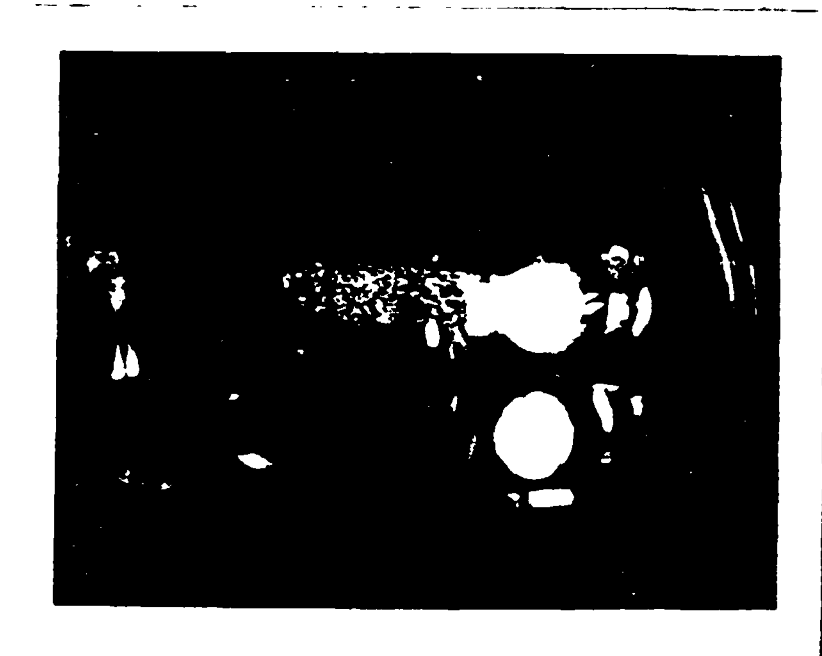

2"

b

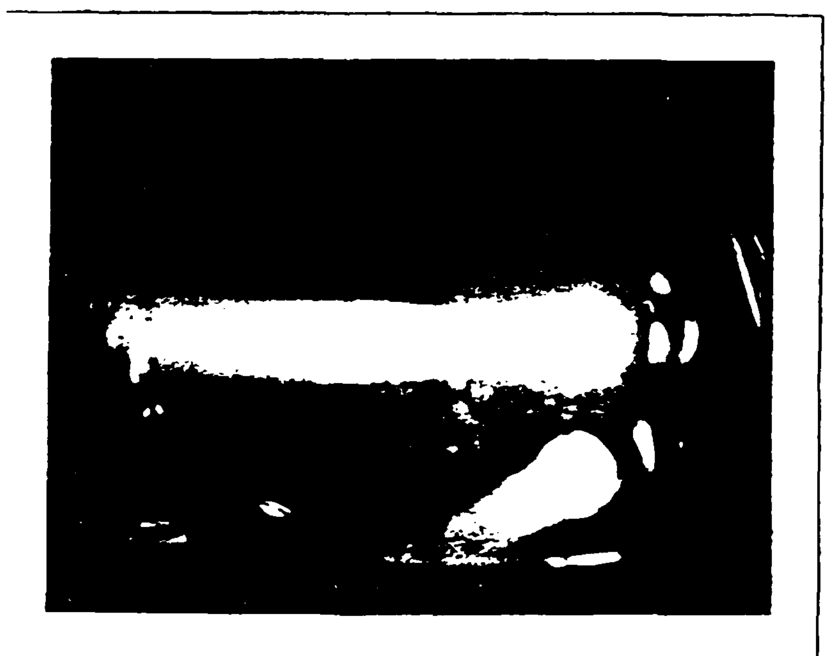

Figure 18 a) Cloud produced on natural aerosol in an expansion cloud chamber.

b) Cloud produced on acetylene soot in an expansion cloud chamber.

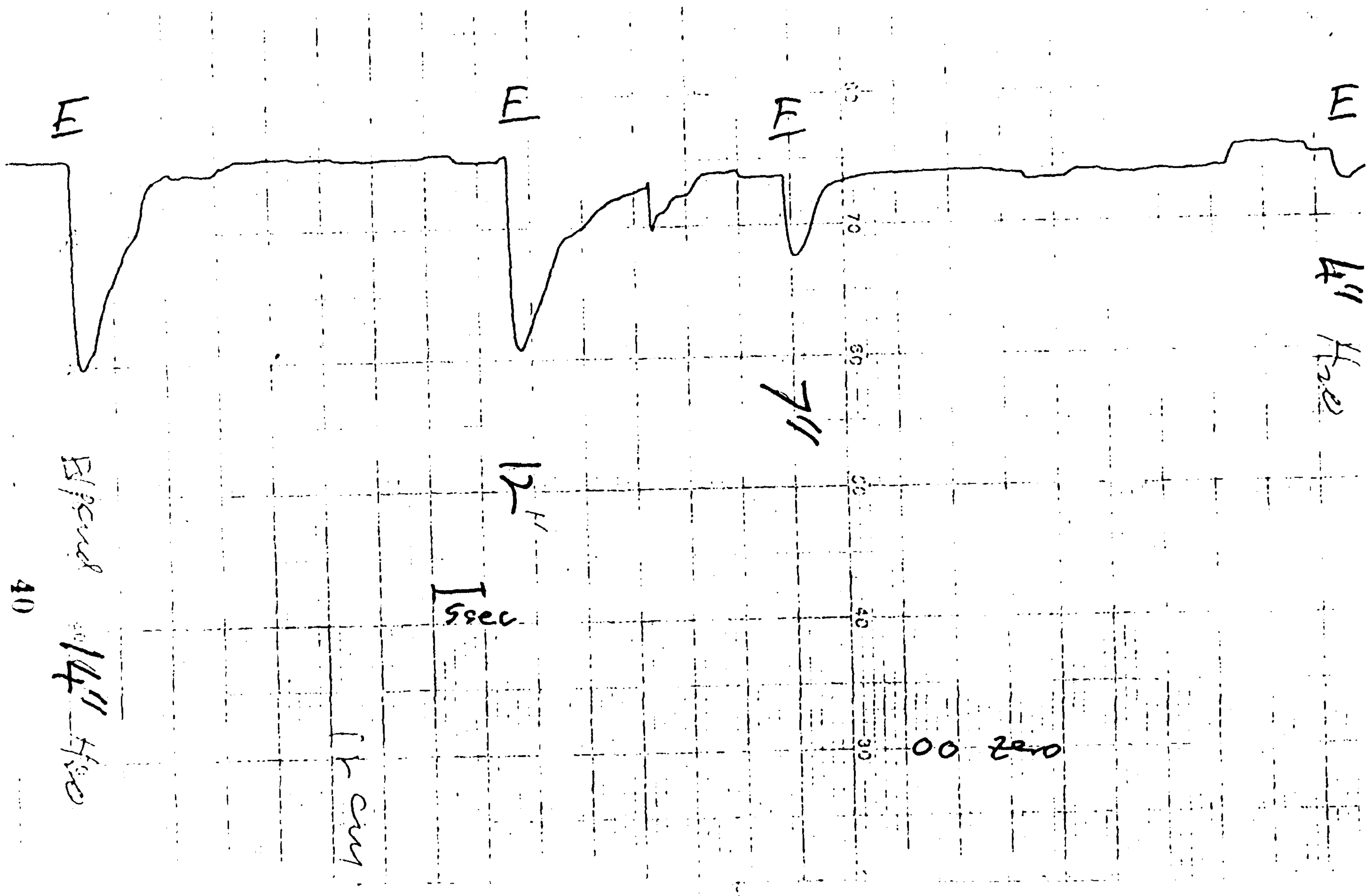

FIG. 19: EXTINCTION MEASUREMENT AFTER EXPANSION AND RECOMPRESSION FOR A ACETYLENE SOOT NUCLEATED WATER CLOUD

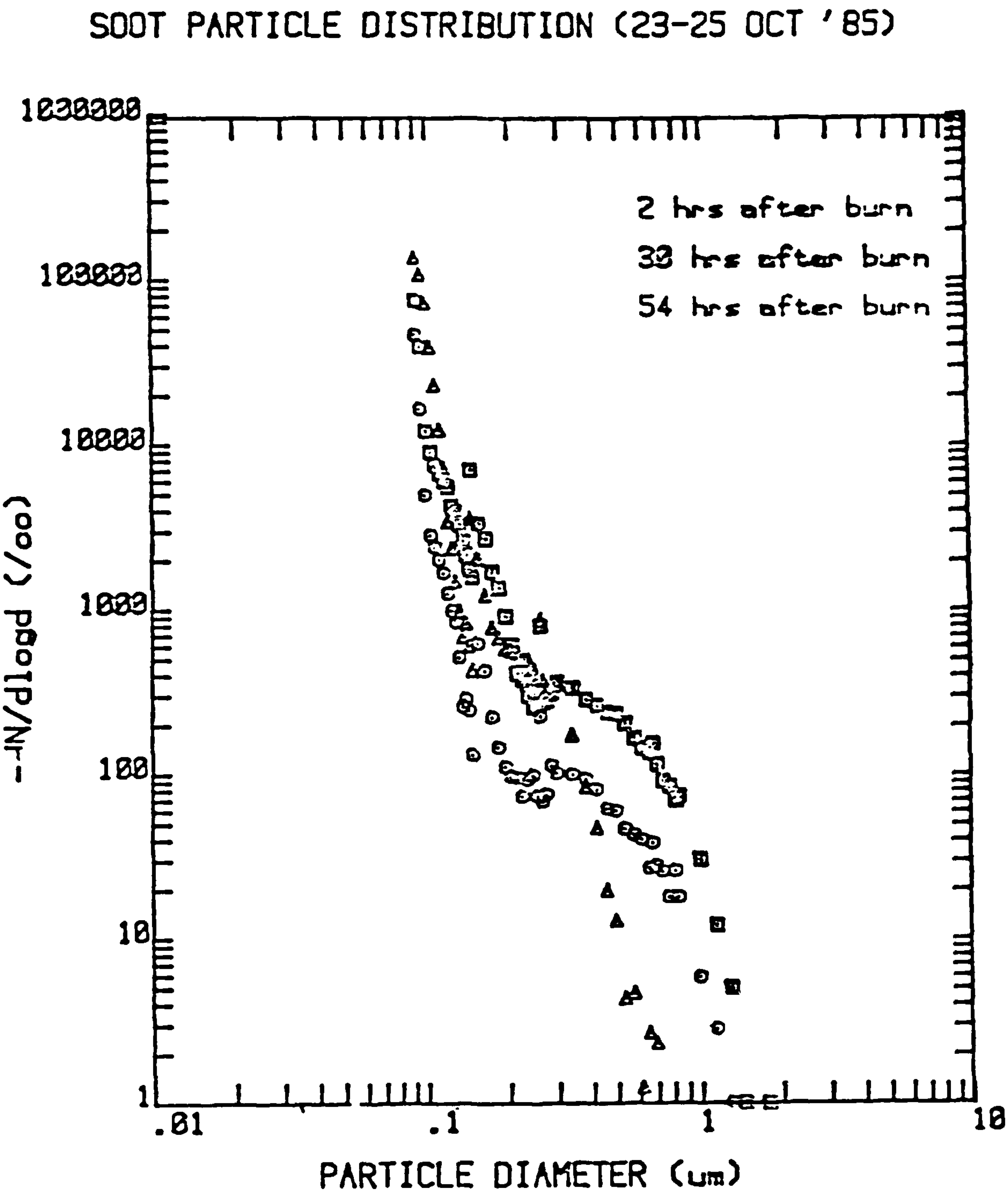

Figure 20: ASASP-X size spectra

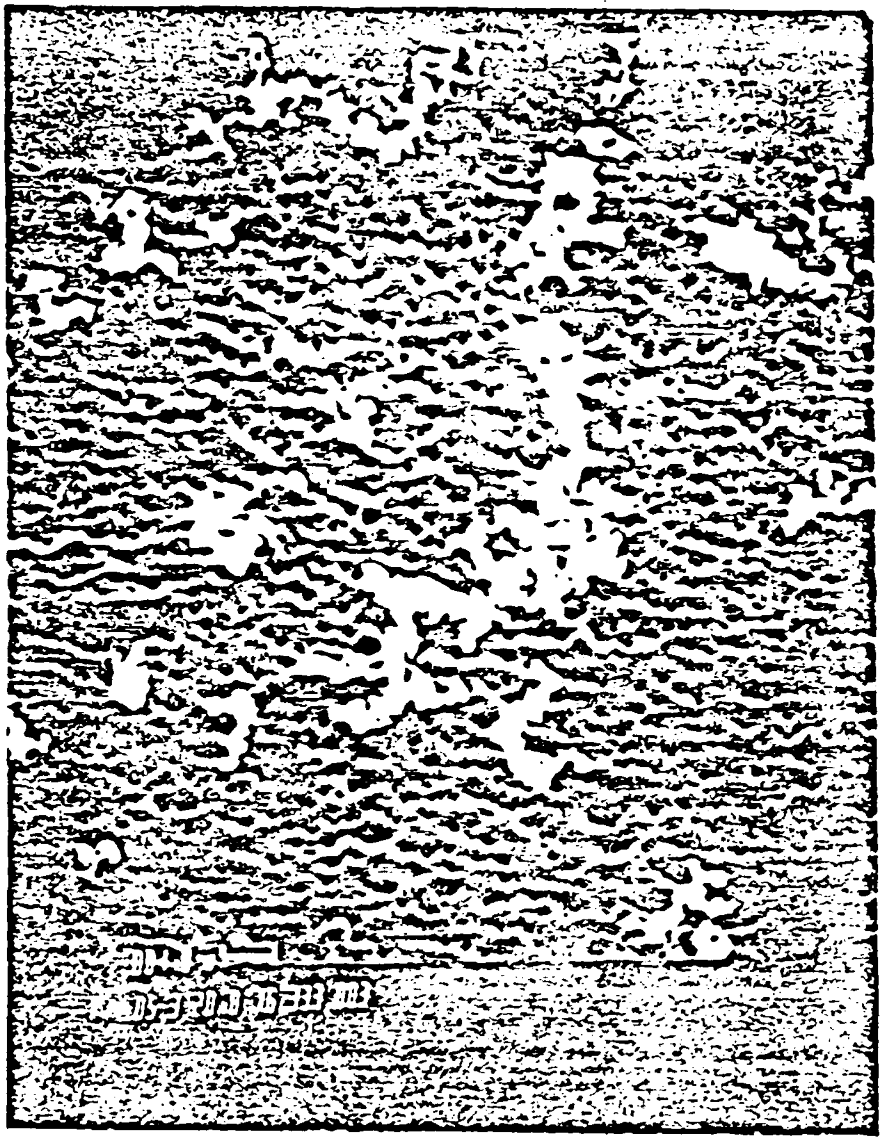

FILTER 26

Figure 21: October 23, 1985 sample. Filter exposed at 5.5 hours, from 8 m^3 bag.

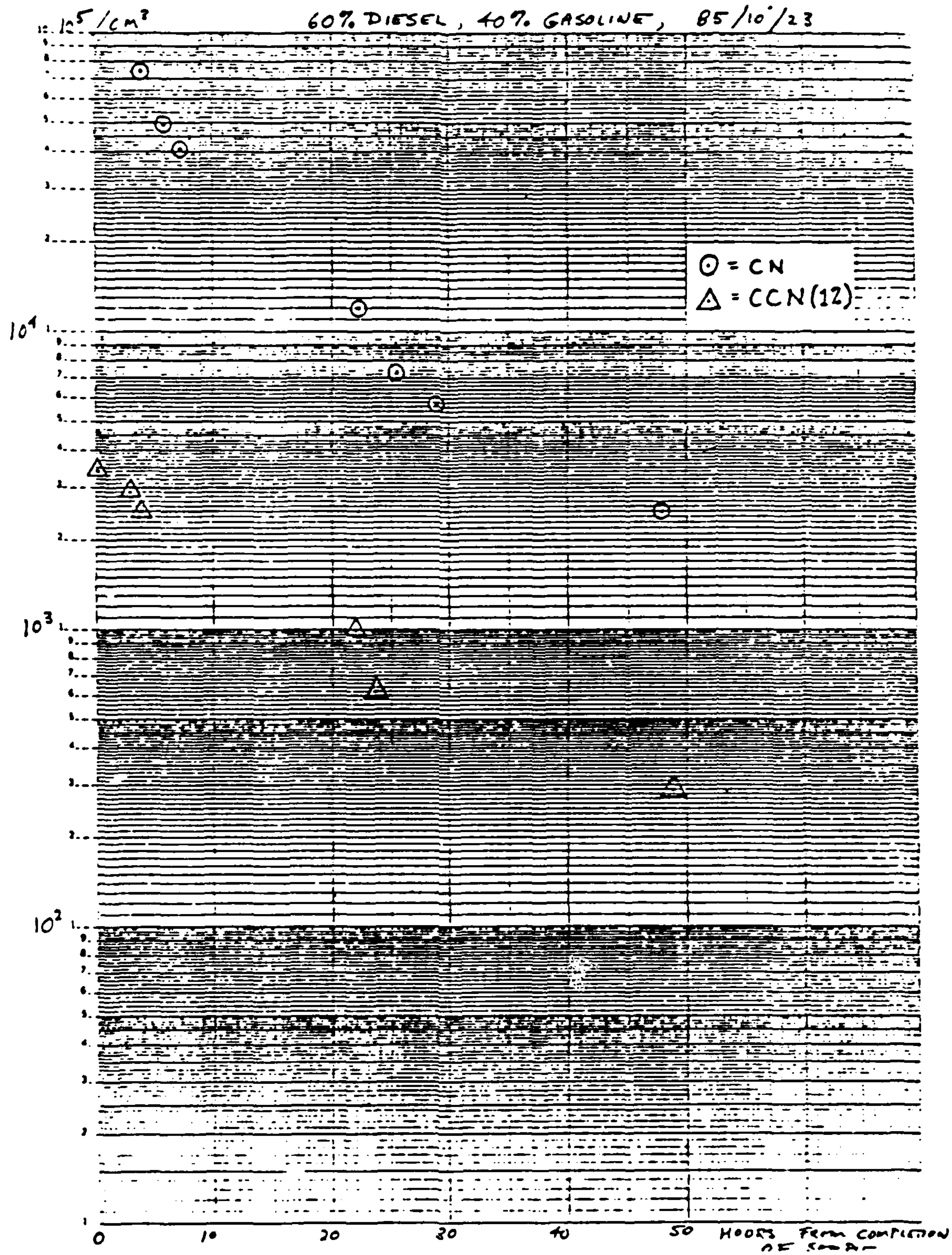

Figure 22: CN and CCN active at 1%; October 23, 1985 sample.

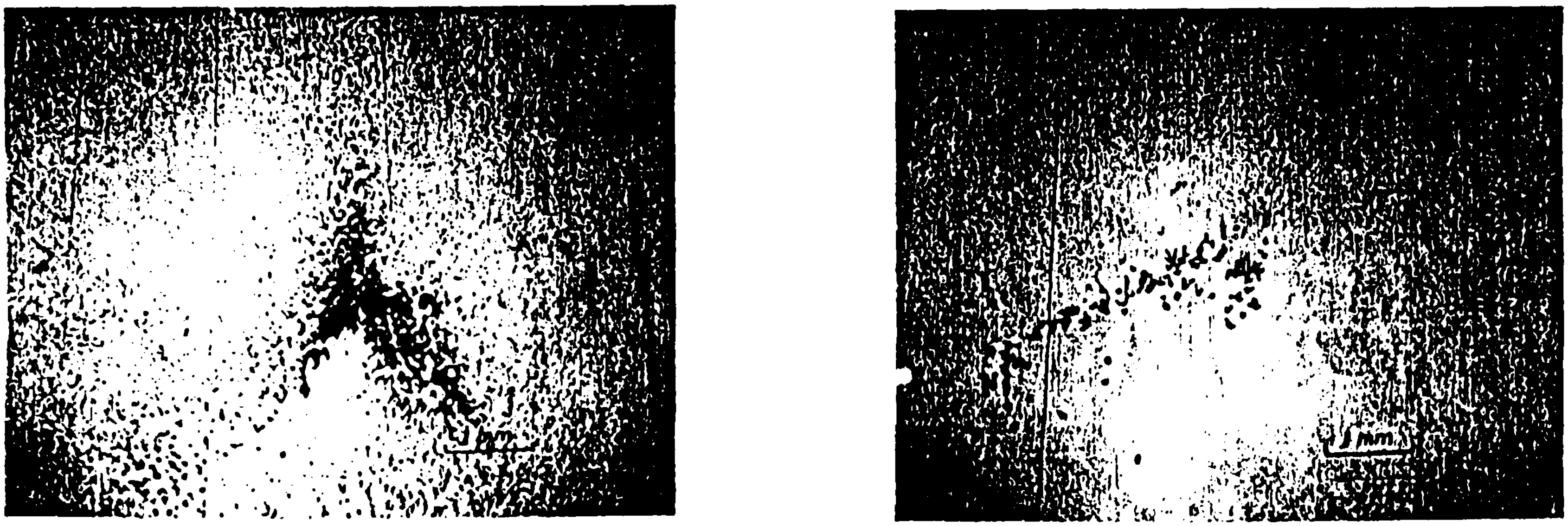

FIGURE 23: SOOT FLAKES FROM ACETYLENE COLLECTED ON FORMVAR REPLICATOR. LABORATORY TEST.

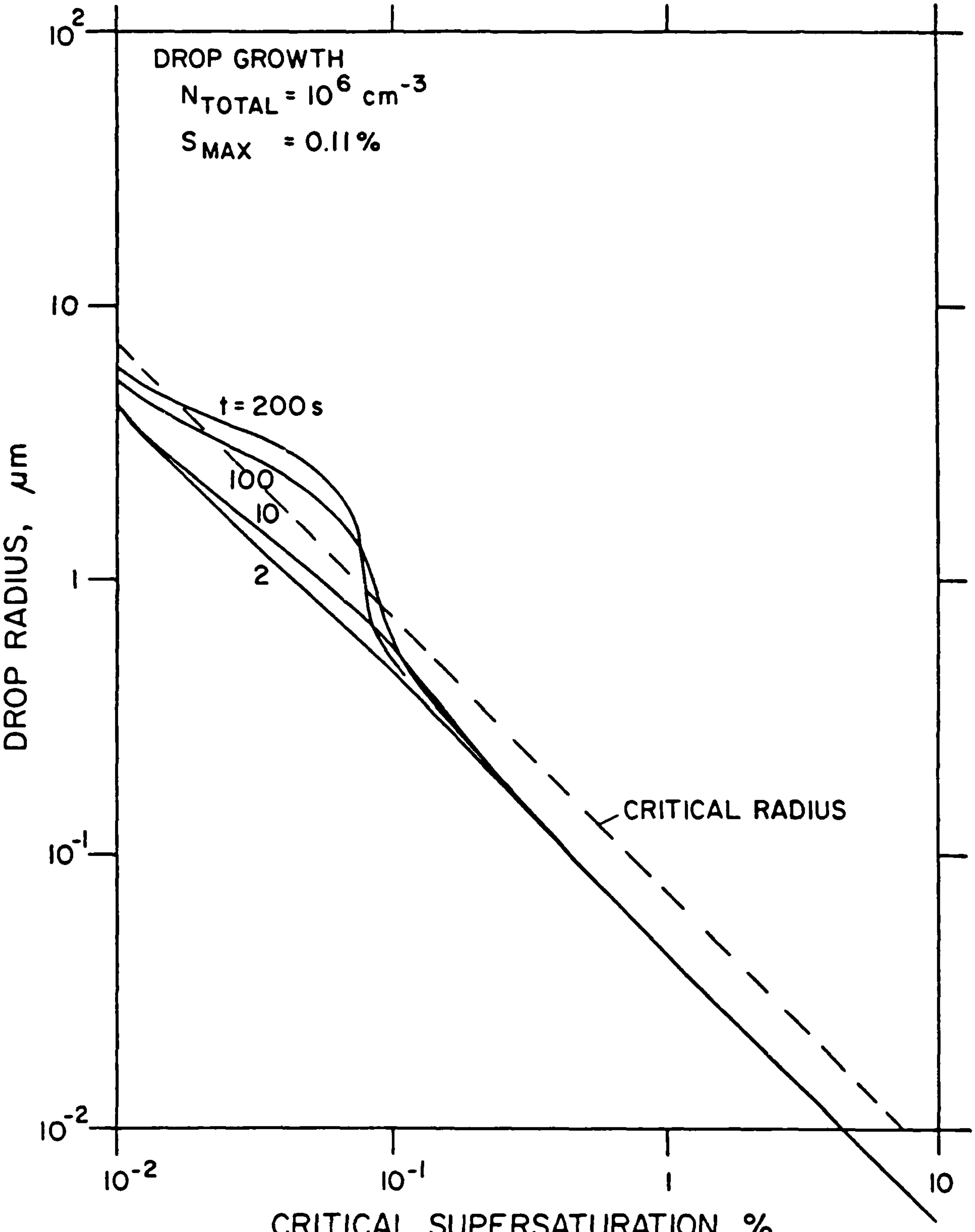

FIG. 24: MODEL DROPLET GROWTH $10^6\ cm^{-3}$

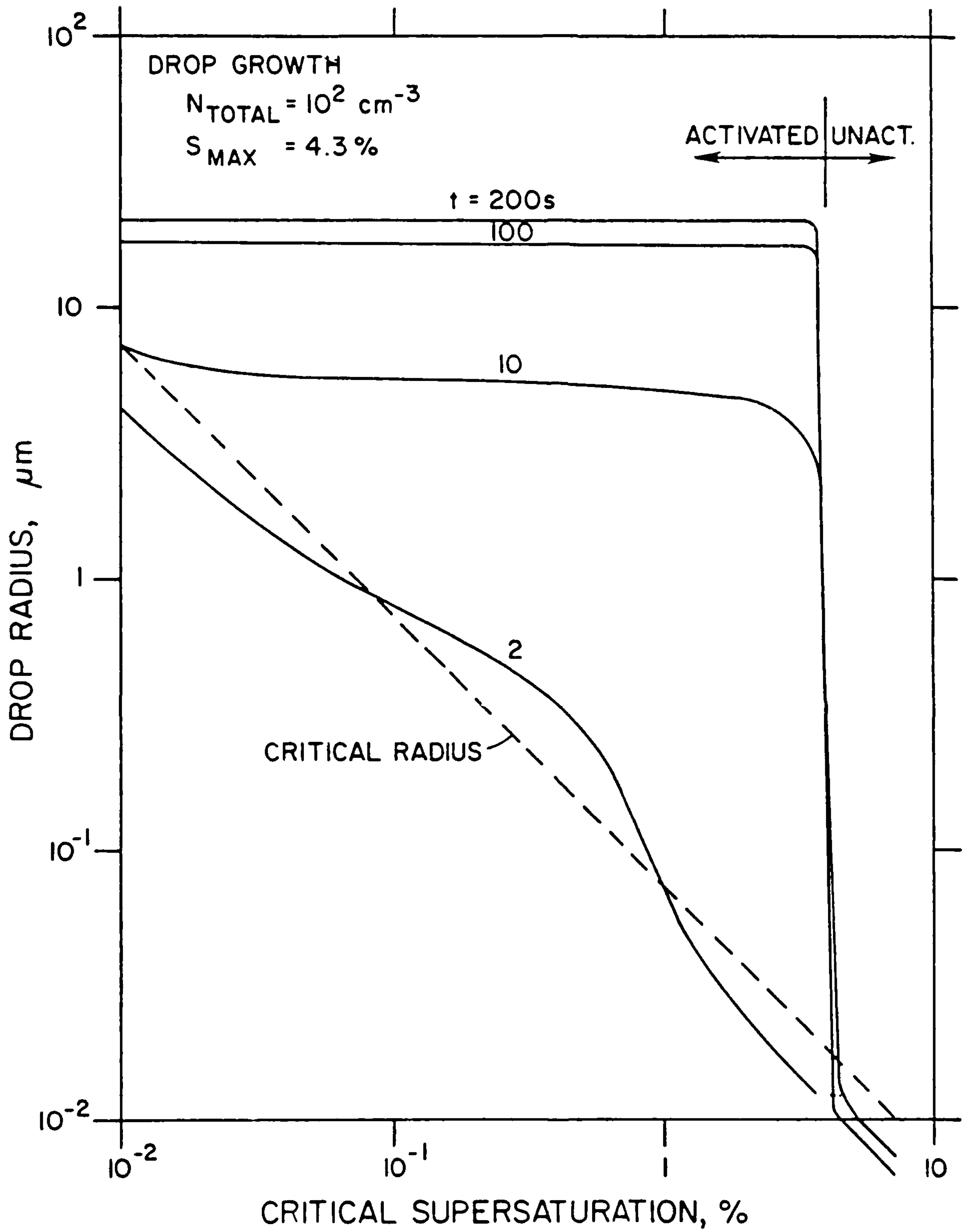

FIG. 25: MODEL DROPLET GROWTH 100 cm^{-3}

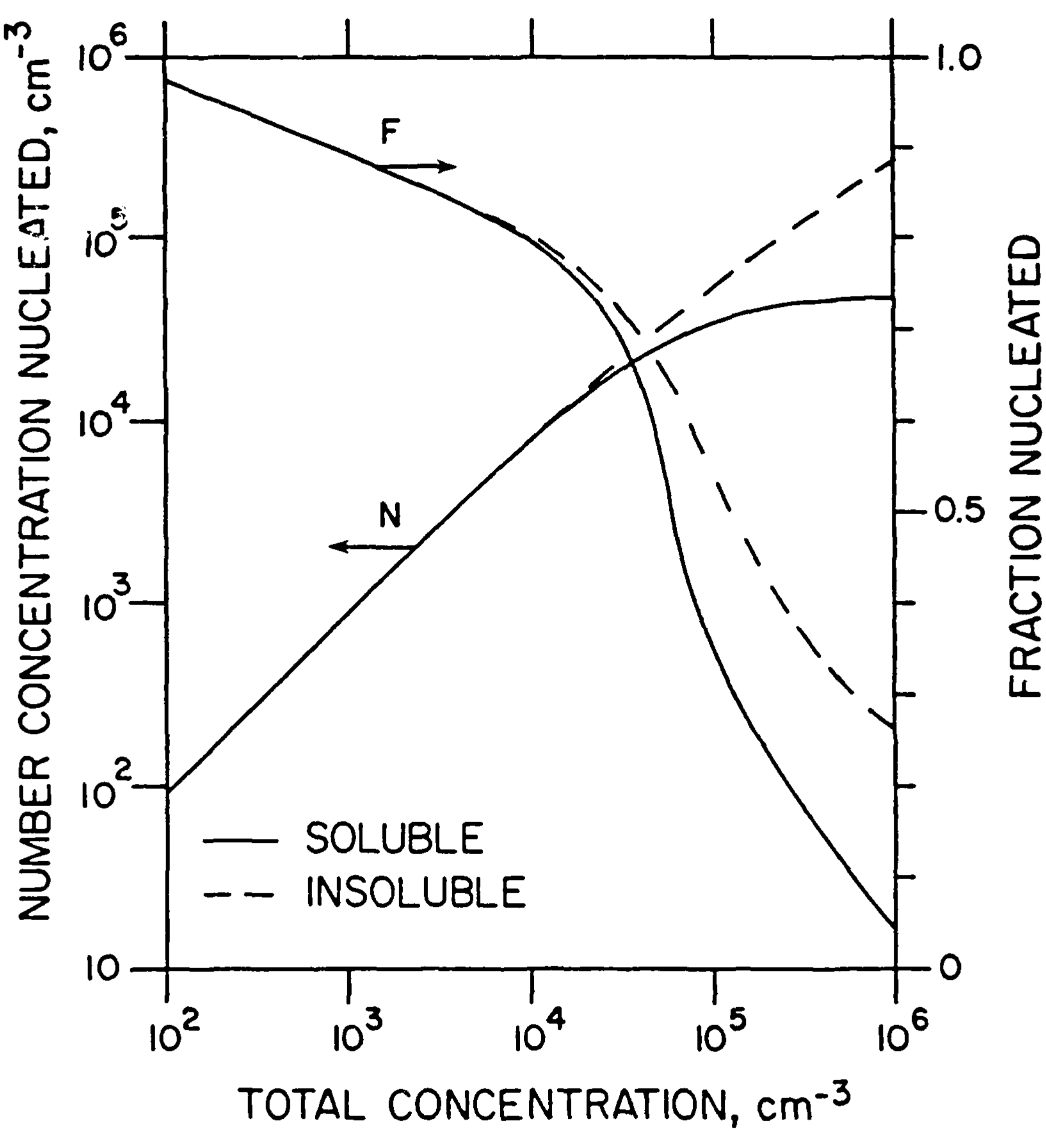

FIG. 26: MODEL NUMBER AND FRACTION ACTIVATED

CONCLUSIONS FROM OUR STUDY:

1). Lab/field soot complex; 0.1 to 100 μm.

2). Lab soot acetylene/crude oil $\frac{CCN}{CN}$ ratio few to 10% increasing with time.

3). Ice nucleation unexciting.

4). Soot collects on outside of drops mm - 50 μm as evaporation proceeds.

- (i) Independent particles
- (ii) lily pads
- (iii) solidified surface
- (iv) collapsed soccer ball
- (v) surface resuspension

5). Sooty cloud doesn't change extinction over 10^3s by scavenging.

6). CCN - cloud droplets - ice removal or coalescence; only partial pluvial constipation.

FUTURE WORK:

i. evaporated cloud droplets and soot coagulation.

ii. scattering + extinction of sooty cloud.

iii. role of growth/evaporation in scavenging process (a) droplets, (b) ice

iv. soot in a supercooled cloud - rime growth.

FIELD:

i. soot from oil fire. CN, CCN, replica.

ii. cloud droplets on replica, modification and scavenging in cap cloud. (Lodi?)

iii. deeper cloud and ice role in scavenging. Ice from replica (Chapleau?)

MAJOR PROBLEM:

Firestorm dynamics to give right microphyics for maximum scavenging.

Chemical Scavenging in the Atmosphere: Smoke-Ozone Reactions

N. deHaas, R. M. Fristrom, M. J. Linevsky and D. M. Silver
Applied Physics Laboratory, The Johns Hopkins University
Laurel, Maryland 20707

ABSTRACT

A laboratory apparatus has been constructed to examine the reaction of smoke particles with ozone. A stopped-flow experimental procedure has been developed that permits (1) a measurement of the total extinction of a He-Ne laser beam by ozone(Chappuis band) and/or by various sub-micron smoke particles; (2) a measurement of the right-angle scattering of a Nd-Yag laser by the smoke particles; and (3) a sampling of particulates for examination under the scanning electron microscope. Ozone (without smoke) is stable in the apparatus over a period of hours; smoke (without ozone) is also stable over a period of hours. Smoke-ozone mixtures begin decaying immediately and, under the experimental conditions employed, they have half-lives of a half-hour to two hours depending on the fuel source of the smoke particles. Specifically, the half-life is defined to be the time in which the optical extinction at 6328 Å is reduced to one-half its initial value. Translating these results to "nuclear winter" atmospheric conditions yields half-lives in the range of a month. These experiments provide solid qualitative evidence for the existence of atmospheric chemical scavenging of smoke and ozone.

This work was supported in part by the Naval Sea Systems Command under Contract N00024-85-C-5301.

Submitted for presentation at the DNA Global Effects Program Technical Meeting, 25-27 February 1986 by D. M. Silver, (301) 953-6265.

TABLE V - SOOT CLOUD SCAVENGING (LIMITED BY TURBULENT ENTRAINMENT WHICH IN TURN IS DIFFUSION LIMITED BELOW THE MINIMUM MIXING SCALE LENGTH)

Alt (Km)	$t_{1/2}(O_3)$ Scale 1 Meter sec	$t_{1/2}(O_3)$ Scale 10 Meters sec
8	1170	$1.2X10^5$ (1 1/2 da)
10	500	$5X10^4$ (1/2 da)
12	160	$1.6X10^4$ (5 hrs)

$$t_{1/2} = \frac{1/2 \text{ Number of C atoms in Minimal Eddy}}{\text{Minimal Eddy Area *Diffusion Velocity *Concentration *Reaction Probability}}$$

$$t_{1/2} = \frac{1/2\, V_E * f * N_T}{A_E * V_D * N_i}$$

$$t_{1/2} = 1X10^{-4}\, P*(300/T)^{1.67} * N_T/N_i * d_E^{\,2}$$

$$V_E/A_E = d_E/6$$

$f = 4.8X10^{-3}$ (Ref. C. Fenimore, Chemistry of Premixed Flames, Pergamon (1964) p. 65)

$$V_D = 2D_i/L_c = \left(\frac{2D_0}{PL_C}\right)\left(\frac{T}{300}\right)^{1.67}$$

SMOKE-OZONE APPARATUS

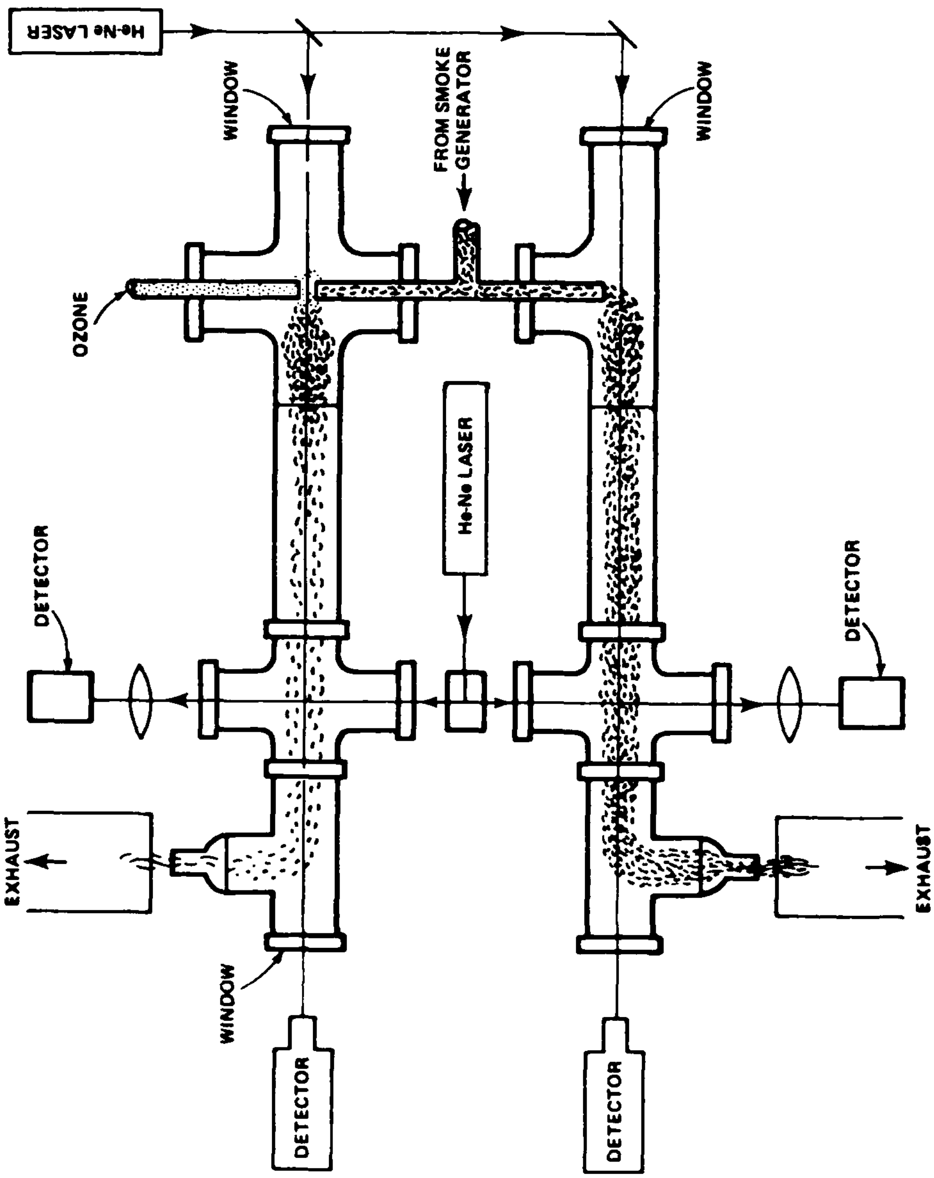

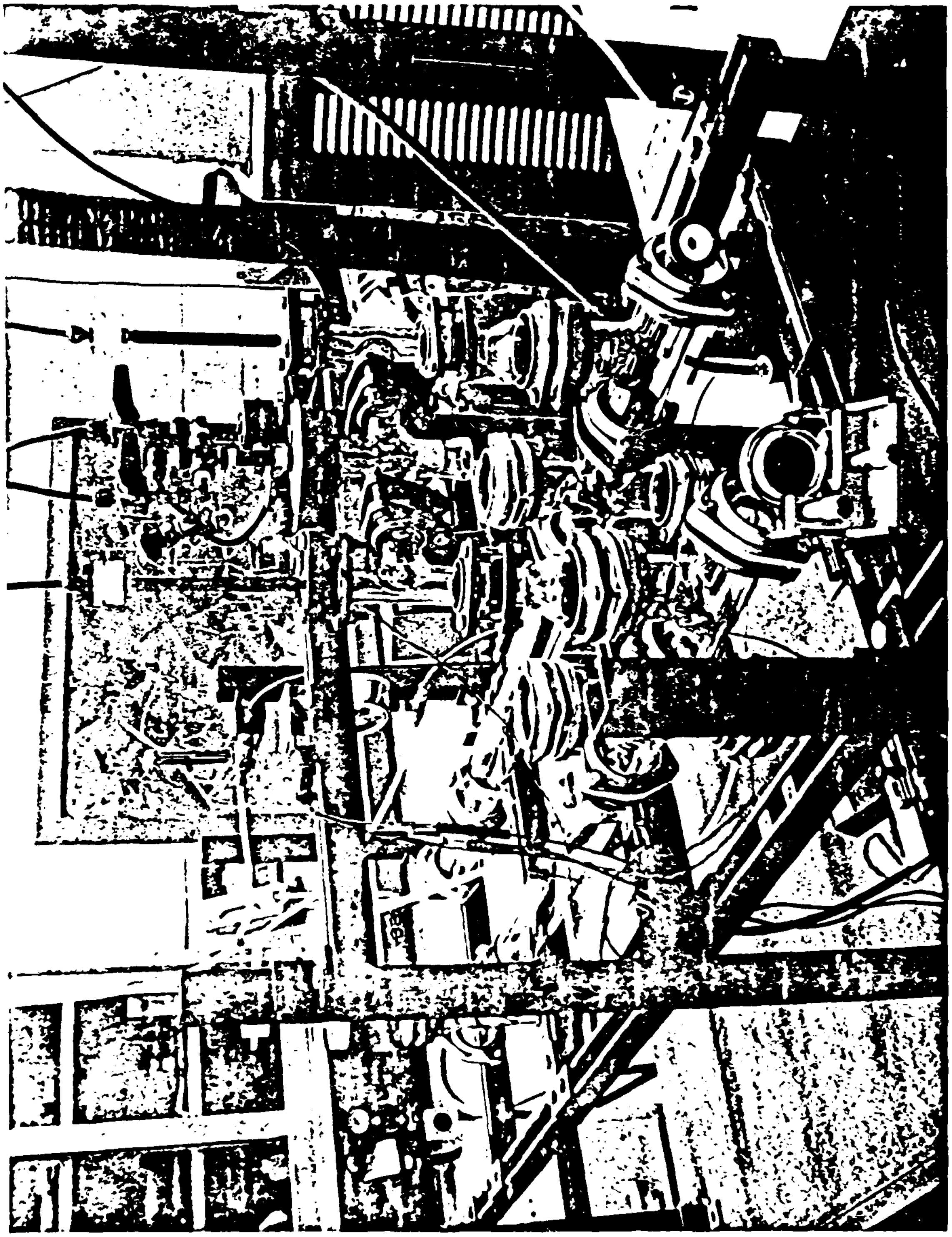

Smoke - Ozone Apparatus

Cellulosic Smoke (SEM 3600 x)

Xylenic Smoke (SEM 3600 x)

Transmission of light through smoke column

$$I = I_0 \exp(-a b c_s)$$

a = extinction coefficient
b = length of smoke column
c_s = concentration of smoke

$\ln(I_0/I)$ is linearly proportional to smoke concentration

$$\ln(I_0/I) = a b c_s$$

Rate of disappearance of smoke

$$-\frac{dC_s}{dt} = k\, C_o\, C_s$$

k is second-order rate constant
C_o is concentration of ozone
C_s is concentration of smoke

With excess ozone, rate is pseudo first-order in smoke concentration: (C_o assumed constant)

$$\therefore\ C_s = A \exp(-k\, C_o\, t)$$

But $\ln(I_o/I)$ is proportional to C_s

$$\therefore\ \ln \ln(I_o/I) = A' - kC_o t$$

i.e., linearly proportional to time if the reaction is pseudo first-order in smoke concentration

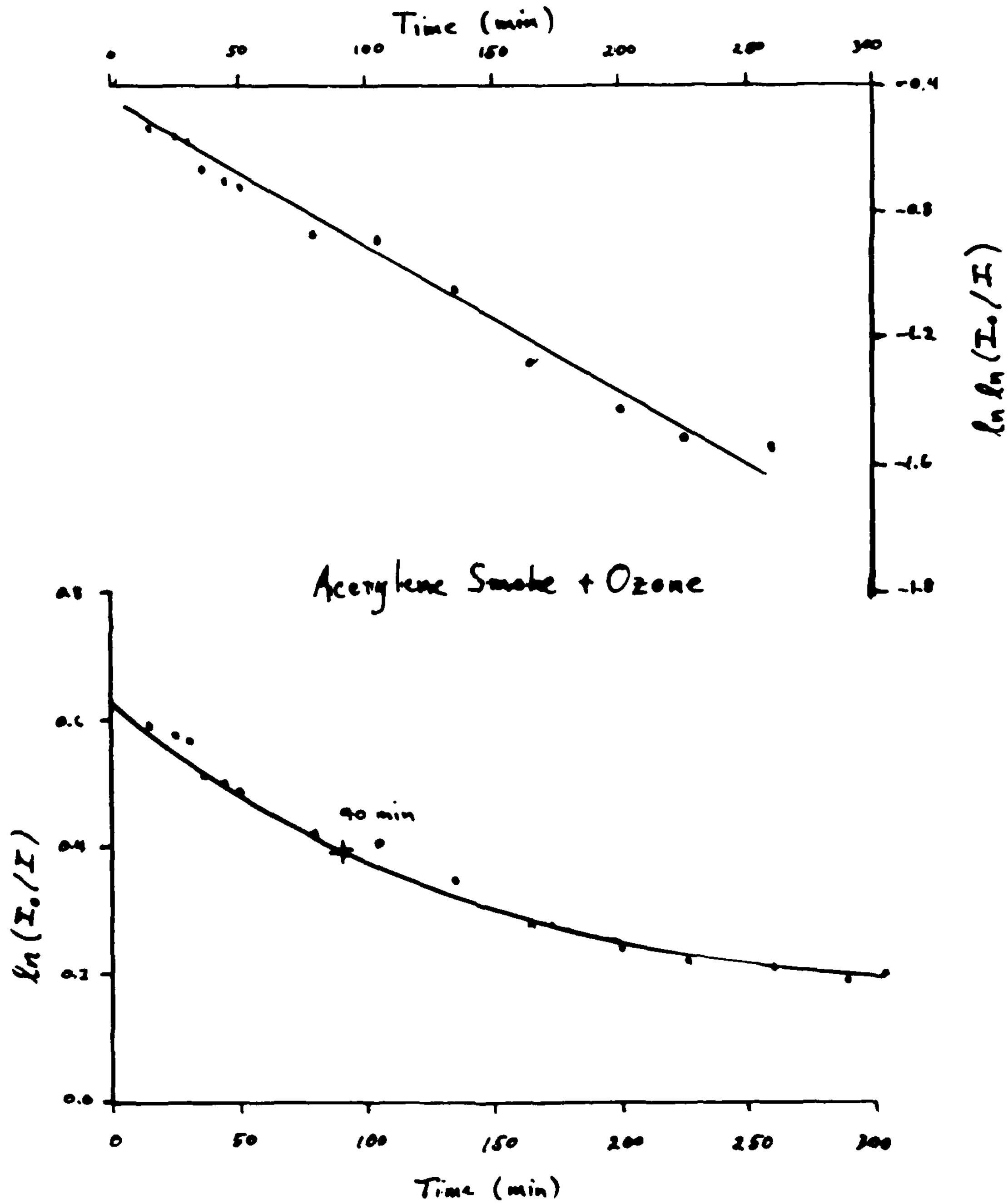

Time (min)
0
50
100
150
200
250
300
-0.4
-0.8
-1.2
-1.6
-1.8
ln ln(I₀/I)
Acetylene Smoke + Ozone
0.8
0.6
0.4
0.2
0.0
90 min
ln(I₀/I)
0
50
100
150
200
250
300
Time (min)

1.29

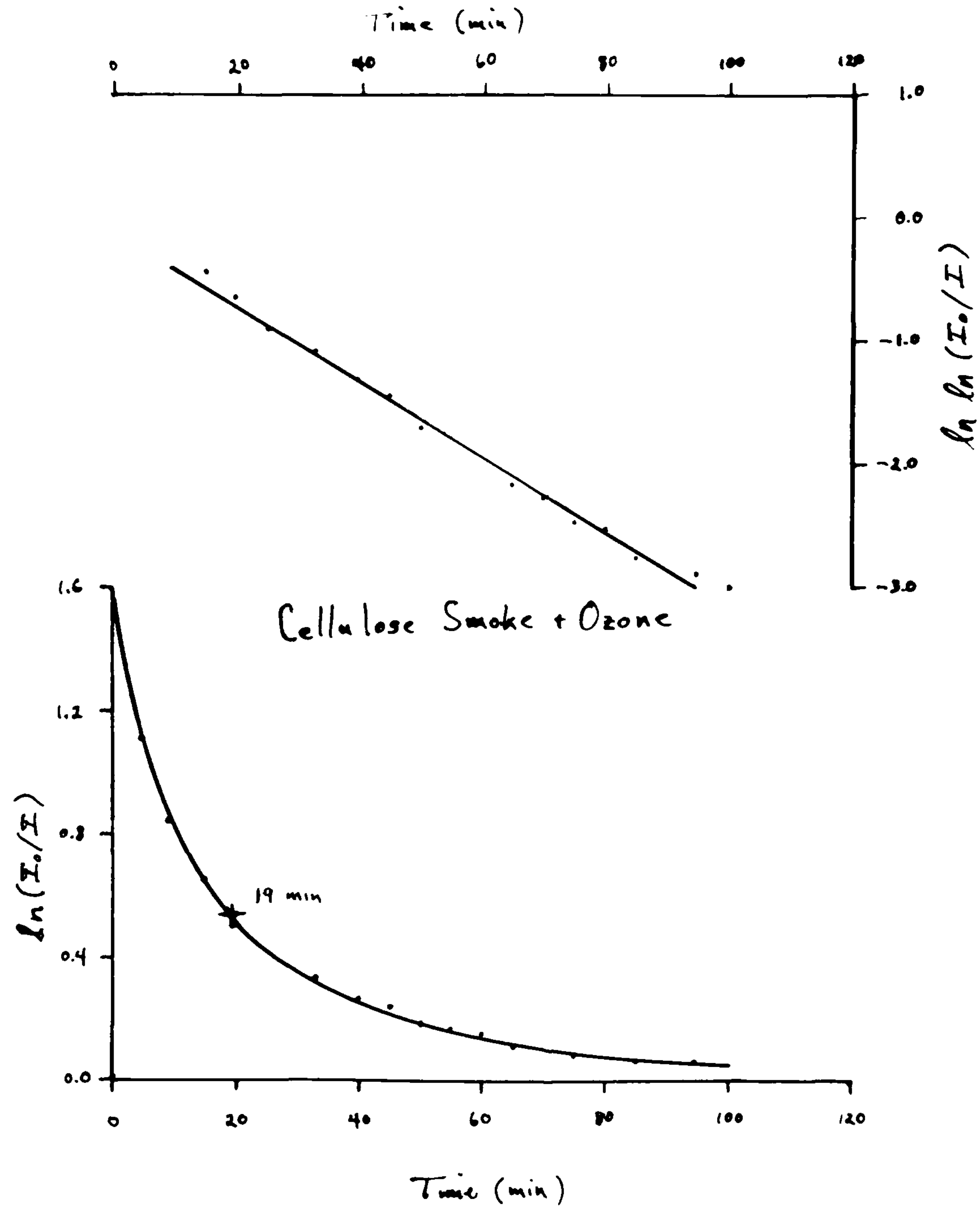

Time (min)
0
20
40
60
80
100
120
1.0
0.0
-1.0
-2.0
-3.0
ln ln (I₀/I)
Cellulose Smoke + Ozone
1.6
1.2
0.8
0.4
0.0
ln (I₀/I)
19 min
0
20
40
60
80
100
120
Time (min)

1.20

Ozone (without smoke) is stable in apparatus over a period of hours (no change in absorption in the Chappuis bands).

Smoke (without ozone) is stable in apparatus over a period of hours (no change in optical extinction at 6328 Å).

Smoke-ozone mixtures show a time-dependent decay in optical extinction at 6328 Å

- Half-life depends on source of smoke
- Kinetics appear to have first-order dependence on smoke concentration

Translated to "nuclear winter" atmospheric conditions, optical extinction is estimated to be reduced to one-half its initial value in a time range of a month.

REACTION OF STRATOSPHERIC CARBON AEROSOL WITH OZONE

L. R. MARTIN, H. S. JUDEIKIS, R. B. COHEN

THE AEROSPACE CORPORATION

$$C + O_3 \longrightarrow CO + O_2$$

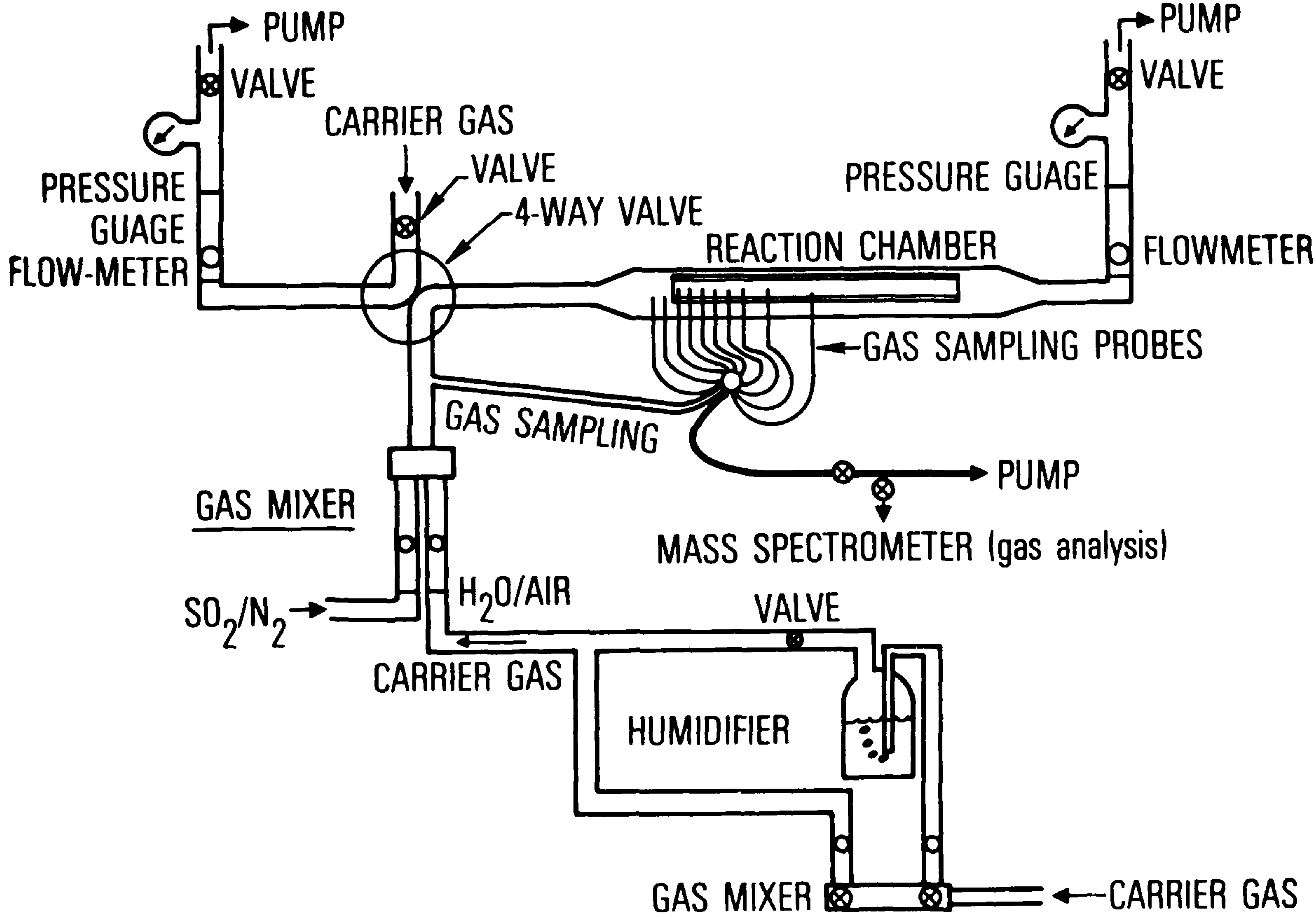

PUMP
VALVE
CARRIER GAS
VALVE
4-WAY VALVE
PRESSURE
GUAGE
FLOW-METER
PUMP
VALVE
PRESSURE GUAGE
FLOWMETER
REACTION CHAMBER
GAS SAMPLING PROBES
GAS SAMPLING
PUMP
MASS SPECTROMETER (gas analysis)
GAS MIXER
SO_2/N_2
H_2O/AIR
VALVE
CARRIER GAS
HUMIDIFIER
GAS MIXER
CARRIER GAS

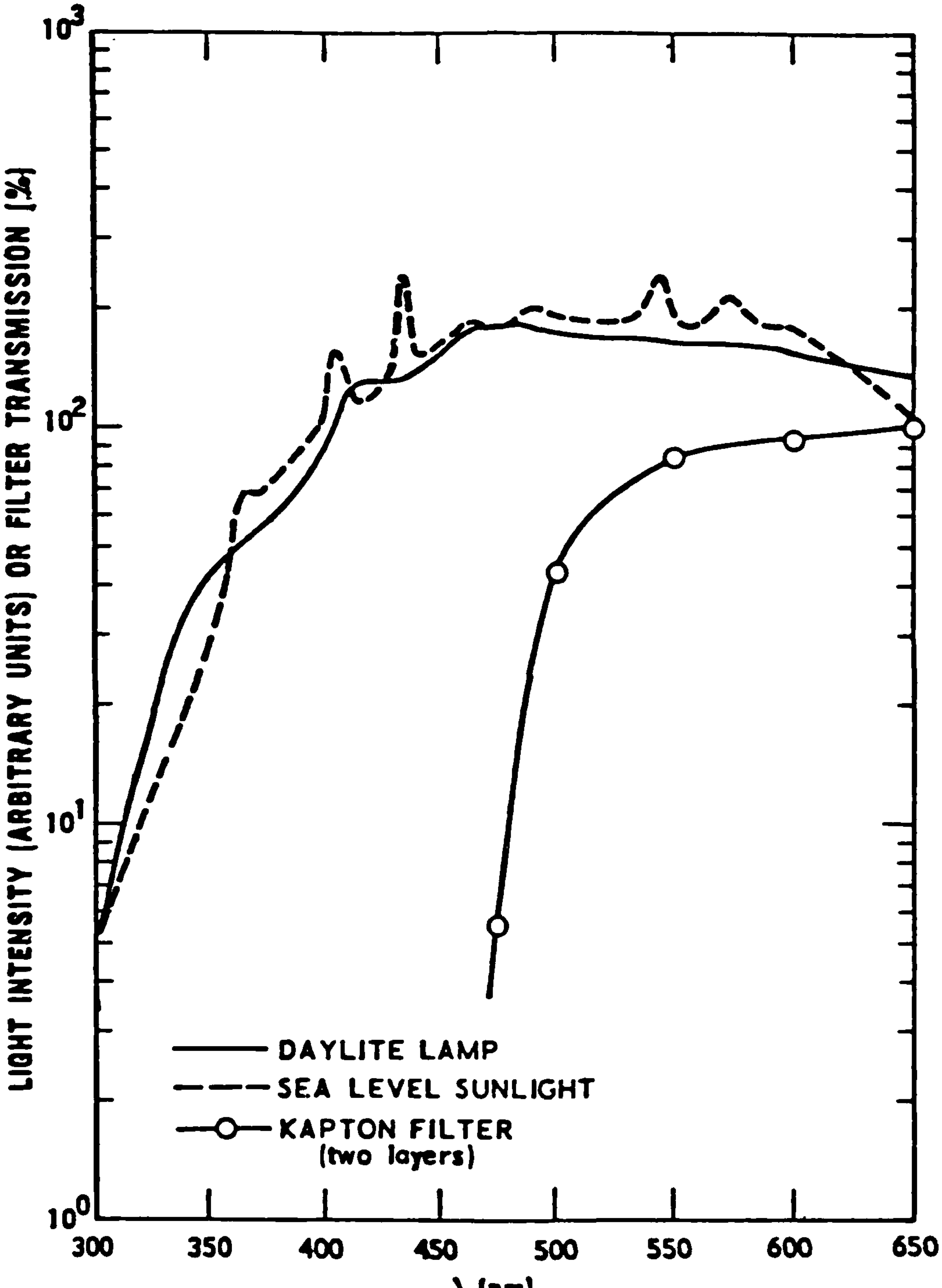

LIGHT INTENSITY (ARBITRARY UNITS) OR FILTER TRANSMISSION (%)
10^3
10^2
10^1
10^0
300
350
400
450
500
550
600
650
λ (nm)
DAYLITE LAMP
SEA LEVEL SUNLIGHT
KAPTON FILTER
(two layers)

CHEMICAL ANALYSES

- GAS PHASE
  - ON-LINE MASS SPEC
  - CO, CO_2, OTHERS
- ADSORBED PRODUCTS
  - DESORPTION AND MASS SPEC
  - DISSOLUTION AND HPLC

$$D\left(\frac{\partial^2 C}{\partial R^2} + \frac{1}{R}\frac{\partial C}{\partial R} + \frac{\partial^2 C}{\partial Z^2}\right) - V_Z \frac{\partial C}{\partial Z} = 0$$

WHERE $C = \frac{[SO_2]}{[SO_2]_0}$

BOUNDARY CONDITIONS

$$C = 1 \text{ AT } Z = 0$$

$$C = 0 \text{ AT } Z = \infty$$

$$\frac{\partial C}{\partial R} = 0 \text{ AT } R = 0$$

$$D\frac{\partial C}{\partial R} = \phi K_R C \text{ AT } R = R$$

GENERAL SOLUTION

$$C = \sum_I F_I(R) E^{-\beta_I Z}$$

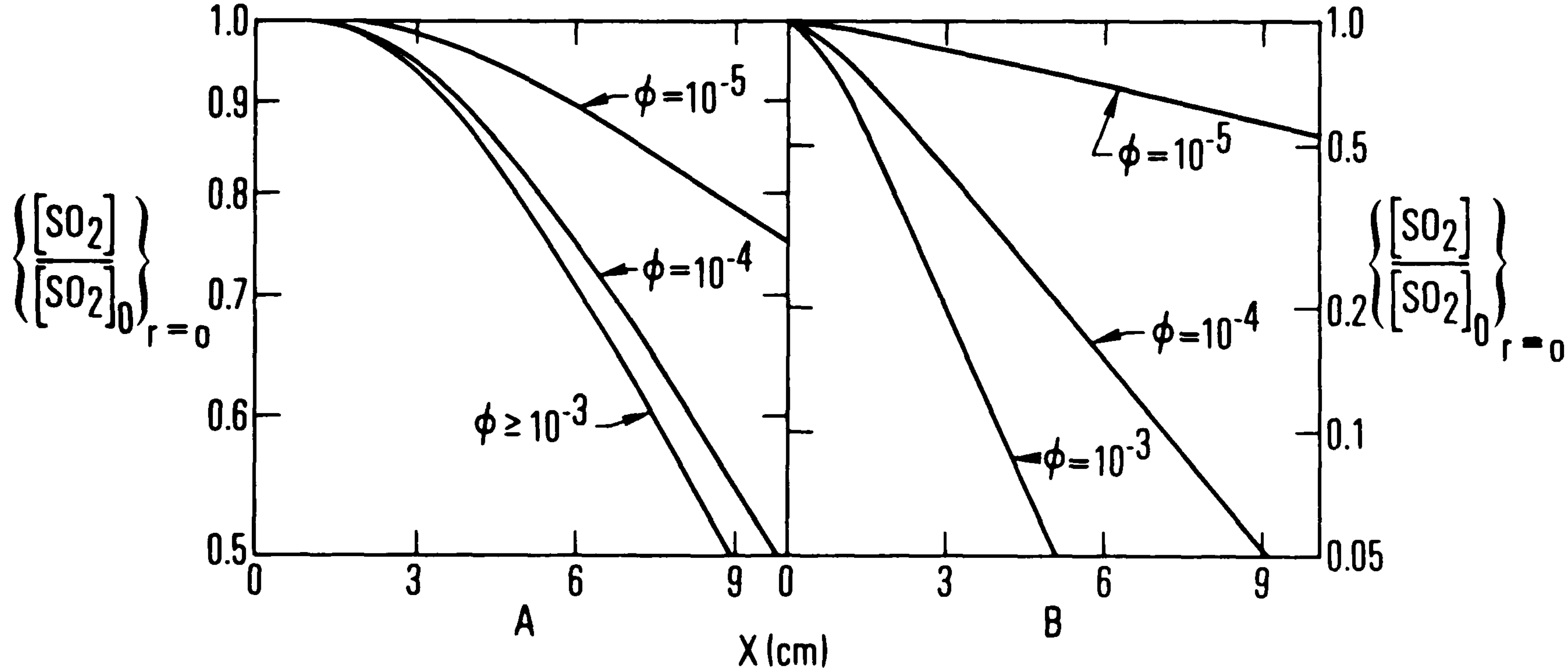
1.0
0.9
0.8
0.7
0.6
0.5
$\left\{\frac{[SO_2]}{[SO_2]_0}\right\}_{r=o}$
$\phi=10^{-5}$
$\phi=10^{-4}$
$\phi\geq10^{-3}$
0
3
6
9
A
X (cm)
$\phi=10^{-5}$
$\phi=10^{-4}$
$\phi=10^{-3}$
0
3
6
9
B
1.0
0.5
0.2
0.1
0.05
$\left\{\frac{[SO_2]}{[SO_2]_0}\right\}_{r=o}$

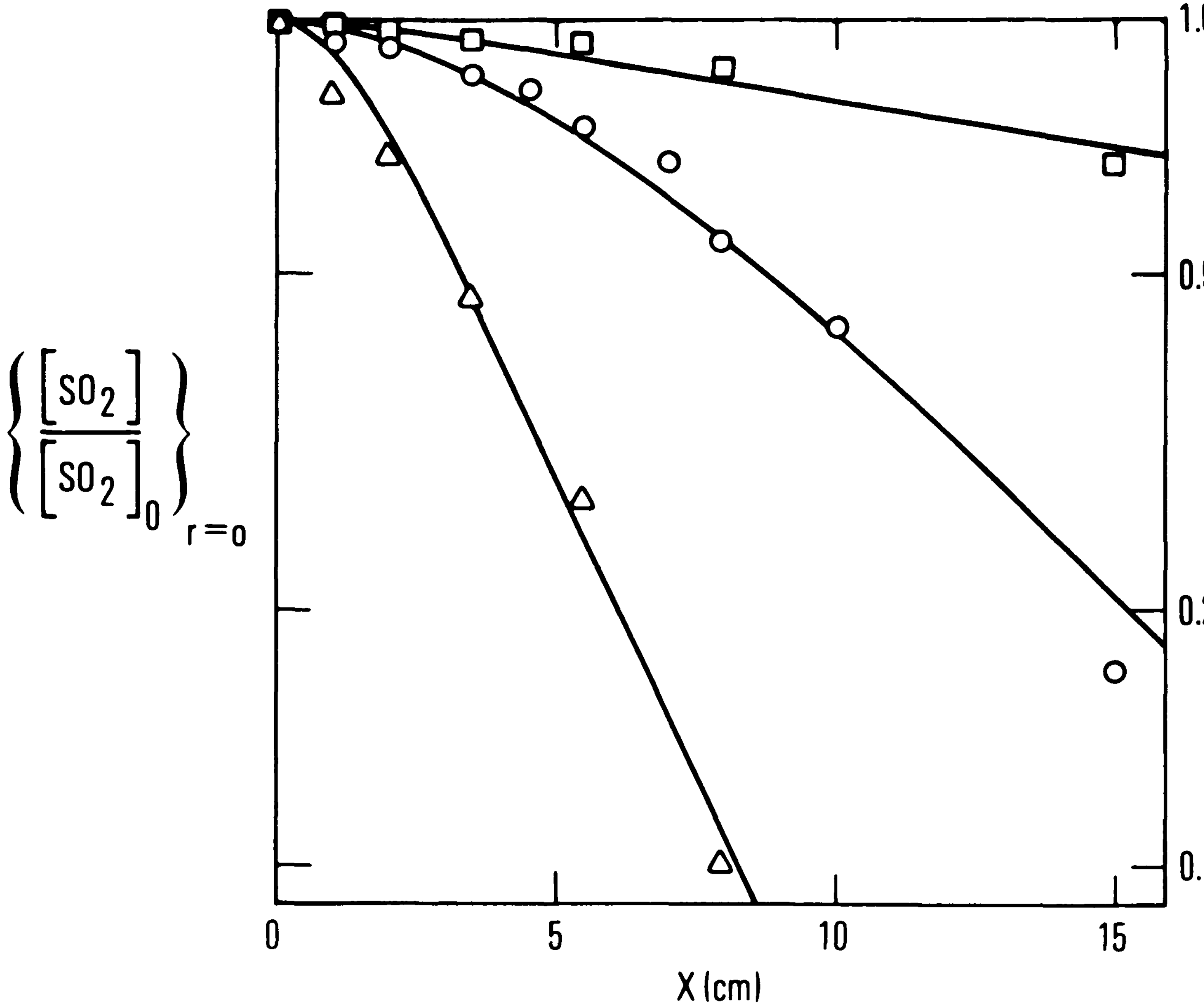
$\left\{\frac{[SO_2]}{[SO_2]_0}\right\}_{r=0}$
1.0
0.5
0.2
0.1
0
5
10
15
X (cm)

ATMOSPHERIC MODEL

$$\text{AEROSOL REACTION RATE} = \frac{3\,AD}{R^2}\,G\,C_{O_3}$$

$$G = 1\left[+ K_N \left(\frac{1.33 + 0.7\,K_N^{-1}}{1 + K_N^{-1}} + \frac{4}{3}\,\frac{1-\gamma}{\gamma} \right) \right]^{-1}$$

FOR $K_N \gg 1$

$$\frac{C}{C_O} = \left(1 - 0.009\,\frac{\gamma}{R_O}\,T\right)^3$$

$$\frac{R}{R_O} = \left(1 - 0.009\,\frac{\gamma}{R_O}\,T\right)$$

AEROSOL DESTRUCTION

γ	DESTRUCTION TIME FOR R_0 (μ) = 0.1	0.2	0.5
10^{-3}	3 HR	6 HR	15 HR
10^{-4}	1 DAY	2 DAYS	5 DAYS
10^{-5}	13 DAYS	26 DAYS	65 DAYS
10^{-6}	4 MOS.	8 MOS.	20 MOS.
10^{-7}	4 YRS.	8 YRS.	20 YRS.

AEROSOL DESTRUCTION

$D_0 = 0.3\mu$

$\gamma = 1 \times 10^{-5}$

$O_3 = 3 \times 10^{12}/cc$

T (DAYS)	AEROSOL RADIUS (μ)	% AEROSOL MASS REMAINING
0	0.30	100.00
3	0.28	78.44
6	0.25	60.22
9	0.23	45.07
12	0.21	32.70
15	0.18	22.83
18	0.16	15.18
21	0.14	9.46
24	0.11	5.40
27	0.09	2.70
30	0.07	1.10
33	0.04	0.30
36	0.02	0.03
39	0.00	0.00

HETEROGENEOUS REACTIONS IN A SOOT LADEN ATMOSPHERE

DAVID M. GOLDEN
MICHEL J. ROSSI
LUDWIG BROUWER
SHERRY STEPHENS

DEPARTMENT OF CHEMICAL KINETICS
CHEMICAL PHYSICS LABORATORY
SRI INTERNATIONAL

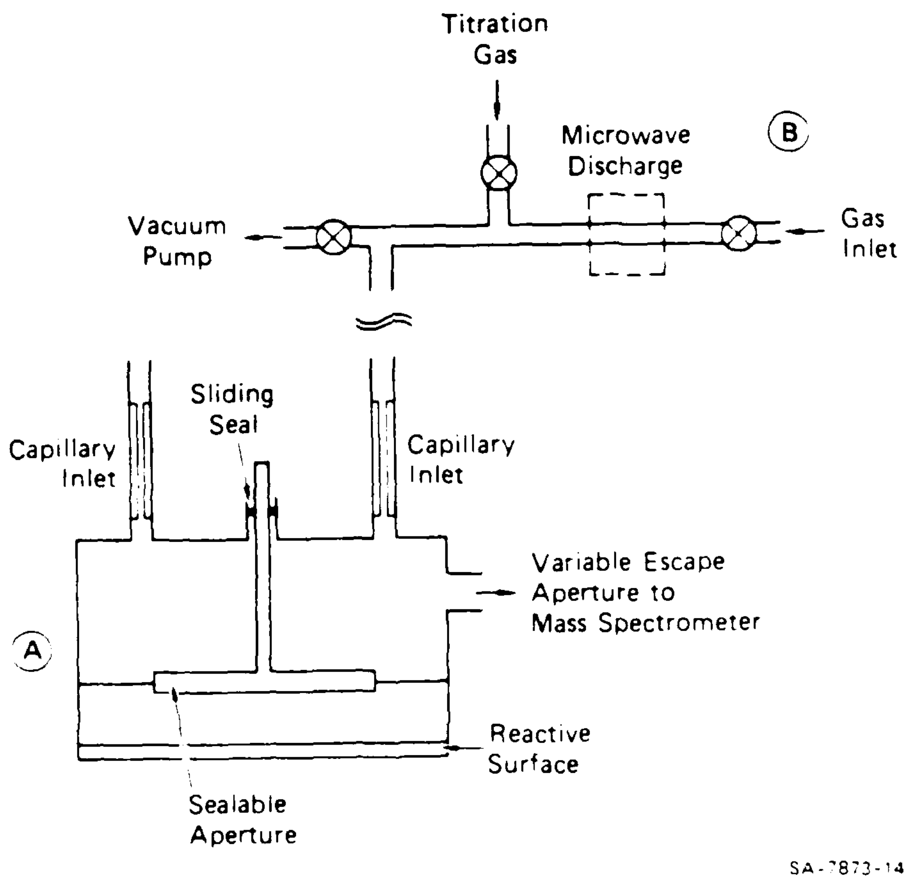
Titration Gas
Microwave Discharge
B
Vacuum Pump
Gas Inlet
Sliding Seal
Capillary Inlet
Capillary Inlet
Variable Escape Aperture to Mass Spectrometer
A
Reactive Surface
Sealable Aperture
SA-7873-14

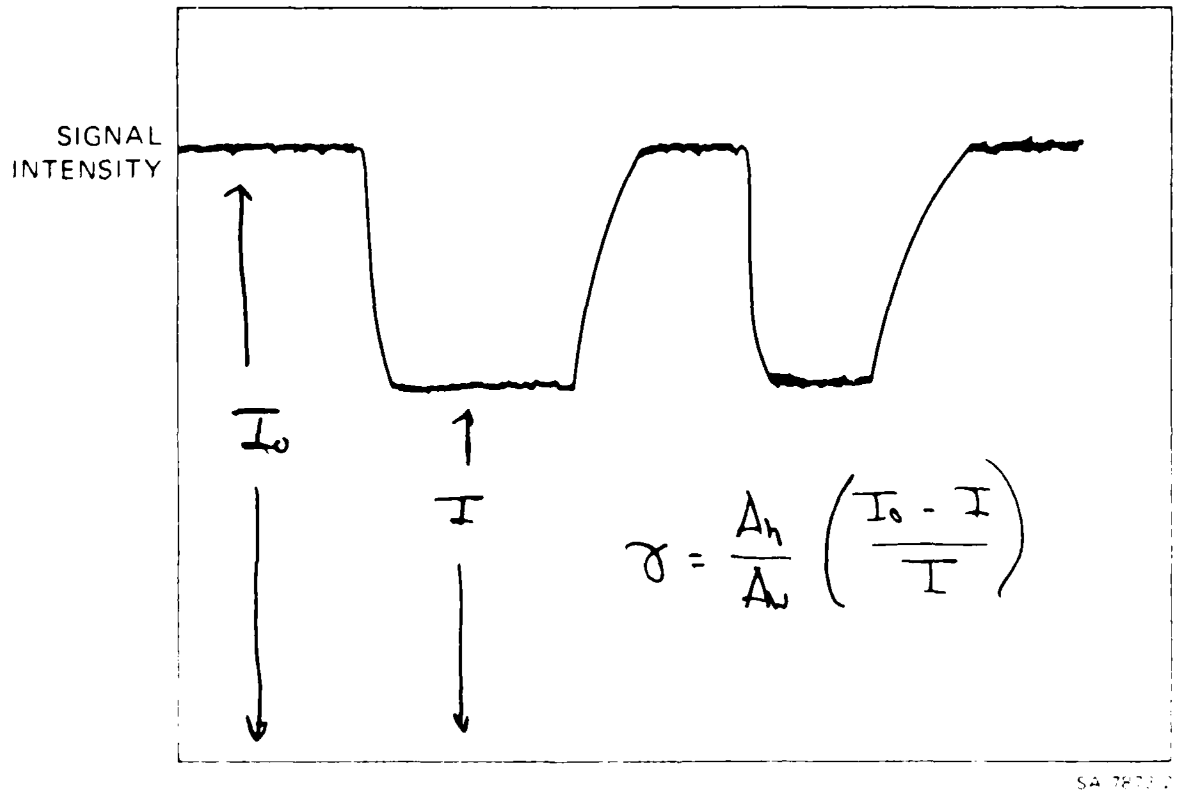

FIGURE TYPICAL EXPERIMENTAL DATA

Table 1. Collisional reaction probabilities on a H_2SO_4 surface at 300 K.

Species	Collisional reaction probability (γ)
H_2O_2	7.8×10^{-4}
HNO_3	$\geq 2.4 \times 10^{-4}$
HO_2NO_2	2.7×10^{-5}
$ClONO_2$	1.0×10^{-5}
N_2O_5	$\geq 3.8 \times 10^{-5}$
H_2O	$\sim 2.0 \times 10^{-3}$
NH_3	$> 1.0 \times 10^{-3}$
OH	4.9×10^{-4}
O_3	$< 1.0 \times 10^{-6}$
NO	$< 1.0 \times 10^{-6}$
NO_2	$< 1.0 \times 10^{-6}$
SO_2	$< 1.0 \times 10^{-6}$
Alkenes	$< 1.0 \times 10^{-6}$
Alkanes	$< 1.0 \times 10^{-6}$
CF_4	$< 1.0 \times 10^{-6}$
CCl_2F_2	$< 1.0 \times 10^{-6}$
$O(^3P)$	$< 1.0 \times 10^{-6}$
N	$< 1.0 \times 10^{-6}$

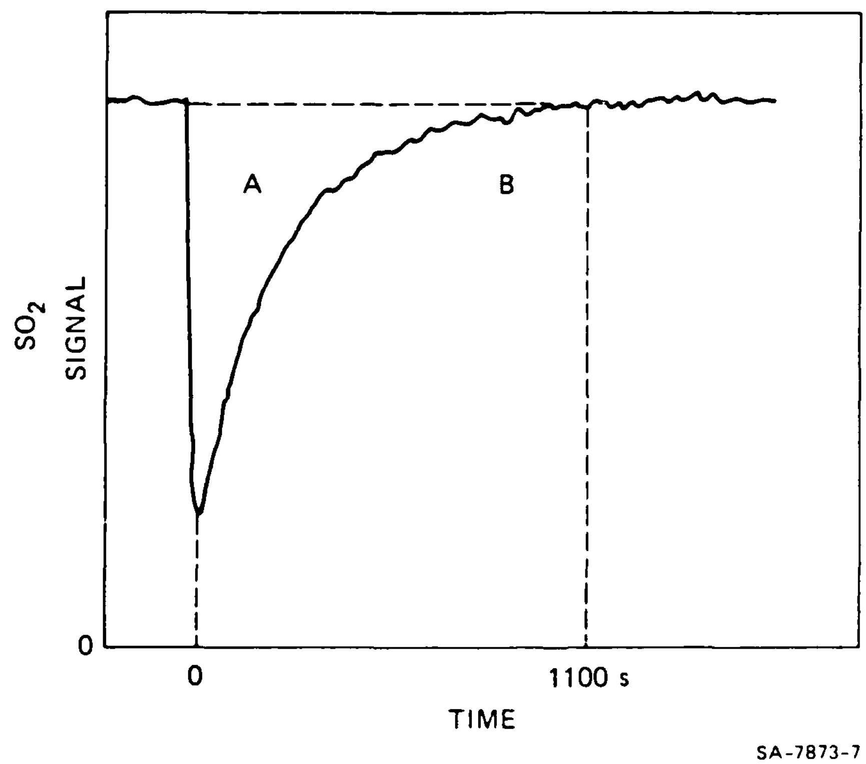

SO_2
SIGNAL
A
B
0
0
1100 s
TIME
SA-7873-7

H_2O MASS SPECTROMETER SIGNAL ($m/e = 18$) IN THE SYSTEM N_2O_5/H_2O ON CARBON

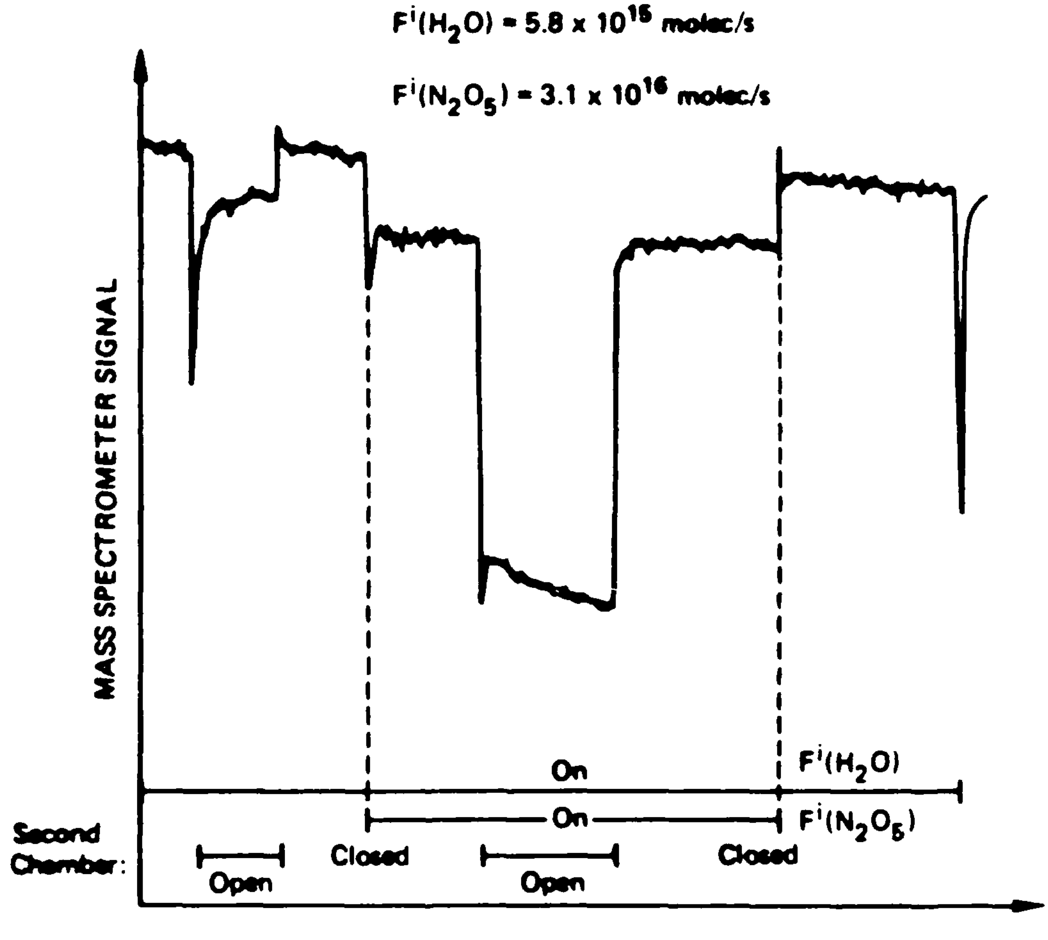

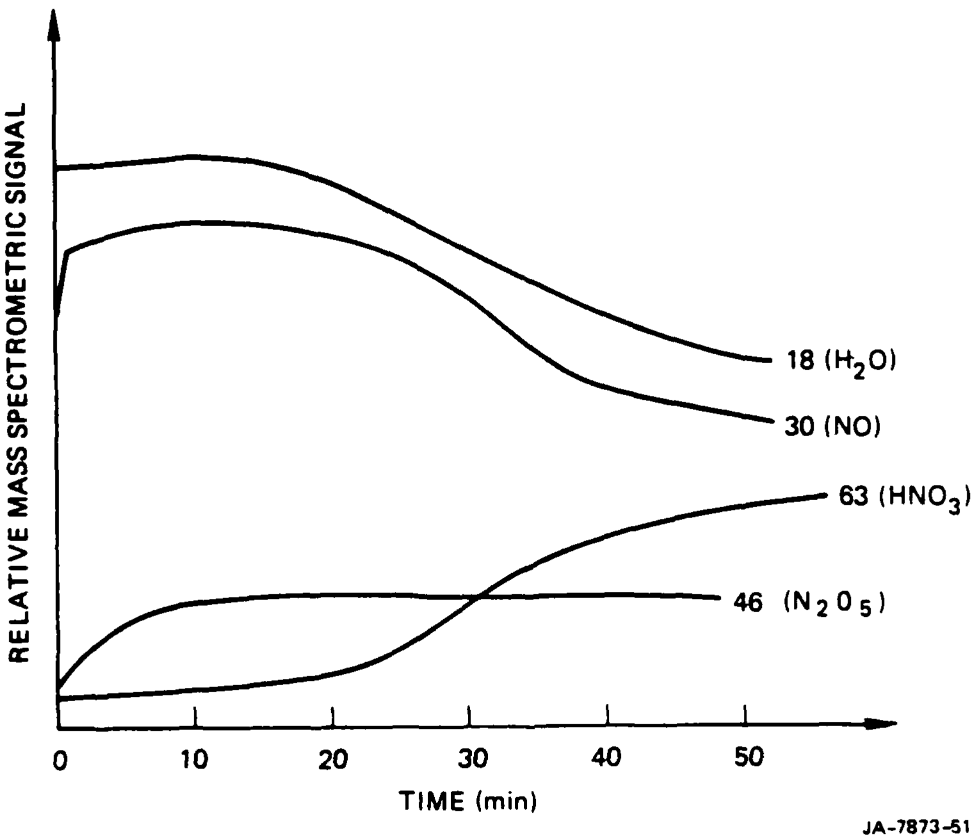
RELATIVE MASS SPECTROMETRIC SIGNAL
18 (H_2O)
30 (NO)
63 (HNO_3)
46 (N_2O_5)
0
10
20
30
40
50
TIME (min)
JA-7873-51

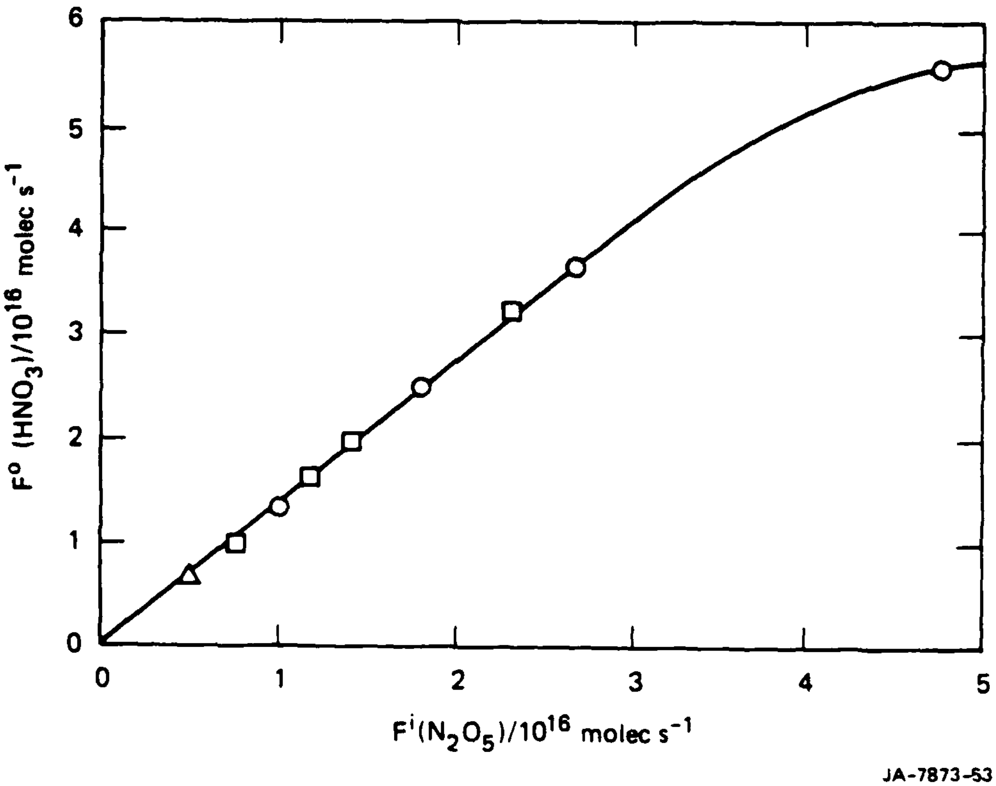

6
5
4
3
2
1
0
0
1
2
3
4
5
F° (HNO3)/10^16 molec s^-1
F^i(N2O5)/10^16 molec s^-1
JA-7873-53

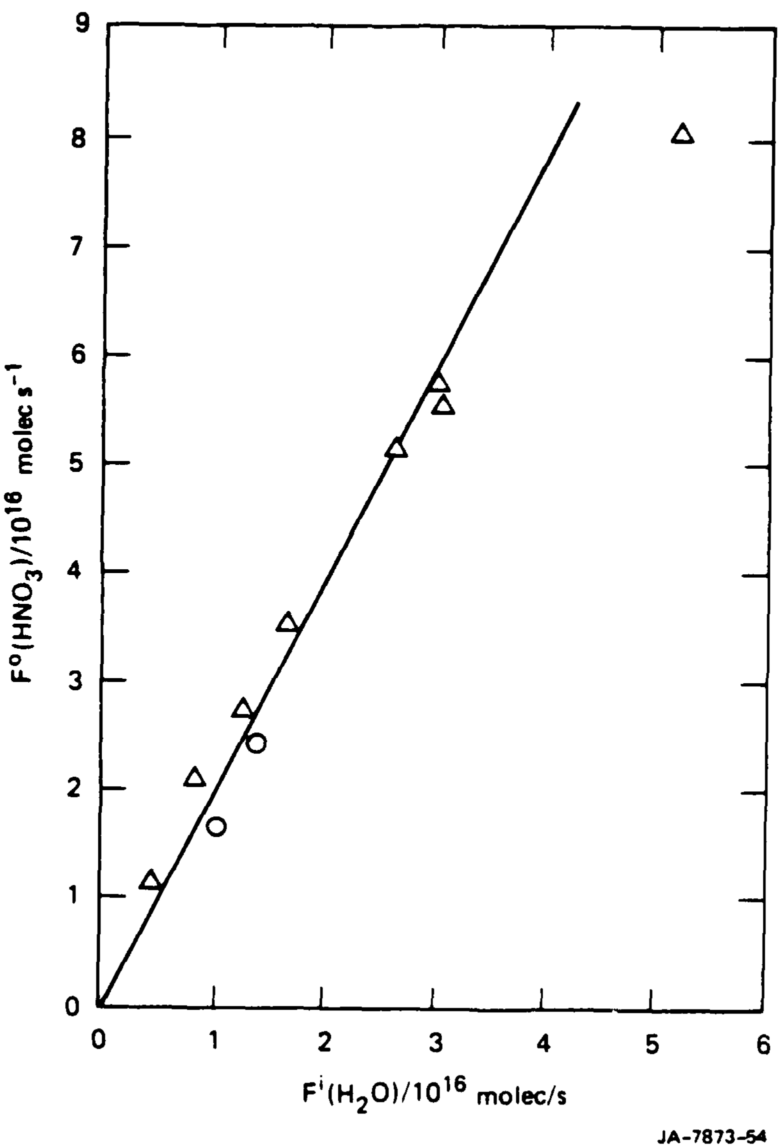

9
8
7
6
5
4
3
2
1
0
0
1
2
3
4
5
6
$F^o(HNO_3)/10^{16}$ molec s^{-1}
$F^i(H_2O)/10^{16}$ molec/s
JA-7873-54

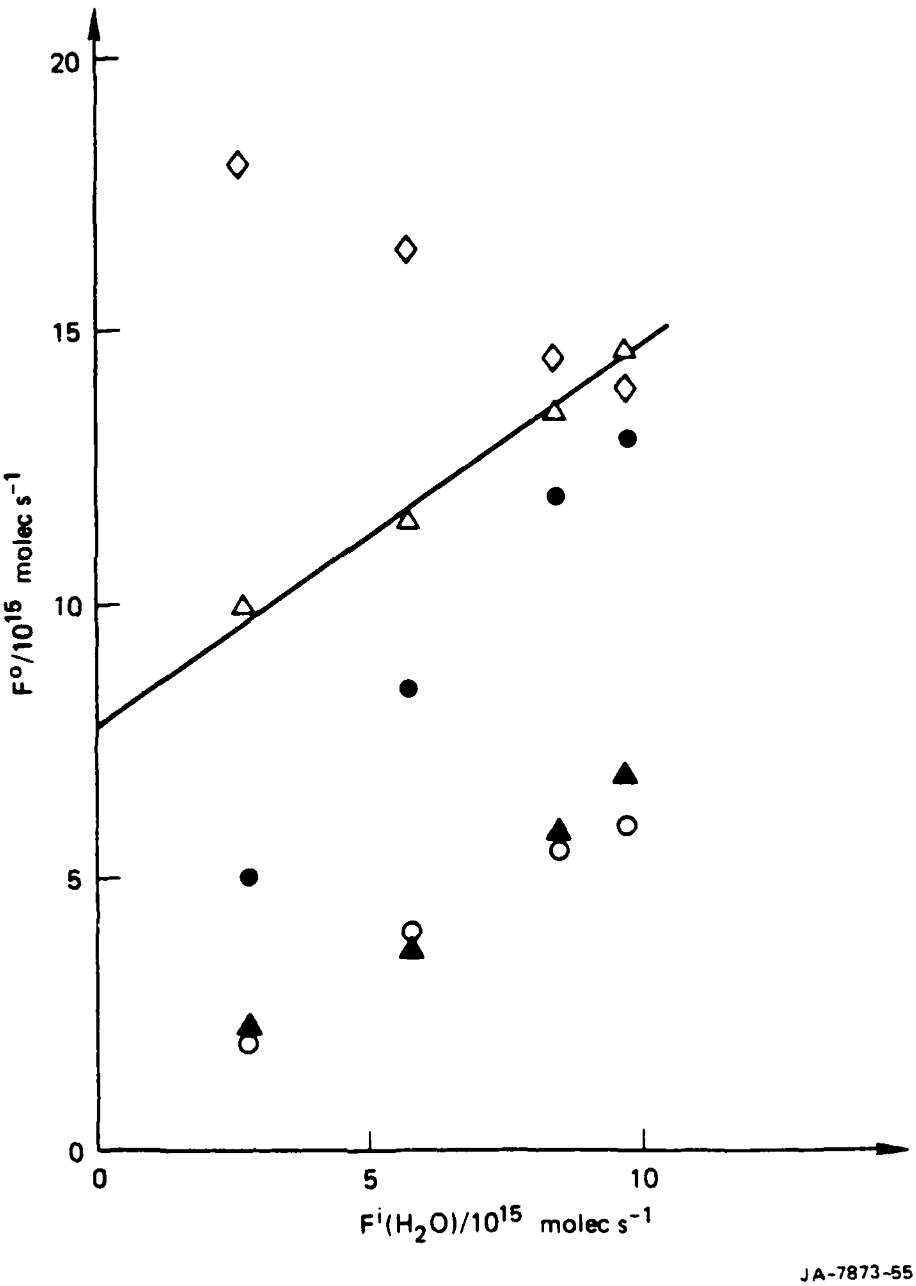

20
15
10
5
0
0
5
10
$F^o/10^{15}$ molec s^{-1}
$F^i(H_2O)/10^{15}$ molec s^{-1}
JA-7873-55

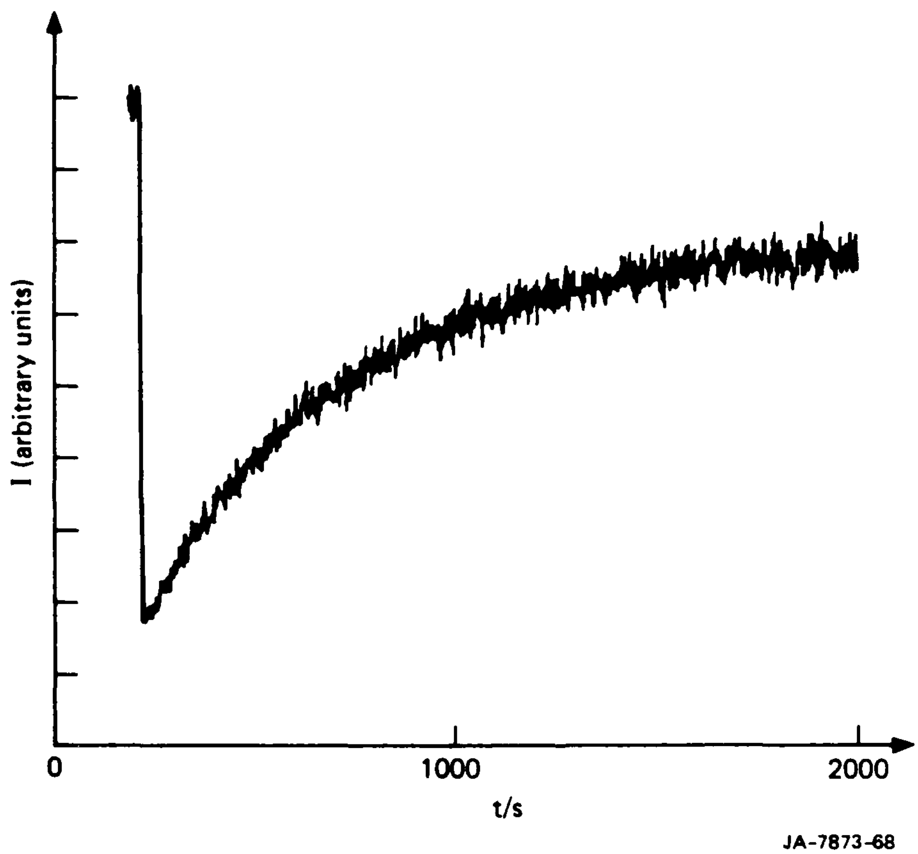
I (arbitrary units)
0
1000
2000
t/s
JA-7873-68

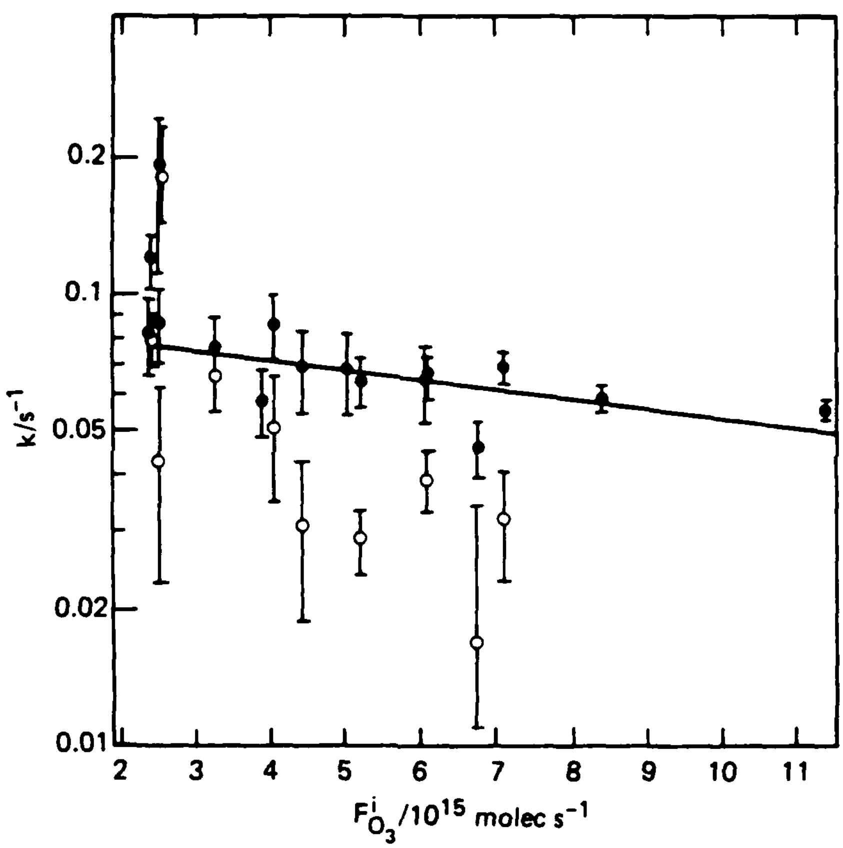

JA-7873-64

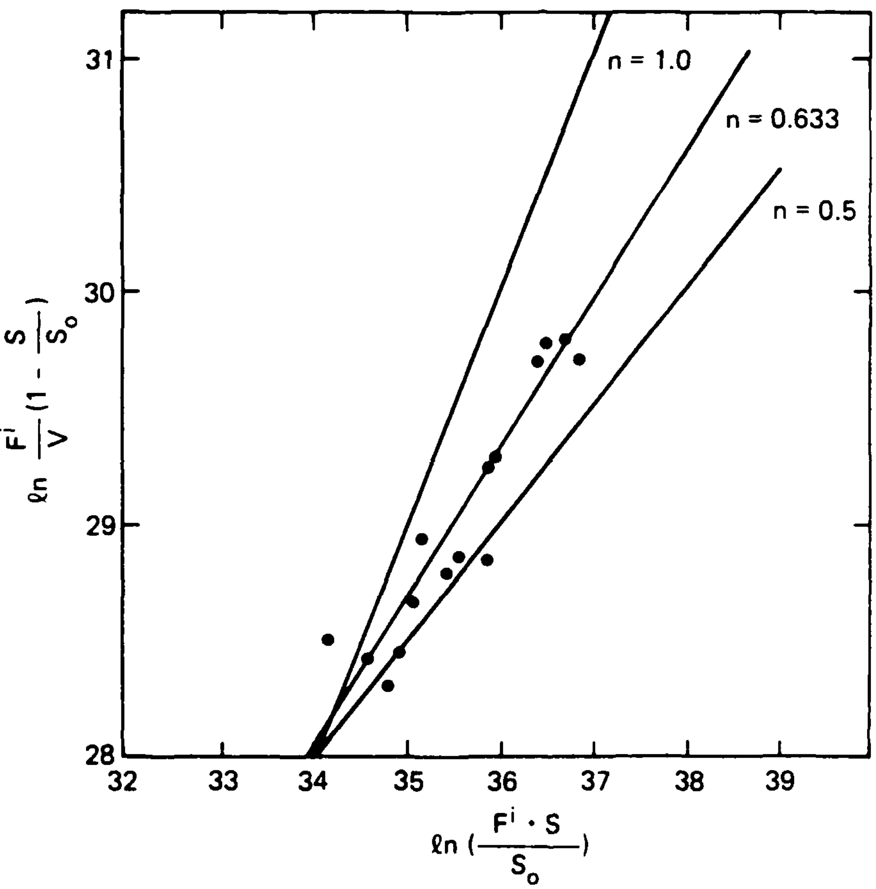

n = 1.0
n = 0.633
n = 0.5
31
30
29
28
32
33
34
35
36
37
38
39
$\ell n \frac{F^i}{V}(1 - \frac{S}{S_o})$
$\ell n (\frac{F^i \cdot S}{S_o})$

JA-7873-63

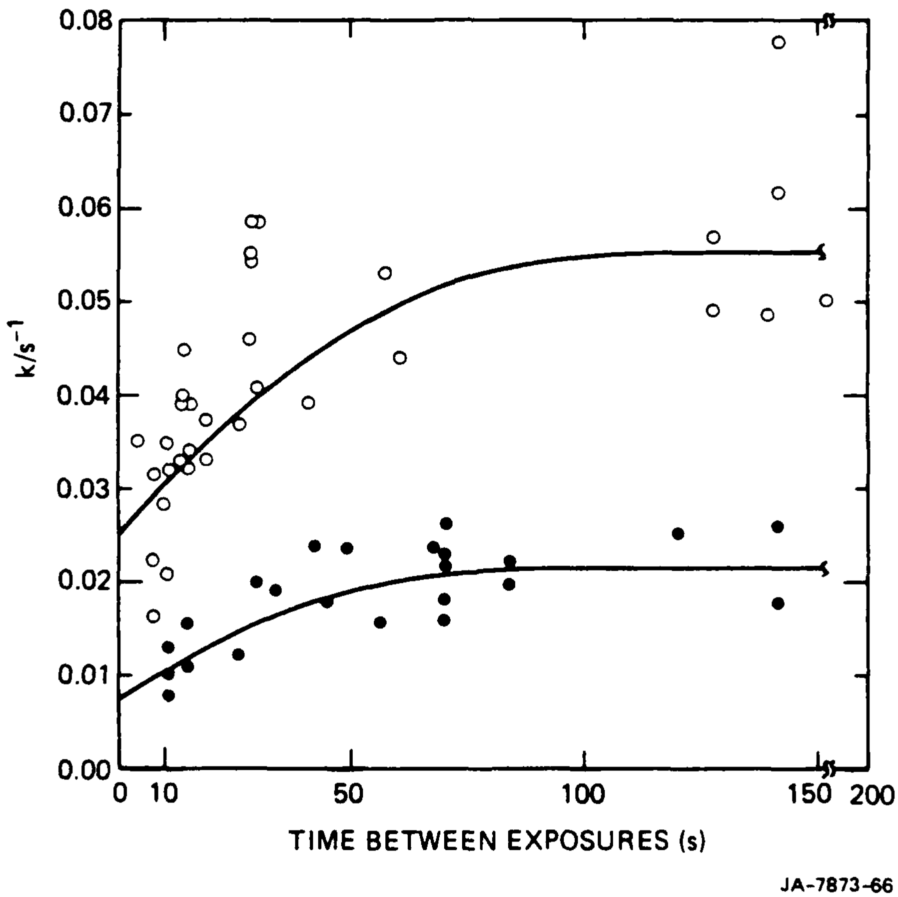

0.08
0.07
0.06
0.05
0.04
0.03
0.02
0.01
0.00
k/s^{-1}
0 10
50
100
150 200
TIME BETWEEN EXPOSURES (s)
JA-7873-66

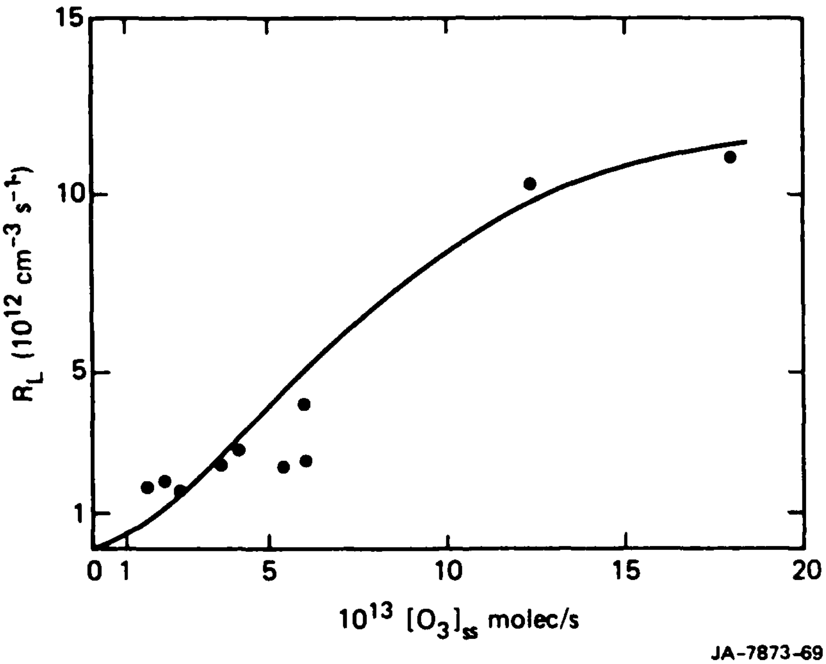
15
10
5
1
0
1
5
10
15
20
R_L (10^{12} cm^{-3} s^{-1})
10^{13} $[O_3]_{ss}$ molec/s
JA-7873-69

PROPOSED MODELING STUDIES ON REMOVAL BY CLOUD PROCESS OF MASSIVE EMISSIONS OF PARTICLES

In Young Lee

Atmospheric Physics Program
Environmental Research Division
Argonne National Laboratory, Argonne, IL 60439

ABSTRACT

In general, atmospheric aerosols originate by several processes: (1) condensation and sublimation of vapors and the formation of smokes in combustion, (2) reactions among trace gases, (3) mechanical disruption and dispersal of matter at the earth's surface as mineral dusts, and (4) coagulation of nuclei to produce larger particles of mixed constitution. The particles participate actively during cloud formation either as cloud condensation nuclei or ice-forming nuclei, or passively by being removed by cloud droplets and raindrops through processes of collision and coalescence. The evolution of dust and smoke particles is additionally controlled by dynamic processes such as transport, turbulent mixing and deposition. These natural processes of aerosol evolution would be greatly affected if extraordinary amounts of dust and smoke particles were injected into the atmosphere by blasts or large fires.

The scavenging efficiency for aerosols produced by blasts and fires can be examined in numerical simulations which describe coagulational processes involving aerosols, cloud droplets and raindrops. The investigation of the evolution

within clouds of dust and smoke particles of very high concentrations is important for clear understanding of the resulting global budget of aerosols and for better assessment of the potential climatic impact. The collision efficiency between particles can be formulated from a combination of theoretical analyses and available experimental data. A numerical module for wet removal can be used to evaluate scavenging efficiency, modification of cloud properties, and applicability of cloud microphysics parameterizations currently in use.

A cloud model originally developed at Argonne to study cloud microphysics parameterizations has been modified to examine the behavior of submicron aerosols in clouds. Lagrangian computations following a rising parcel of air were made in order to understand and identify mechanisms that control the fate of smoke and dust particles in clouds. The air parcel was assumed to be saturated initially and to contain aerosols of high number density ($1650\ cm^{-3}$). Some portion of the aerosols in the parcel could be activated to form cloud droplets and the rest could remain inactivated due mainly to the Kelvin effect. Thereafter, the spectrum was allowed to evolve and form raindrops. The model treated particle sizes ranging from 0.04 μm to 164 μm in radius.

Computations have been made for 40 min of simulated time. The spectral evolution and the role of each microphysical mechanism in the spectral evolution are presented in Figs. 1 and

2, respectively. Figure 1 shows that the spectrum evolves quickly during the first five minutes of cloud development due mainly to condensation, which affects the growth of particle sizes approximately up to the mode radius near 10 μm. The spectral evolution starts to produce raindrops, associated with sizes greater than about 50 μm in radius, after 10 min of simulated time. The submicron size particles are not removed or activated until simulated time exceeds 20 min, but thereafter they are quickly scavenged as the cloud starts to accumulate drops greater than about 100 μm in radius. In Fig. 2, we see clearly that the combined processes of condensation and coagulation can remove submicron particles much more effectively than either process alone. We also found that the removal of submicron particles is augumented if precipitation is included.

Figure 1. Number distributions of aerosols, cloud droplets and raindrops after various periods of simulation.

Figure 2. The role of cloud microphysical processes of condensation and coagulation in the spectral evolution of particles.

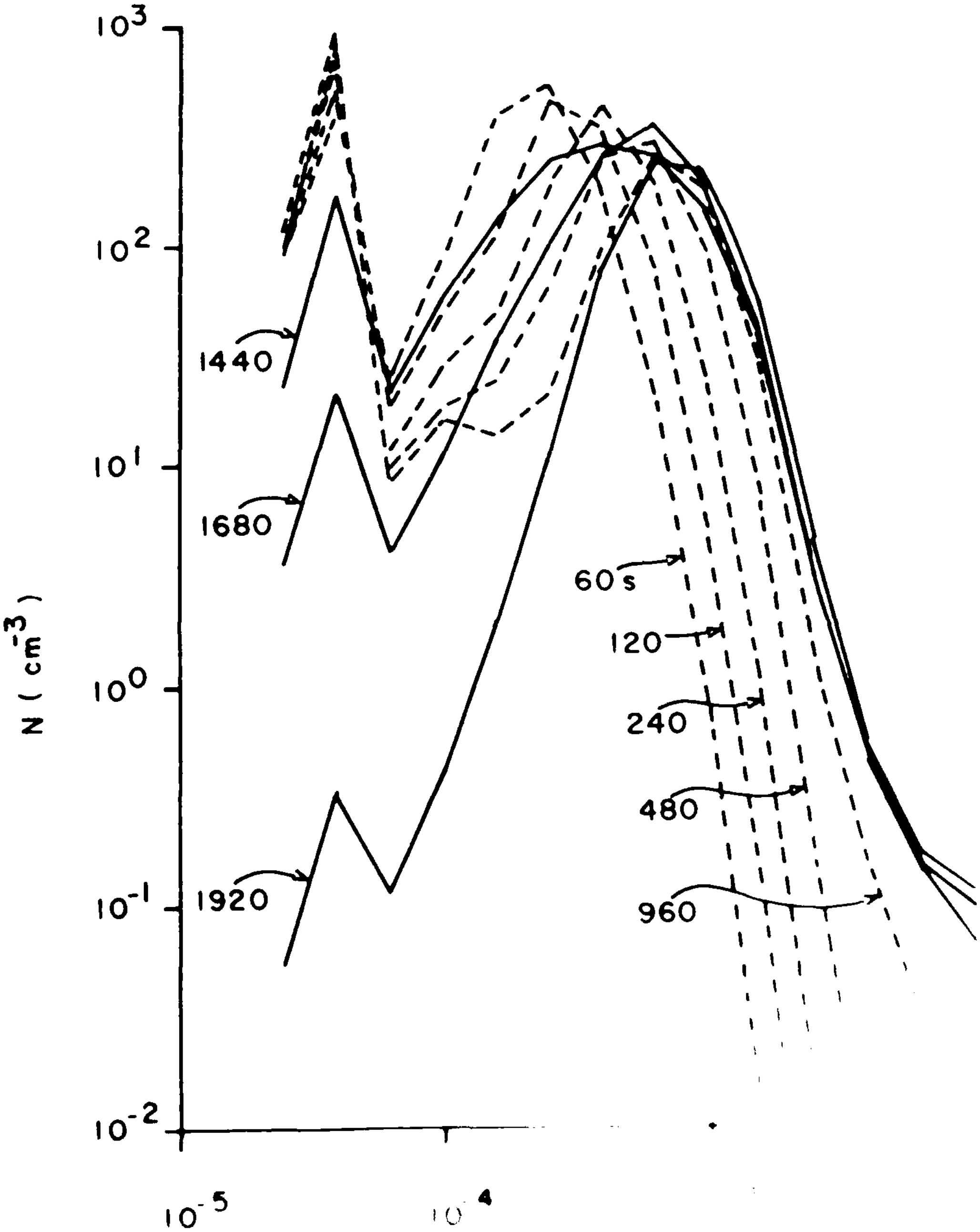

10^3
10^2
10^1
10^0
10^{-1}
10^{-2}
N (cm^{-3})
10^{-5}
10^{-4}
1440
1680
1920
60 s
120
240
480
960

AD-A185 150 TECHNICAL PAPERS PRESENTED AT THE DEFENSE NUCLEAR AGENCY GLOBAL EFFECTS R..(U) DOD NUCLEAR INFORMATION AND ANALYSIS CENTER SANTA BARBARA CA.. 15 MAY 86 2/4

UNCLASSIFIED DASIAC-TN-86-29-VOL-2 DNA001-82-C-0274 F/G 15/6.4 NL

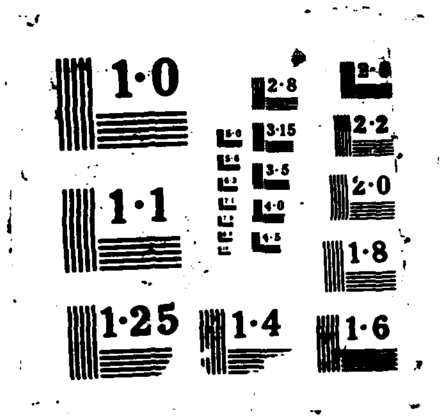
1·0
2·8
3·15
3·5
4·0
2·2
2·0
1·1
1·8
1·25
1·4
1·6

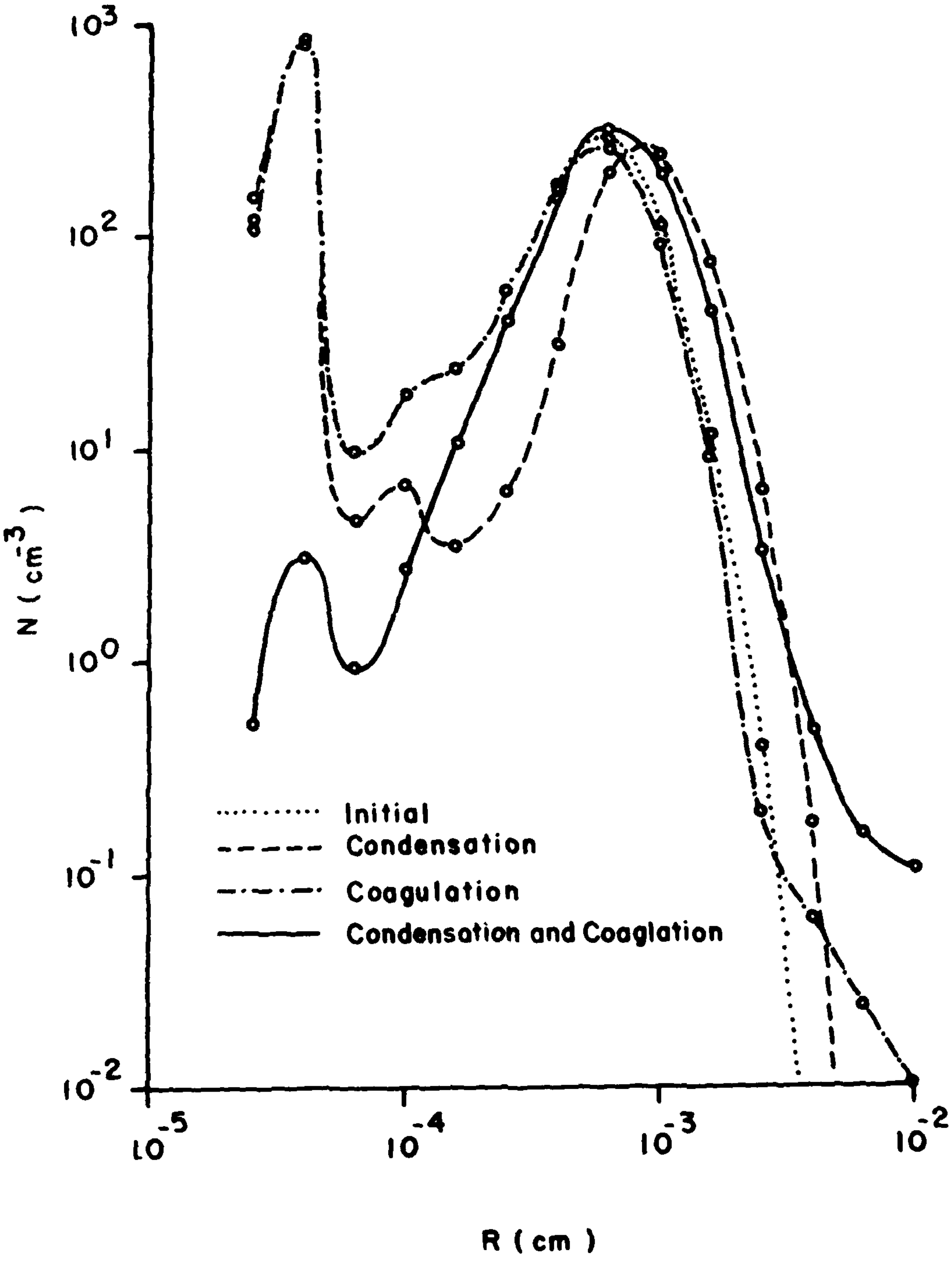

N (cm⁻³)
R (cm)
Initial
Condensation
Coagulation
Condensation and Coaglation

The University of Missouri-Rolla Cloud Simulation Chambers

Daniel R. White
Donald E. Hagan
John C. Carstens

Graduate Center for Cloud Physics Research
University of Missouri-Rolla

THE UMR CLOUD SIMULATION CHAMBERS

The UMR cloud simulation program is based on two cooled-wall expansion chambers designed to produce uniform cooling comparable to that produced in cloud updrafts. The smaller chamber, called Proto II, is currently producing cloud, and the larger--more sophisticated--Romulus chamber is scheduled for completion in the summer of 1985.

These chambers feature thermoelectric modules to cool the walls at the same rates as the expansion cools the gas. Thermal wall effects are thus effectively removed and a closed parcel thermodynamic environment similar to that found in the core of a convective cloud in the absence of turbulent mixing can be simulated.

After a sample of moist aerosol-laden air has been introduced into the chamber, the sensitive volume undergoes a controlled expansion which cools the gas and produces the increased relative humidity required for cloud formation. The chamber's initial condition can be set at any desired state of relative humidity less than 100%. The cooling capability is sufficient to allow ice nucleation and crystal growth studies to be carried out.

The creation of a viable cloud simulation program has necessitated developmental work on a broad front so that the required science and technology would come together to support the experimental effort at about the same time. Much of this effort has gone into the development of the following peripheral and supporting equipment:

1. Air preconditioning system for drying and filtering large volumes of air (see Fig. A2) for flushing the chamber and for use by aerosol generation equipment.
2. Precision saturator columns and thermal regulation columns for relative humidity (see Fig. A3).
3. A variety of aerosol generation techniques have been developed for the production of artificial nuclei. Much effort has gone into characterizing aerosols and rendering them monodispersed. Natural nuclei can be employed.
4. Precision continuous flow thermal diffusion chamber (CFDs) for characterizing the critical activation supersaturation spectrum of the condensation nuclei have been developed. Three vertical plate CFDs are currently operational. Three vertical plate CFDs are currently under construction. These will operate simultaneously, two in the CFD mode and one in the isothermal mode, to cover the entire CCN spectrum with high resolution and will provide automatic data acuisition in a format for immediate assimilation by the simulation chamber minicomputer system to aid in establishing last minute parameters for experiment control.
5. Optical and electrical aerosol characterization equipment for measuring the size distribution of both wet and dry aerosol particles. A GE CNC counter and a UMR Aitken nucleus counter are also available for mesuring total particle concentrations and sensing the Aitken nuclei content of sample air. This makes possible scavenging experiments.

6. Laser light scattering equipment enables one to determine the Mie scattering intensity at one angle. The total attenuation of a light beam (from a light emitting diode operating at a different wavelength from the argon ion laser) is also measured with a precision of three parts in 10^4. A photograph is also taken with flash illumination in order to verify the droplet concentration at specified intervals. These optical systems are described in more detail in Appendix C.

7. The digital data acquisition and control system is built around a NOVA 840 and a NOVA 3 minicomputer. When both are operational, a greater real time computational capacity is available for experiments. State-of-the-art techniques are employed extensively through the system, particularly in the measurement and control of temperature and pressure.

8. A wide variety of simulation chamber control options have been developed. These can be readily configured to best suit the demands of individual experiments. It is possible to run various microphysical models in real time on one of the minicomputers and use the output in the control of the chamber or to compare with the output of the various optical sensors. In this area we envision a continuous evolution of capability as new experiments are developed.

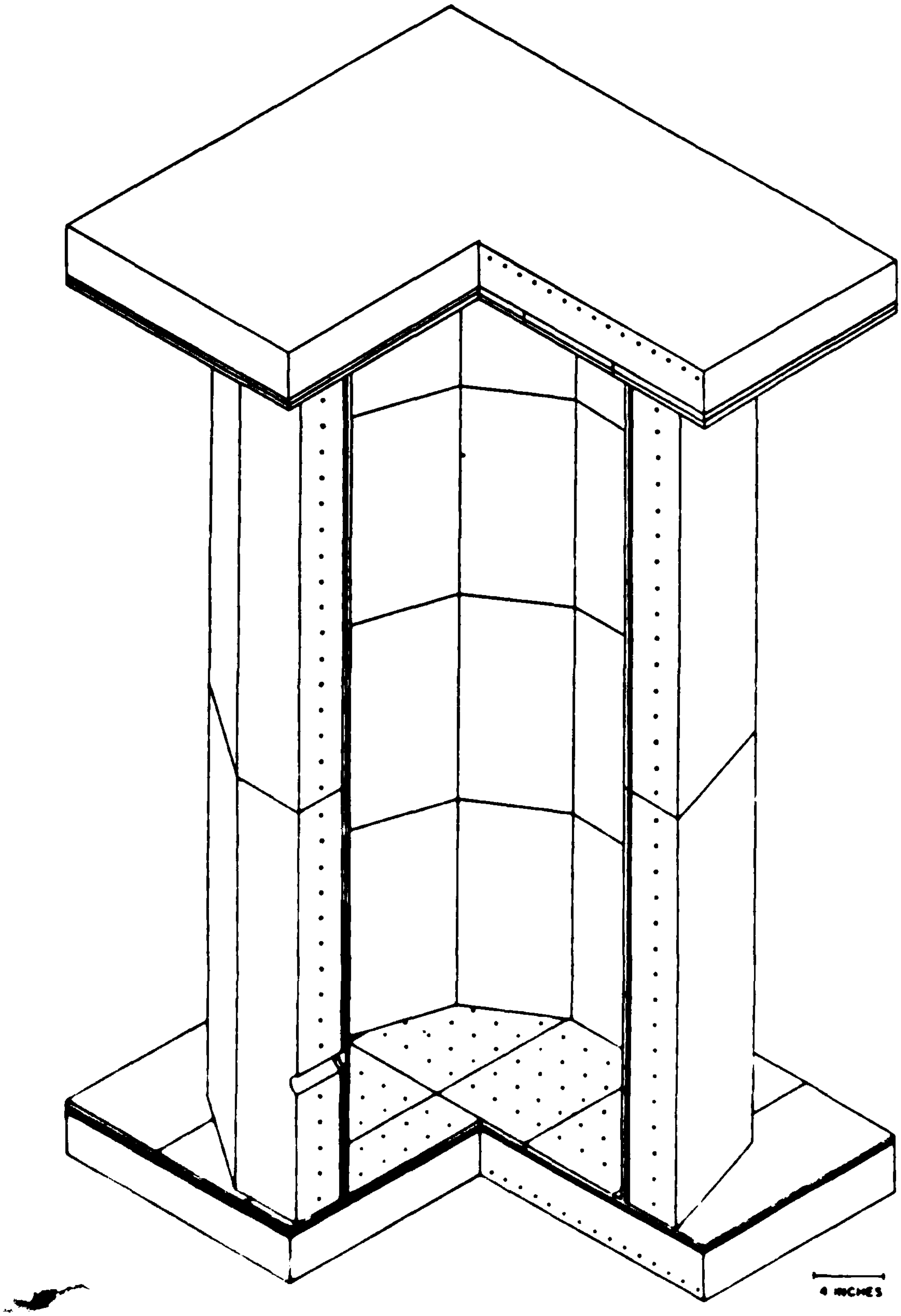

Fig. A1 Prot[illegible] Cloud Simulation Chamber

UMR CLOUD SIMULATION FACILITY

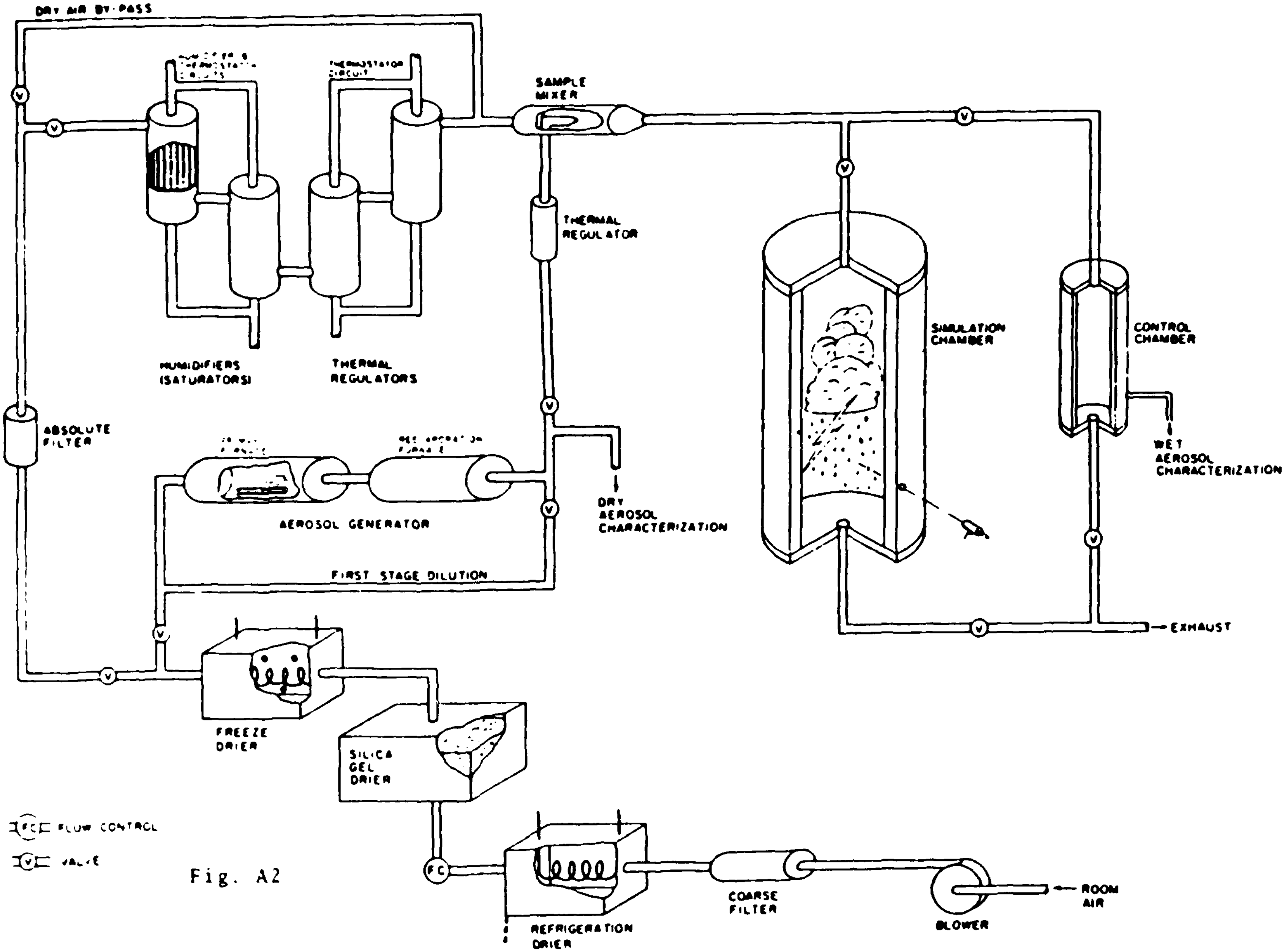

Fig. A2

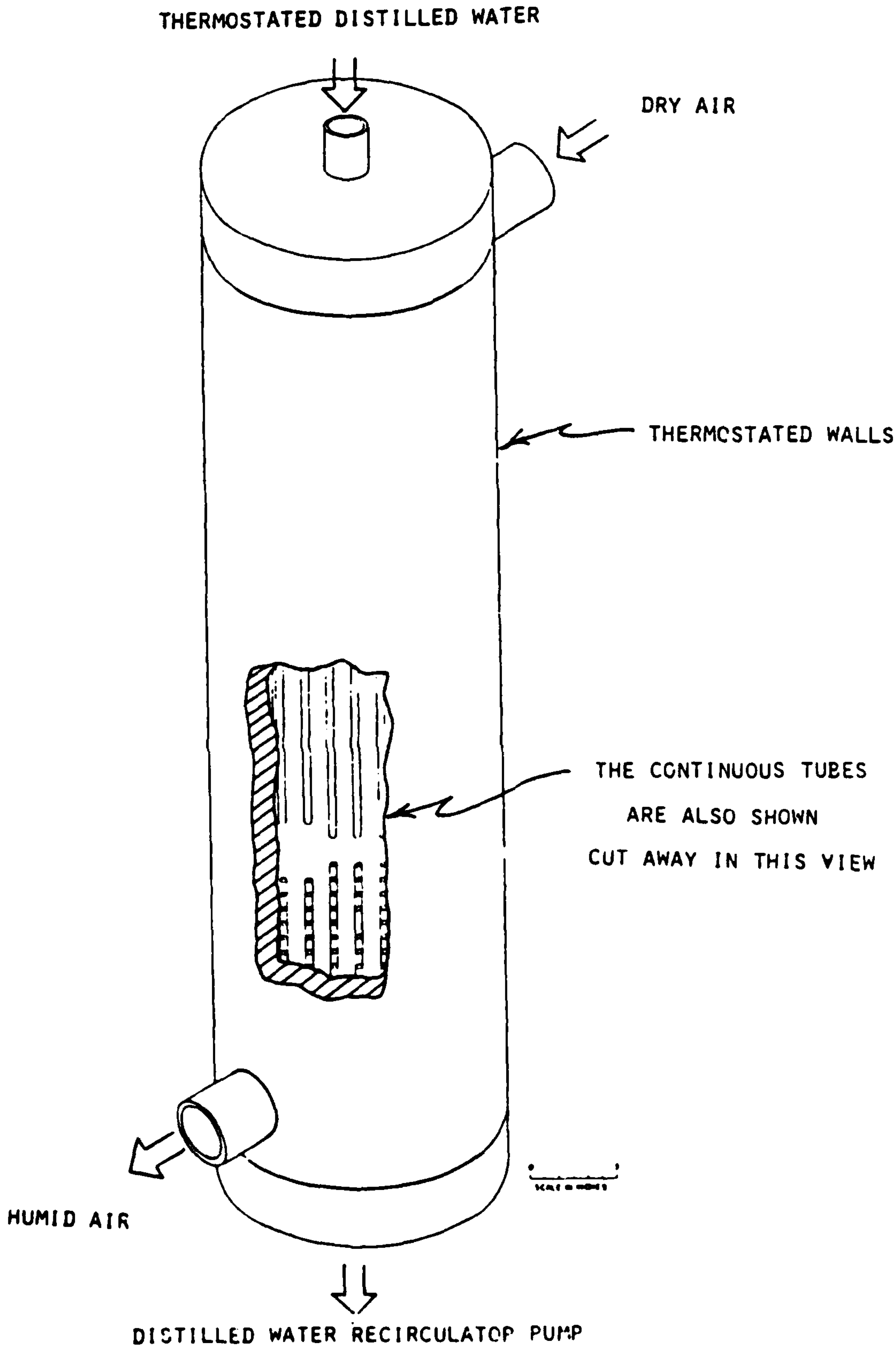

Fig. A3 Humidifier

TABLE I
PROTO II CHAMBER SPECIFICATIONS

Temperature		Prototype Chamber
Range		40° to -40°C
Control		
Holding:	At fixed temperature RMS deviation from spatial average, 40 sensors	0.030°C
Cooling Mode:	Maximum rate, at least	10°C/min.
	Wall temperature lag from control point	0.01°C/(°C/min.)*
	RMS deviation from spatial average	0.080°C @ 6°C/min. 0.040°C @ 3°C/min.
Wall Measurement Precision		±0.002°C
Pressure		
Reference pressure absolute accuracy		±0.01%, dead weight pressure gauge
Dynamic sensor range		0 to 100 Torr differential
Resolution		±0.05 Torr
Control:		
Holding:	Standard deviation (time)	0.5 Torr
Expansion:	Maximum rate	3.9 Torr/sec 12 (C/min. wet adiabatic)
Offset from command valve		0.5 Torr
Standard deviation with (time)		0.36 Torr
Wall Cooling Method		Thermoelectric modules plus fluid heat exchange in heat sink
Volume		48 cm dia x 61 cm ht OR 48 cm dia x 122 cm ht

*Cooling Rate

SECTION 2

PLUME DYNAMICS AND CLOUD PHYSICS

Scavenging of submicron aerosols by clouds.

R.F.Pueschel, NASA Ames Research Center, Moffett Field, CA 94040.

Scavenging by clouds and precipitation is the most effective mechanism by which aerosols are removed from the atmosphere. Data on the relationships between aerosol and cloud spectra and concentrations before, during and after cloud formation show the extent and time scales with which the aerosol-cloud interaction occurs. Specifically, the following results will be discussed:

(1) The accumulation mode, the longest lived portion of the atmospheric aerosol, provides the cloud condensation nuclei around which drops form. Particles as small as 0.1 um diameter are ingested into cloud drops during the cloud's formation; the nucleation scavenging of submicron particles is the more efficient the larger their size.

(2) In polluted airmasses, there are more submicron particles removed from the aerosol than there are cloud drops formed. This is different from clean air situations where a 1:1 relationship between the loss of submicron particles and the formation of cloud drops exists. Thus, in polluted air a mechanism in addition to nucleation scavenging has to be invoked to account for the aerosol losses. Stephan flow, a hydrodynamical movement of a vapor-gas mixture normal to the surface of a condensing liquid, to compensate for gas diffusion away from the surface, is a possible explanation.

(3) Nucleation scavenging during cloud formation is 180 times faster than is in-cloud attachement of the residual aerosol after the cloud has formed.

THE ROLE OF BUOYANCY INDUCED TURBULENCE IN SCAVENGING PARTICULATES FROM LARGE SCALE FIRES

R. B. Edelman

Science Applications International Corporation

Combustion Science and Advanced Technology Department

Chatsworth, CA 91311

Presented at the Global Effects Program Technical Meeting,

February 25 – 27, 1986

NASA – Ames Research Center

Moffet Field, CA

TOPICS

- Area of Interest
- Problem Definition
- Objective
- Method of Approach
- Summary

AREA OF INTEREST

- Uncertainty in Predicting Amount and Structure of Soot and other Particulates Reaching High Altitudes
- Scavenging and Coagulation can have a Strong Effect

PROBLEM DEFINITION

- Local Plume Properties are Required
- Spatial and Temporal Variations in Temperature, Concentration and Velocity are Important in Plume Flow Fields
- Properties Depend upon Mixing Rates which, in Turn, Depend Upon Buoyancy–Induced Turbulence and Entrainment Rates

SAIC

OBJECTIVES

- To Describe Local Properties in the Near and Intermediate Plume Flow Fields with Emphasis on Buoyancy – Induced Turbulence and Entrainment Processes

Science Applications International Corporation

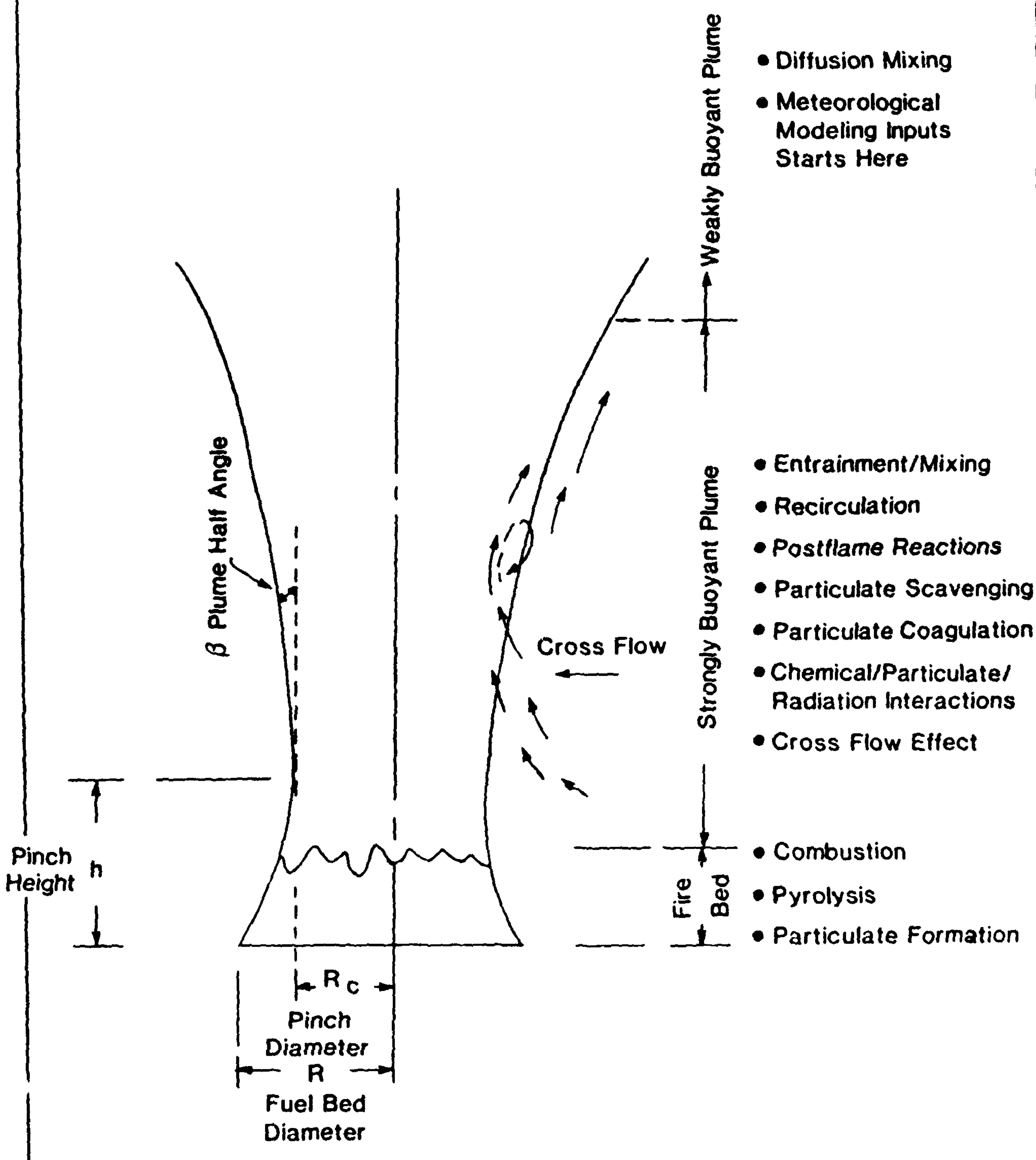

Single Plume Characteristic Regions

SAIC

Science Applications International Corporation

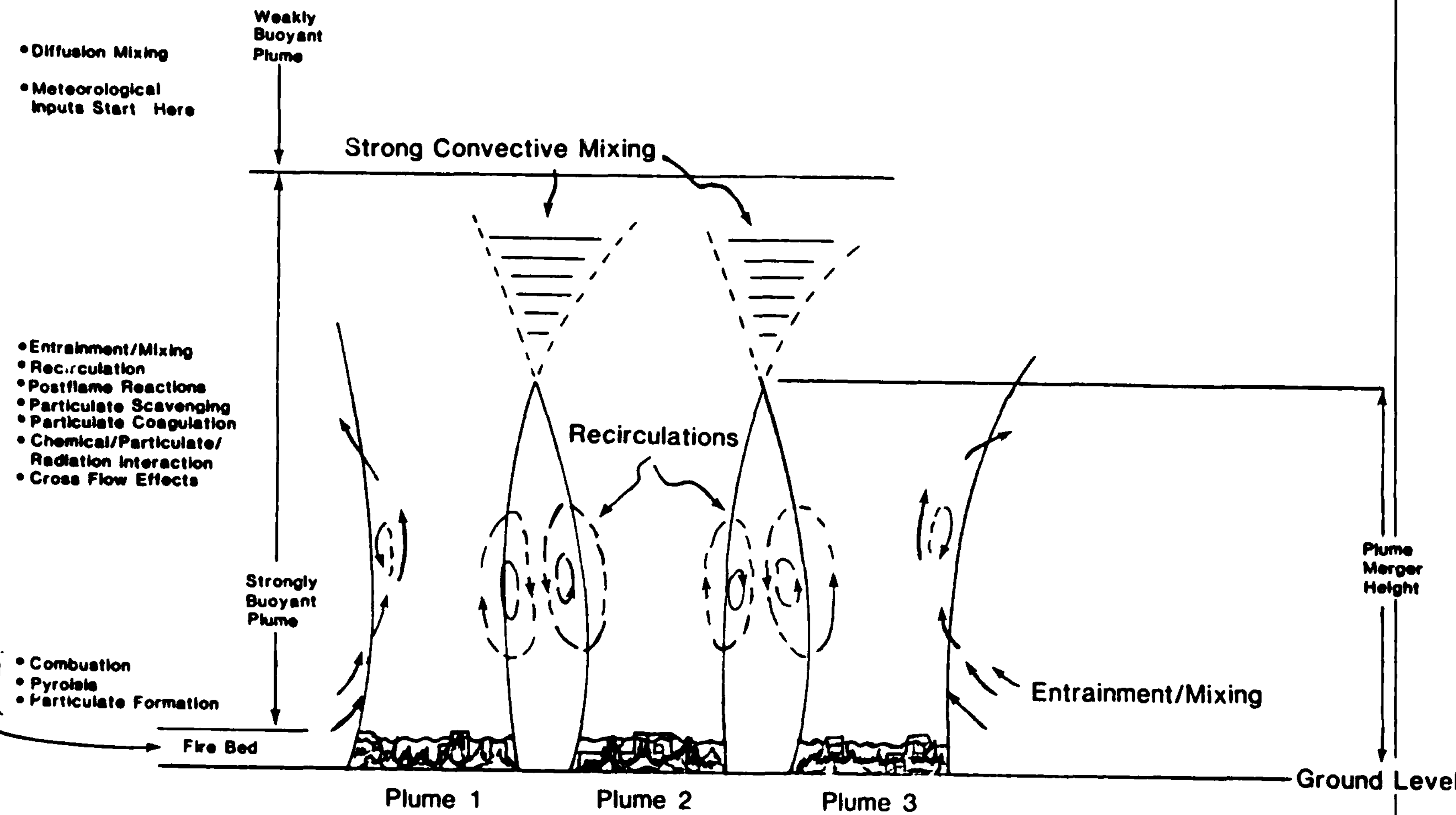

Interacting Plume Phenomena.

SUMMARY OF OBSERVATIONS

- Complex Interplay of Time Dependent Entrainment and Mixing Processes
- Combustion Completion and Secondary Rate Processes are Relatively Slow and therefore are Non – Equilibrium Processes
- Mass Fire is Likely Comprised of Small Multiple Fire Plumes Interacting with One Another, Merging to Form a Single Large Scale Plume

SAIC

METHOD OF APPROACH

- Single Plume Modeling
  - Axisymmetric
  - Steady
  - Transient
- Multiple Plume Modeling
  - 3-D
  - Steady
  - Transient
- Plume Structure
  - Local Properties
  - Scaling

PRELIMINARY RESULTS ON TURBULENT PLUMES

- Buoyancy Induced Mean Flow Acceleration
- Buoyancy Induced Turbulence

BUOYANCY GENERATED TURBULENCE

$$\underbrace{\frac{\partial k}{\partial t}}_{\substack{\text{rate}\\ \text{of}\\ \text{change}}} + \underbrace{U_j \frac{\partial k}{\partial x_j}}_{\text{convection}} = \underbrace{- \frac{\partial}{\partial x_j} \left[\overline{u_j \left(\frac{u_i u_i}{2} + \frac{p}{\rho} \right)} - \nu \frac{\partial k}{\partial x_j} \right]}_{\text{diffusive transport}}$$

$$\underbrace{- \overline{u_i u_j} \frac{\partial U_i}{\partial x_j}}_{\substack{\text{production}\\ \text{by shear}}} \qquad \underbrace{- \beta g_i \overline{u_i T'}}_{\substack{\text{production}\\ \text{by buoyancy}\\ \text{forces}}} \qquad \underbrace{- \nu \overline{\frac{\partial u_i}{\partial x_j} \frac{\partial u_i}{\partial x_j}}}_{\text{dissipation}}$$

where,

$$k = \frac{1}{2} \overline{u_i u_i}$$

SAIC

Science Applications International Corporation

k−ε−q *TURBULENCE MODEL*

1. TURBULENT KINETIC ENERGY

$$\rho u \frac{\partial k}{\partial x} + \rho v \frac{\partial k}{\partial r} = \frac{1}{r}\frac{\partial}{\partial r}\left(\frac{r\mu_T}{Pr_k}\frac{\partial k}{\partial r}\right) + \mu_T\left(\frac{\partial u}{\partial r}\right)^2 - \rho\varepsilon + \rho g\frac{\beta}{2}(qk)^{\frac{1}{2}}$$

2. TKE DISSIPATION RATE

$$\rho u \frac{\partial \varepsilon}{\partial x} + \rho v \frac{\partial \varepsilon}{\partial r} = \frac{1}{r}\frac{\partial}{\partial r}\left(r\frac{\mu_T}{Pr_\varepsilon}\frac{\partial \varepsilon}{\partial r}\right) + 1.44\frac{\varepsilon}{k}\mu_T\left(\frac{\partial k}{\partial r}\right)^2 - 1.92\frac{\rho\varepsilon^2}{k} + \rho g\beta\varepsilon\left(\frac{q}{k}\right)^{\frac{1}{2}}$$

3. TEMPERATURE $[q \equiv (T'^2)^{1/2}]$

$$\rho u \frac{\partial q}{\partial x} + \rho v \frac{\partial q}{\partial r} = \frac{1}{r}\frac{\partial}{\partial r}\left(r\frac{\mu_T}{Pr_q}\frac{\partial q}{\partial r}\right) + 2.7\,\mu_T\left(\frac{\partial T}{\partial r}\right)^2 - 1.8\,\frac{\rho\varepsilon}{k}q - 2k\left(\frac{\partial q^{\frac{1}{2}}}{\partial r}\right)^2$$

$Pr_k = 0.6$

$Pr = 0.6$

$Pr_q = 0.7$

$\mu_T = 0.09\,\rho\frac{k^2}{\varepsilon}$

SAIC

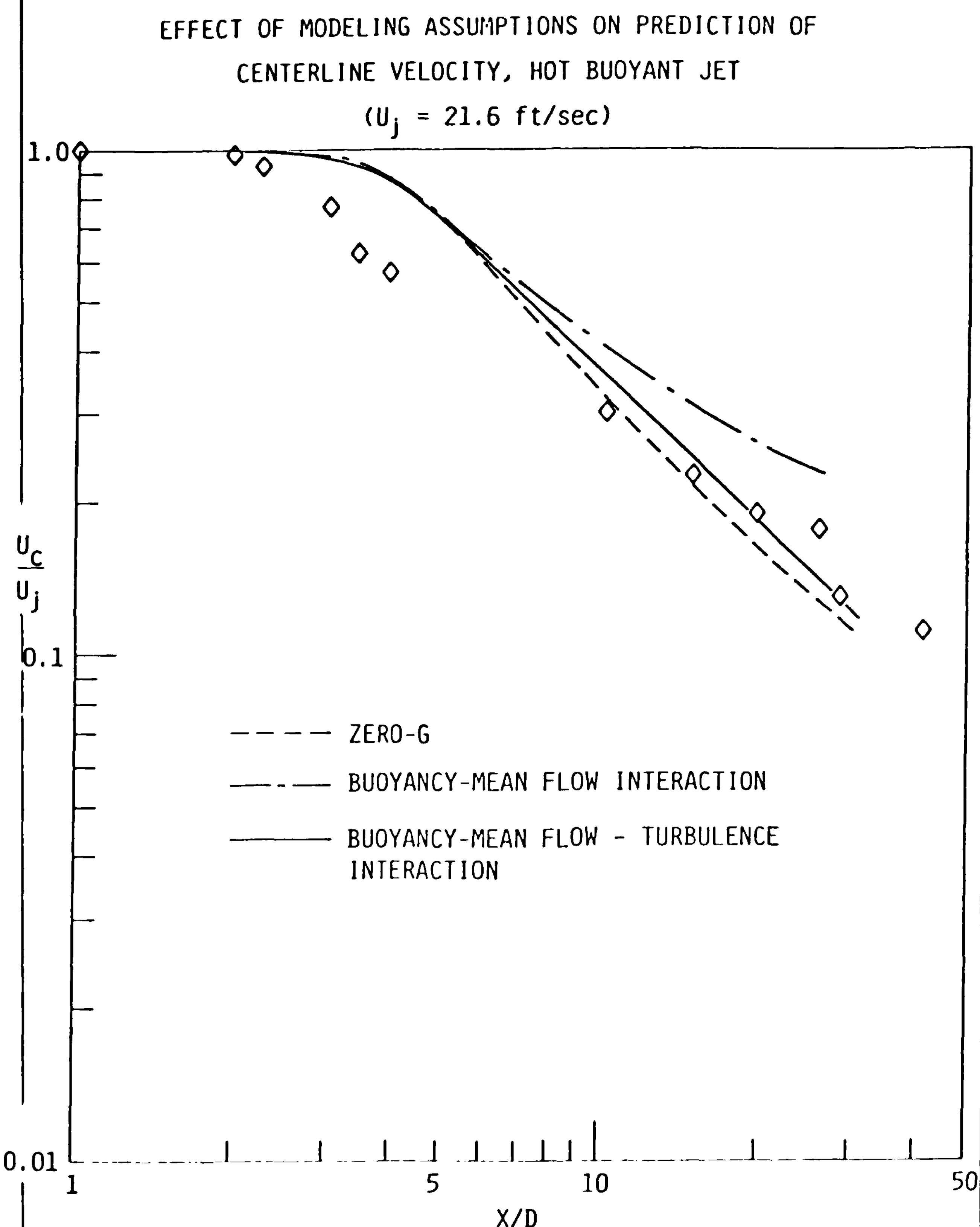
EFFECT OF MODELING ASSUMPTIONS ON PREDICTION OF
CENTERLINE VELOCITY, HOT BUOYANT JET
(U_j = 21.6 ft/sec)
1.0
0.1
0.01
$\frac{U_c}{U_j}$
1
5
10
50
X/D
ZERO-G
BUOYANCY-MEAN FLOW INTERACTION
BUOYANCY-MEAN FLOW - TURBULENCE INTERACTION

EFFECT OF MODELING ASSUMPTIONS ON PREDICTION OF CENTERLINE TEMPERATURE, HOT BUOYANT JET (U_j = 21.6 ft/sec)

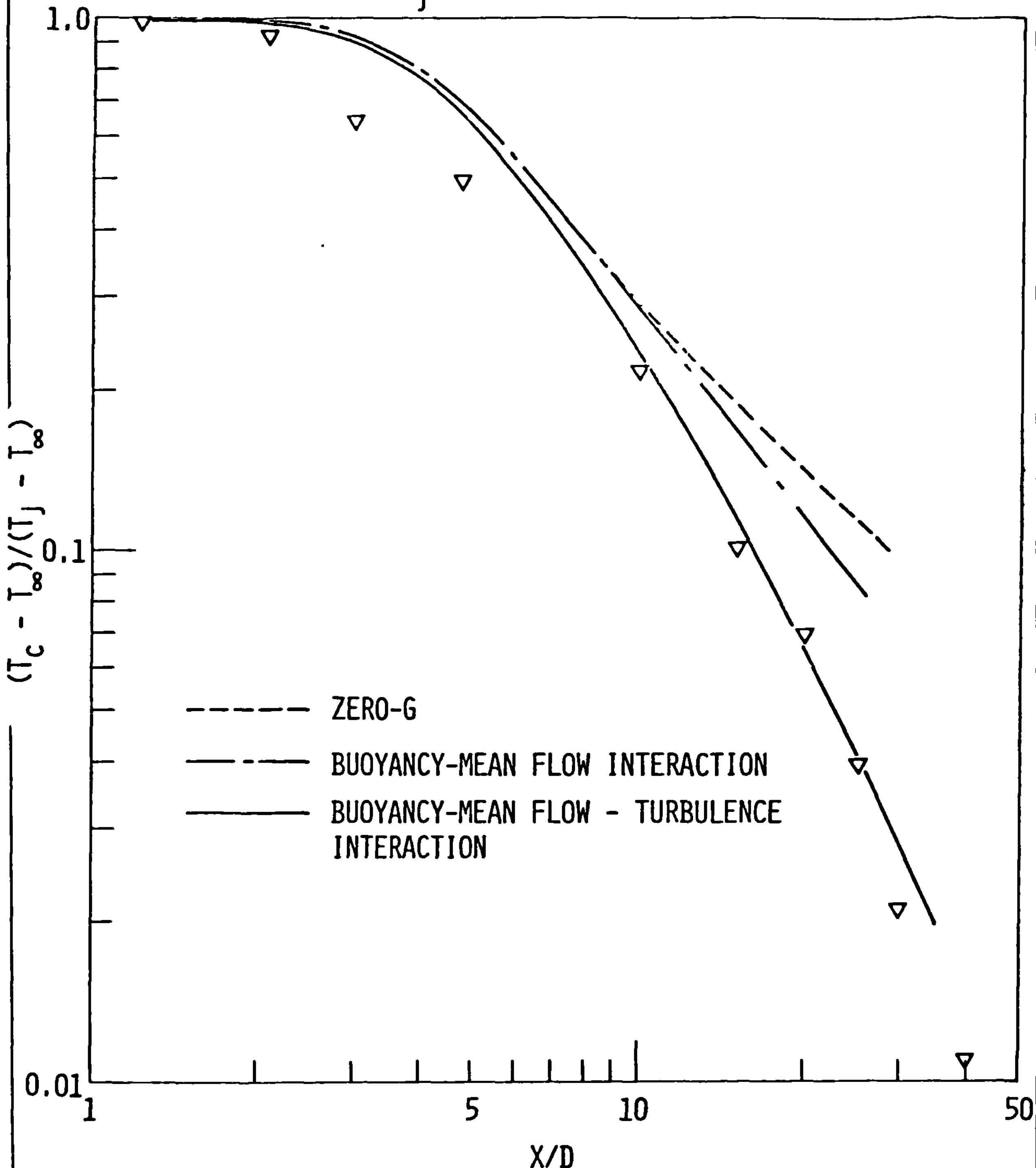

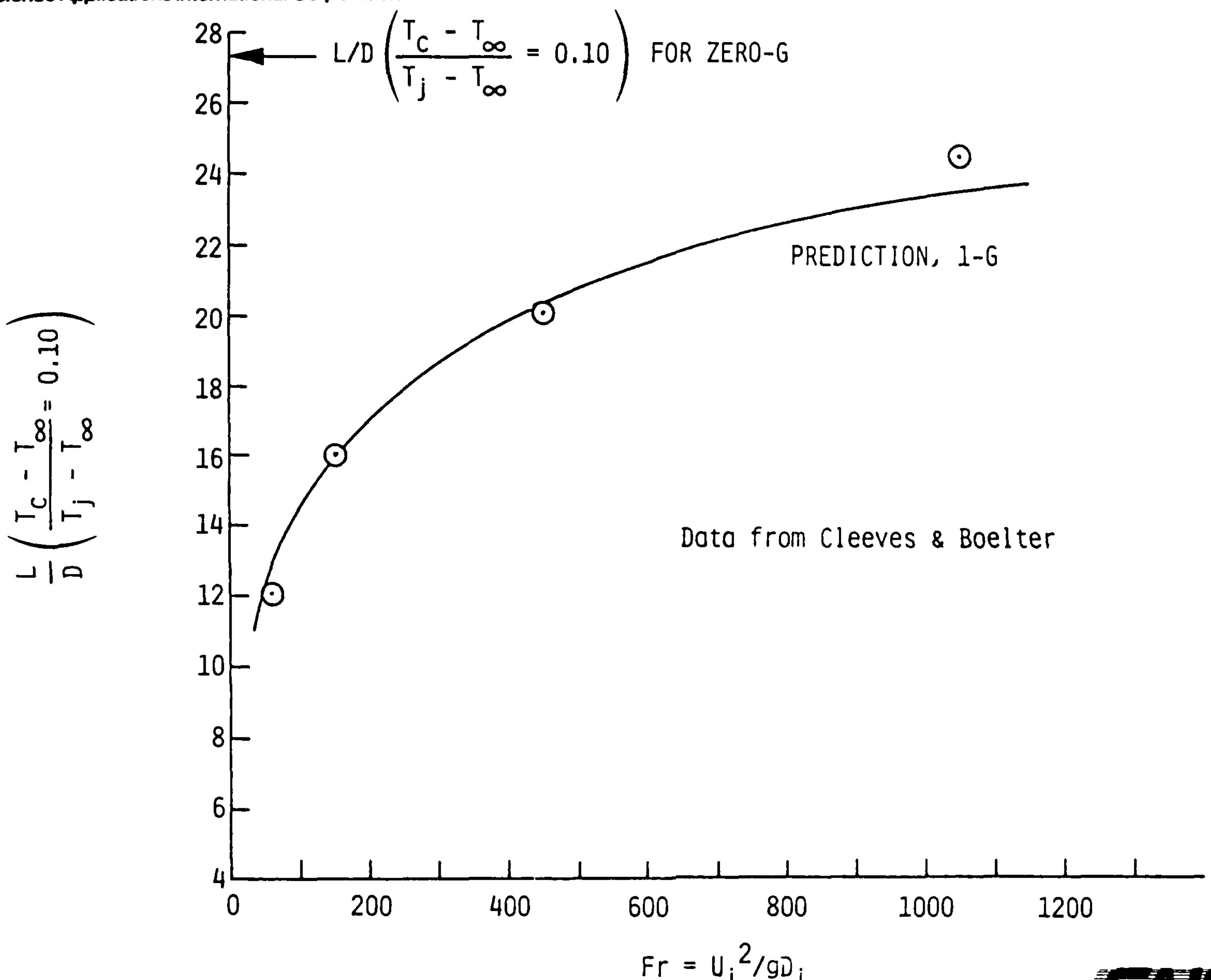

$L/D \left(\frac{T_c - T_\infty}{T_j - T_\infty} = 0.10 \right)$ FOR ZERO-G
PREDICTION, 1-G
Data from Cleeves & Boelter
$\frac{L}{D} \left(\frac{T_c - T_8}{T_j - T_8} = 0.10 \right)$
$Fr = U_j^2/gD_j$
28
26
24
22
20
18
16
14
12
10
8
6
4
0
200
400
600
800
1000
1200

COMPARISON OF PREDICTED AND MEASURED
BUOYANT PLUME LENGTHS

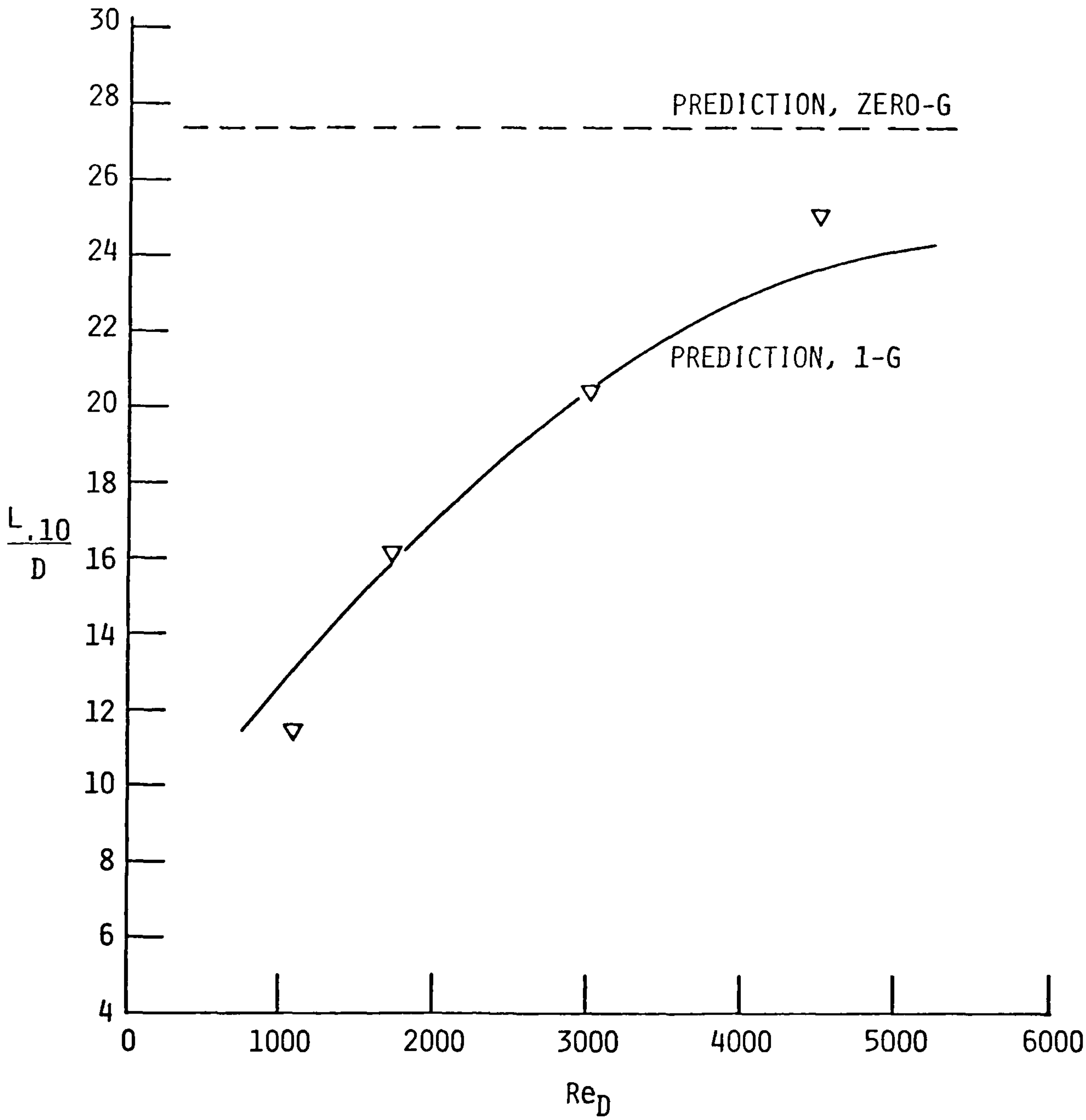

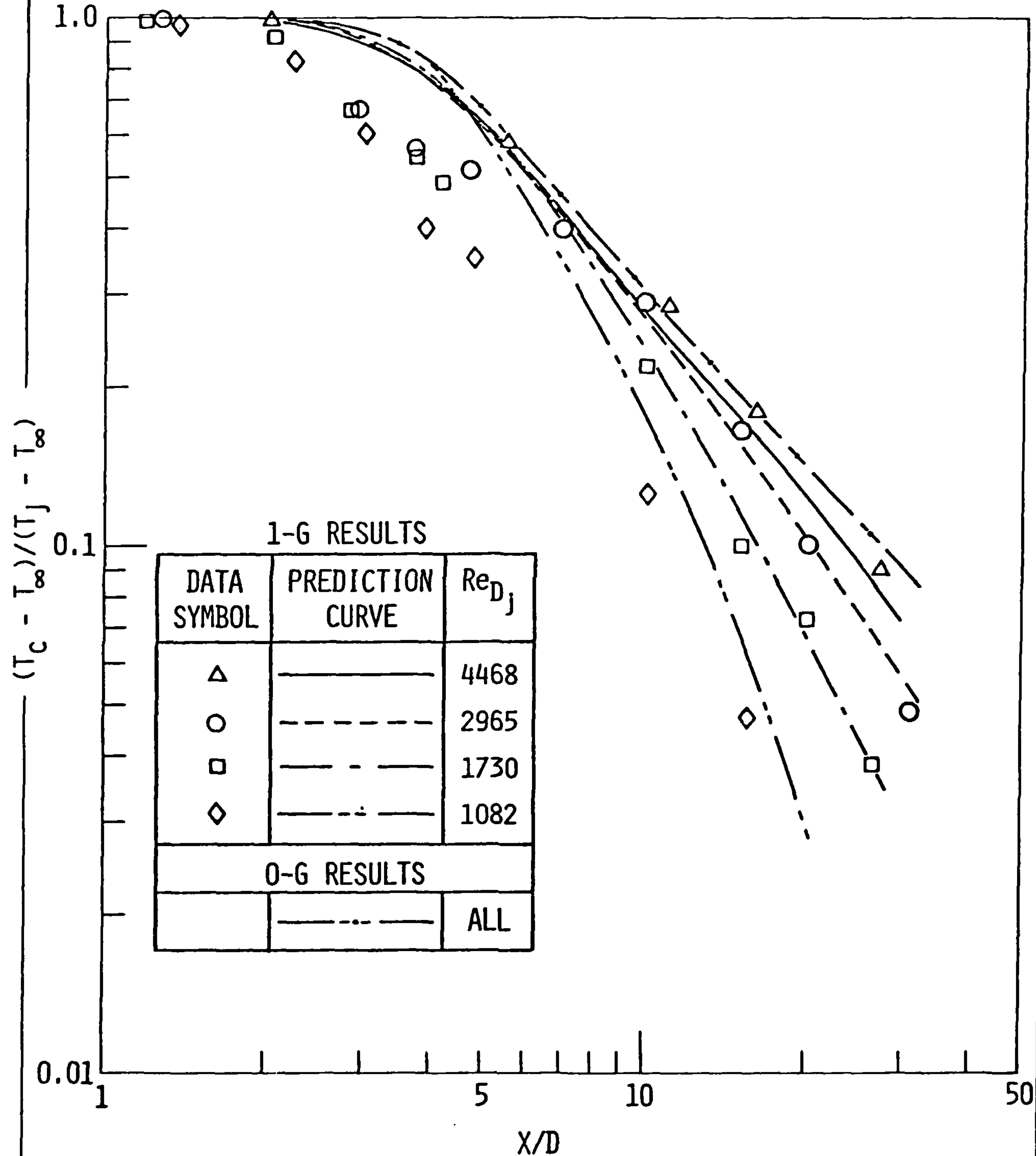
1.0
0.1
0.01
$(T_c - T_8)/(T_j - T_8)$
1
5
10
50
X/D
1-G RESULTS
DATA SYMBOL
PREDICTION CURVE
Re_{D_j}
4468
2965
1730
1082
0-G RESULTS
ALL

SUMMARY OF REQUIREMENTS

- Modeling
  - Application of Existing Multidimensional Analyses and Computer Codes Developed through the Incorporation of Appropriate Buoyancy–Induced Turbulence and Entrainment Submodels
    - Axisymmetric
    - 3–D
    - Chemical and Physical Processes
- Data
  - Laboratory Scales (cms)
  - Intermediate Scale (meters)
  - Large Scale (up to 100 meter)
- Various Programs of Differing Levels can be Defined to Address
  - Scaling
  - Multiple Plume Interactions
  - Fuel Effects

SAIC

On the Scavenging of Aerosol Particles by Snow Crystals

Pao K. Wang
Department of Meteorology
University of Wisconsin
Madison, WI 53706

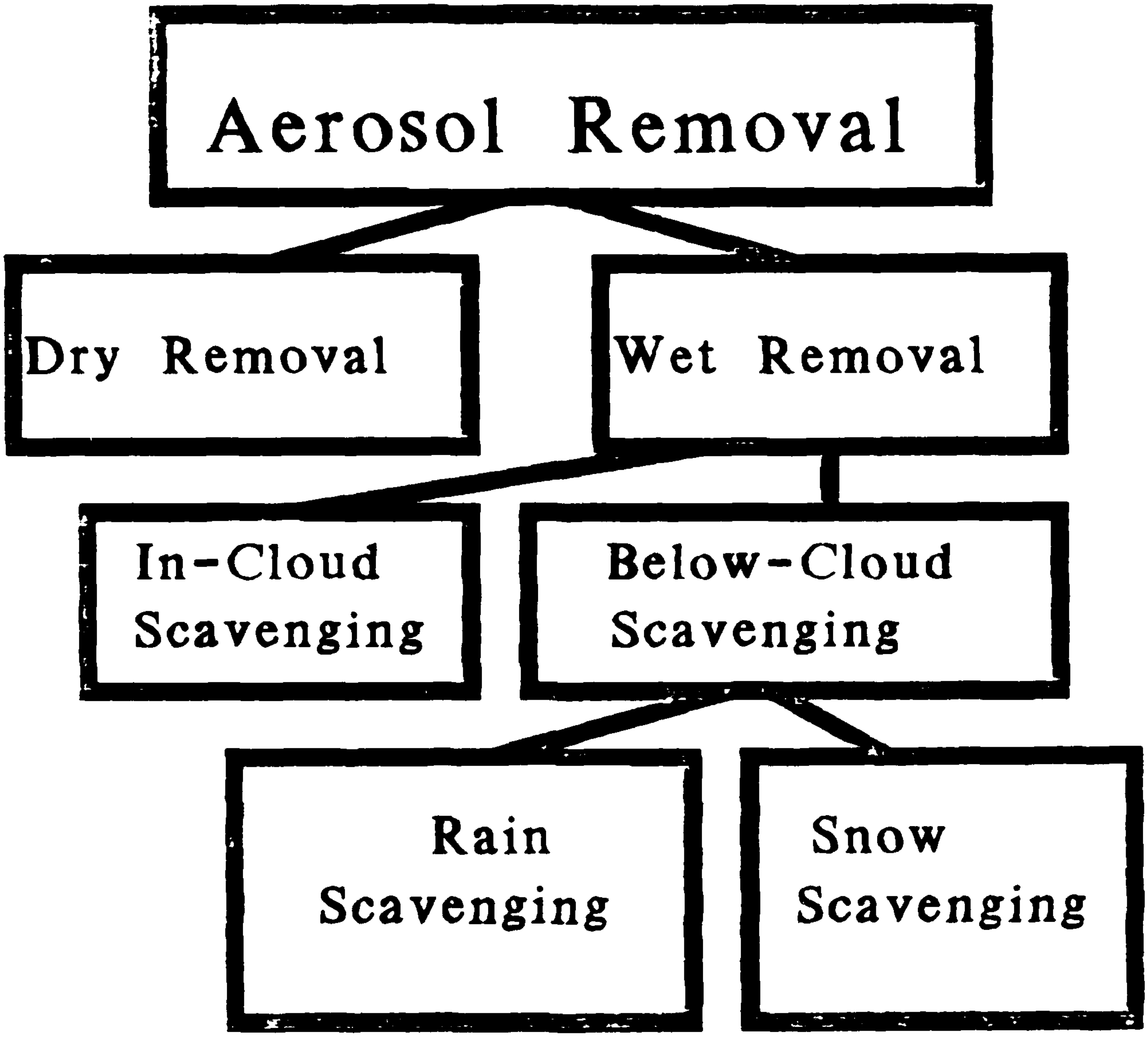
Aerosol Removal
Dry Removal
Wet Removal
In-Cloud Scavenging
Below-Cloud Scavenging
Rain Scavenging
Snow Scavenging

Previous Research In Precipitation Scavenging

1. Rain Scavenging

Wang, P.K., and H.R. Pruppacher, 1977b
"An experimental determination of the efficiency with which aerosol particles are collected by water drops in subsaturated air"
J. Atmos. Sci., 34, 1664-1669.

Wang, P.K., S.N. Grover, and H.R. Pruppacher, 1978
"On the effect of electric charges on the scavenging of aerosol particles by clouds and small raindrops"
J. Atmos. Sci., 35, 1735-1743.

Wang, P.K., 1979a
"Particular solutions to the steady-state diffusion equation and their application to aerosol scavenging problems"
Pap. Meteor. Res. (Taipei), 2, 37-42.

Wang, P.K., and H.R. Pruppacher, 1980a
"The effect of an external electric field on the scavenging of aerosol particles by cloud and small raindrops"
J. Coll. Interf. Sci., 75, 286-297.

Walcek, C., P.K. Wang, J.H. Topalian, S.K. Mitra, and H.R. Pruppacher, 1981
"An experimental test of a theoretical model designed to determinate the rate at which freely falling water drops scavenge SO2 in air"
J. Atmos. Sci., 38, 871-876.

Wang, P. K., 1983b
"Collection of aerosol particles by a conducting sphere in an external electric field-continuum regime approximation"
J. Coll. Interf. Sci., 94, 301-318.

2. Snow Scavenging

Wang, P. K., and H. R. Pruppacher, 1980b
"On the efficiency with which aerosol particles of radius less than 1 micron are collected by columnar ice crystals"
Pure Appl. Geophys., 118, 1090-1108.

Martin, J.J., P.K. Wang, and H.R. Pruppacher, 1980a
"On the efficiency with which aerosol particles of radius larger than
Pure Appl. Geophys., 118, 1109-1129.

2. Snow Scavenging (cont'd)

Martin, J.J.,P.K.Wang, and H.R. Pruppacher,1980b
"A theoretical determination of the efficiency with which aerosol particles are collected by simple ice plates"
J.Atmos.Sci.,37,1628-1638.

Martin, J.J.,P.K. Wang, and H.R. Pruppacher,1980c
"A theorectical study of the effect of electric charges on the efficiency with which aerosol particles are collected by ice crystal plates"
J.Coll.Interf.Sci.,78,44-56.

Wang, P.K., and S.M. Denzer,1983
"Mathematical description of the shape of plane hexagonal snow crystals"
J. Atmos. Sci.,40,1024-1028.

Wang, P. K.,1983a
"On the definition of collision efficiercy of atmospheric particles"
J. Atmos. Sci., 40, 1051-1052.

Wang, P.K., 1985
" A potential and stream function analysis of two-dimensional steady state convective diffusion equations involving Laplace fields"
Int. J. Heat Mass Transfer, 28, 1089-1095.

Wang, P. K., C. H. Chuang, and N. L. Miller, 1985
" Electrostatic, temperature, and vapor density fields surrounding stationary columnar ice crystals"
J. Atmos. Sci.,42, 2371-2379.

Wang, P. K.,1985
"A convective diffusion model for the scavenging of submicron aerosol particles by snow crystals of arbitrary shapes"
accepted by J. de Rech. Atmos.

Wang, P. K.,1985
" Brownian diffusion of charged fine particles surrounding a conducting cylinder in the presence of an external electric field"
accepted by J. Aerosol Sci.

Wang, P. K., and D. Sauter
" Experimental measurements of the snow scavenging efficiencies of aerosol particles "
(to be submitted to J. Atmos. Sci.)

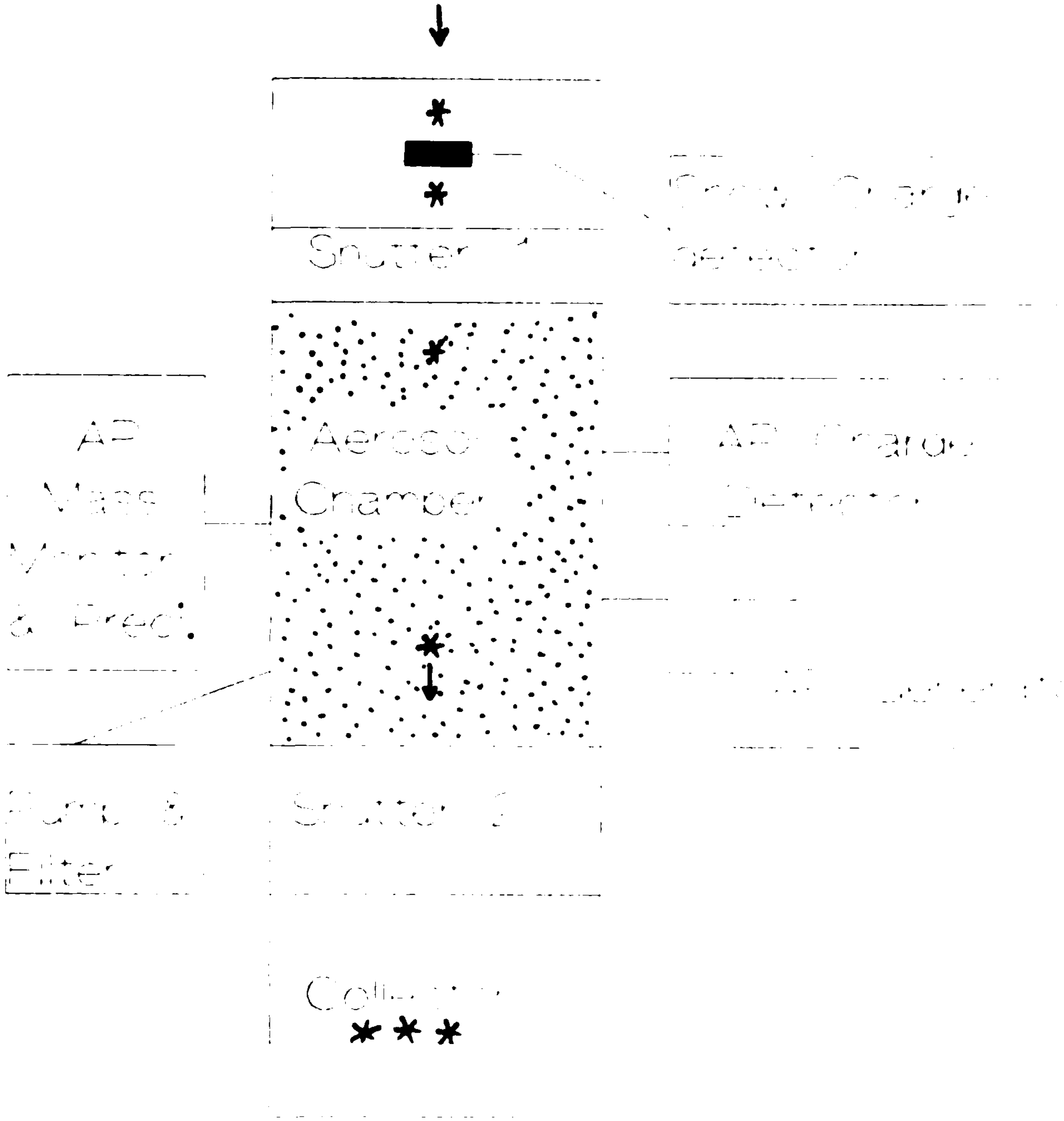
& Pred.
Chamber
Filter

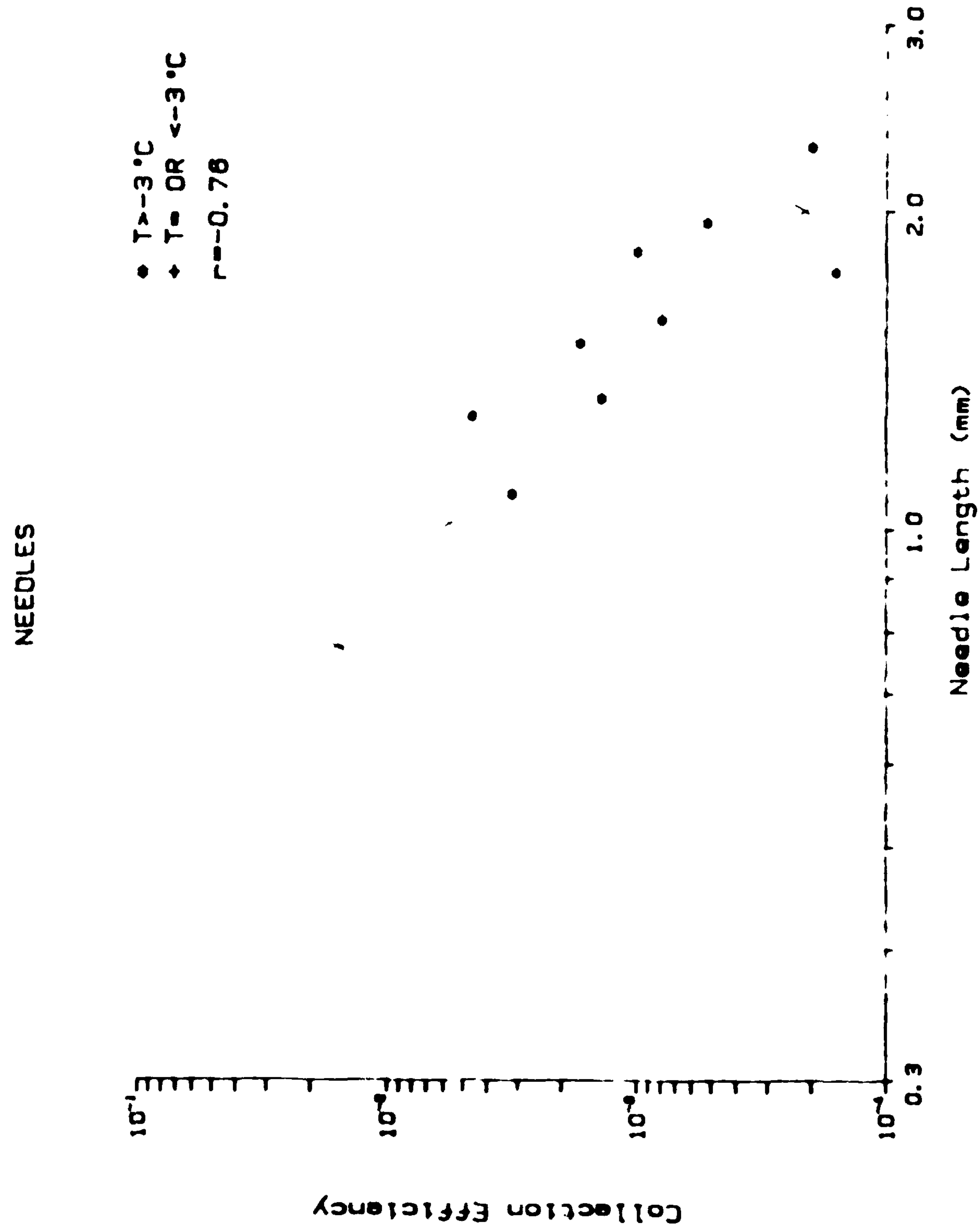
NEEDLES
• T>-3°C
+ T= OR <-3°C
r=-0.78
Needle Length (mm)
0.3
1.0
2.0
3.0
Collection Efficiency

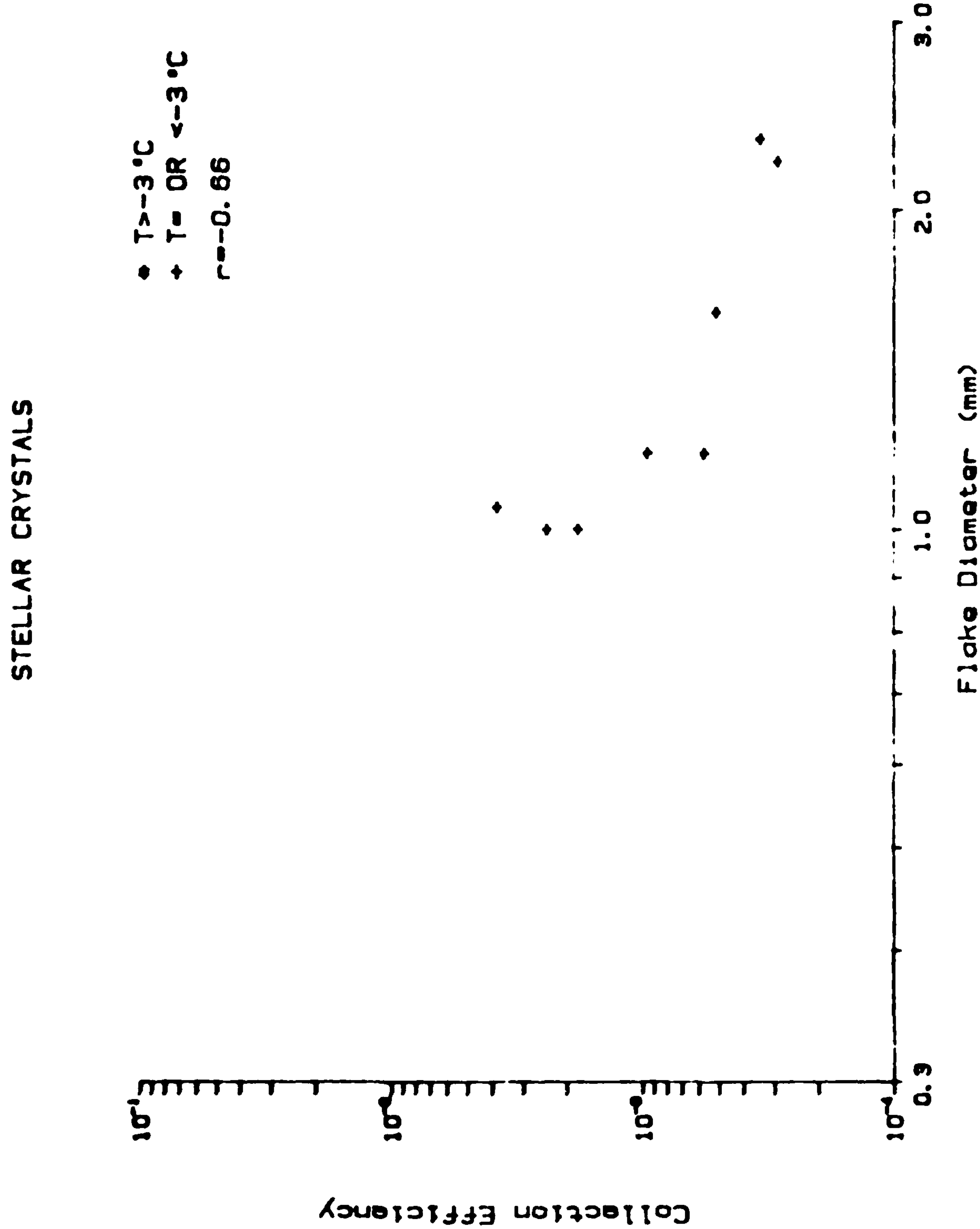
STELLAR CRYSTALS
T>-3°C
T= OR <-3°C
r=-0.66
Collection Efficiency
Flake Diameter (mm)
0.0
1.0
2.0
3.0

Fig 4.11

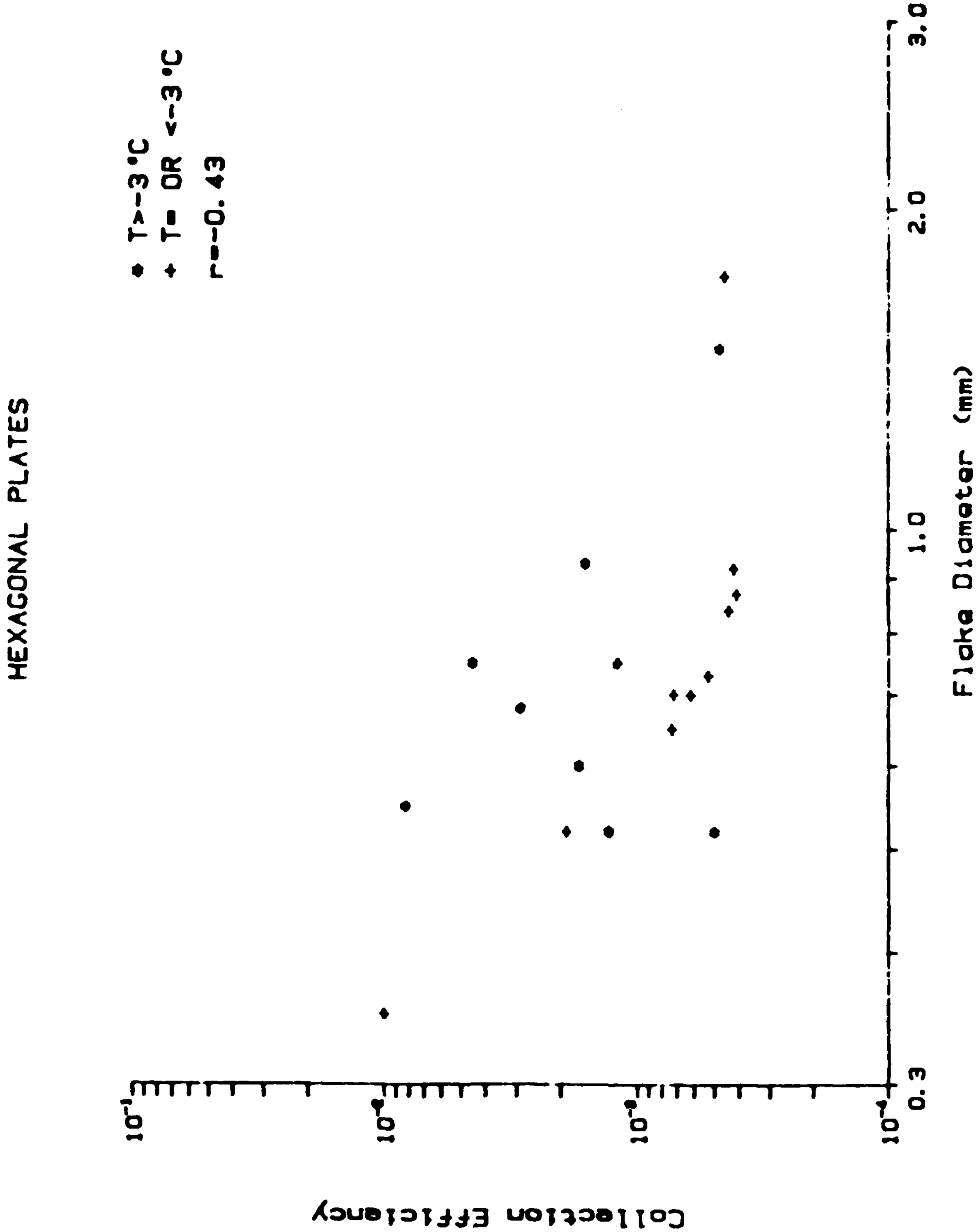

HEXAGONAL PLATES
• T>-3°C
+ T= OR <-3°C
r=-0.43
Flake Diameter (mm)
Collection Efficiency
0.3
1.0
2.0
3.0
10^{-1}
10^{-2}
10^{-3}
10^{-4}

Fig 4.21

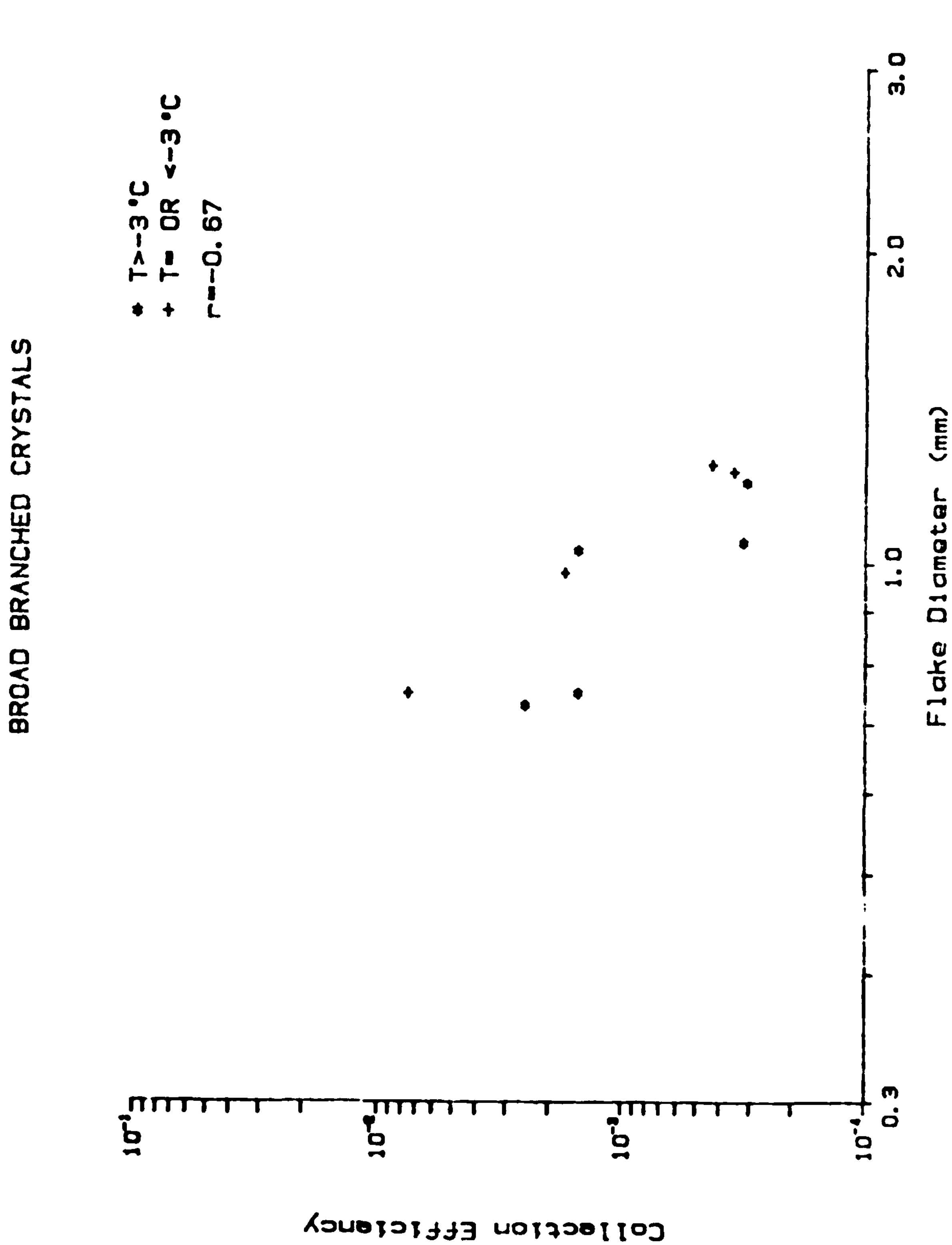

BROAD BRANCHED CRYSTALS
* T>-3°C
+ T= OR <-3°C
r=-0.67
Collection Efficiency
10^{-1}
10^{-2}
10^{-3}
10^{-4}
0.3
1.0
2.0
3.0
Flake Diameter (mm)

Fig 4.16

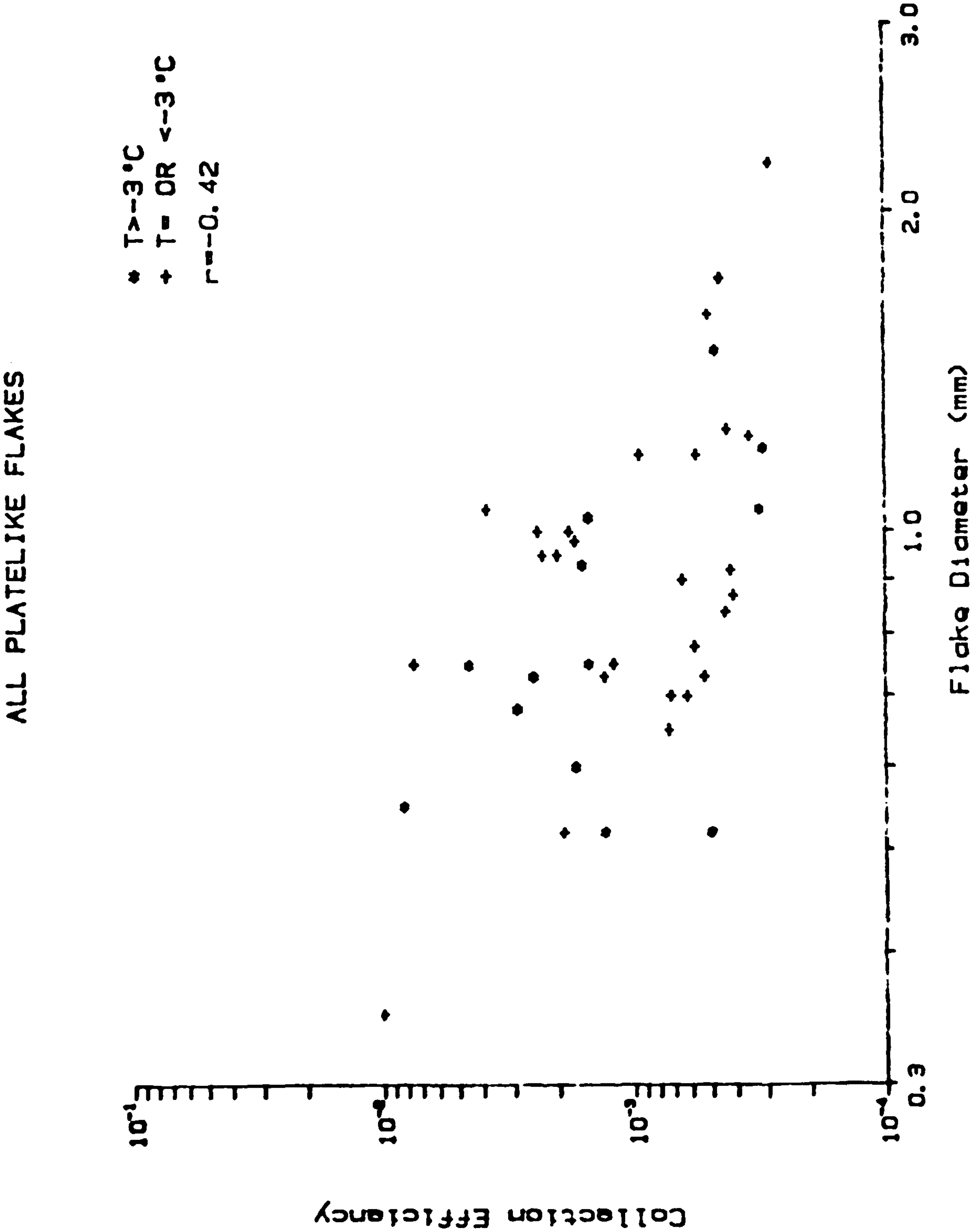
ALL PLATELIKE FLAKES
* T>-3 °C
+ T= OR <-3 °C
r=-0.42
Collection Efficiency
10^-1
10^-2
10^-3
10^-4
0.3
1.0
2.0
3.0
Flake Diameter (mm)

Fig 4.1

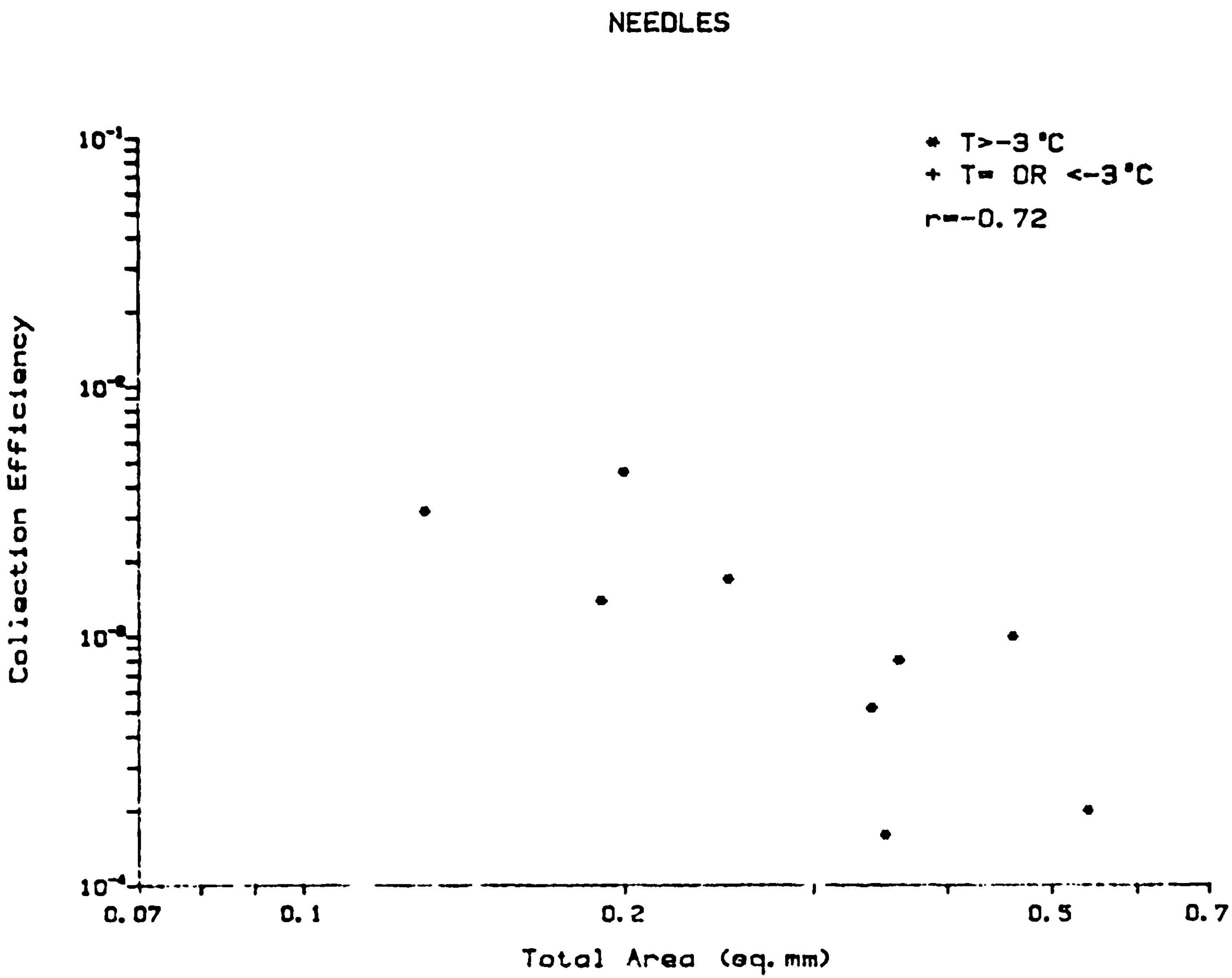
NEEDLES
* T>-3 °C
+ T= OR <-3 °C
r=-0.72
Collection Efficiency
10^{-1}
10^{-2}
10^{-3}
10^{-4}
0.07
0.1
0.2
0.5
0.7
Total Area (sq. mm)

Fig 4.9

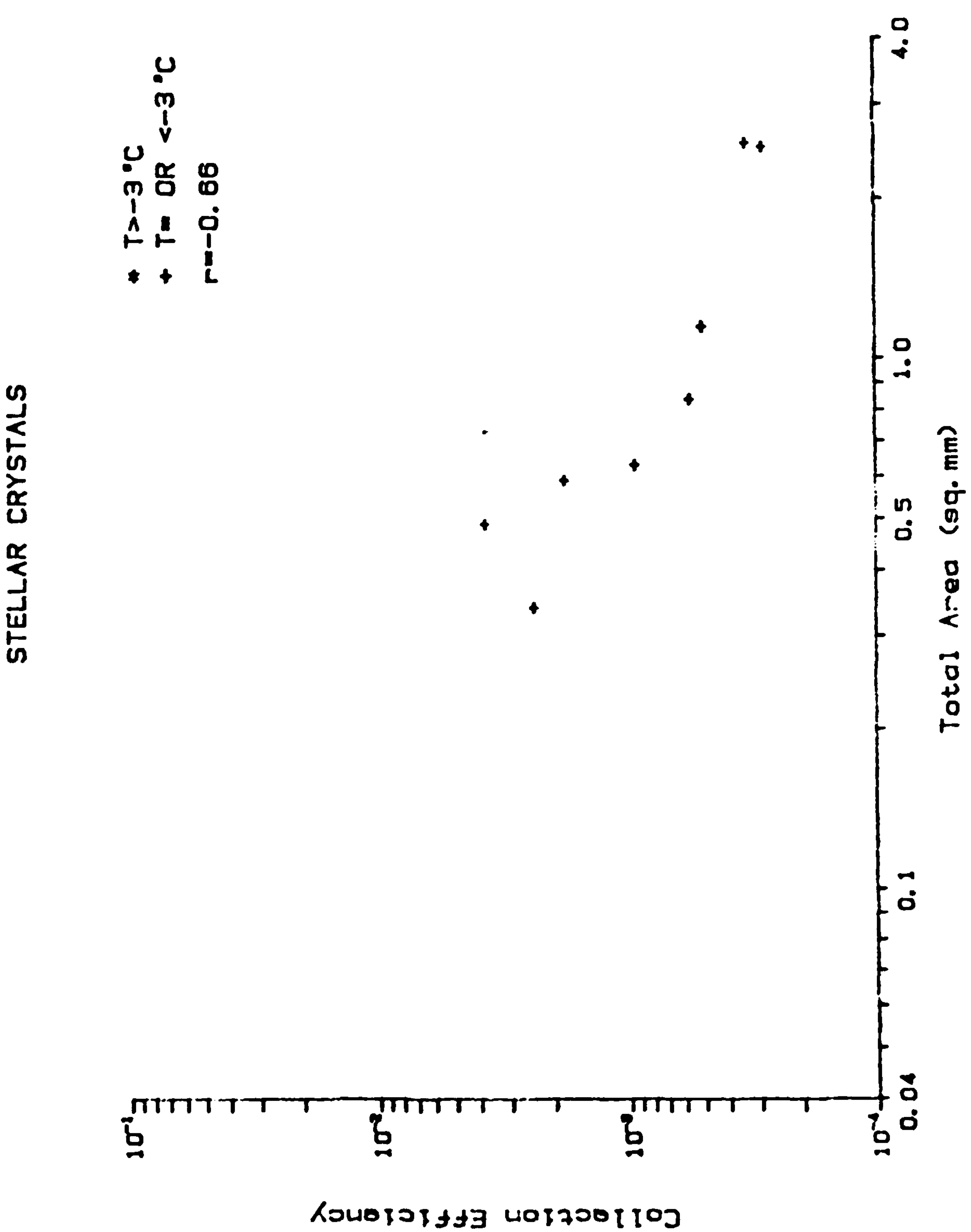
STELLAR CRYSTALS
* T>-3°C
+ T= OR <-3°C
r=-0.66
Total Area (sq. mm)
0.04
0.1
0.5
1.0
4.0
Collection Efficiency

Fig 4.14

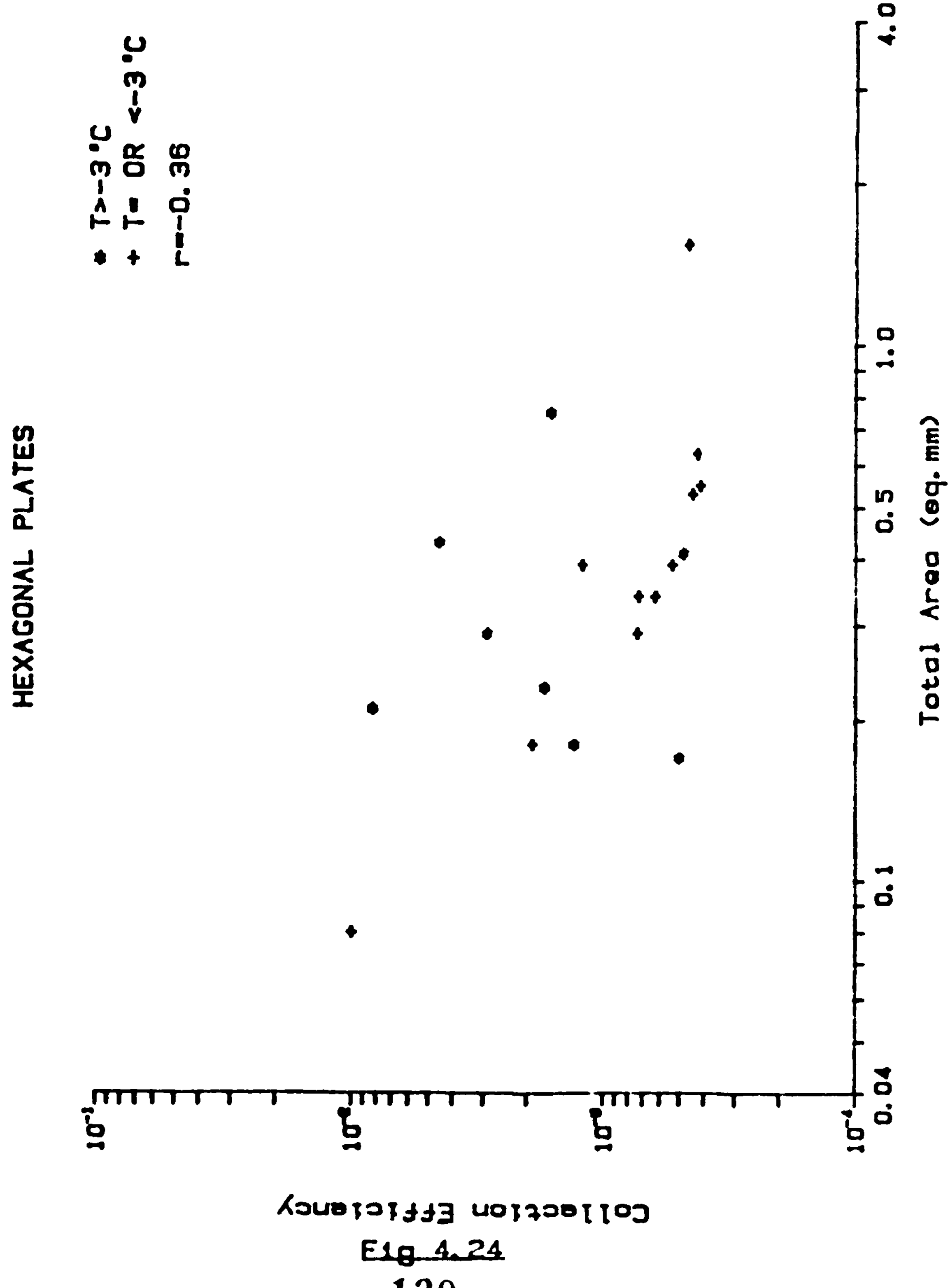

HEXAGONAL PLATES
* T>-3°C
+ T= OR <-3°C
r=-0.36
Total Area (sq. mm)
0.04
0.1
0.5
1.0
4.0
10^{-1}
10^{-4}
Collection Efficiency

Fig 4.24

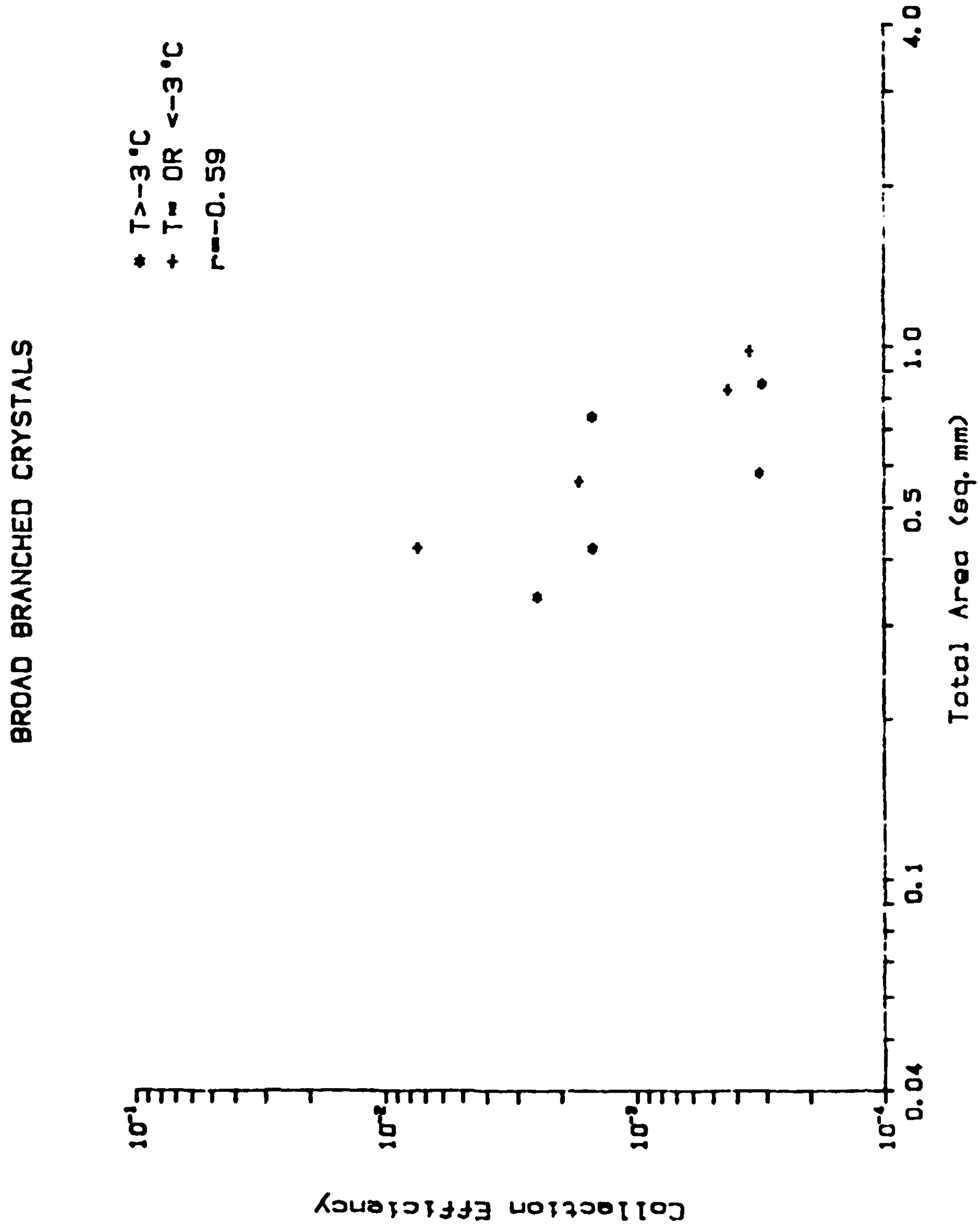

BROAD BRANCHED CRYSTALS
* T>-3°C
+ T= OR <-3°C
r=-0.59
Total Area (sq. mm)
0.04
0.1
0.5
1.0
4.0
Collection Efficiency
10^{-1}
10^{-2}
10^{-3}
10^{-4}

Fig 4.19

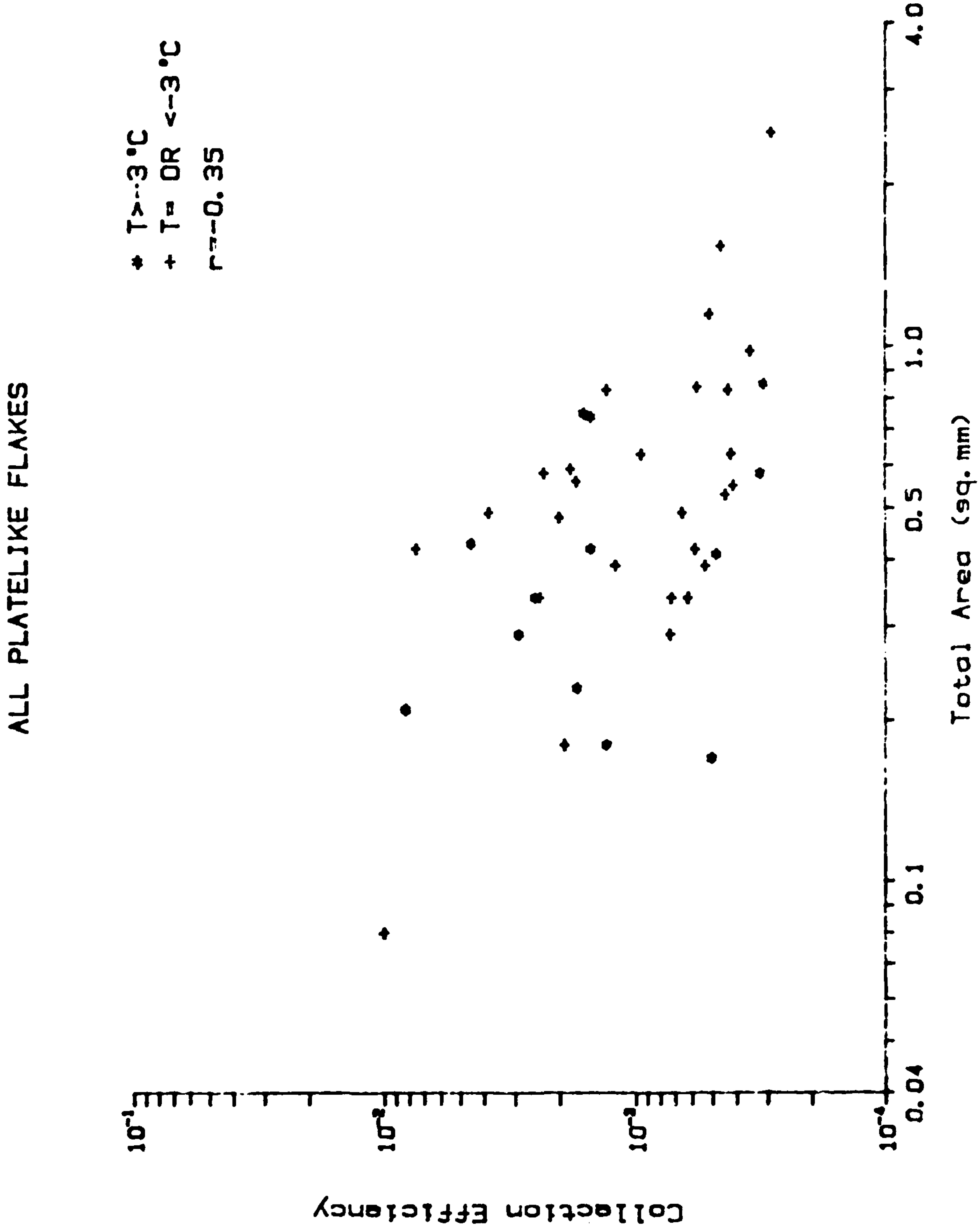
ALL PLATELIKE FLAKES
* T>-3°C
+ T= OR <-3°C
r=-0.35
Collection Efficiency
10⁻¹
10⁻²
10⁻³
10⁻⁴
0.04
0.1
0.5
1.0
4.0
Total Area (sq. mm)

Fig 4.4

Theoretical Consideration

Basically a convective diffusion problem

The mechanisms involved are:

1. Inertial impaction
2. Brownian diffusion
3. Thermophoresis
4. Diffusiophresis
5. Electric forces
   - –Static charges
   - –Extrenal electric field
6. Turbulence

Models:

1. Trajectory Model – Brownian diffusion not treated
   valid for particle radius > 0.5 micron.
2. Flux Model – inertial impaction not treated
   valid for particle radius <= 0.5 micron.

$\boxed{\text{Flux Model}}$: (Good for $r \le 0.5\ \mu m$) ④

Convective Diffusion Equation (CDE)

$$D\nabla^2 n - B\vec{F}\cdot\nabla n = 0 \qquad \text{--- (1)}$$

Ventillation- Ehanced CDE

$$\bar{f}_p D\nabla^2 n - B\sum \bar{f}_i \vec{F}_i \cdot \nabla n = 0 \qquad \text{---(2)}$$

where $\bar{f}_i$'s are overall ventillation factors.

B.C. $\begin{cases} n = 0 & \text{at } \phi = \phi_0 \text{ (Surface)} \\ n = n_\infty & \text{at } R \to \infty \end{cases}$ .. (3)

where ϕ is the force potential.

Solution of (2) :

$$n = n_\infty \left[e^{\frac{B}{D\bar{f}_p}(\phi-\phi_0)} - 1 \right] \Big/ \left(e^{\frac{B\phi_0}{D\bar{f}_p}} - 1 \right) \quad \text{.. (4)}$$

Resulting collection kernel:

$$K = -\frac{1}{n_\infty}\frac{\partial N}{\partial t} = -\frac{1}{n_\infty}\oint \left(nB\vec{F} - Df_p \nabla n \right) \cdot d\vec{S}$$

$$= \frac{B}{e^{\frac{B}{Df_p}\phi_o} - 1} \oint \vec{F} \cdot d\vec{S} \qquad \left(\vec{F} = \sum_i f_i \vec{F}_i \right) \quad \cdots (5)$$

Collection Efficiency

$$E = \frac{K}{K^*} \qquad \cdots\cdots (6)$$

Consider the following external forces:

$$\vec{F} = \vec{F}_e + \vec{F}_{th} + \vec{F}_{df} \qquad \cdots\cdots (7)$$

$\vec{F}_e$: Electric force , $\vec{F}_{th}$: Thermophoretic force

$\vec{F}_{df}$: Diffusiophoretic force.

⑥

Applying electrostatic theory,

$$\oint \vec{F}_e \cdot d\vec{S} = 4\pi C \xi (V_s - V_\infty) = 4\pi Q \xi$$

$$\oint \vec{F}_{th} \cdot d\vec{S} = 4\pi C \bar{f}_h Z_{th} (T_s - T_\infty)$$

$$\oint \vec{F}_{df} \cdot d\vec{S} = 4\pi C \bar{f}_h Z_{df} (\rho_{v,s} - \rho_{v,\infty})$$

V: Electric potential, T: Temp., ρ_v: Vapor density

C: Capacitance (different for different shapes + sizes)

$$Z_{th} = \frac{12\pi\eta_a r (k_a + 2.5 k_p N_{kn}) k_a}{5(1+3N_{kn})(k_p + 2k_a + 5k_p N_{kn}) P}$$

$$Z_{df} = \frac{6\pi\eta_a r (0.74 D M_a)}{(1+\alpha N_{kn}) M_w \rho_a}$$

(7)

Therefore the collection kernel is

$$K = -\frac{4\pi B\left[Q\dot{g} + C\bar{f}_h Z_{th}(T_s - T_\infty) + C\bar{f}_h Z_{df}(\rho_{v,s} - \rho_{v,\infty})\right]}{e^{\frac{B}{Df_p}\phi_0} - 1}$$

$$= -\frac{4\pi B \phi_0 C}{e^{\frac{B}{D\bar{f}_p}\phi_0} - 1}$$

For sphere : $C = a$ (radius)

For complicated shapes such as snow flakes, C can be measured experimentally.

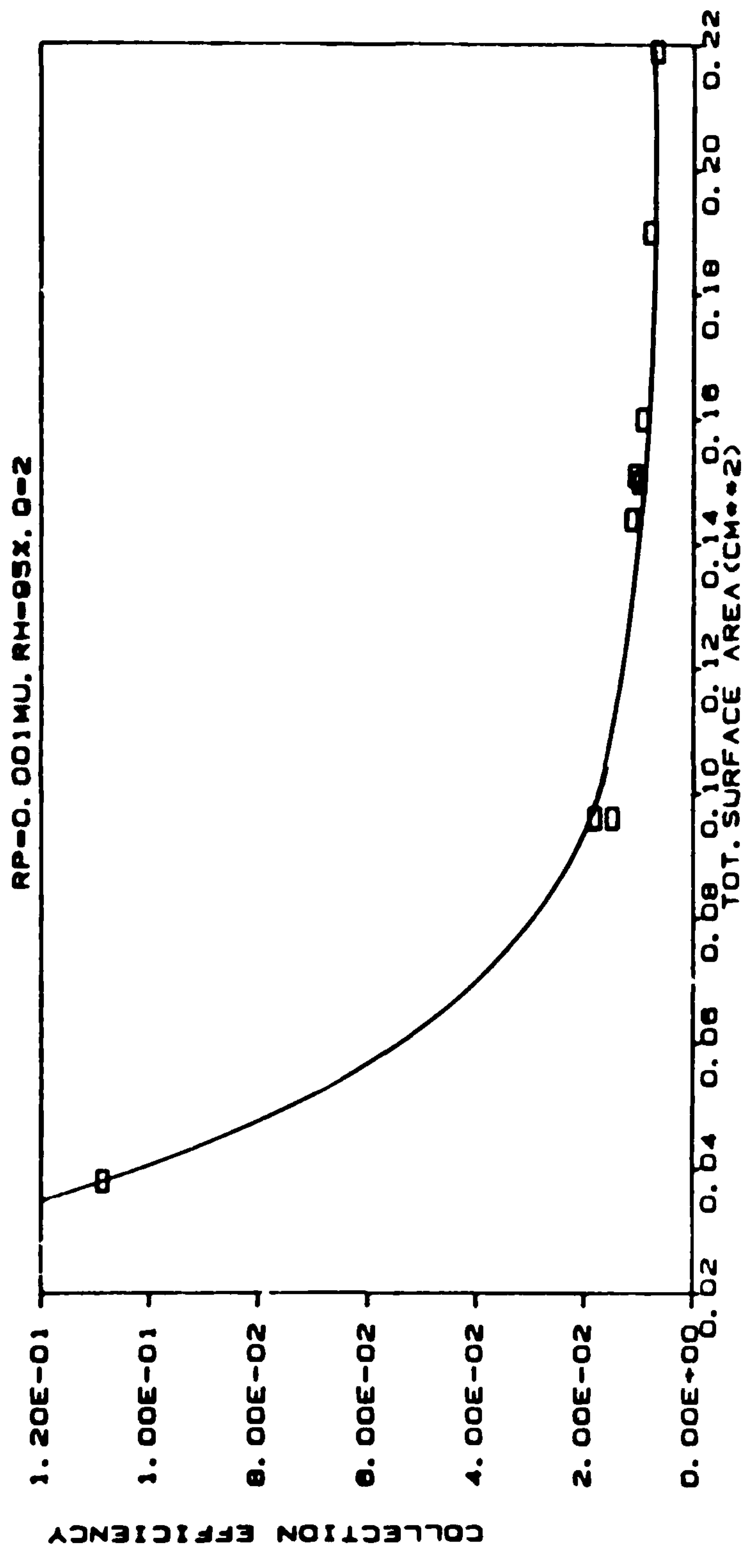
RP=0.001MU, RH=95%, D=2
COLLECTION EFFICIENCY
1.20E-01
1.00E-01
8.00E-02
6.00E-02
4.00E-02
2.00E-02
0.00E+00
0.02
0.04
0.06
0.08
0.10
0.12
0.14
0.16
0.18
0.20
0.22
TOT. SURFACE AREA (CM**2)

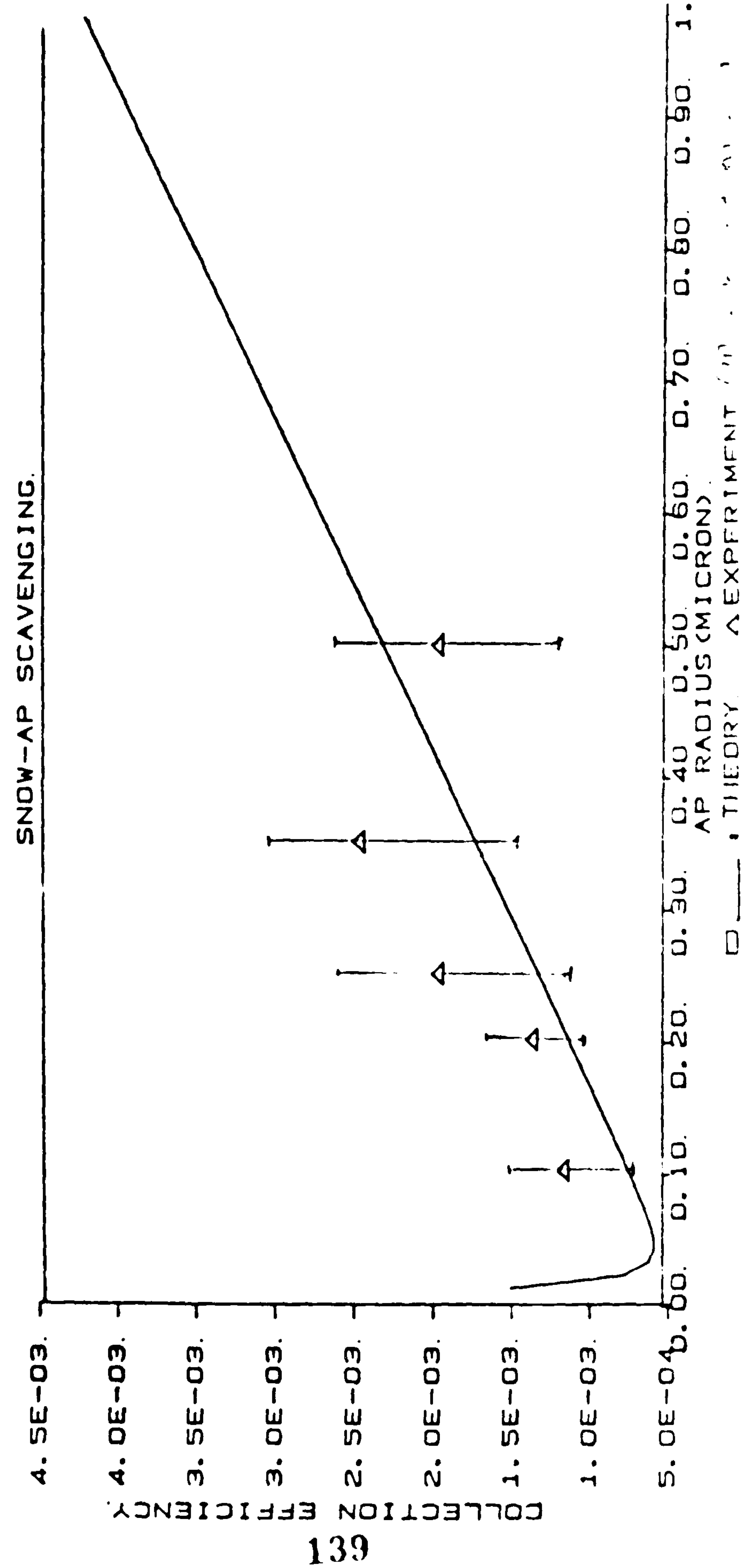

SNOW-AP SCAVENGING.
COLLECTION EFFICIENCY.
4.5E-03
4.0E-03
3.5E-03
3.0E-03
2.5E-03
2.0E-03
1.5E-03
1.0E-03
5.0E-04
0.00
0.10
0.20
0.30
0.40
0.50
0.60
0.70
0.80
0.90
1.
AP RADIUS (MICRON)
THEORY
EXPERIMENT

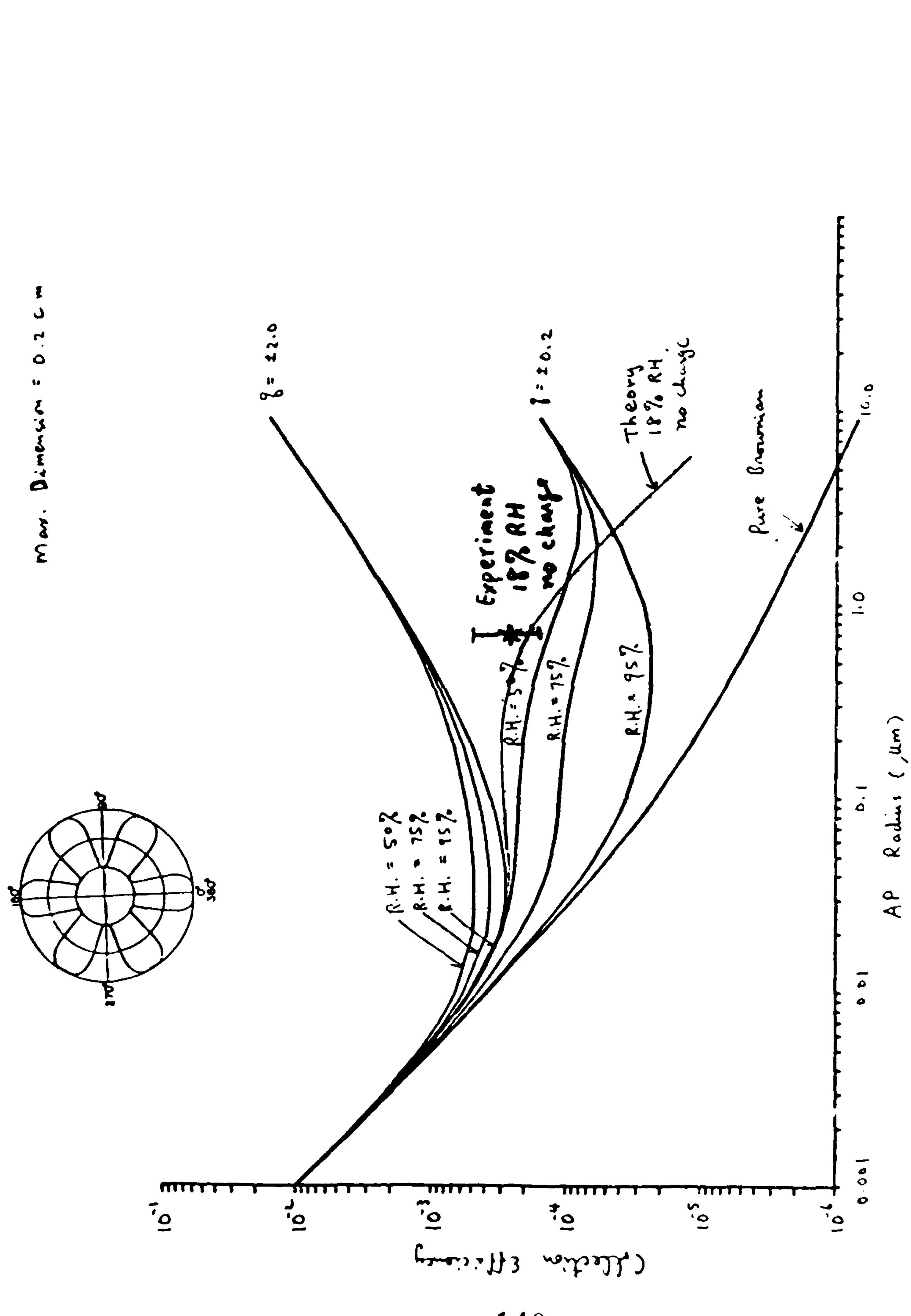

Max. Dimension = 0.2 cm
δ = ±2.0
δ = ±0.2
Theory
18% RH
no charge
Experiment
18% RH
no charge
Pure Brownian
R.H. = 50%
R.H. = 75%
R.H. = 95%
Collection Efficiency
AP Radius (μm)
0.001
0.01
0.1
1.0
10.0
10^{-1}
10^{-2}
10^{-3}
10^{-4}
10^{-5}
10^{-6}

CLOUD MODEL SENSITIVITY STUDIES ON THE VERTICAL PENETRATION OF SOOT

R. Banta
Air Force Geophysics Lab.
AFGL/LYC
Hanscom AFB, MA
(617) 861-2948

OVERVIEW

- Review 3-D cloud model results

  dependence of upward soot penetration on atmospheric conditions

- Offers hope for simple parameterization of vertical soot profiles

- Atmospheric stability indices - distributions

  by season

  by region

- Sample procedure: how distribution approach might be used to estimate amount of soot initially entering stratosphere

- Forest fire (and other) smoke plume heights – sensitive to atmospheric stability, moisture content, in addition to fire intensity – (NRC, '85)

- If urban fires have larger heat fluxes (10x), are those larger fires also sensitive to atmospheric structure?

- 3-D numerical cloud simulations indicate that they are.

3-D Cloud Model Simulations

- standard atmosphere + moisture, winds
- to 30 min (60 min w/ reduced heat flux)
- cloud microphysics (cloud, rain, ice, "snow", graupel/hail)
- soot tracer

see descriptions by Tripoli & Cotton

SAMPLE OUTPUT

- 3-D pictures
- 2-D cross sections
- numerical output fields

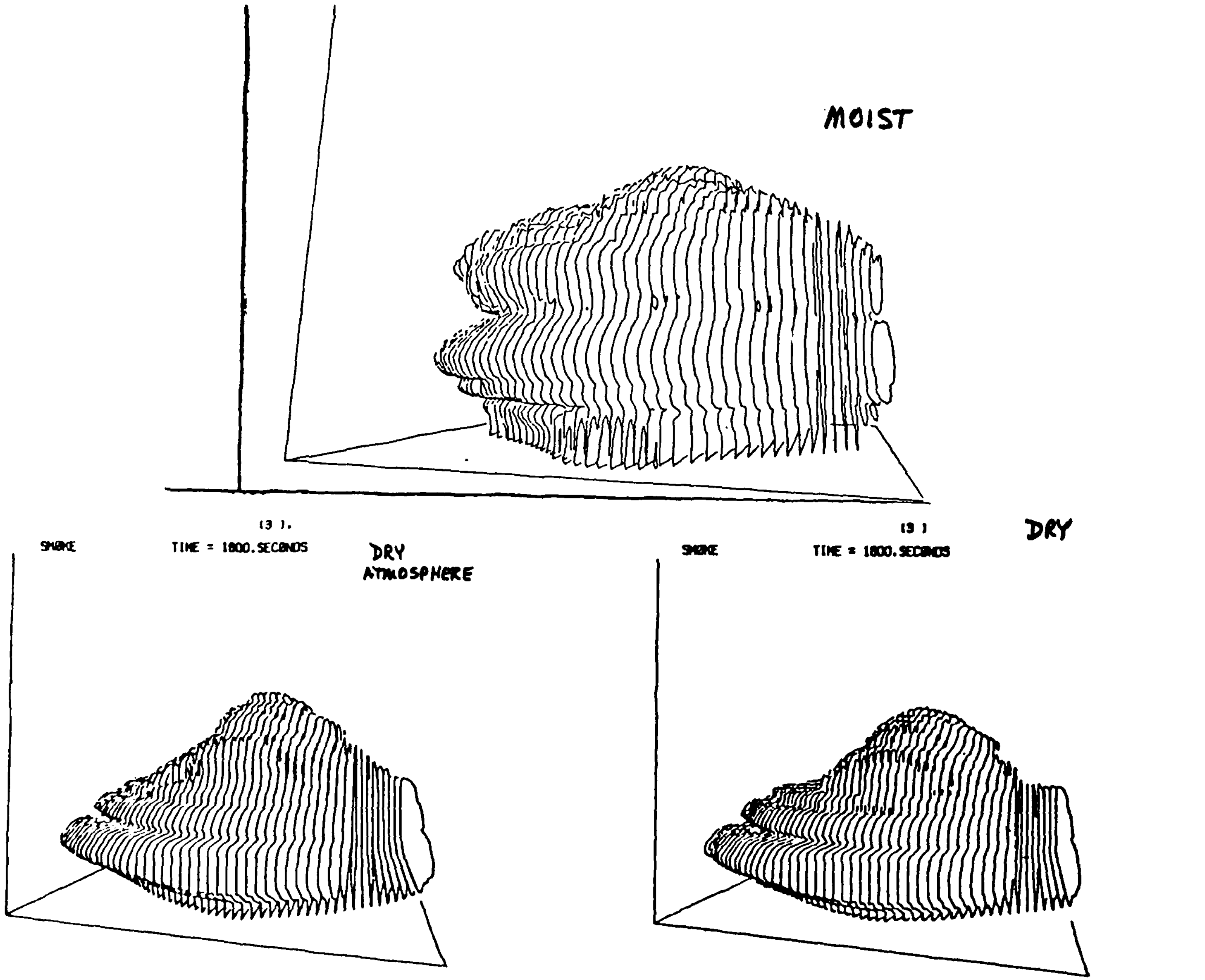
MOIST
(3).
SMOKE
TIME = 1800.SECONDS
DRY
ATMOSPHERE
(3)
SMOKE
TIME = 1800.SECONDS
DRY

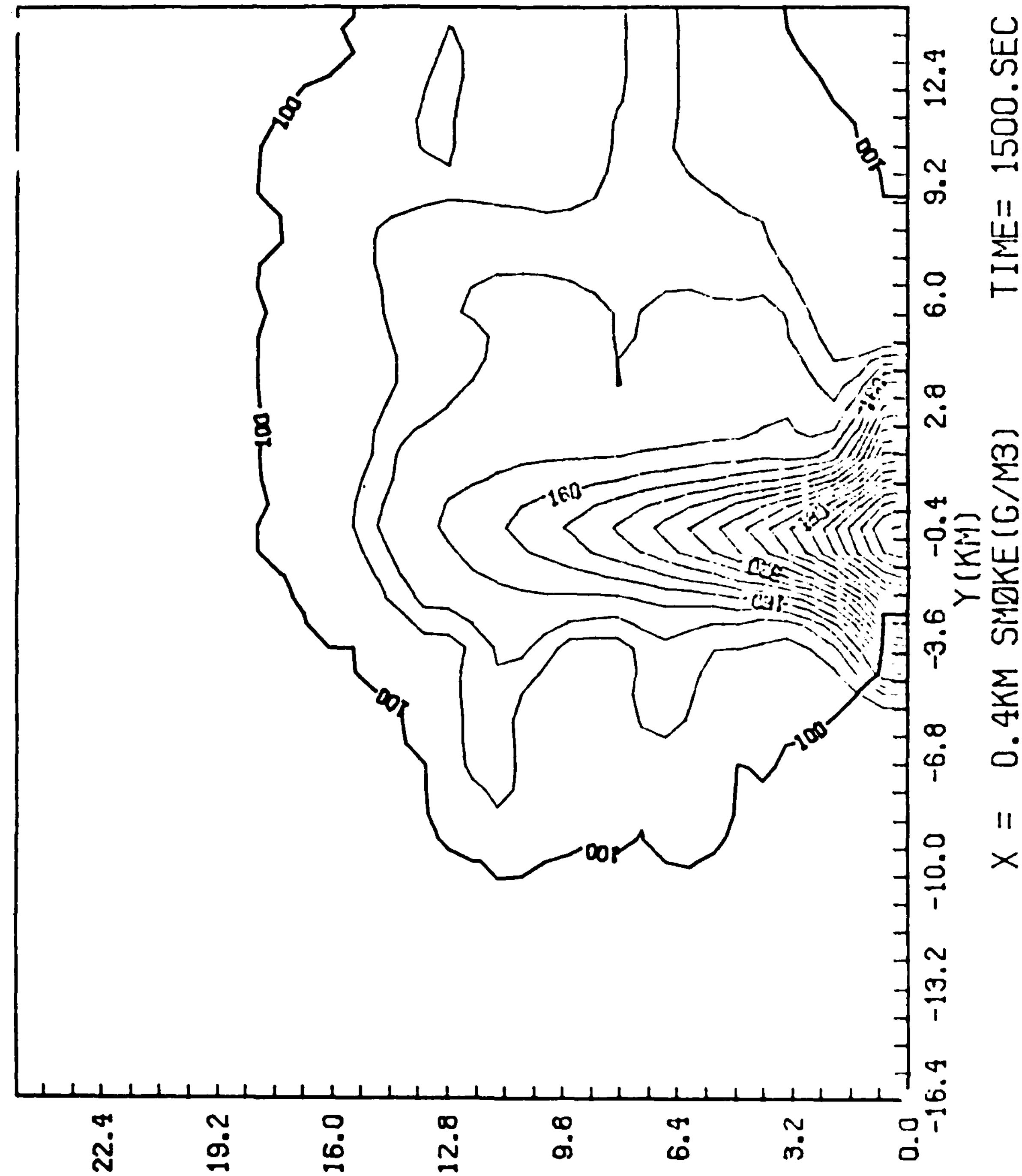

X = 0.4KM SMØKE(G/M3)
TIME= 1500.SEC
Y(KM)
-16.4 -13.2 -10.0 -6.8 -3.6 -0.4 2.8 6.0 9.2 12.4
0.0 3.2 6.4 9.6 12.8 16.0 19.2 22.4
100
160

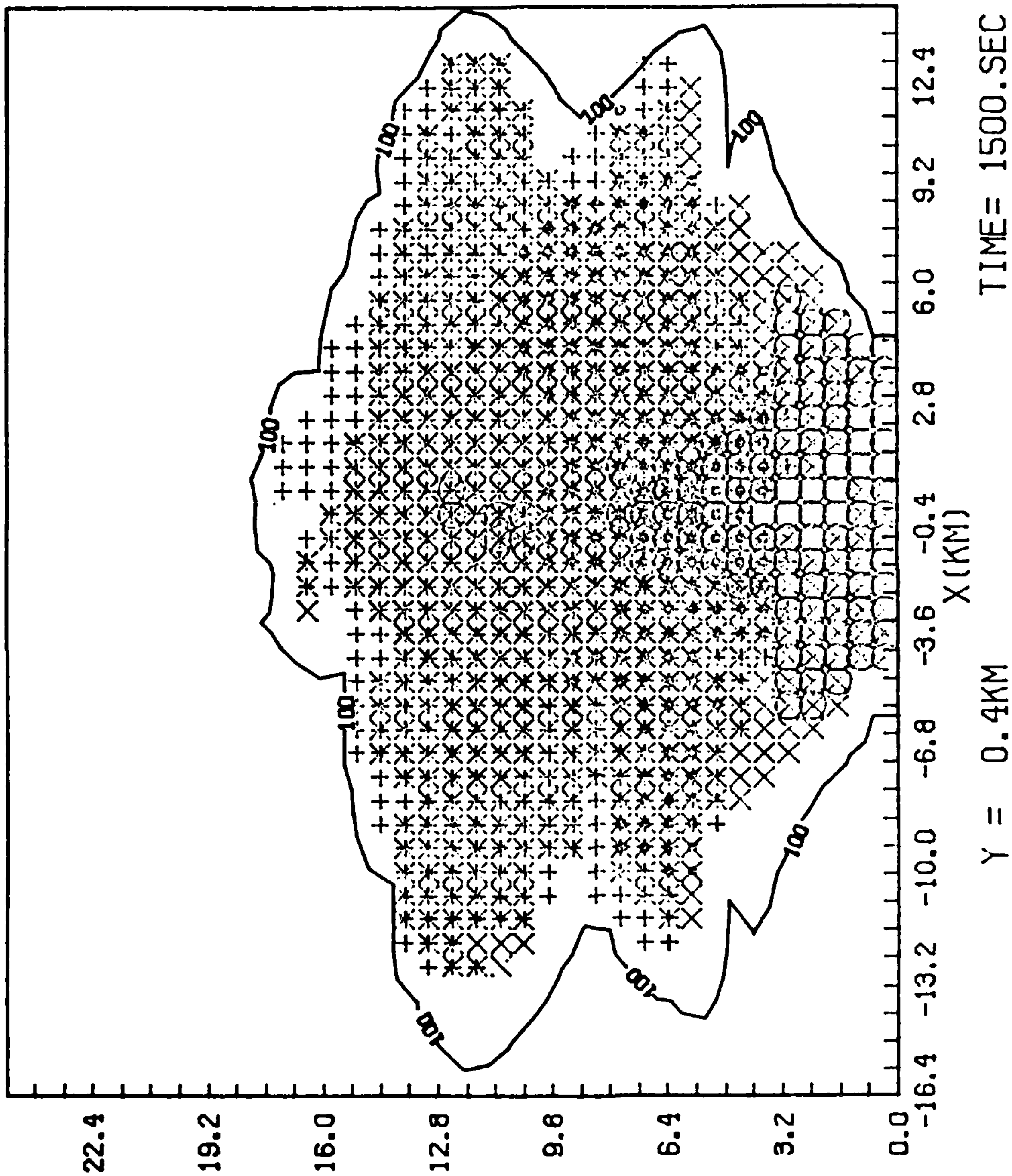

TIME= 1500.SEC
Y = 0.4KM
X(KM)
-16.4 -13.2 -10.0 -6.8 -3.6 -0.4 2.8 6.0 9.2 12.4
0.0 3.2 6.4 9.6 12.8 16.0 19.2 22.4
100

SUMMARY OF MODEL-RUN COMPARISONS

Stability
- unstable (Cotton & Tripoli): 44% into stratosphere
- stable (std. atmos): 22% " "

Moisture (std atmos)
- with 40-50% RH in troposphere: 22% into stratosp
- with 0 moisture <1% " "

Heat flux (std atmos)
- 100% - smoke penetrated to 14 km.
- 10% - no smoke above 6 km.

Large heat-flux fires - sensitive to atmosphere

MODEL-RUN COMPARISONS

One more issue - CCN concentrations

5000 cm^{-3} 22% into stratosphere

50 cm^{-3} 11% into stratosphere

(attempt to represent some large nuclei)

less latent heat of fusion

but with the phoretic effects modeled,
< 2% scavenging in both cases

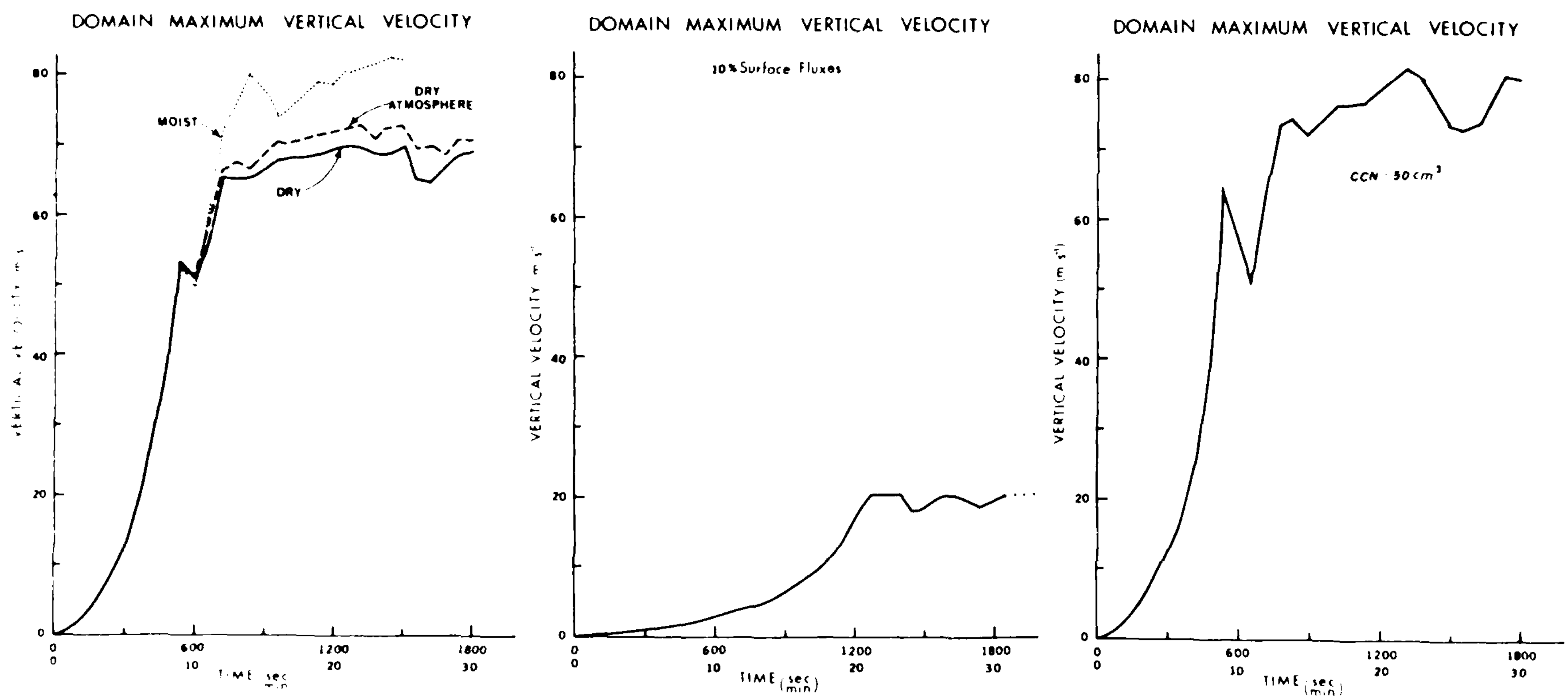
DOMAIN MAXIMUM VERTICAL VELOCITY
MOIST
DRY ATMOSPHERE
DRY
DOMAIN MAXIMUM VERTICAL VELOCITY
10% Surface Fluxes
VERTICAL VELOCITY (m s⁻¹)
TIME (sec/min)
DOMAIN MAXIMUM VERTICAL VELOCITY
CCN 50 cm⁻³
VERTICAL VELOCITY (m s⁻¹)
TIME (sec/min)

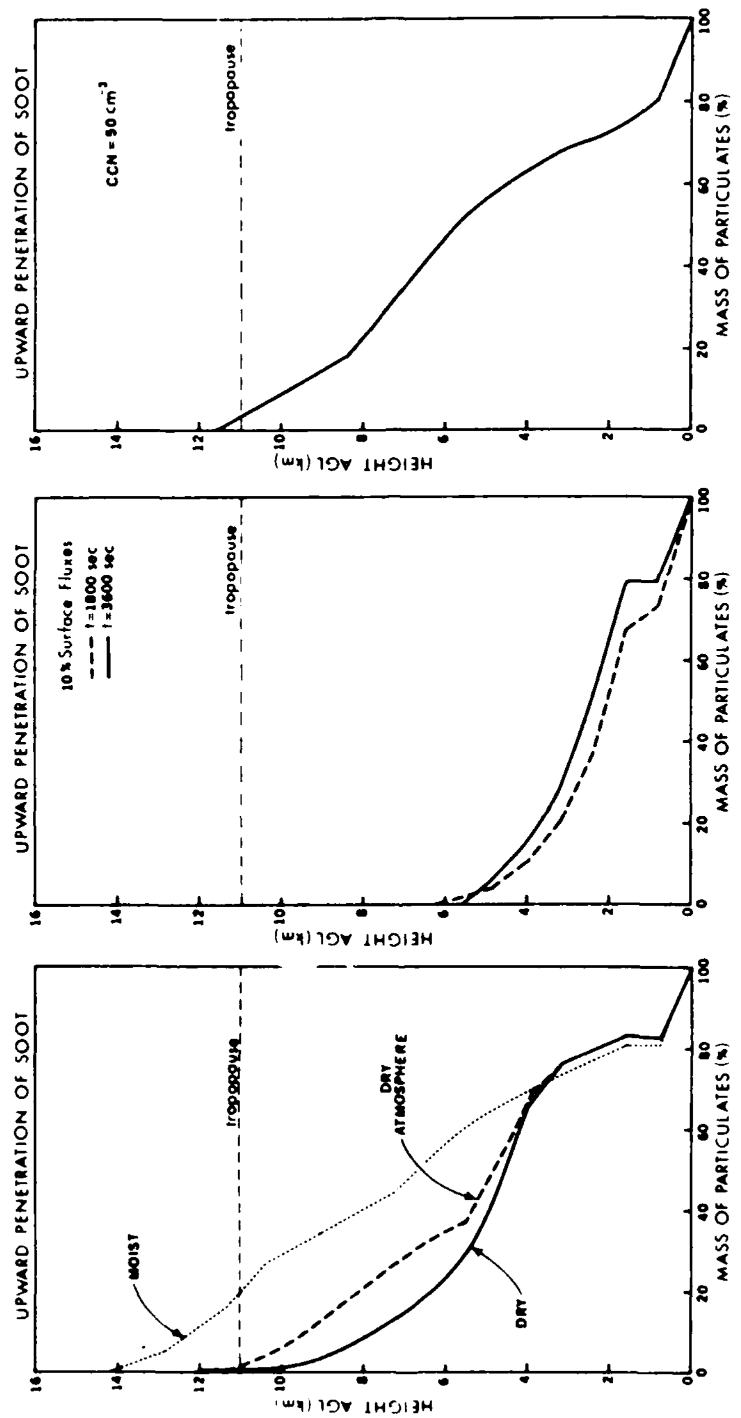
UPWARD PENETRATION OF SOOT
MOIST
tropopause
DRY ATMOSPHERE
DRY
HEIGHT AGL (km)
MASS OF PARTICULATES (%)
UPWARD PENETRATION OF SOOT
10% Surface Fluxes
t=1800 sec
t=3600 sec
tropopause
HEIGHT AGL (km)
MASS OF PARTICULATES (%)
UPWARD PENETRATION OF SOOT
CCN = 50 cm^{-3}
tropopause
HEIGHT AGL (km)
MASS OF PARTICULATES (%)

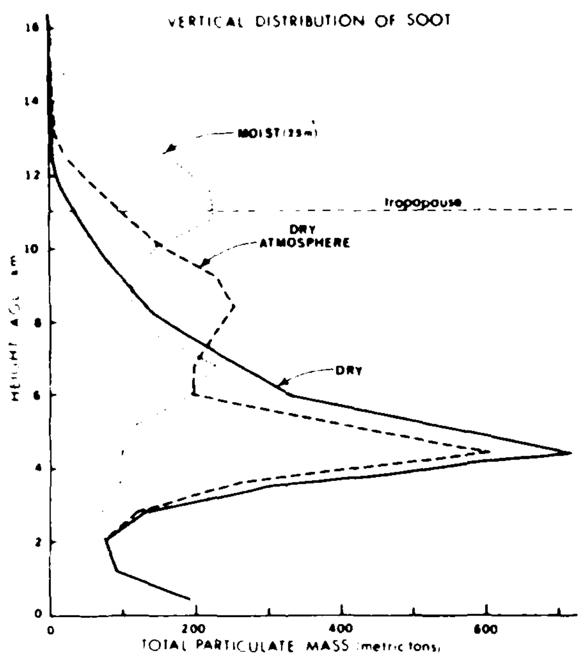
VERTICAL DISTRIBUTION OF SOOT
MOIST (25 m)
DRY ATMOSPHERE
DRY
tropopause
HEIGHT AGL (km)
TOTAL PARTICULATE MASS (metric tons)

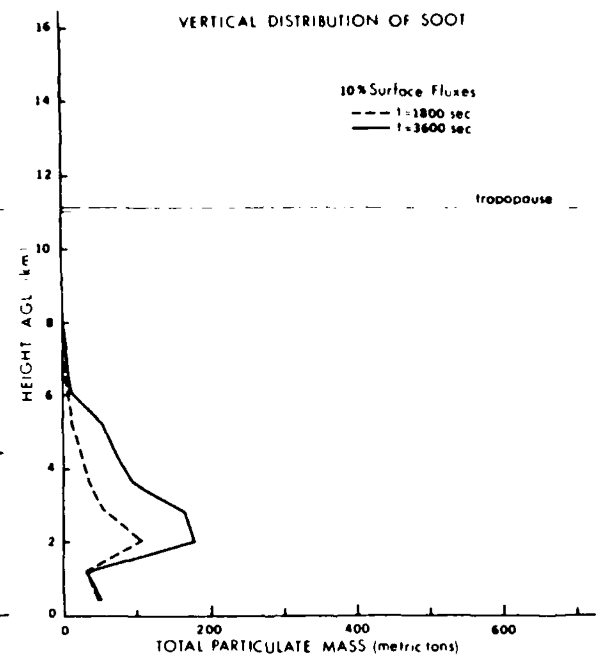
VERTICAL DISTRIBUTION OF SOOT
10% Surface Fluxes
t = 1800 sec
t = 3600 sec
tropopause
HEIGHT AGL (km)
TOTAL PARTICULATE MASS (metric tons)

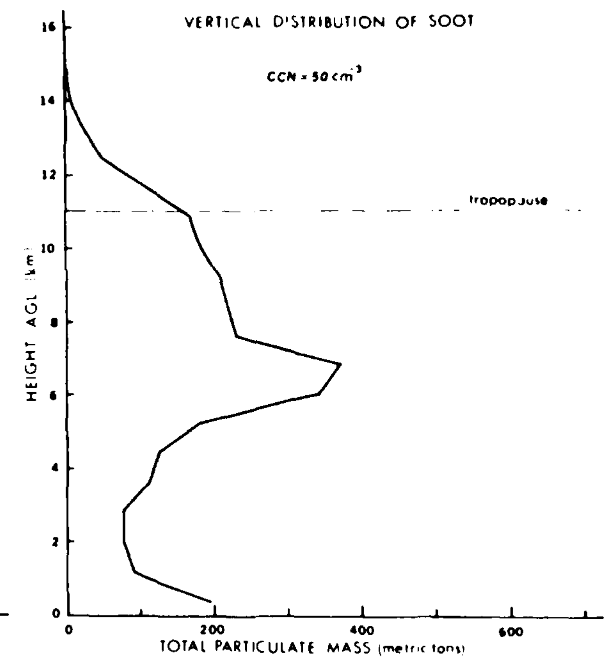
VERTICAL DISTRIBUTION OF SOOT
CCN = 50 cm^-3
tropopause
HEIGHT AGL (km)
TOTAL PARTICULATE MASS (metric tons)

PARAMETERIZATION OF VERTICAL INJECTION PROFILE

Previous results suggest that vertical injection profiles can be parameterized in terms of some stability (etc.) parameter as input into larger-scale models. Need

- profile shape
  - uniform
  - detrainment curve

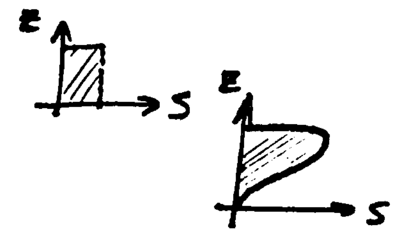

- height of plume
  - fire heat flux
  - atmospheric stability
  - atmospheric moisture (low-level, precipitable water)
  - wind profile
  - tropopause height (normalize?)
  - etc.

VARIABILITY OF STABILITY INDICES
BY SEASON, BY REGION

Analog of the desired parameter

Stability Indices, e.g.

- simple: Showalter Stability Index (SSI)
  850mb tmp, humidity; 500mb tmp.

- complex: SWEAT Severe Weather Threat Index
  mixture of tmp, moisture, wind shear values at various levels

Both compiled by U.S. Air Force's Environmental Technical Applications Center (ETAC)

12-year period ('73-'84)

~ 8,000 obs per month (12-yr sample)

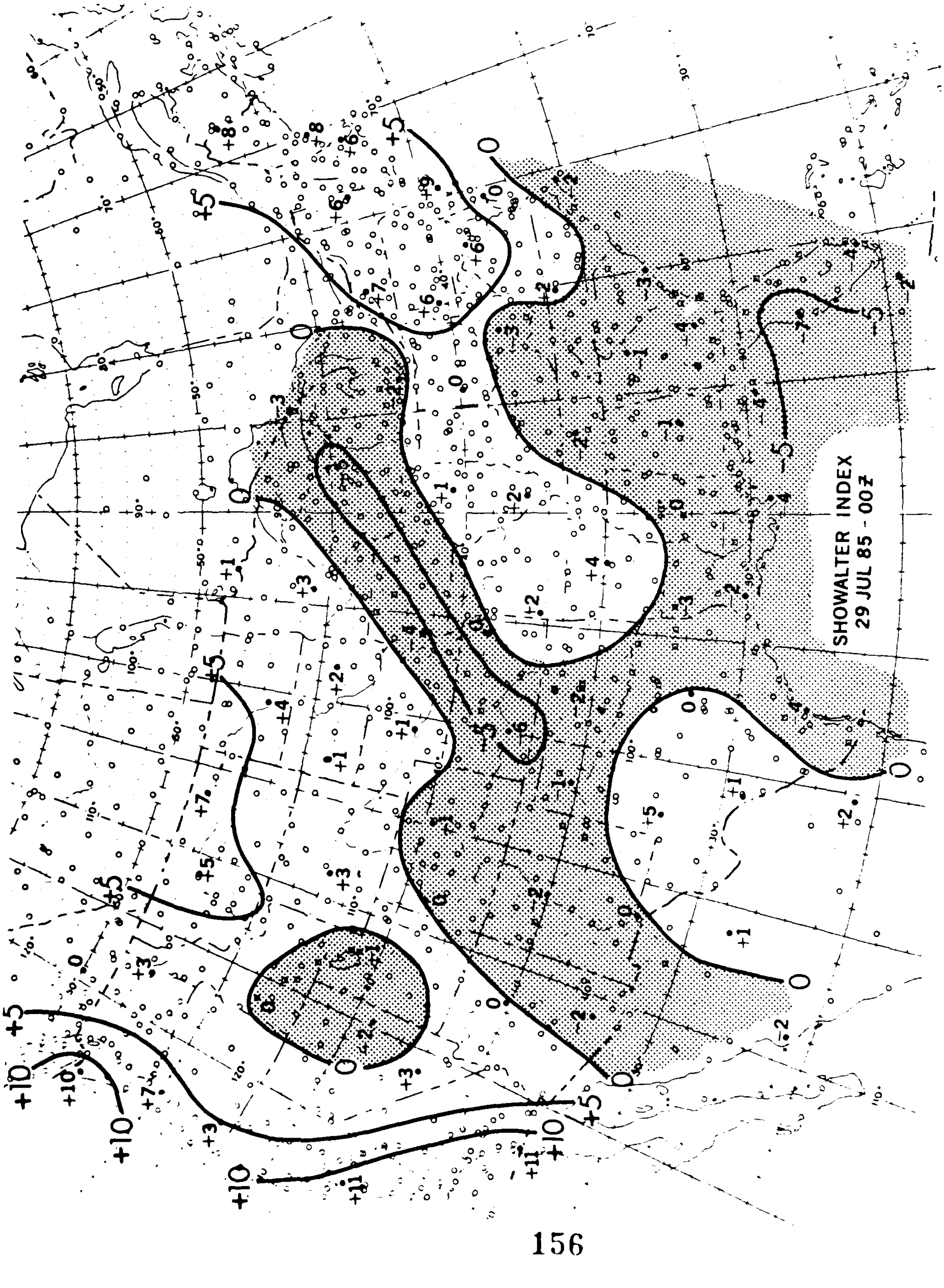
SHOWALTER INDEX
29 JUL 85 - 00Z

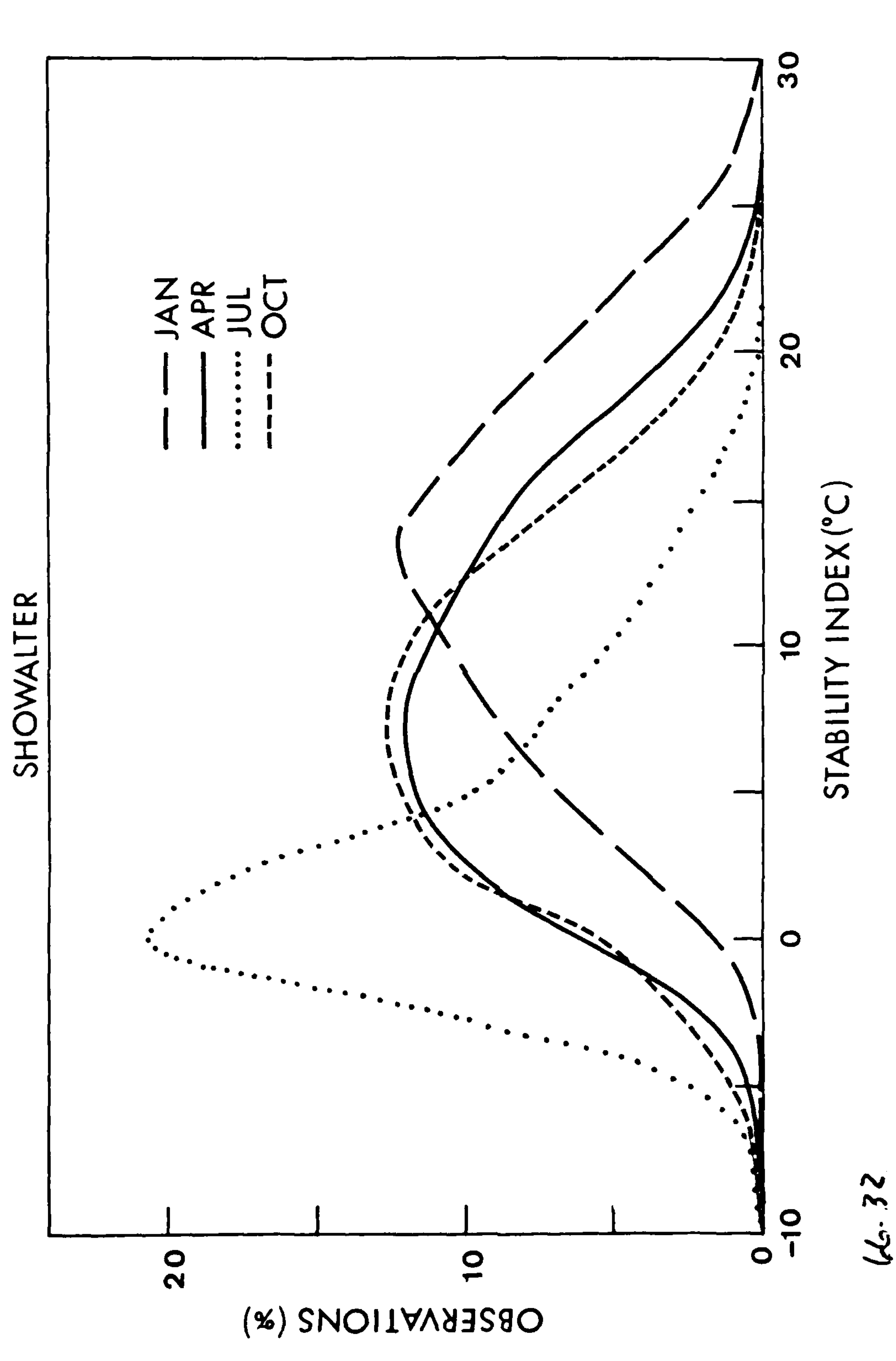
SHOWALTER
JAN
APR
JUL
OCT
OBSERVATIONS (%)
20
10
0
-10
0
10
20
30
STABILITY INDEX (°C)

fig. 32

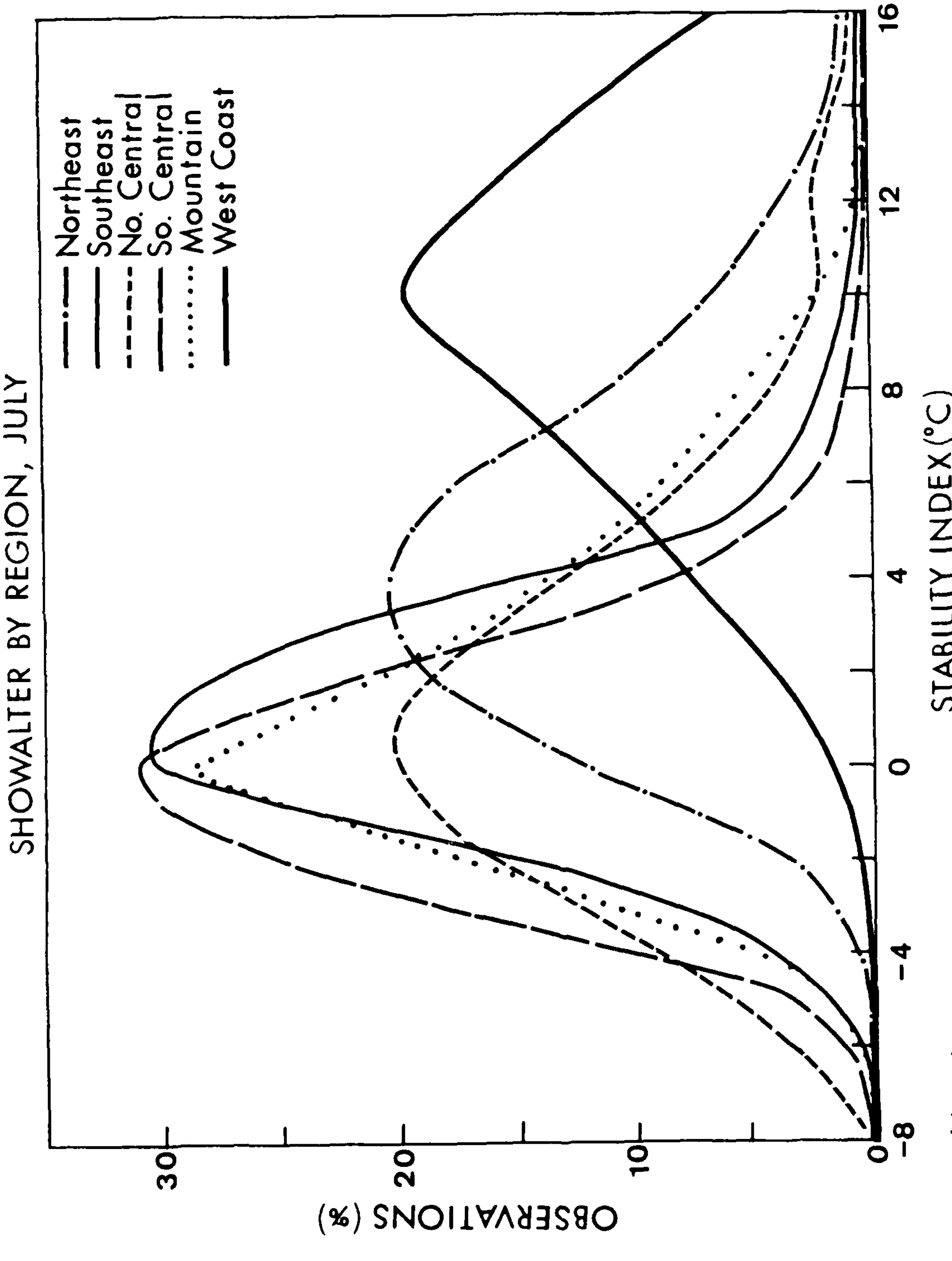
SHOWALTER BY REGION, JULY
Northeast
Southeast
No. Central
So. Central
Mountain
West Coast
OBSERVATIONS (%)
0
10
20
30
-8
-4
0
4
8
12
16
STABILITY INDEX (°C)

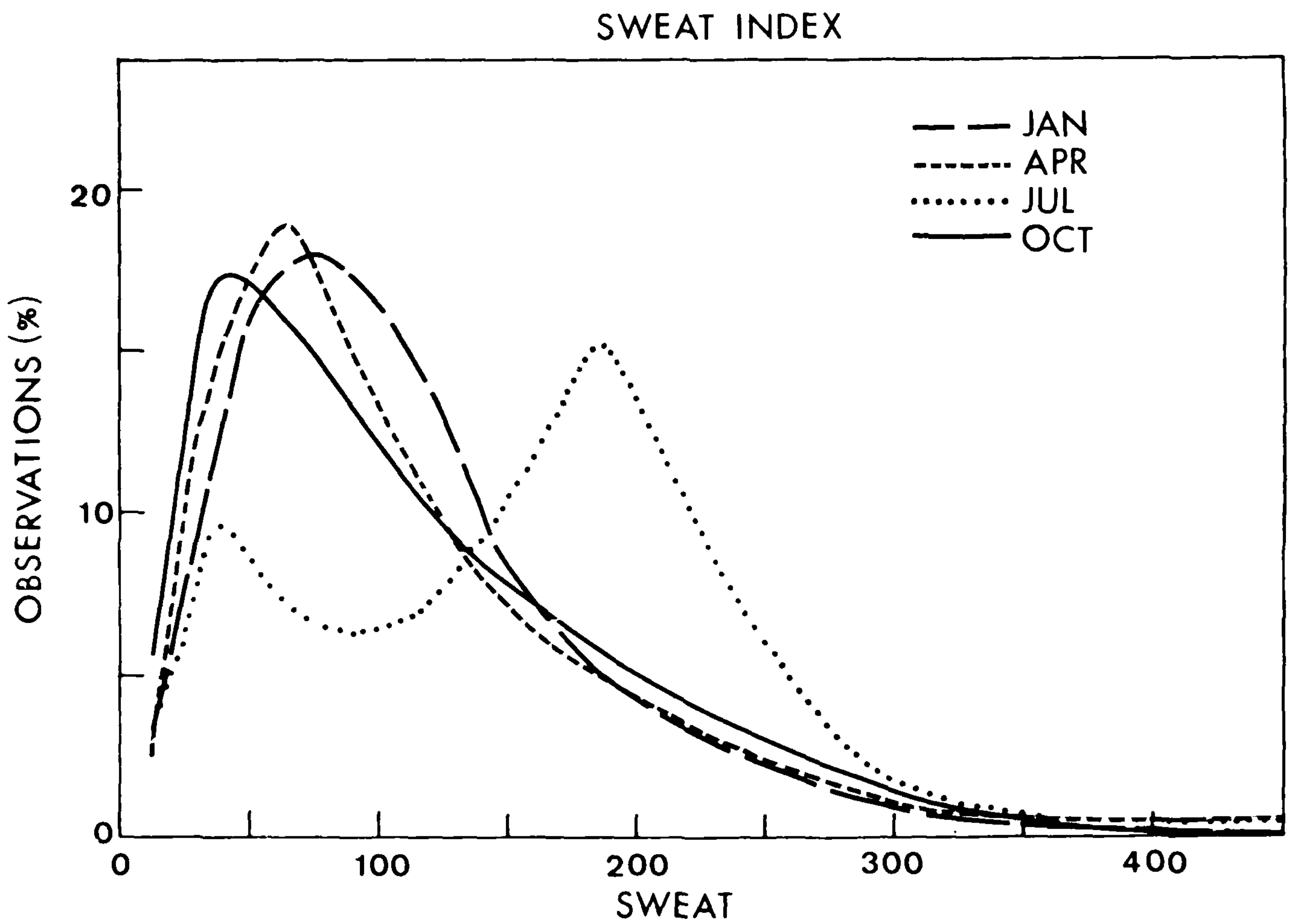
SWEAT INDEX
JAN
APR
JUL
OCT
OBSERVATIONS (%)
0
10
20
0
100
200
300
400
SWEAT

66.29

SWEAT BY REGION, JULY

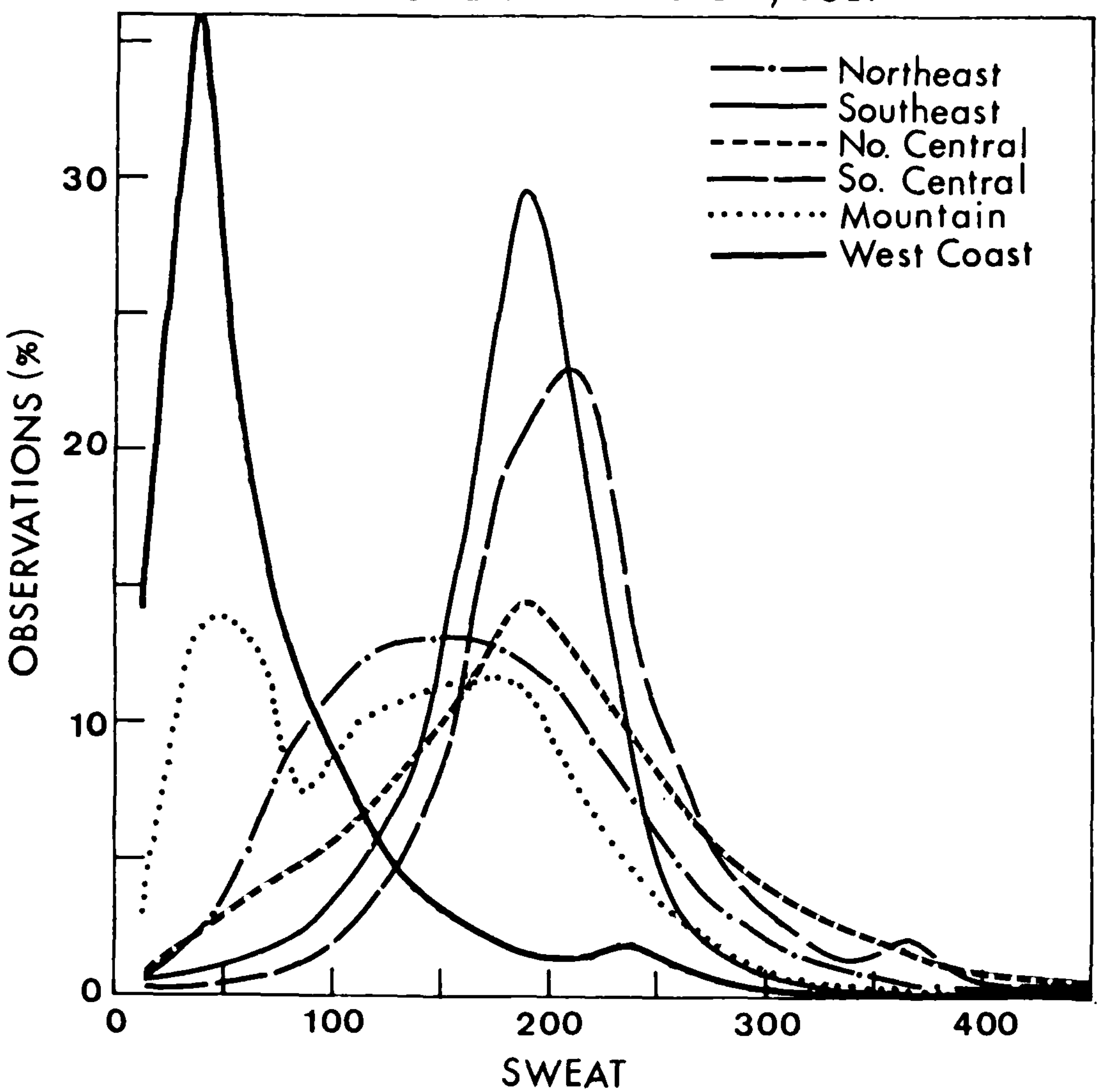

66·30

APPROACH: CRUDE EXAMPLE (using SSI)

Assume vertical smoke distribution can be described by

(1.)

$$p(z) = 30\,(z^4 - z^5) \qquad 0 \le z \le 1 \qquad \sim B(5,2)$$

cumulative distribution

$$S(z) = \begin{cases} 0 & z \le 0 \\ 6z^5 - 5z^6 & 0 < z < 1 \\ 1 & z \ge 1 \end{cases}$$

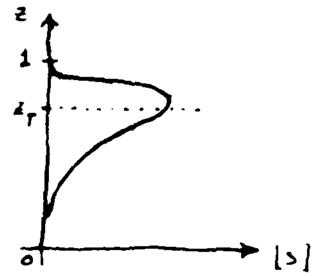

If z_T is taken to be the tropopause height, then

$S(z_T)$ represents the amount of smoke in troposphere

$1 - S(z_T)$ " amount of smoke in stratosphere

DISTRIBUTION APPROACH

Where does tropopause fall in the distribution of smoke?

(2.) let $z_T = z_T\,(SSI)$

e.g. $z_T = 0.9 + SSI/50$

Then:

SSI	z_T	$S_Z(z_T)$	$1 - S_Z(z_T)$
+5	1.0	1.00	0.0
0	0.9	0.89	0.11
−5	0.8	0.66	0.34

Now use observed SSI distributions to estimate stratospheric injection of smoke.

RESULTS: STRATOSPHERIC SMOKE INJECTION

	% of soot	T_g (NRC)	Optical Depth ½ hemisphere
JULY	7.5	11.3	0.5
JAN	0.6	0.9	0.04

STABILITY DISTRIBUTION APPROACH

(1.) Vertical soot profile – determine

here - assumed a B detrainment-like profile

(2) Relate stability (etc.) parameter to level of tropopause in this distribution

here - simple linear $z_T = 0.9 + \frac{SSI}{50}$

(3a) Climatological: use observed stability-parameter distributions to determine amount of soot at levels of interest

e.g. above tropopause

(3b) Model input (larger-scale): use model-derived values to calculate stability (etc.) parameter, then obtain geometric altitudes by multiplying distribution heights by actual tropopause height / z_T

SUMMARY

- Vertical soot profile, max. heights related to fire, atmosphere properties
- Should be able to determine a parameter which takes all these effects into account (?)
- How would such a parameter behave
  - Clues from stability indices - by season, region
- How could such a parameter be used to estimate vertical smoke profile info?
  - Crude example using SSI, assuming B dist'n of smoke in vertical
  - Estimated 7.5 % of smoke would enter stratosphere in July case. Corresponds to optical depth of 0.5 using NRC baseline data.

WHY BOTHER?

Framework, guidance in interpreting cloud observations and cloud model results.

Use model, obs:

- to find a suitable parameter
- to find an appropriate vertical soot profile
- to relate the two
- to evaluate the scheme.

Then use climo data to determine distributions of the parameter.

MULTIPLE PLUME FLOW FIELDS

HOWARD R. BAUM
NATIONAL BUREAU OF STANDARDS
GAITHERSBURG, MD. 20899

MASS FIRE BURN GEOMETRY

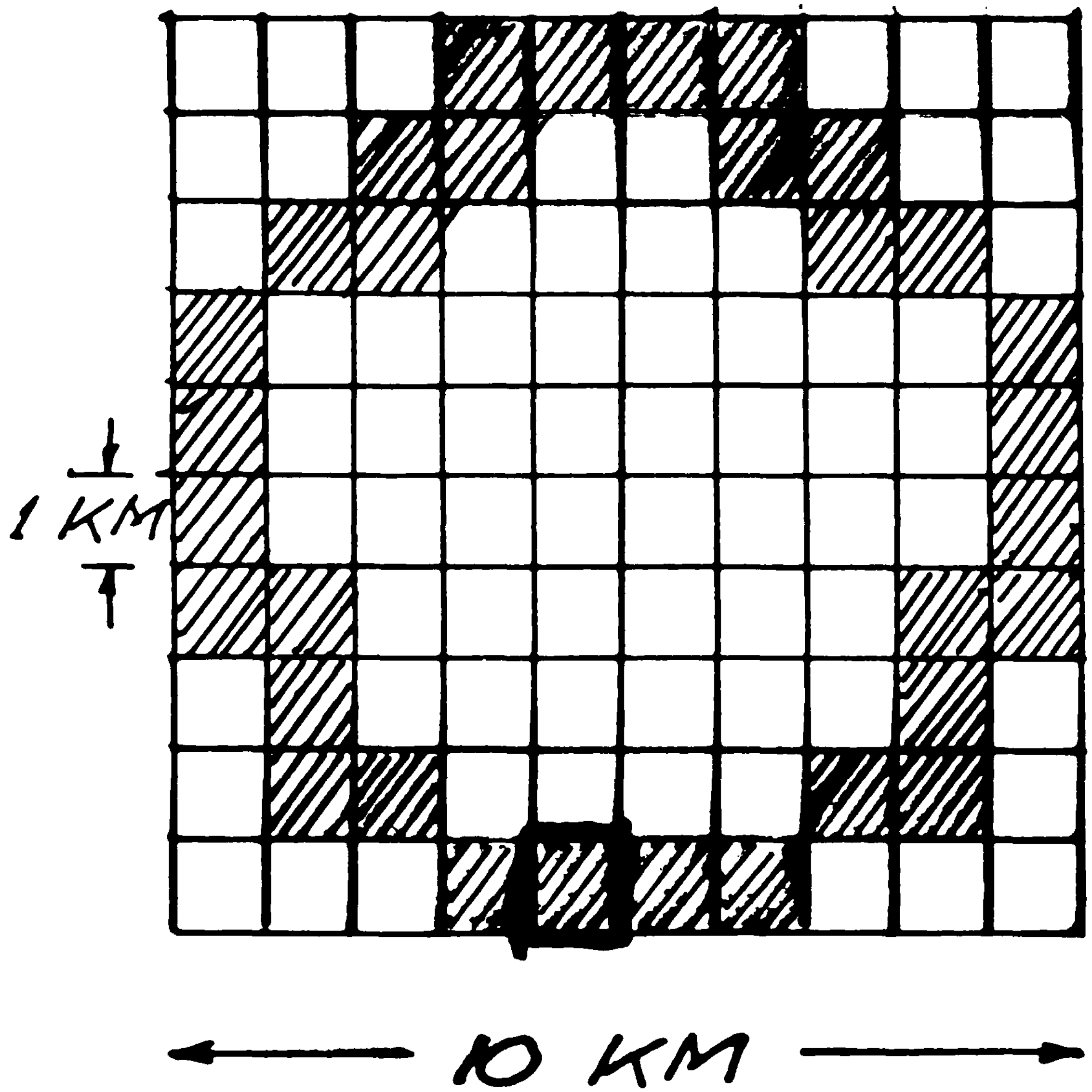

CROSS HATCH INDICATES BURNING AREA AT 1 KM RESOLUTION

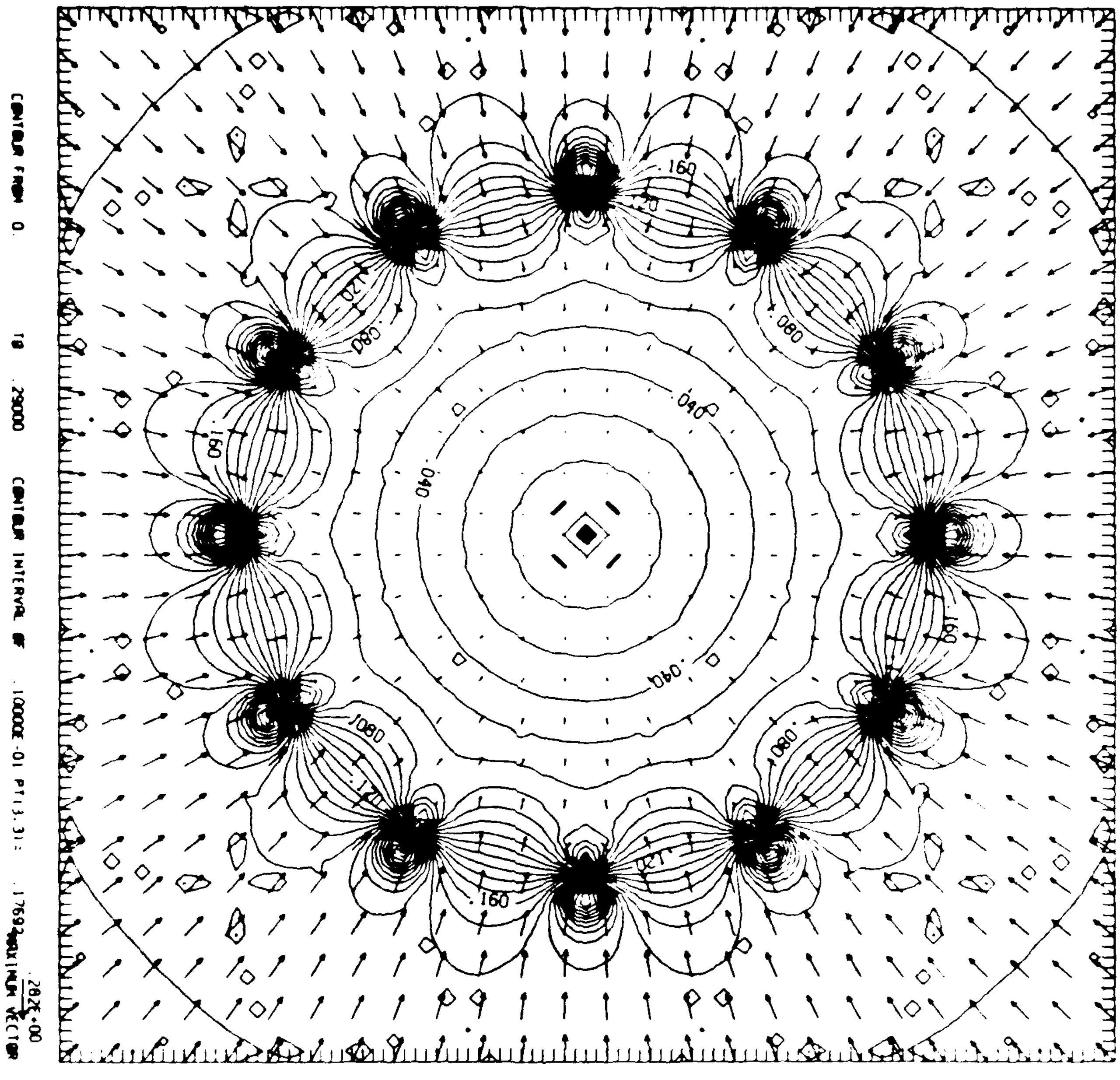
CONTOUR FROM 0. TO .29000 CONTOUR INTERVAL OF .10000E-01 PT(3,3)= .17692
MAXIMUM VECTOR .283E+00
.160
.120
.080
.040

VELOCITY DECOMPOSITION

$$\vec{u} = \nabla\phi + \vec{V}$$

$$\phi = \sum_i \phi_i$$

$$\vec{V} = \sum_i \vec{V}_i$$

$$\nabla^2\phi_i = \frac{\gamma-1}{\gamma P_0} Q_i$$

$$\nabla\cdot\vec{V}_i = 0$$

$$\nabla\times\vec{V}_i = \vec{\omega}_i$$

NOTE THAT ALTHOUGH EACH COMPONENT OF THE FLOW IS AXIALLY SYMMETRIC WITH RESPECT TO A LOCAL ORIGIN, THE NET RESULTANT FLOW IS THREE DIMENSIONAL.

ROLE OF KINEMATICS

CONSERVATION OF MASS & ENERGY TOGETHER WITH PERFECT GAS LAW YIELD

$$\nabla \cdot \vec{u} = \frac{\gamma - 1}{\gamma P_0} \sum_i Q_i$$

Q_i = LOCAL HEAT RELEASE RATE IN "i" TH PLUME

P_0 = AMBIENT PRESSURE
γ = SPECIFIC HEAT RATIO

THE VORTICITY FIELD $\vec{\omega}$ IS DEFINED IN TERMS OF THE VELOCITY $\vec{u}$ BY

$$\nabla \times \vec{u} = \vec{\omega}$$

GIVEN A REPRESENTATION FOR Q_i AND $\vec{\omega}$, THE VELOCITY FIELD IS DETERMINED UNIQUELY EVERYWHERE

REPRESENTATION OF $\vec{\omega}$

VORTICITY PRIMARILY IN PLUMES

$$\vec{\omega} = \sum_i \vec{\omega}_i$$

$\vec{\omega}_i$ = VORTICITY OF "i"$\underline{\text{TH}}$ PLUME

EACH PLUME IS AXIALLY SYMMETRIC

$$\vec{\omega}_i \cong \omega_\theta \hat{\theta}_i$$

$\hat{\theta}_i$ = UNIT VECTOR IN LOCAL AZIMUTHAL DIRECTION

$$\omega_\theta \cong \frac{\partial u_z}{\partial r}$$

$$= -\frac{2U_0(z)}{R(z)}(r/R)\exp\left\{-(r/R)^2\right\}$$

$U_0(z)$ = CENTRLINE VELOCITY OF PLUME

$R(z)$ = LOCAL PLUME WIDTH

SCALING LAWS

$$D^* = \left\{ Q_0 / \rho_0 C_p T_0 \sqrt{g} \right\}^{2/5}$$

$$\vec{u} = (gD^*)^{1/2} \, \vec{u}^*(r^*, z^*)$$

$$r^* = r/D^* \; ; \; z^* = z/D^*$$

$$\omega_\phi = (g/D^*)^{1/2} \, \omega^*(r^*, z^*)$$

$$\phi = (gD^*)^{1/2} D^* \, \bar{\Phi}^*(r^*, z^*)$$

$$\psi = (gD^*)^{1/2} D^* \, \bar{\Psi}^*(r^*, z^*)$$

THIS SCALING LEADS TO A "UNIVERSAL" FLOW FIELD WHICH DEPENDS ONLY ON THE RADIATED FRACTION OF THE CHEMICAL HEAT RELEASE

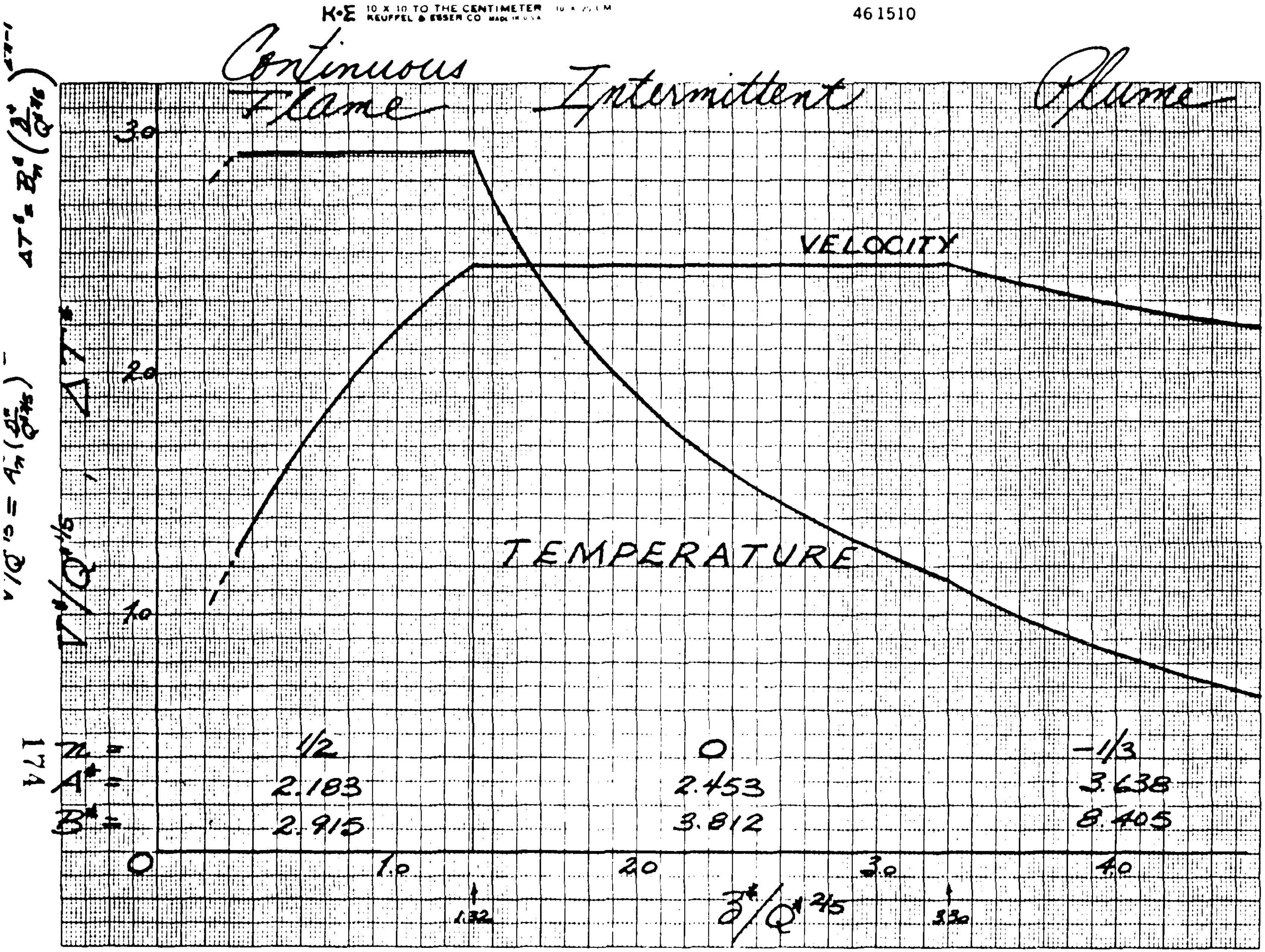

$z^* = z/D$; $Q^* = Q/\rho_\infty C_p T_\infty \sqrt{gD}\, D^2$; $V^* = V/\sqrt{gD}$ · $\Delta T^* = \Delta T/T_\infty$

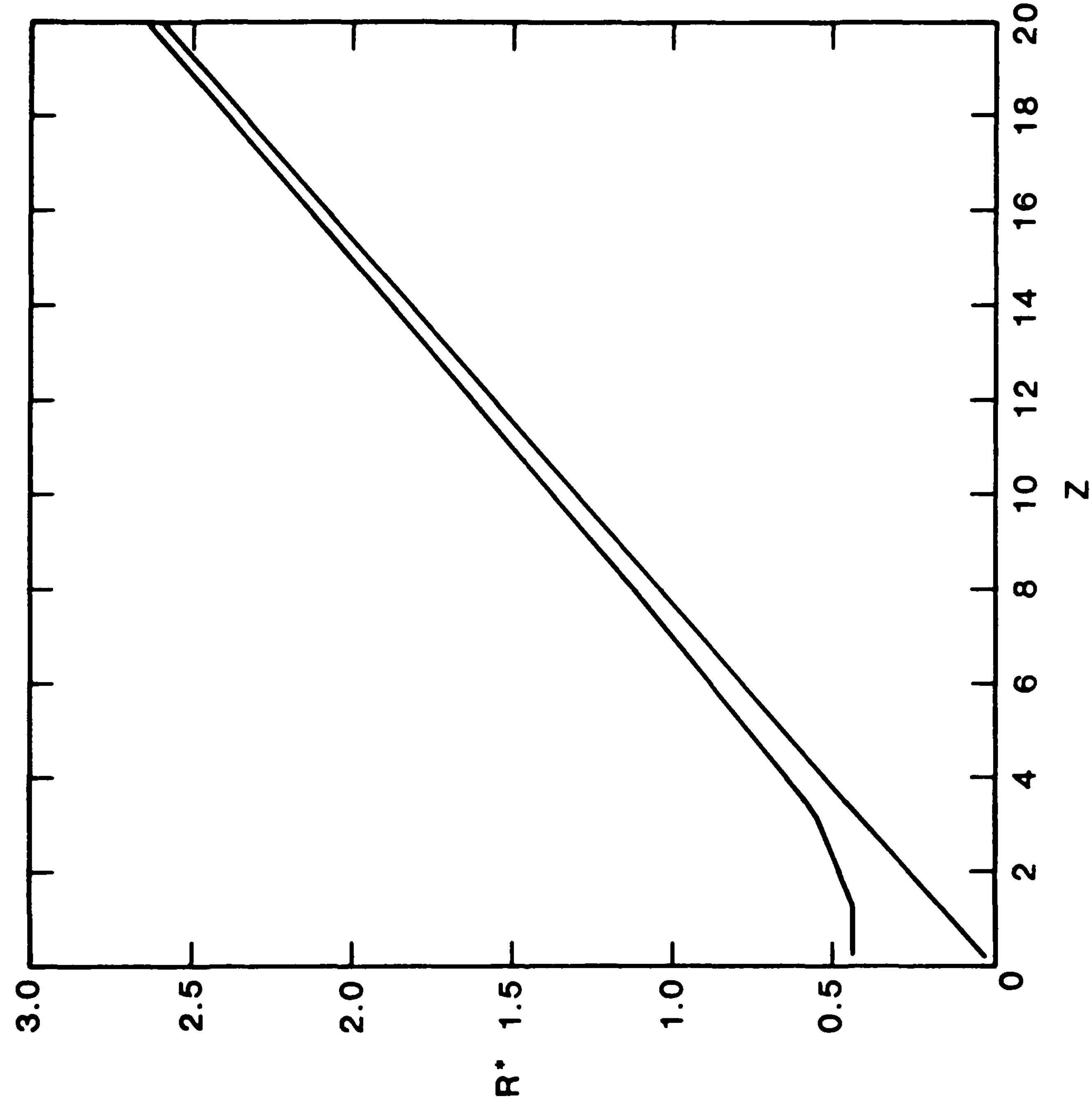
R*
3.0
2.5
2.0
1.5
1.0
0.5
0
2
4
6
8
10
12
14
16
18
20
Z

VECTOR POTENTIAL EQ.

$$\frac{\partial^2 \Psi^*}{\partial z^{*2}} + \frac{\partial^2 \Psi^*}{\partial r^{*2}} - \frac{1}{r^*}\frac{\partial \Psi^*}{\partial r^*} = -r^* \omega^*$$

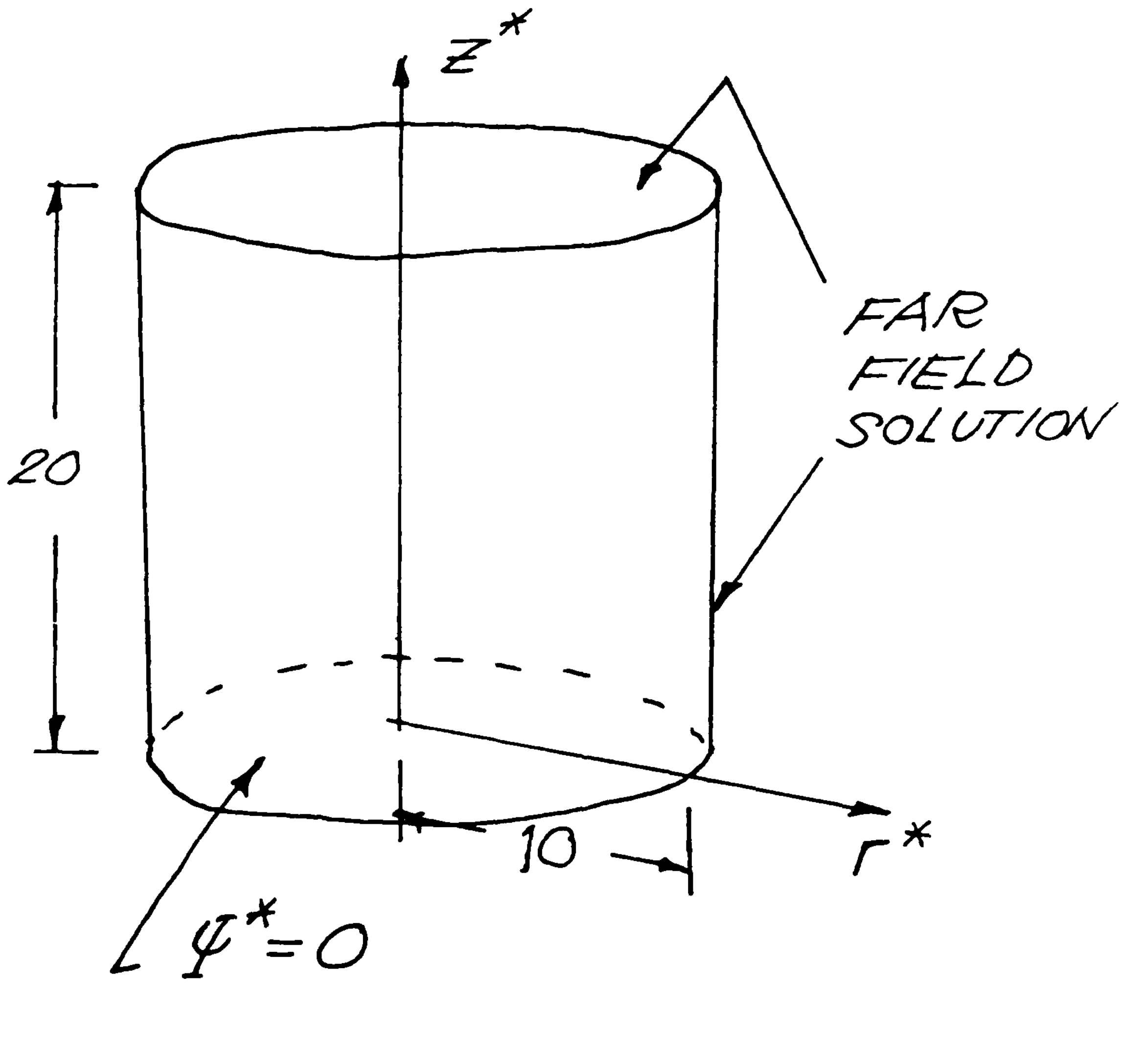

POINT SOURCE PLUME

$$\Psi^* = \rho^{5/3} F(\mu)$$

$$\omega^* = \rho^{-4/3} \Omega(\mu)$$

$$\rho^2 = r^2 + z^2$$

$$\mu = \cos\theta$$

$$\frac{d^2F}{d\mu^2} + \frac{10}{9(1-\mu^2)} F = -\frac{\Omega(\mu)}{\sqrt{1-\mu^2}}$$

$$r = \rho \sin\theta \; ; \; z = \rho\cos\theta$$

$$F(0) = F(1) = 0$$

THE SOLUTION TO THIS PROBLEM GENERATES THE FAR FIELD FOR EACH PLUME

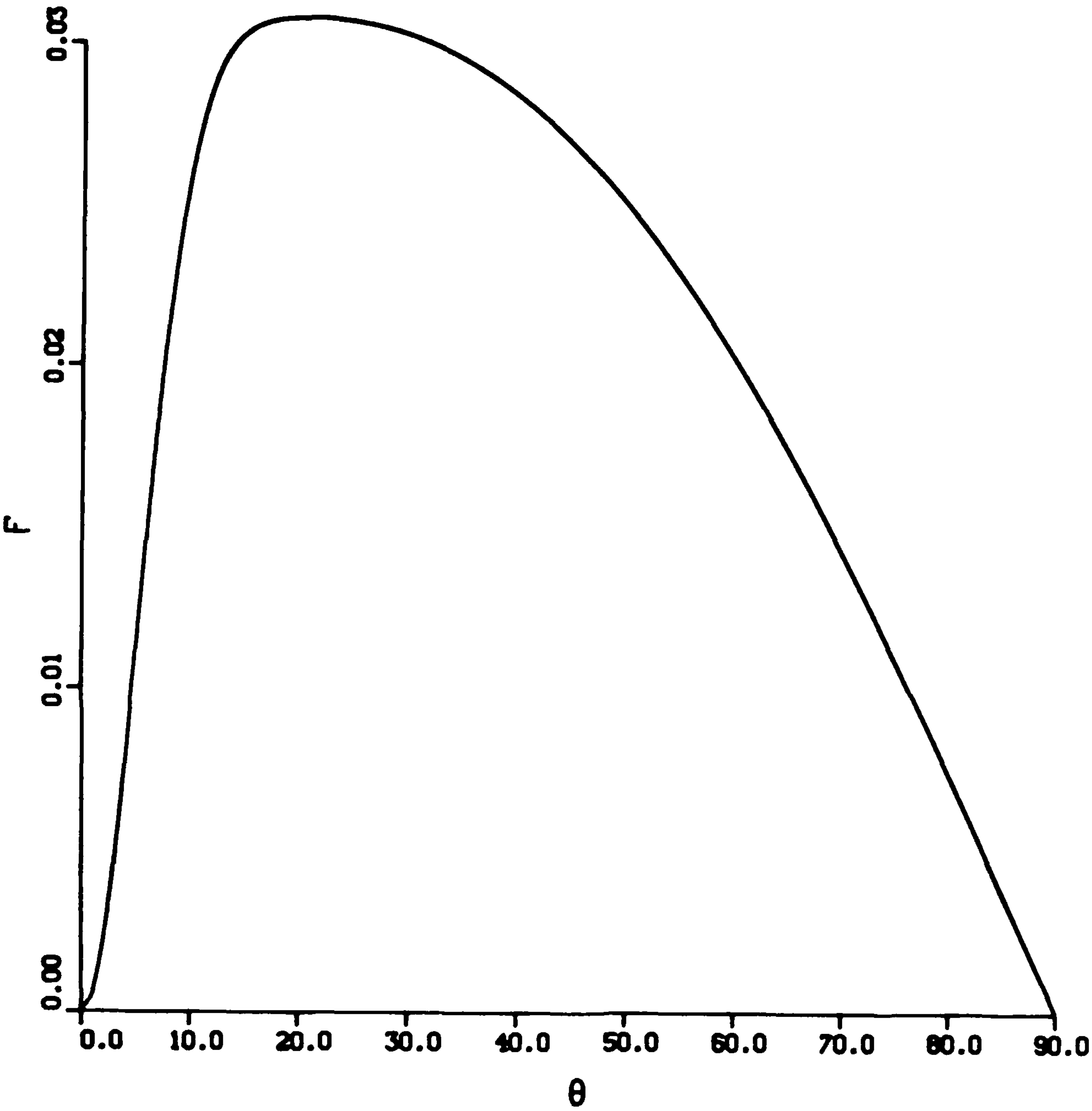

0.03
0.02
0.01
0.00
F
0.0
10.0
20.0
30.0
40.0
50.0
60.0
70.0
80.0
90.0
θ

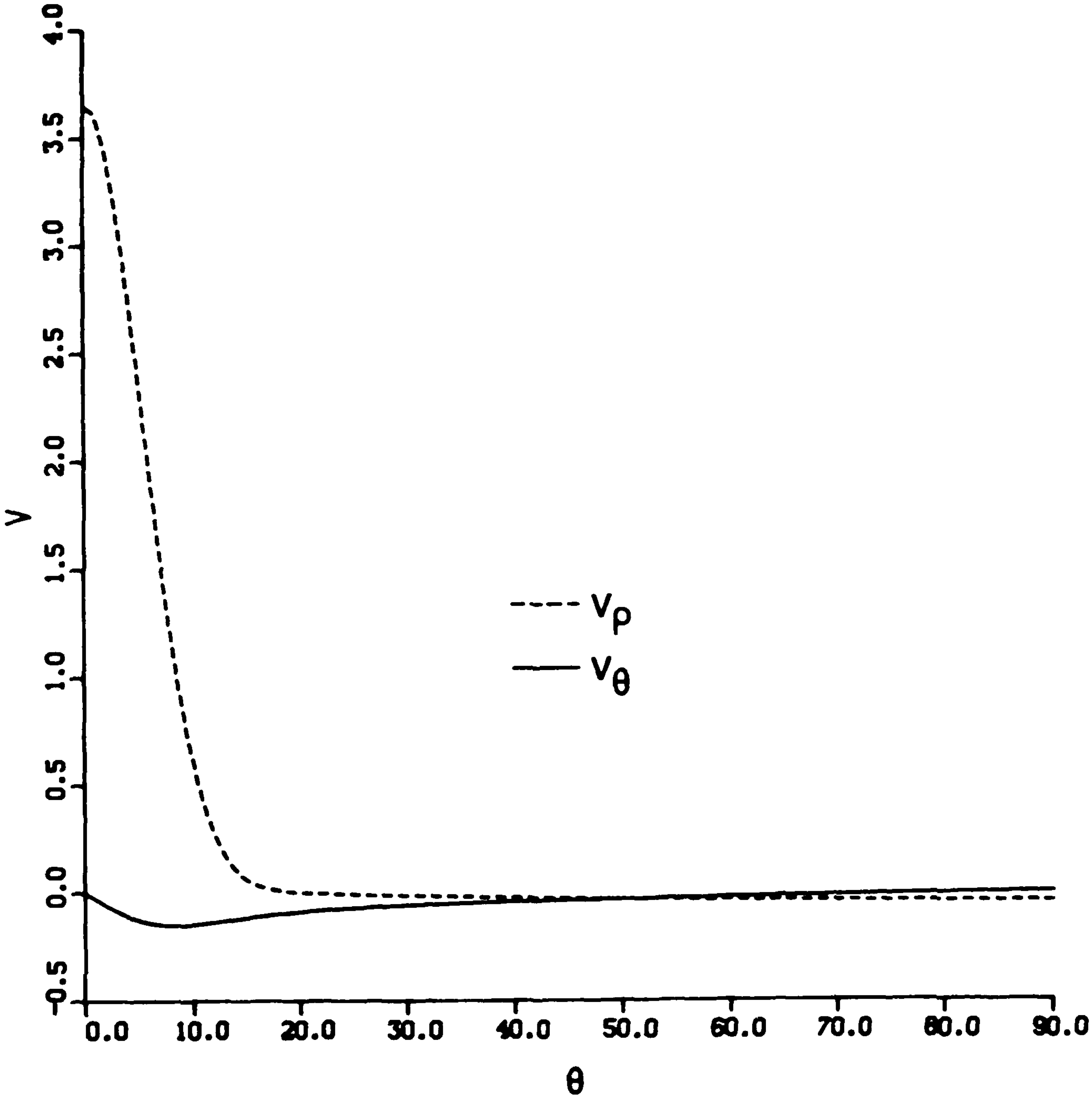

4.0
3.5
3.0
2.5
2.0
1.5
1.0
0.5
0.0
-0.5
V
V_ρ
V_θ
0.0
10.0
20.0
30.0
40.0
50.0
60.0
70.0
80.0
90.0
θ

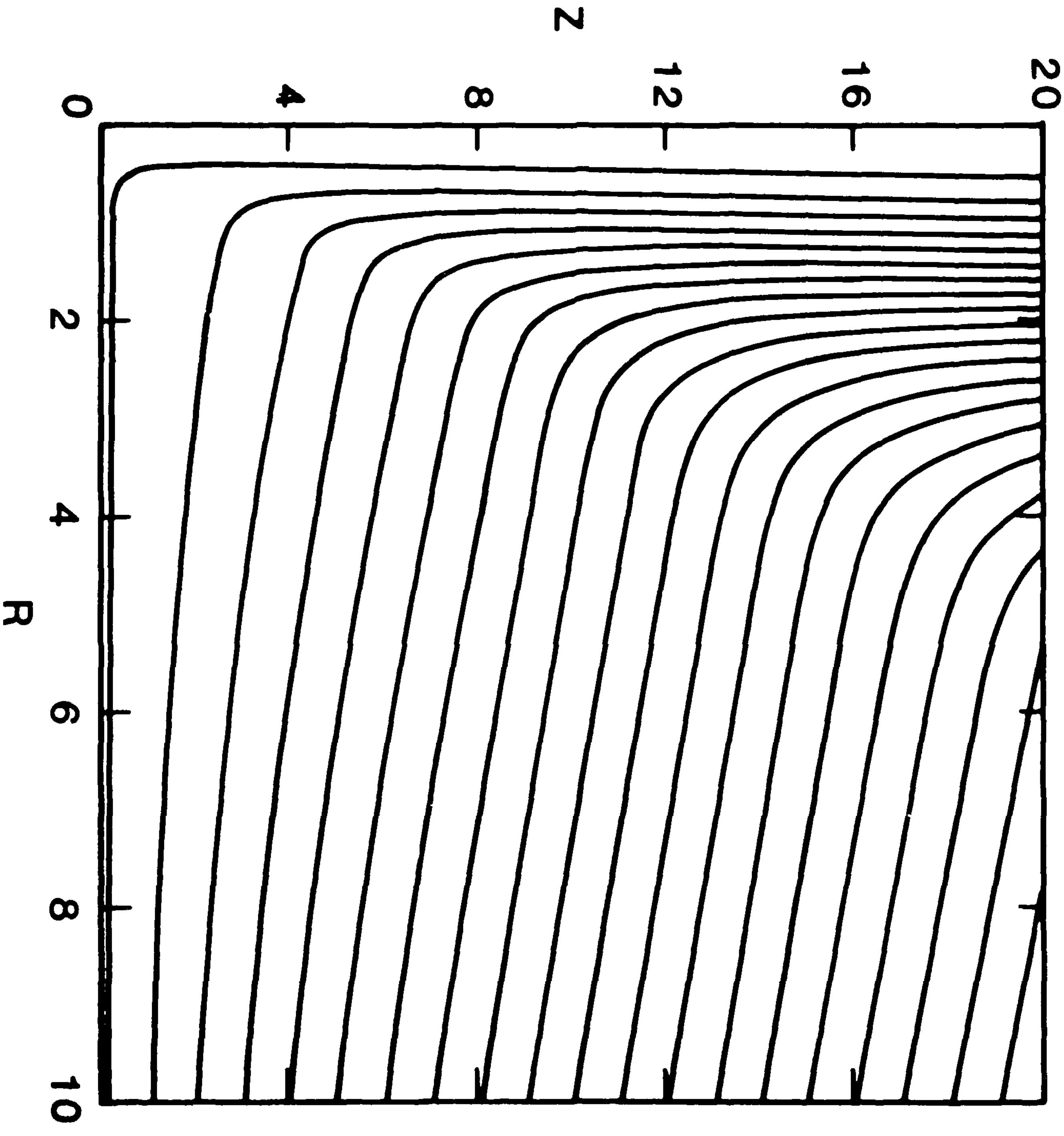
Z
20
16
12
8
4
0
R
2
4
6
8
10

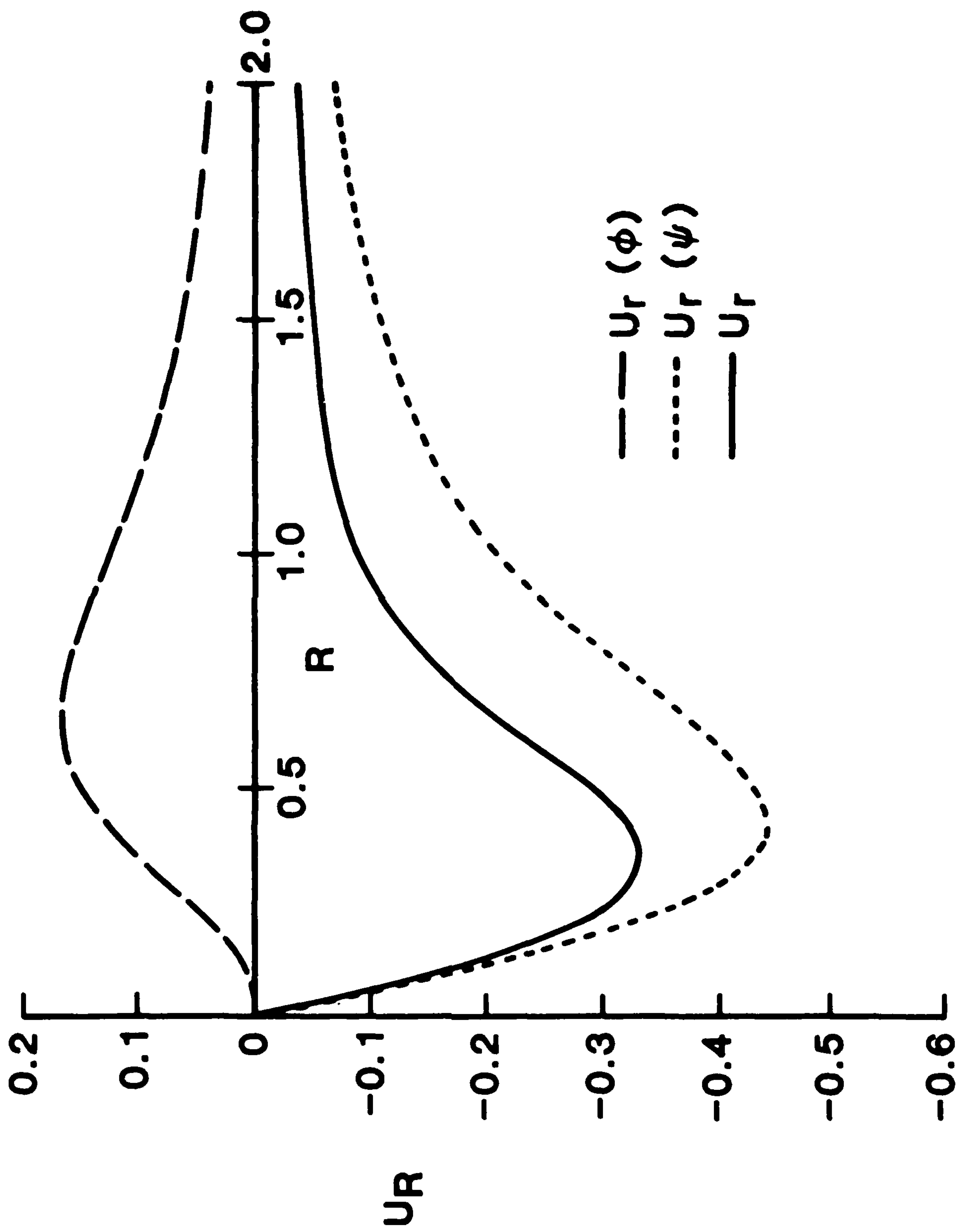

UR
R
0.2
0.1
0
-0.1
-0.2
-0.3
-0.4
-0.5
-0.6
0.5
1.0
1.5
2.0
ur (φ)
ur (ψ)
ur

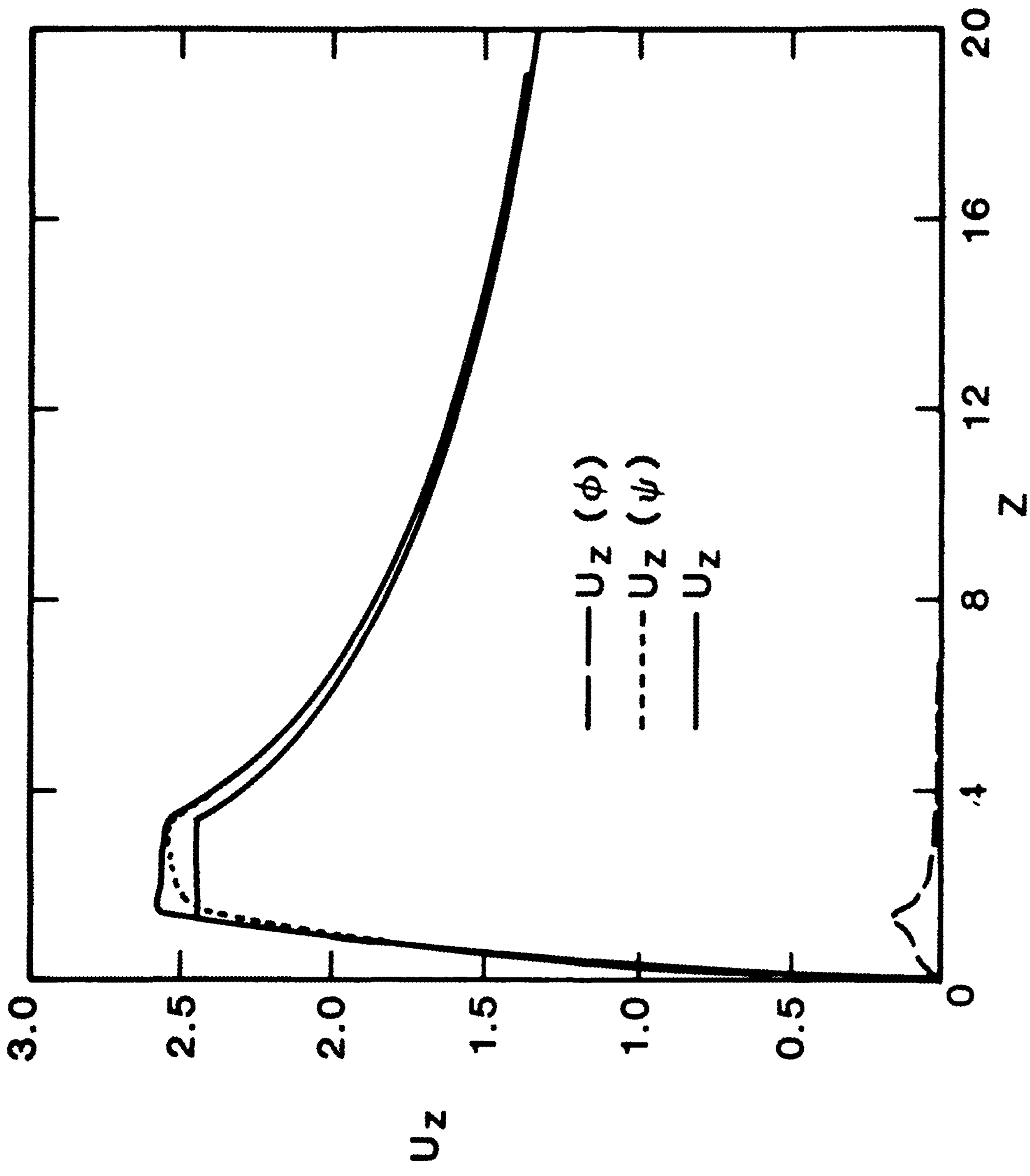

U_z
3.0
2.5
2.0
1.5
1.0
0.5
0
4
8
12
16
20
Z
U_z (ϕ)
U_z (ψ)
U_z

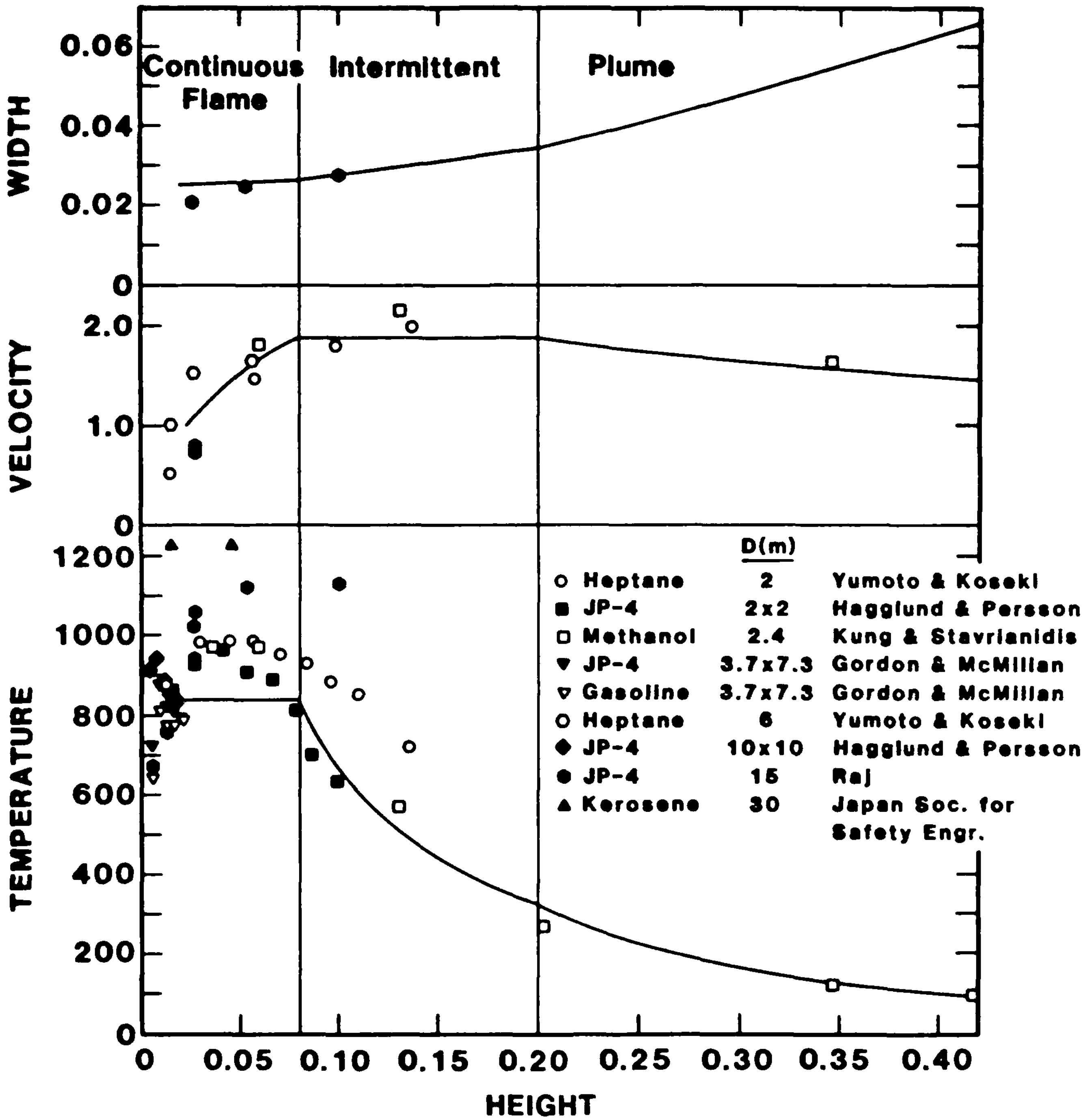

Continuous Flame
Intermittent
Plume
WIDTH
0.06
0.04
0.02
0
VELOCITY
2.0
1.0
0
TEMPERATURE
1200
1000
800
600
400
200
0
HEIGHT
0
0.05
0.10
0.15
0.20
0.25
0.30
0.35
0.40
D(m)
Heptane 2 Yumoto & Koseki
JP-4 2x2 Hagglund & Persson
Methanol 2.4 Kung & Stavrianidis
JP-4 3.7x7.3 Gordon & McMillan
Gasoline 3.7x7.3 Gordon & McMillan
Heptane 6 Yumoto & Koseki
JP-4 10x10 Hagglund & Persson
JP-4 15 Raj
Kerosene 30 Japan Soc. for Safety Engr.

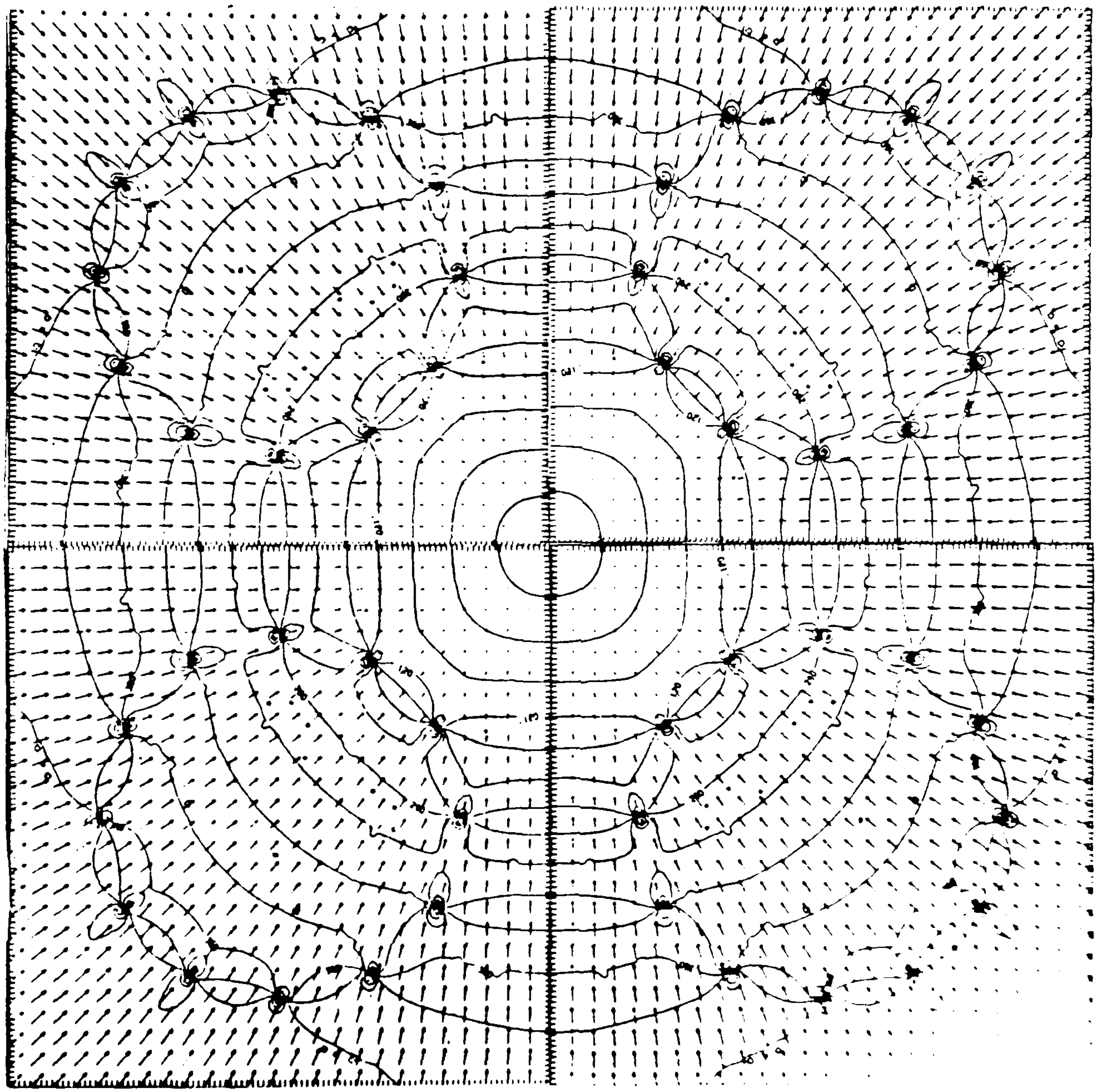

AD-A185 150 TECHNICAL PAPERS PRESENTED AT THE DEFENSE NUCLEAR AGENCY GLOBAL EFFECTS R..(U) DOD NUCLEAR INFORMATION AND ANALYSIS CENTER SANTA BARBARA CA.. 15 MAY 86 3/4

UNCLASSIFIED DASIAC-TN-86-29-VOL-2 DNA001-82-C-0274 F/G 15/6.4 NL

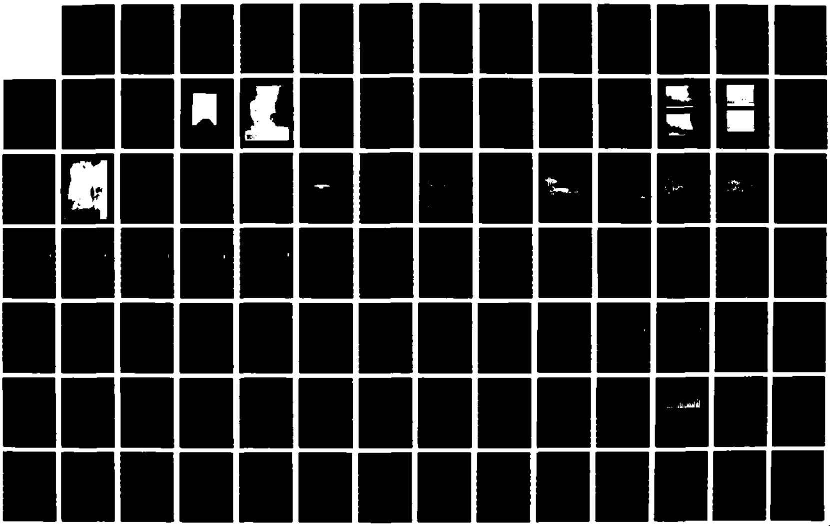

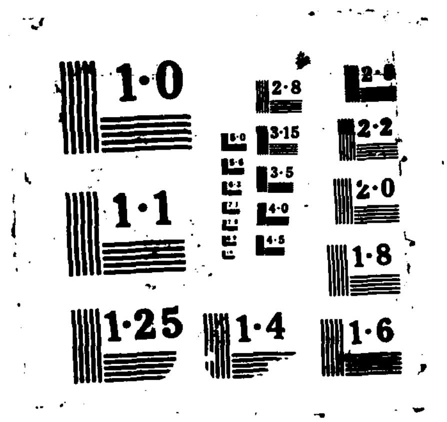
1·0
2·8
3·15
3·5
4·0
4·5
2·2
2·0
1·1
1·8
1·25
1·4
1·6

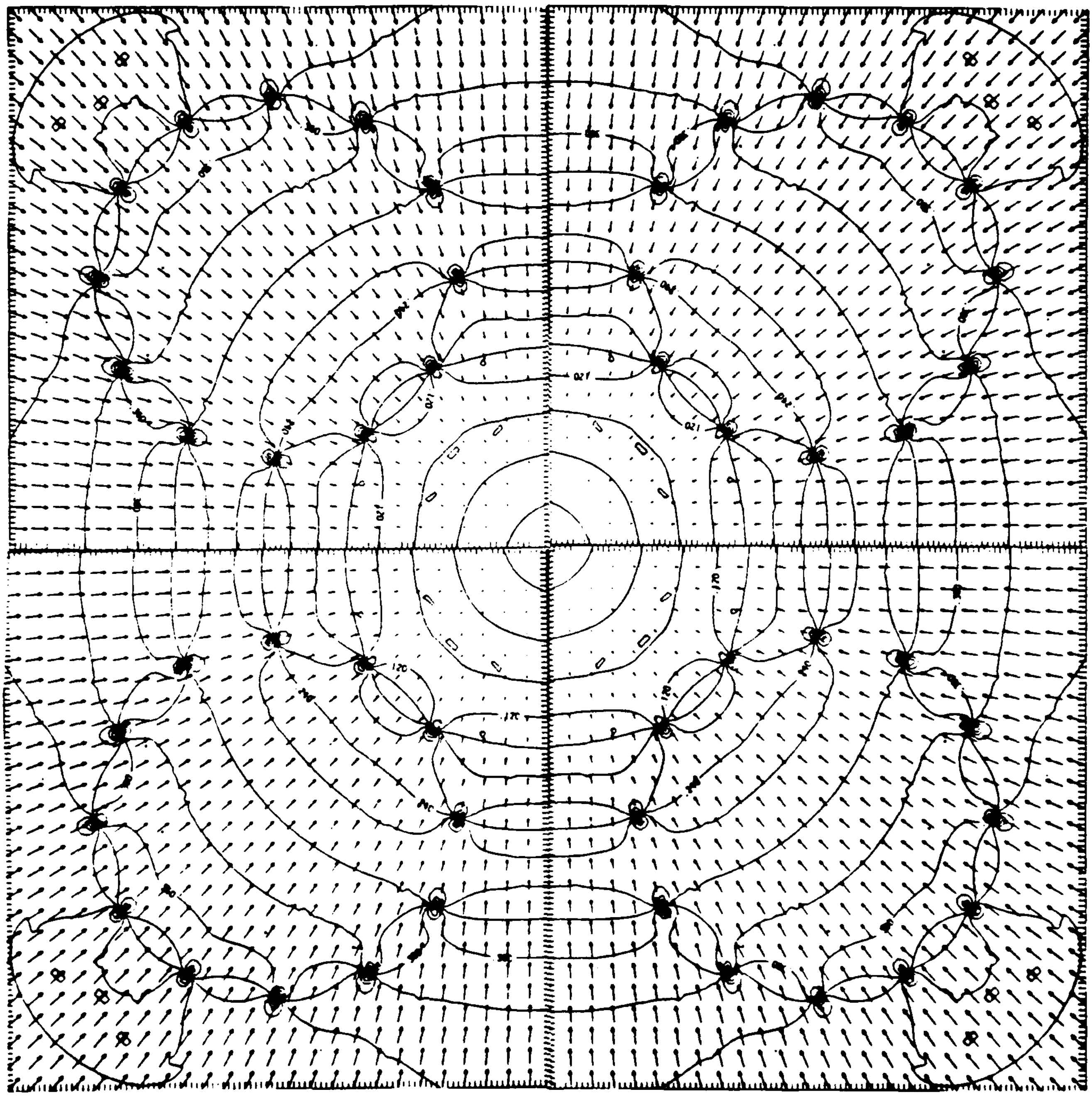

CAPABILITIES

1) VERY GENERAL FIRE PLANFORM

2) PERMITS MODELING FROM ESTABLISHED DATABASE

3) RANDOM AS WELL AS DETERMINISTIC INPUT IN SIZE AND LOCATION

4) HIGH SPATIAL RESOLUTION FOR MODEST COMPUTER RESOURCES

PHYSICAL SIMULATION OF LARGE-AREA FIRE PLUMES*

by

M. Poreh, J. E. Cermak and J. A. Peterka

Fluid Mechanics and Wind Engineering Program
Department of Civil Engineering
Colorado State University
Fort Collins, Colorado 80523

CSU Project 2-95660

This work was sponsored by the Defense Nuclear Agency under
RDT E RMSS Code B3450 83466 G54CMXG D 00002 H2590D

March 1986 CEP85-86MP-JEC-JAP19

---

*Presented at the Global Effect Program Technical Meeting, of the Defense Nuclear Agency, 25-27 February, 1986, NASA Ames Research Center, California.

PHYSICAL SIMULATION OF LARGE-AREA FIRE PLUMES

by

M. Poreh, J. E. Cermak and J. A. Peterka

ABSTRACT

The dynamics of large-area fire plumes has been investigated by physical simulation using small-scale models. The models use heat or helium to generate the buoyancy flux. They neglect the radiative heat transfer and assume a relatively shallow combustion layer, an assumption which is found to be consistent with the measurements in the model, but maintain the correct dimensionless parameters which determine the dynamics of the plume outside the combustion layer.

Four regions of distinct flow characteristics have been identified. A combustion layer whose height is small compared to the horizontal dimension of the fire. A radial convective boundary layer, where radially-inward induced winds carry the rising plume toward the center. A central core and a convective plume above it, which rises to large heights.

Vigorous mixing with the ambient air occurs in the radial convective boundary layer, where the hot burned fuel rises in the form of thermals. Such thermals are formed for both continuous combustion layers and for large fires which are made of many distinct, close, small fires. It is found that these two cases produce similar plumes.

The simulations show that the plume above the burning area contracts considerably as it rises, and that the upper convective plume behaves as a weak plume with a virtual origin below the

surface, at Z/R of the order of -1.5. The subsequent plume rise in an upper stably-stratified atmosphere would thus be much smaller than that of a plume originating from a point source at the ground, with the same buoyancy flux.

The simulations also show that the induced radial velocities of a large-area fire in a calm neutral atmosphere are not as large as those estimated by previous numerical and analytical models. In addition, the study suggests that the kinetics of a single fire, which is surrounded by numerous other fires would not be much different from that of an individual fire in a calm atmosphere, as oxygen depletion is found to decrease with the size of the fire.

SUMMARY OF THE PRESENTATION

Simulation Rationale

- The simulation is based on the conventional approach to fluid modelling. All the important dimensionless parameters and boundary conditions must be the same in the model and prototype ($\pi_m = \pi_p$).
- The Reynolds number in the model cannot be matched with that of the prototype. However, it is shown to be large, so that 'Reynolds number independence' is expected.
- The models neglect radiative effects.
- It is assumed that the relative thickness of the combustion layer (CL) in large-area fires is small compared to the size of the fire. Thus, the model simulates the flow above the relatively shallow CL.
- The flow above the CL is assumed to be governed by

  σ - The buoyancy flux per unit area produced in the CL, which is proportional to the burning ratio (J/sec) $[\sigma] = L^2/T^3$.

  R - The size (radius) of the (assumed circular) CL.

  π_i - Dimensionless boundary conditions describing the ambient wind, ambient circulation and atmospheric stratification.

The presentation focuses on Large Area Fires (LAF) in a calm, neutrally stratified atmosphere. It has been shown, however, that the physical simulation can include the effects of ambient stratification and circulation (Poreh et al., 1986).

The above assumptions imply that the velocity field $u(\vec{x})$ and the effective gravitational field $g'(\vec{x}) = g\Delta\rho(x)/\rho_a$ are given by

$$\frac{u(\vec{x})}{(\sigma R)^{1/3}} = f(\vec{x}/R) \tag{1}$$

and

$$\frac{g'(\vec{x})}{\sigma^{2/3}\ R^{-1/3}} = g(\vec{x}/R) \tag{2}$$

Buoyancy flux in the models have been generated by:

(1) Heat flux, as suggested by R. R. Long.

(2) Flow of lighter-than-air gas (helium) from a porous circular plate.

It is noted that the value of $\Delta\rho/\rho_a$ of helium is approximately equal to that of burned fuel at stoichiometric proportions (BFSP). Namely, ideal burning of the fuel without mixing with surplus air. Thus, the model simulates an area source of buoyancy produced by a flux of BFSP before it mixes with additional air.

Theoretical considerations and previous experience suggest that $\Delta\rho/\rho_a$ of the buoyant gases at the source need not be the same in the model and the prototype, unless a strong whirl is expected. This assumption is confirmed by the experimental results (Fig. 6). The value of $\Delta\rho/\rho_a$ in one of the model ($R = 50$ cm) was matched with the expected value in a $R = 2$ km urban fire.

Experimental Configuration (Figure 1)

- Two circular helium models with $R = 27$ cm and $R = 50$ cm were used.
- A two-dimensional area source (2 m x 2 m) was placed in a 2 m wide test section of a wind tunnel.

Summary of the Experimental Results

- The shape of the plume based on flow visualization and helium concentration measurements is shown in Figures 2 and 3. Considerable necking of the plume is observed, similar to the necking of a 14 acre fire in Project Flambeau (Figure 4).
- Four regions of distinct flow were identified (Figure 3):

(1) A relatively shallow CL.

(2) A radial convective boundary layer.

(3) A central core.

(4) A convective plume. The convective plume which can be described as a plume from a virtual point source at approximately $z_v = -1.5$ R.

The assumption of a relatively small thickness of the combustion layer is based on the flame height correlation of Thomas (1963) shown in Figure 5. The value of $m''/(\rho_o \sqrt{gD})$ for large urban fires is expected to be of the order of 10^{-5}, so that the ratio of the flame height to the size of the fuel bed (L/D) is expected to be, according to this correlation, of the order of 10^{-2}.

The model does not have a CL. However, a 'pseudo combustion layer' (PCL) has been defined by the height where the injected helium mixes with 6 times air by mass. This is the order of the observed mixing at the edge of turbulent combustion layers. The thickness of this PCL in the model was smaller than 1 mm, as shown in Figure 6. This figure, which shows the value of the dimensionless gravity coefficient $g'(z)$ in the two circular models also confirms the validity of Eq. 2. Near the ground; however, the value of g' may be affected by its initial value at the source.

Since g' is proportional to $\Delta\rho/\rho_a$, which is approximately proportional to $\Delta T/T_a$, the order of magnitude of $\Delta T/T_a$ in large-area fires was estimated (Figure 7).

The conclusion that $\Delta T/T_a$ in the fire plume decreases with the size of the fire appears surprising, but it is a direct consequence of Eq. 2. One may also conclude that the average oxygen depletion in large-area fire plumes is smaller than in small-area fires. This conclusion does not imply that large oxygen depletion cannot exist within individual fires burning within a LAF.

Induced Radial Velocities

The induced radially-inward velocities at the edge of the fire were found to be

$$U_R = k(\sigma R)^{1/3}$$

where $k = 0.24 - 0.5$, much smaller than in numerical models and in reports on large-area fires. (It should be stressed that the

above estimate is for fires in a calm, dry, neutrally stratified atmosphere.)

Figure 8 compares the shape of the radial velocity profile for a point source of buoyancy (a) and for an area source of buoyancy (b), which can be described, at $z > R$, as a convective plume from a virtual source at Z_v. The figure demonstrates why, for the same buoyancy flux, the induced radial velocities increase when z_v is decreased. The conclusion is that area sources produce large inward-radial velocities which depend on the effective necking of the plume.

Estimated Plume Rise in a Stably-Stratified Atmosphere

Briggs equation or the analysis of Morton, Turner and Taylor are for a buoyant plume from a point source. The initial mixing in the radial convective boundary layer (CBL) of an area source would decrease the final plume rise.

Figure 9 shows a rough estimate of the plume rise for an area source with a given total buoyancy flux as a function of the position of the virtual origin. The estimate is based on the assumption that the behavior of the plume at $z > 0$ may be calculated using the width of the virtual plume at $z = 0$. The data is for a buoyancy flux produced by a 100 km^2 fire.

The average plume rise for $z_v = 0$ is identical with the estimate given in the NCR report (1985, p. 74). One clearly sees from Figure 10 that the plume rise is reduced drastically with the lowering of the virtual origin. At $z_v/R = -1.5$ one gets an average plume rise of the order of 5 km.

This drastic reduction is initially surprising. However, if one examines the theoretical solution of Morton et al. for the loss of buoyancy flux from a point source with height (Figure 10), which shows that most of the buoyancy flux is lost when the plume achieves a large width, the reason for the large difference in plume rise between point sources and area sources becomes clear.

It is interesting to note that while lowering of z_v decreases the plume rise, it increases the induced radial velocities.

The Nature of the Radial Convective Boundary Layer (CBL)

The CBL is the largest region above the combustion layer. Our study indicates that it is very similar to atmospheric CBL:

- The Monin-Obukhov length is very small $L/R = O(10^{-4})$.
- The effect of the horizontal shear is small and the induced horizontal velocities do not cause mixing.
- Buoyancy flux is in the form of thermals with large upward velocities, $w_z > U_R$.
- To satisfy continuity fresh cool air descends to the ground between the thermals (or the individual fire plumes).
- Rapid dilution of individual fire plumes is expected.

The flow visualization in Figure 11 shows the radial CBL in the two-dimensional fire model. Figure 12 shows, as well, a smoke filament introduced outside the fire.

Figure 13 shows smoke filaments introduced from outside the fire as they enter the CBL. A rapid descent of the fresh air is

observed, as in cases of fumigation. The same pattern was observed in the circular models and in Project Flambeau. Many numerical and analytical models neglect this unique form of mixing.

The Effect of Urban Streets

The effect was simulated by covering the porous source with perforated plates. The porosity of the plates was 12 percent and 30 percent. The gross plume shape appeared in the flow visualization to be unchanged.

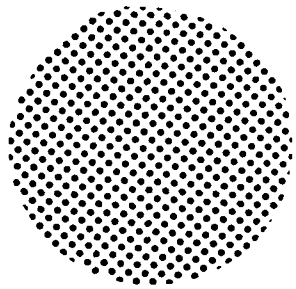

Conclusions

- Physical models can simulate important features of large area fire plumes.
- The rise, in a stably stratified atmosphere, of a plume with a given buoyancy flux decreases with the area of the source.
- Area sources of buoyancy induce larger radial, inward, ground-level velocities than point sources, but the magnitude of these velocities is not as high as previously reported.
- The interaction between simultaneously burning fires over a large area is not expected to be large. This conclusion is based on two observations: the average oxygen depletion in plumes of LAF is not expected to be large. The upward velocities of the individual plumes

within a LAF are expected to be larger than the induced horizontal velocities.

Proposed Future Simulations

- Measure, in small-scale models, the instantaneous temperature (oxygen depletion) LAF and in an individual fire surrounded by other fires.
- Study the detailed effect of streets and noncombustible areas on the flow and temperature field of a LAF.
- Study the behavior of LAF plumes in a stably stratified atmosphere.
- Study the merger of fire plumes from close area fires.

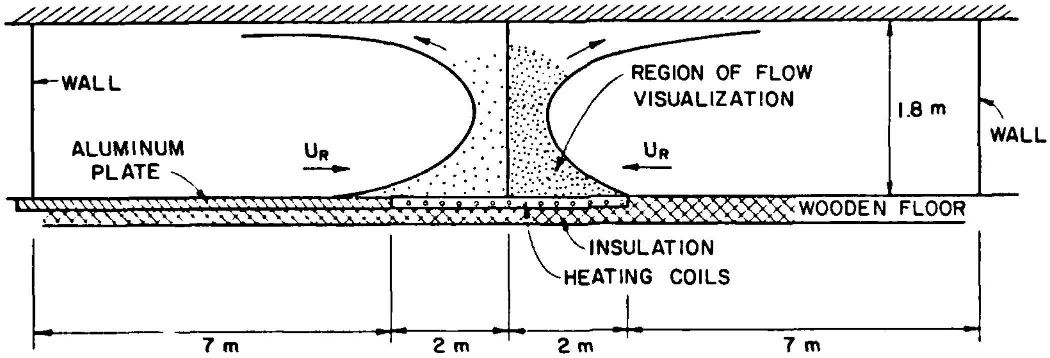

The two-dimensional fire model in the Meteorological Wind Tunnel.

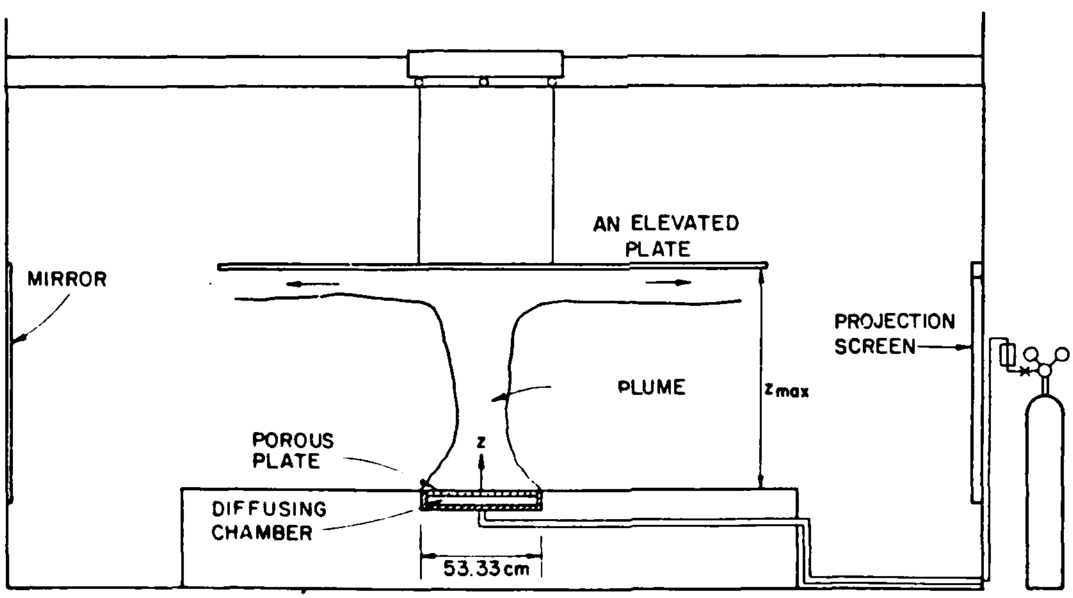

The circular fire model.

Figure 1. Schematic description of the experimental configurations.

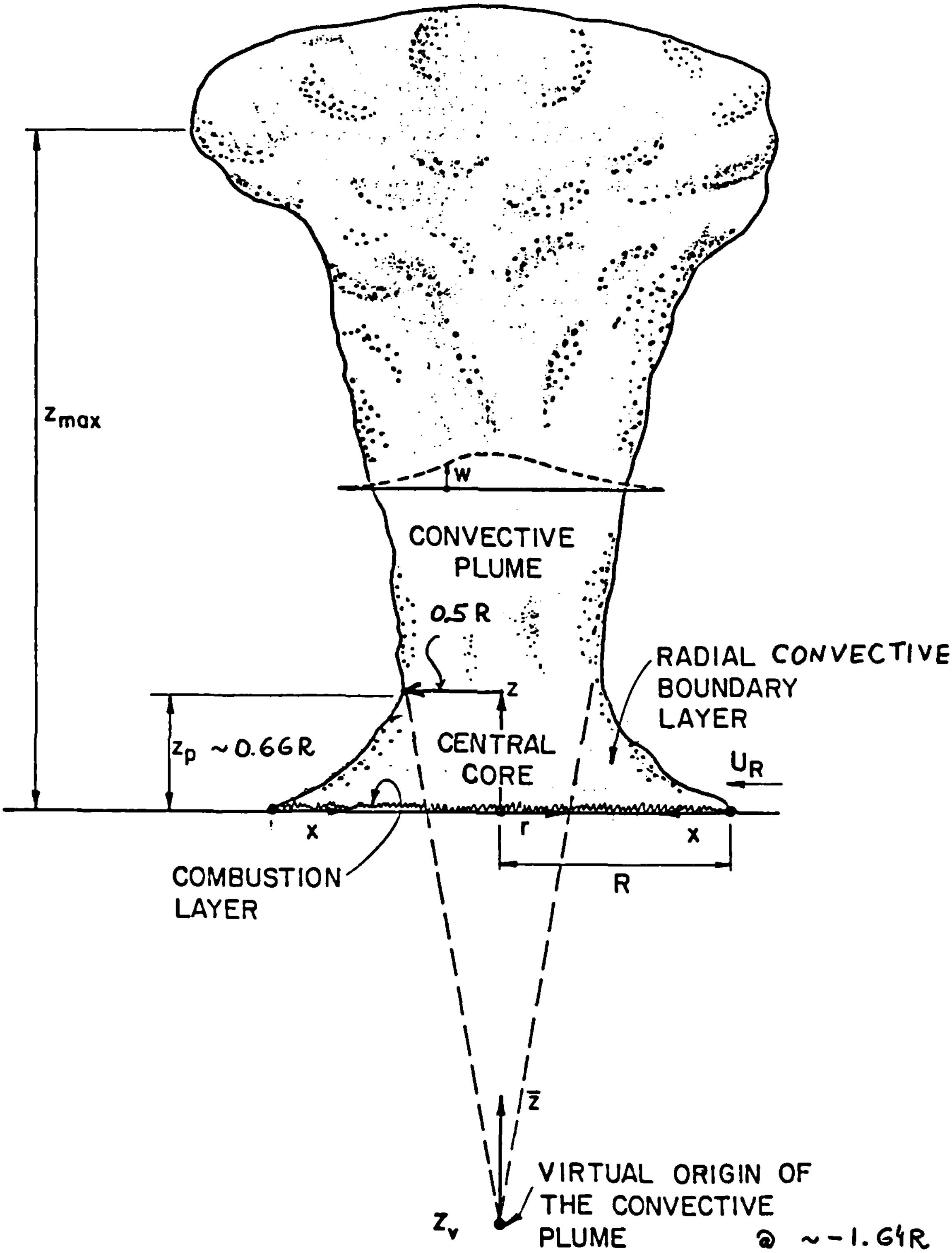

Figure 2. Schematic description of a large fire.

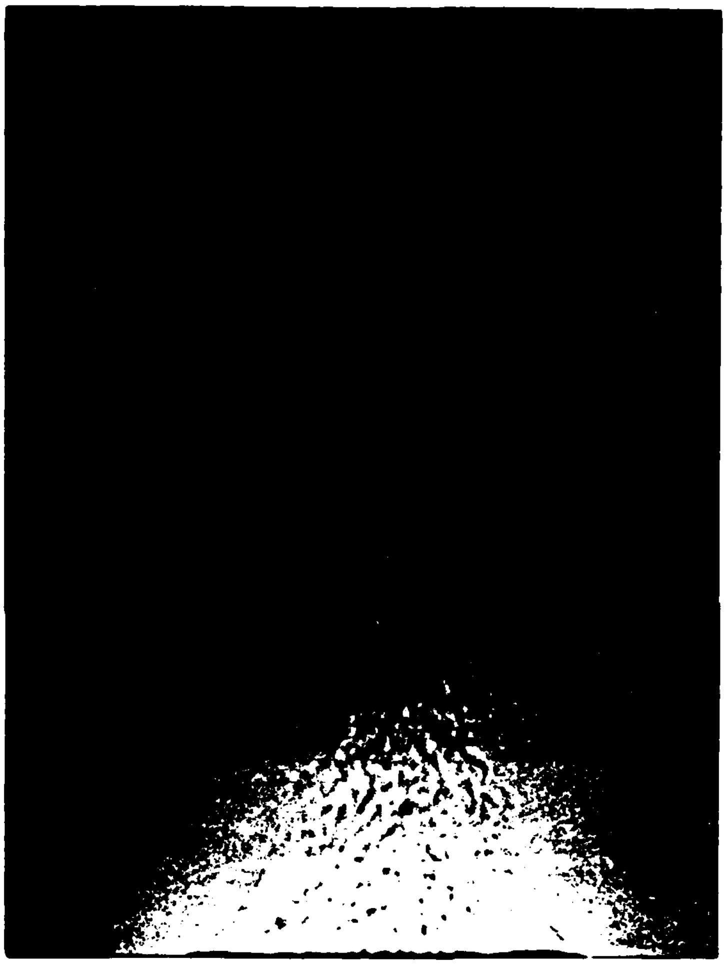

Figure 3. A photograph of the plume shadowgraph.

Figure 4. A 15-acre fire in the Flambeau Project. Trees in foreground are 12 ft high.

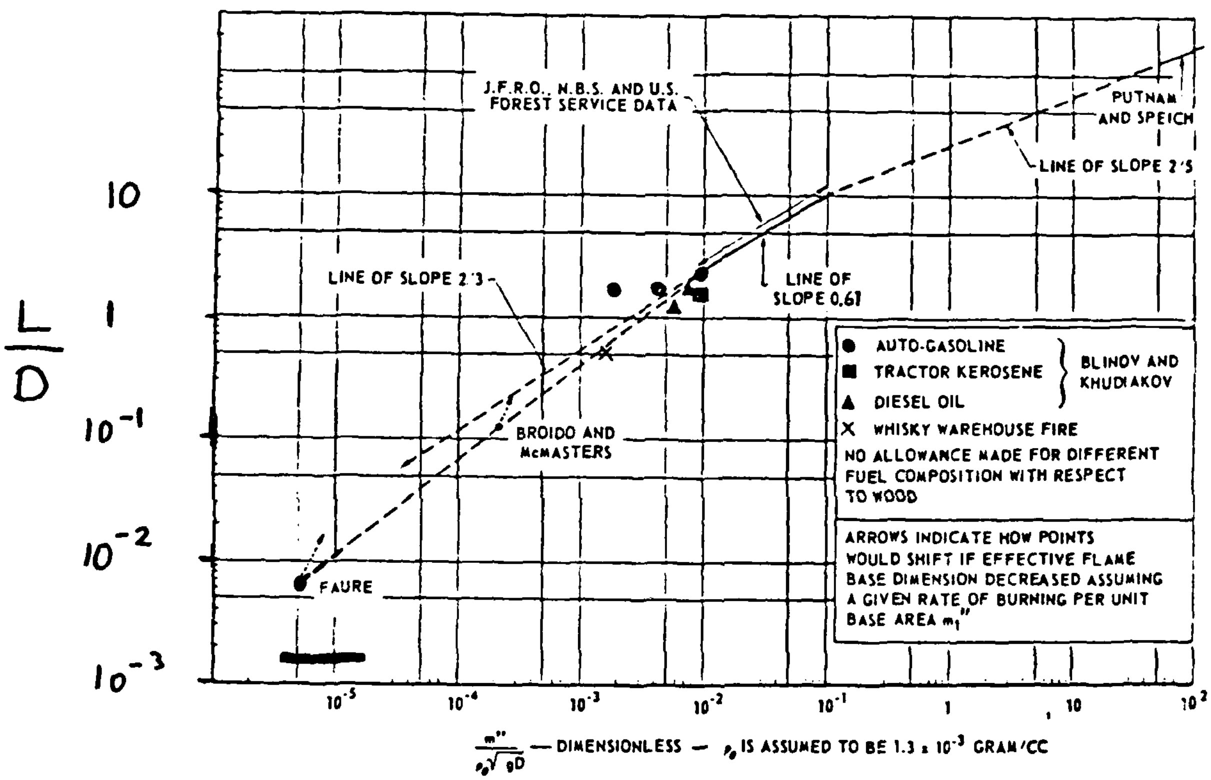

FIG. 4. Flame height correlation.

Figure 5. Flame height correlation according to P.H. Thomas (1963).

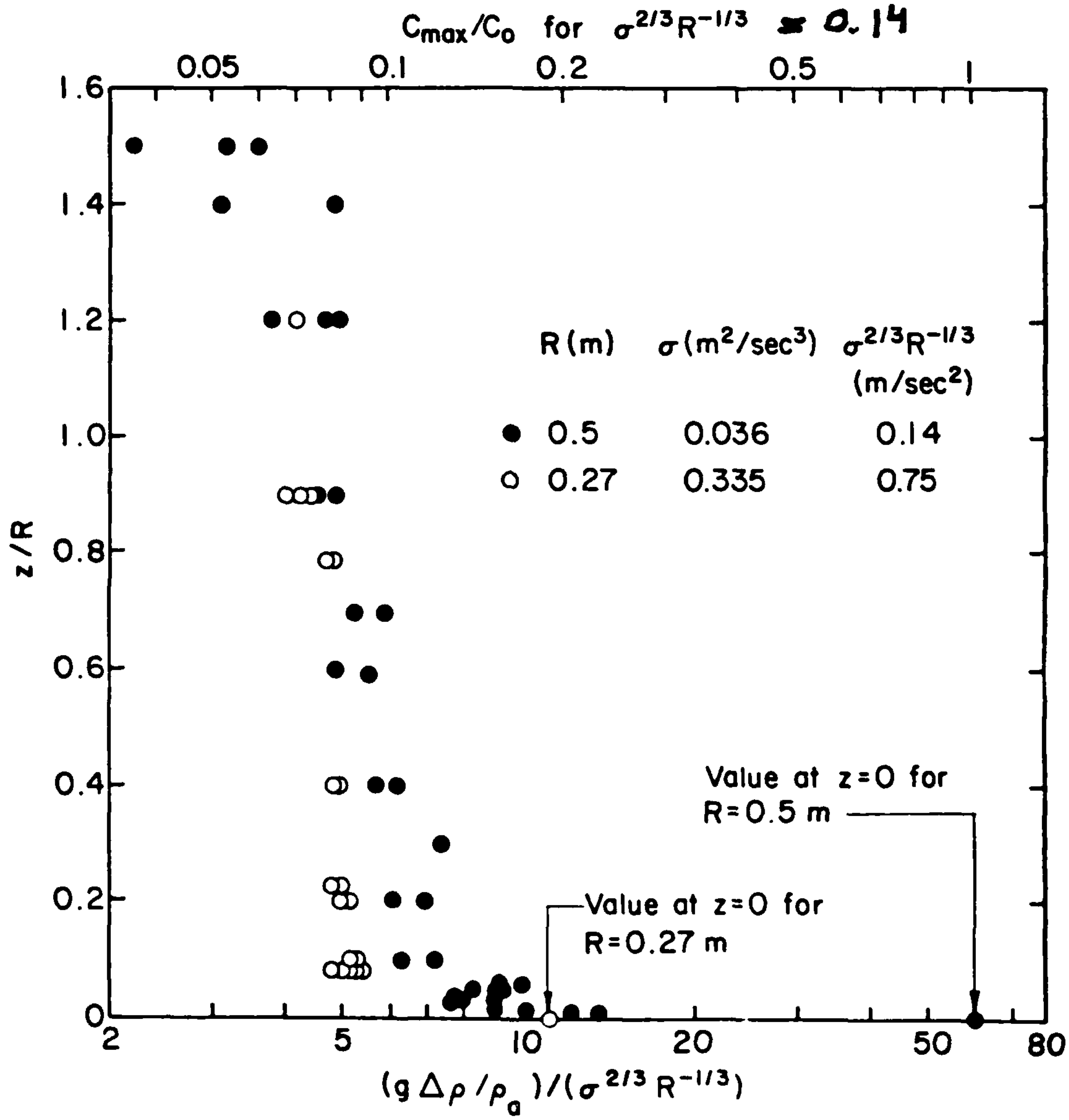

Figure 6. Measured dimensionless buoyancy parameter at the center of the plume in two physical models.

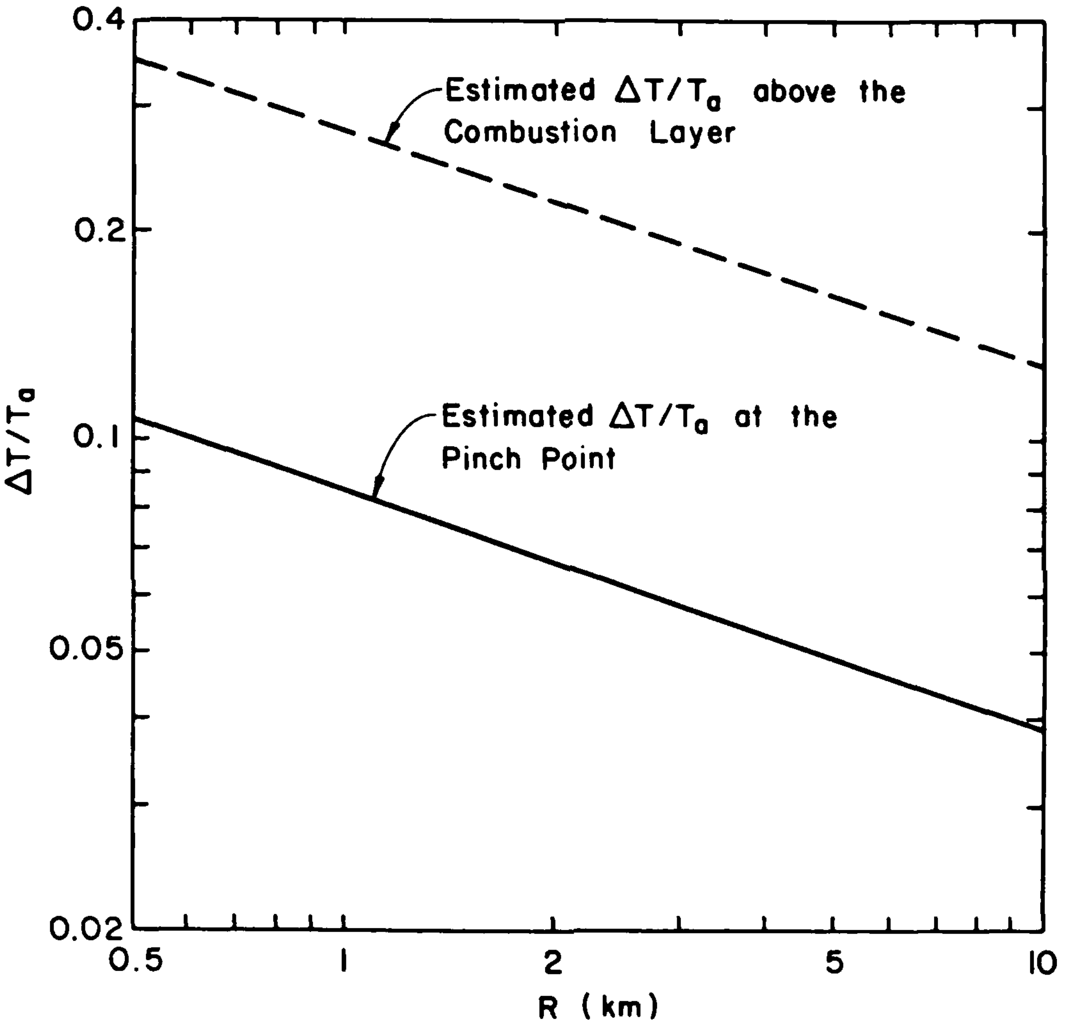

Figure 7. Estimated increase of plume temperatures for different size fires.

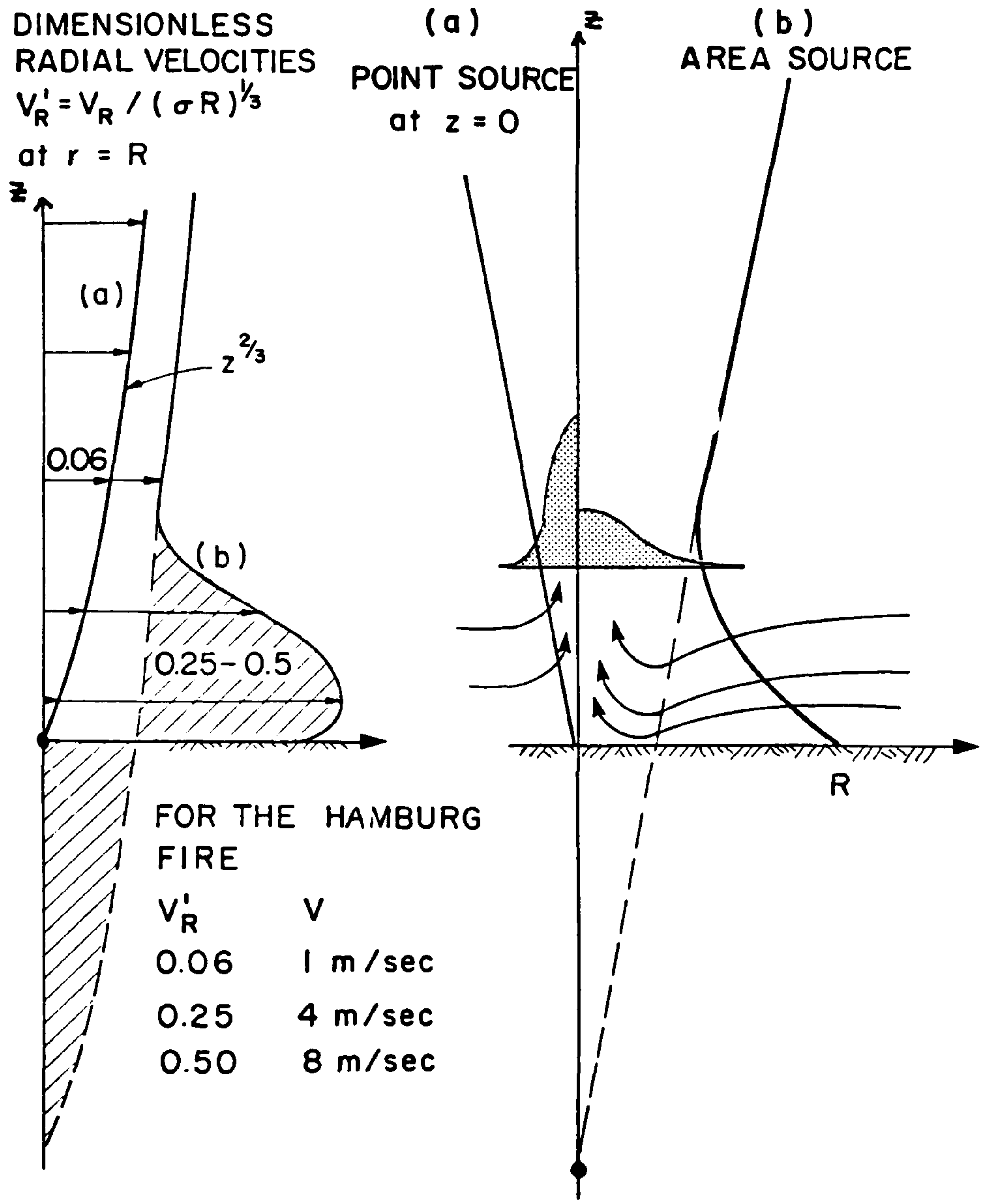

Figure 8. Schematic description of induced radial velocities for a point source (a) and an area source (b). (The correlation between the dimensionless velocities and expected velocities for the Hamberg Fire are shown in the figure).

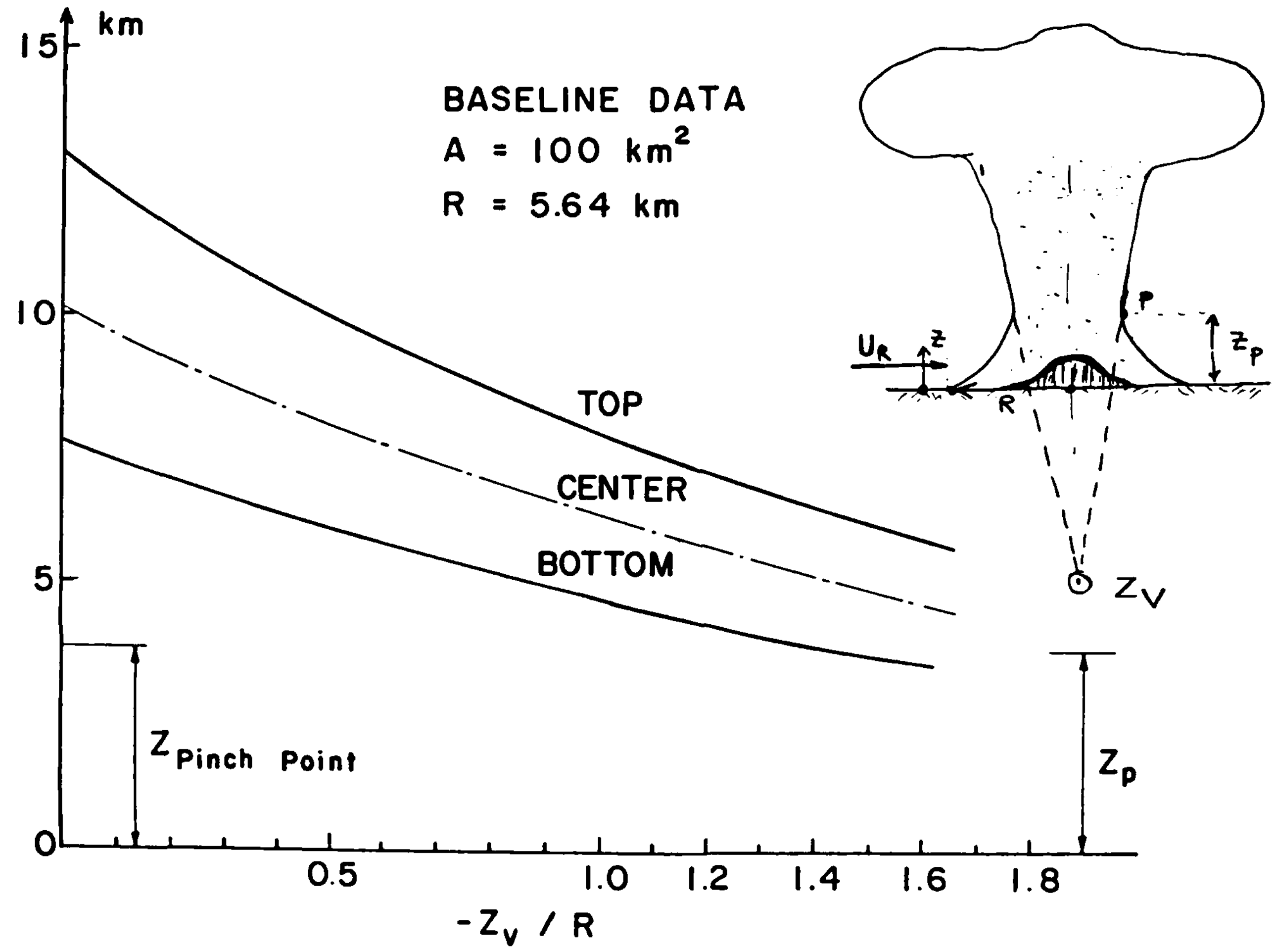

Figure 9. Estimate plume rise for a 100 km fire in a stably stratified atmosphere as a function of the position of the virtual source.

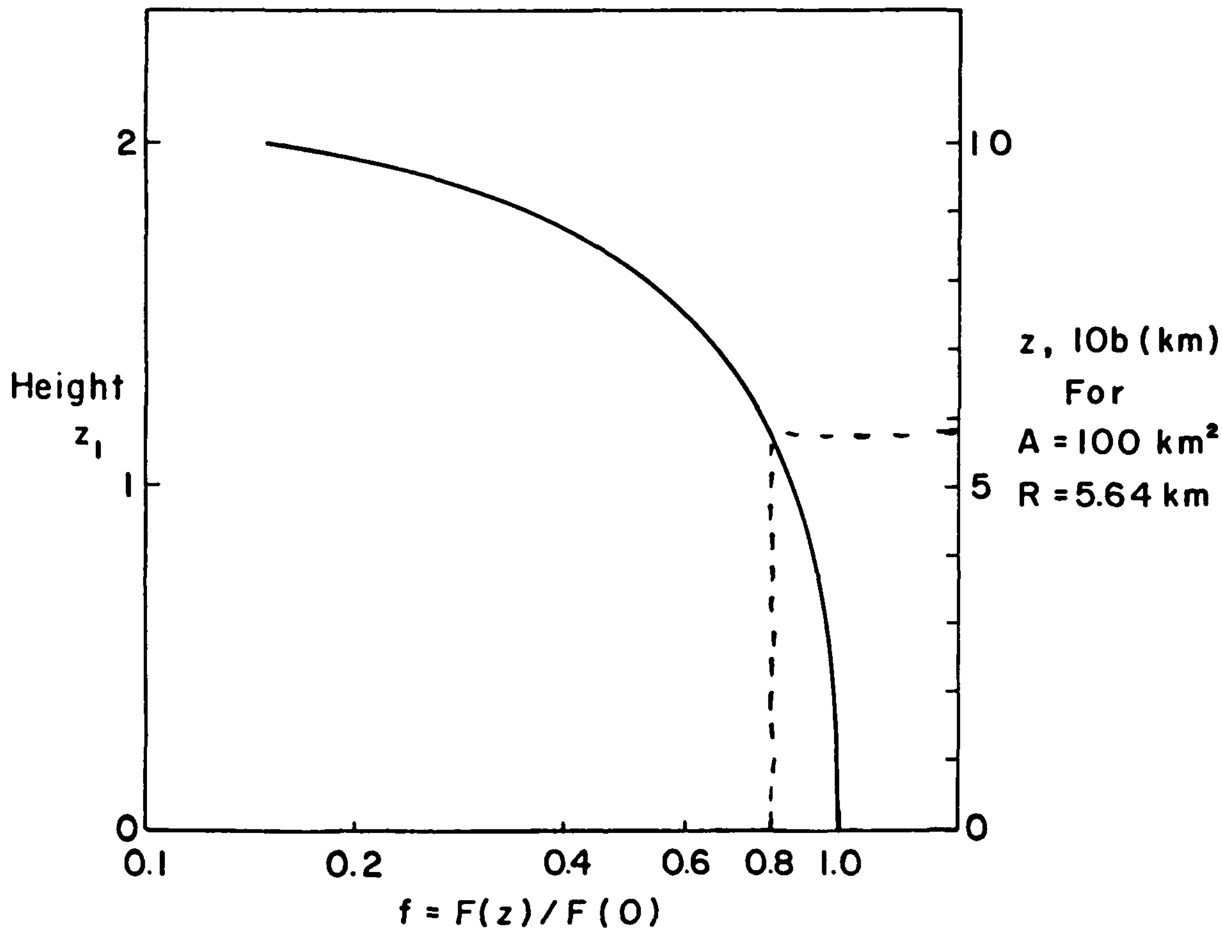

Figure 10. The relative reduction of buoyancy flux F with the height z in a stably stratified atmosphere according to Morton et al. (1956). (Note that most buoyancy flux disappears at large heights after the plume has increased its width.)

Figure 11. Photographs of the outer developing CBL in the two-dimensional fire model.

Figure 12. Photographs of the CBL in the two-dimensional fire model together with a smoke filament released above the layer.

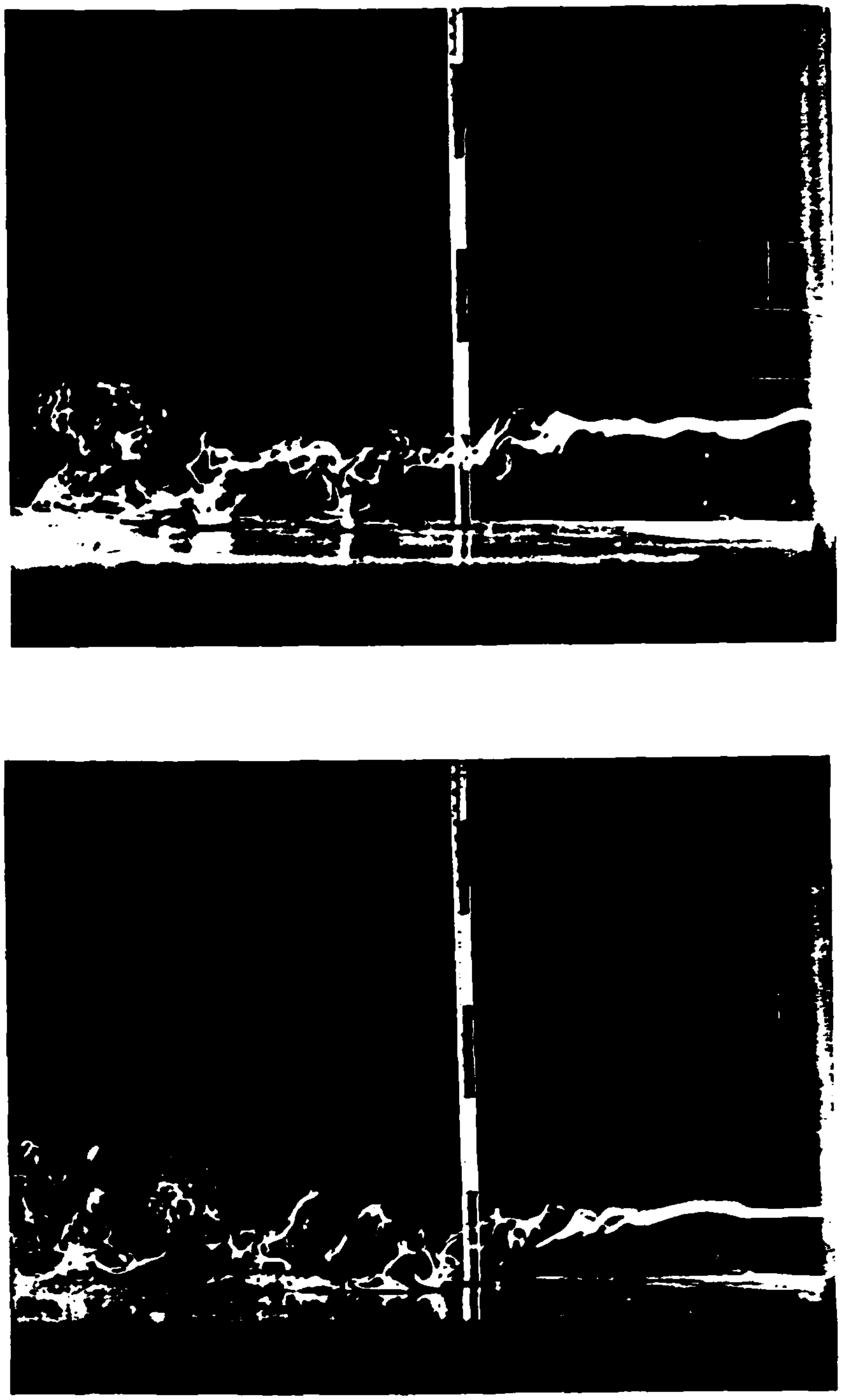

Figure 13. Photographs of smoke filaments released above the CBL in the two-dimensional fire model. (Note the rapid decent of the filaments in the CBL.)

SMOKE PLUMES
FROM LARGE AREA FIRES

A. KARAGOZIAN,

D. REMETCH

R. D. SMALL

GLOBAL EFFECTS PROGRAM MEETING

February 26-27, 1986

PSR
EATON

LARGE AREA FIRE IN THE ATMOSPHERE

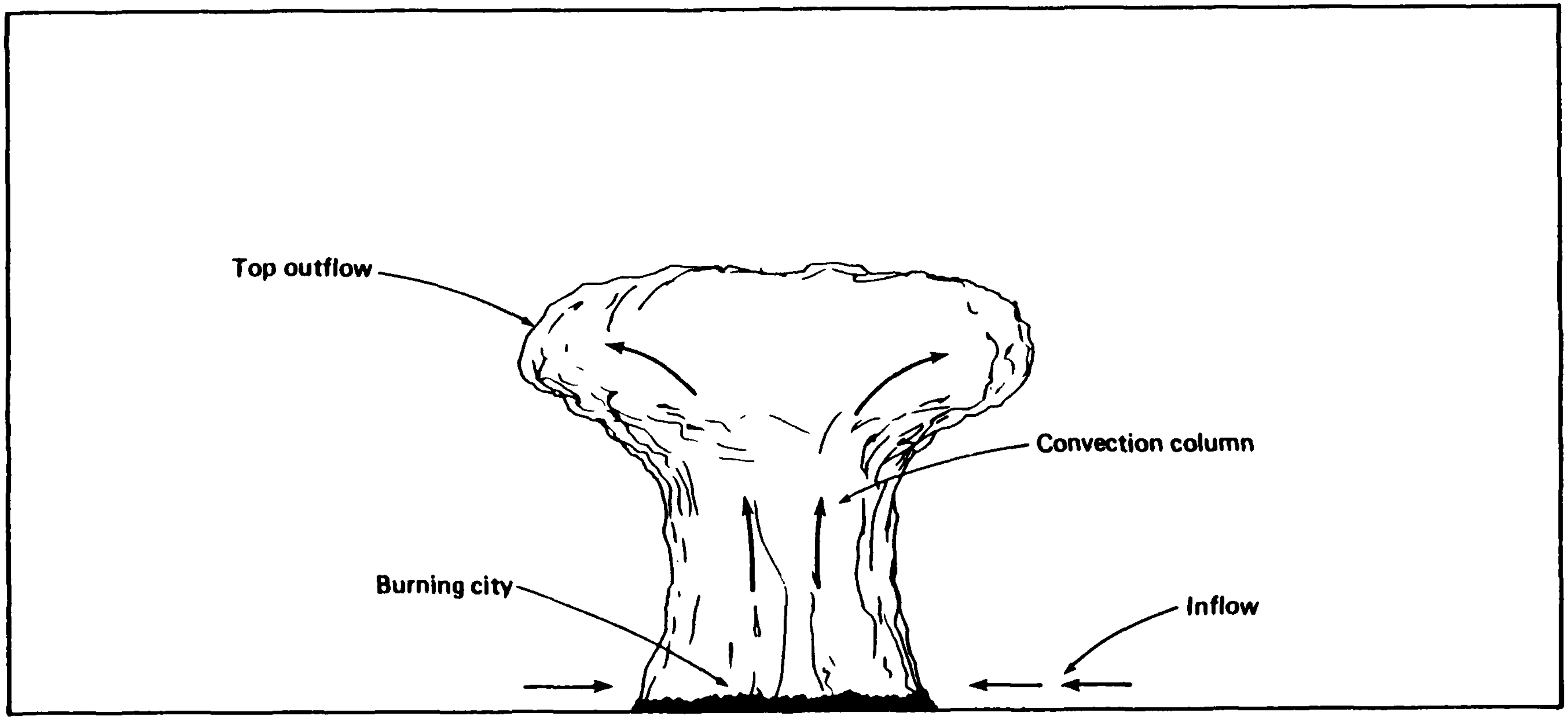

HYDROCODE APPROXIMATION OF LARGE SMOKE PLUMES

- VARIABLES
  - FIRE SIZE AND INTENSITY; BURNING TIME
  - ATMOSPHERE TEMPERATURE PROFILE
  - INVERSION HEIGHT
  - HUMIDITY PROFILE

- MODELING ASSUMPTIONS
  - HEAT RELEASE
  - TURBULENCE
  - TWO-DIMENSIONAL/AXISYMMETRIC
  - RESOLUTION
  - CITY STRUCTURE

- VALIDATION
  - FLAMBEAU
  - METEOTRON
  - CHAPLEAU

PSR
EATON

FLAMBEAU FIRE 460-7-66

- DATA
  - 30 ACRE TEST SITE
  - 240 15 m X 15 m FUEL PILES
  - 7.5 m AISLES
  - 330 m CROSS SECTION
  - 40,000 LB/PILE - MIXED JUNIPER AND PINON
  - HEAT RELEASE MEASURED
  - VELOCITIES MEASURED
- SIMULATION
  - MEASURED HEAT RELEASE USED
  - TWO-DIMENSIONAL WITH AMBIENT WIND
  - FUEL BED - AISLES MODELED
- RESULTS
  - MERGING OF PLUMES CALCULATED
  - PLUME RISE IN CROSSWIND
  - FAIR AGREEMENT WITH MEASURED VELOCITIES

PSR
EATON

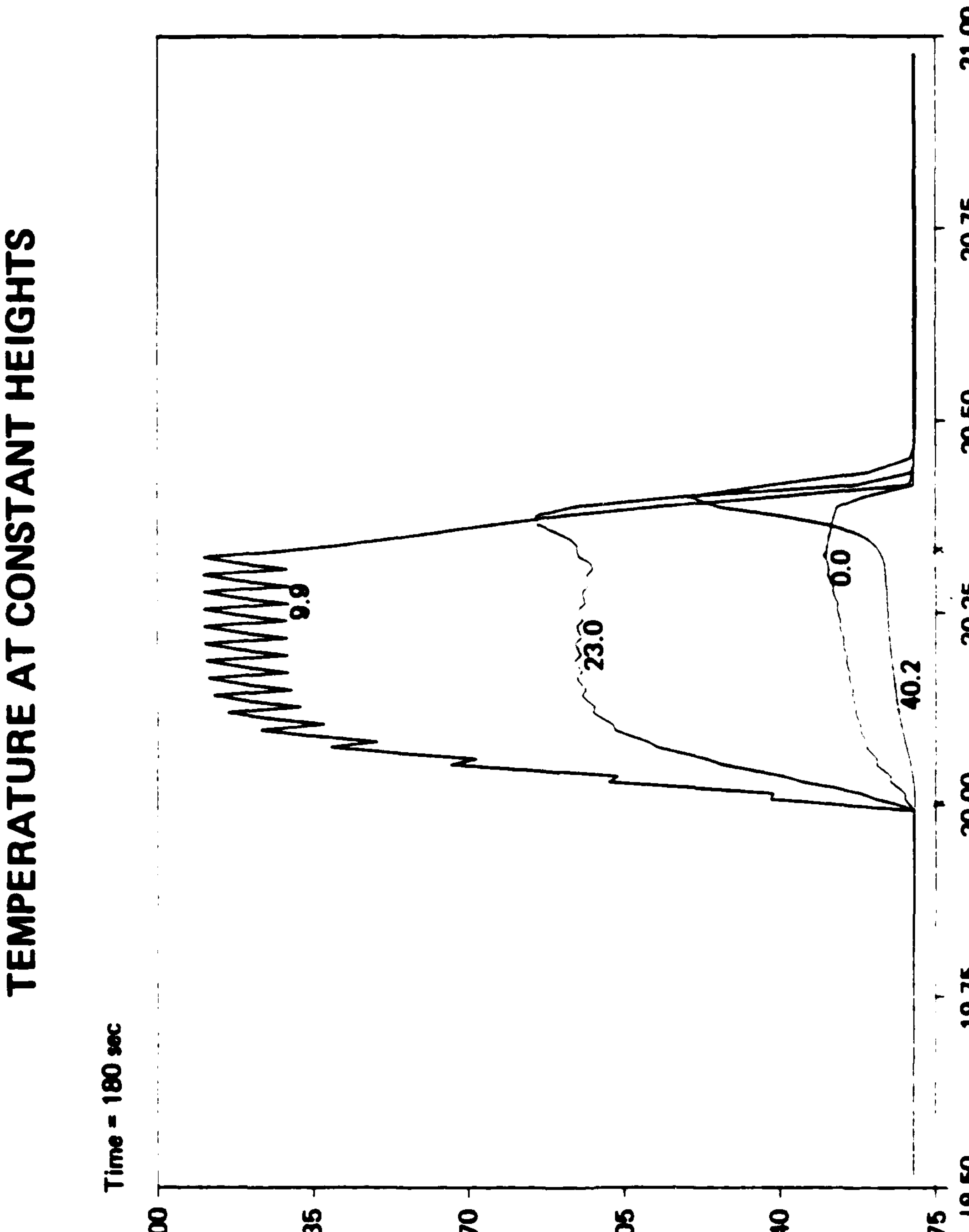
TEMPERATURE AT CONSTANT HEIGHTS
Time = 180 sec
Temperature (°K)
1100
935
770
605
440
275
19.50
19.75
20.00
20.25
20.50
20.75
21.00
Horizontal distance (km)
9.9
23.0
0.0
40.2

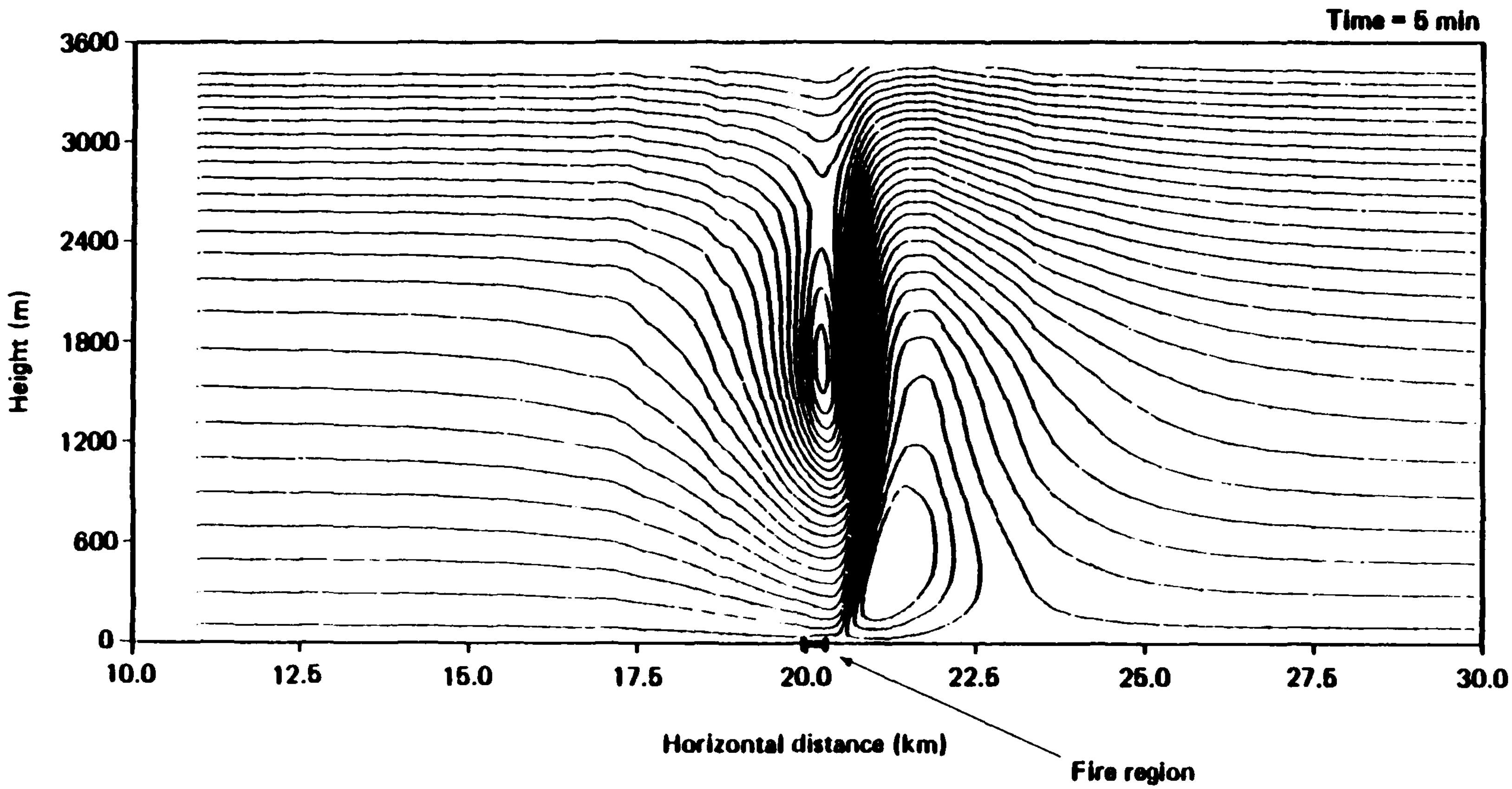

Streamlines: Flambeau fire 460-7-66.

EXAMPLE CASES

- FIRE RADIUS 10 km
- FIRE ZONE HEIGHT 100 m
- HEAT RELEASE RATES 1 $kW/m^3 \rightarrow 2.5\ kW/m^3$
- FUEL CONSUMPTION 2 $g/cm^2/hr$
- SMOKE EMISSION FACTOR 3 PERCENT
- RELATIVE HUMIDITY RATIOS 0, 0.5, 0.77
- U.S. STANDARD ATMOSPHERE TEMPERATURE PROFILE
- TROPOPAUSE AT 11 km

PSR EATON

1 KW/M3 LARGE AREA FIRE:
U. S. STANDARD ATMOSPHERE

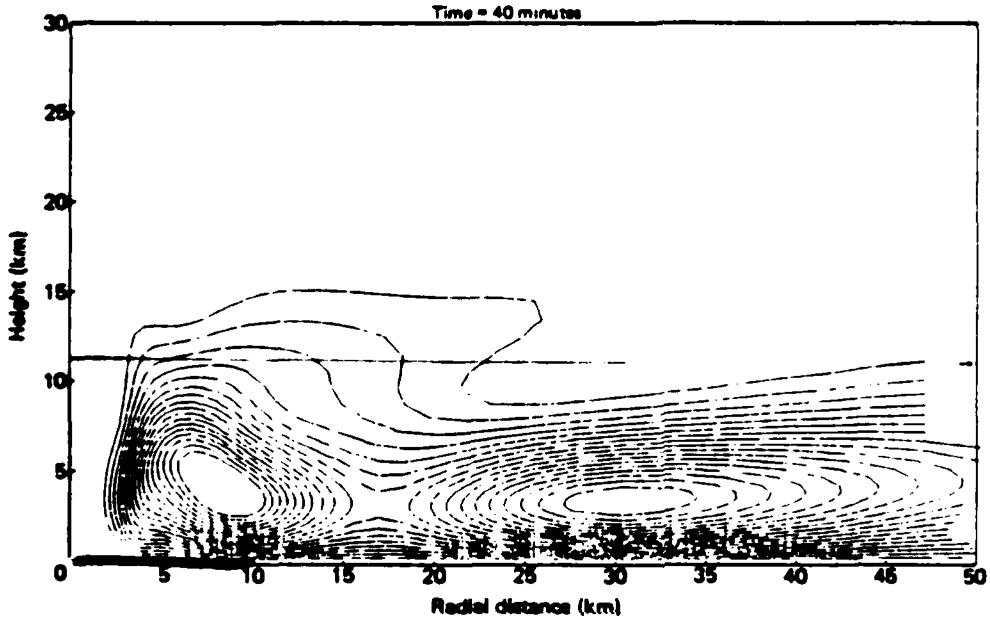

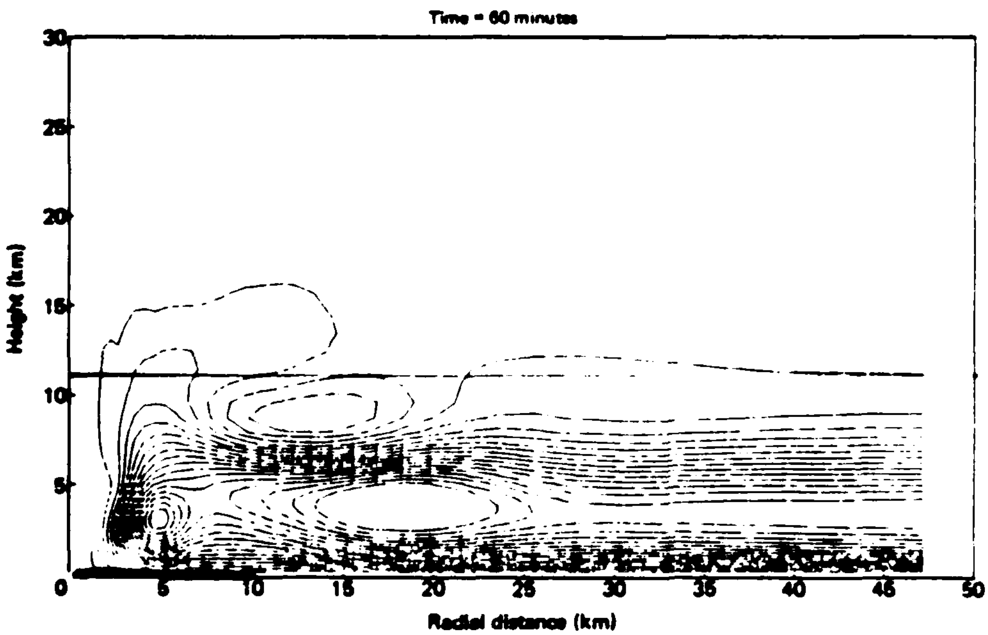

1 KW/M3 LARGE AREA FIRE:
U. S. STANDARD ATMOSPHERE

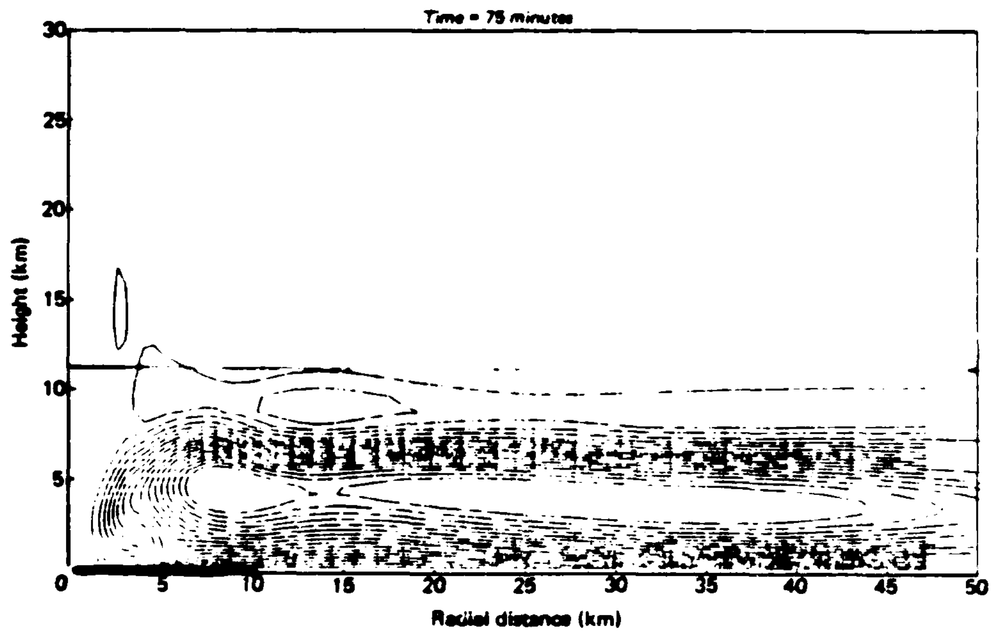

Smoke tracers: 10-km radius area fire; $Q = 1 kW/m^3$; $\phi_0 = 0$.

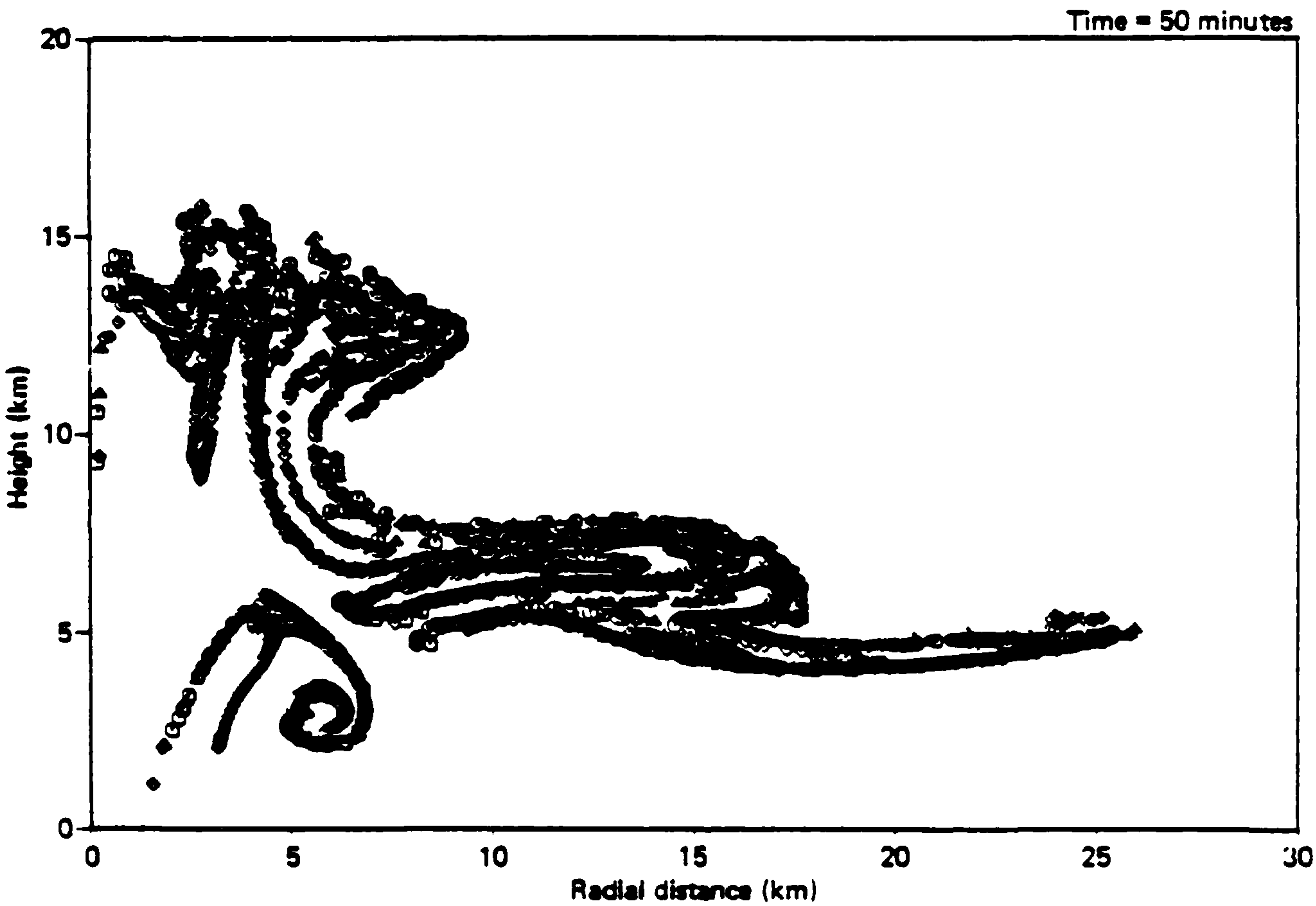

Streamlines: 10-km radius area fire; $Q = 1$ kW/m^3; $\phi_o = 0.77$.

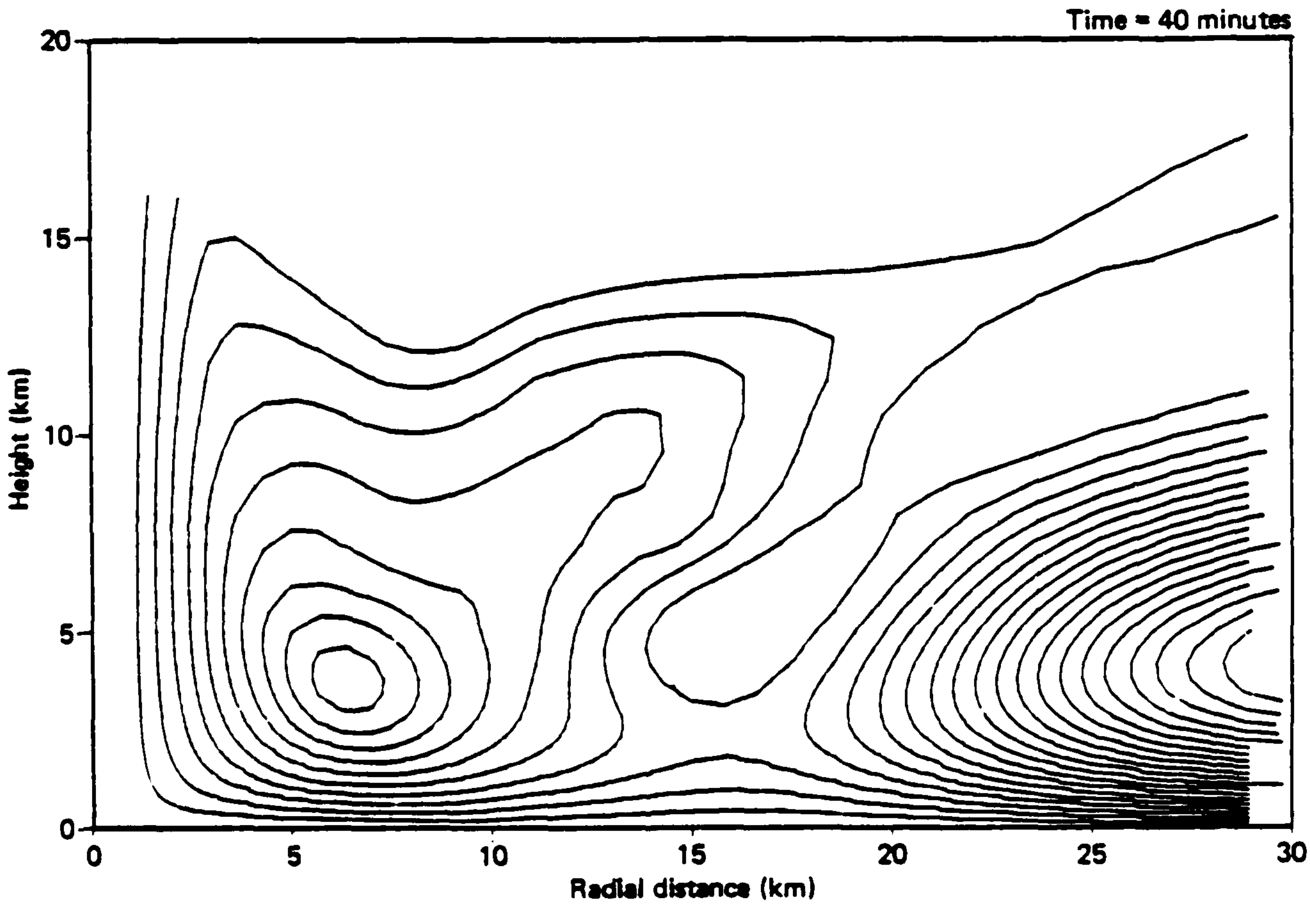

Smoke tracers: 10-km radius area fire; $Q = 1$ kW/m^3; $\phi_0 = 0.77$.

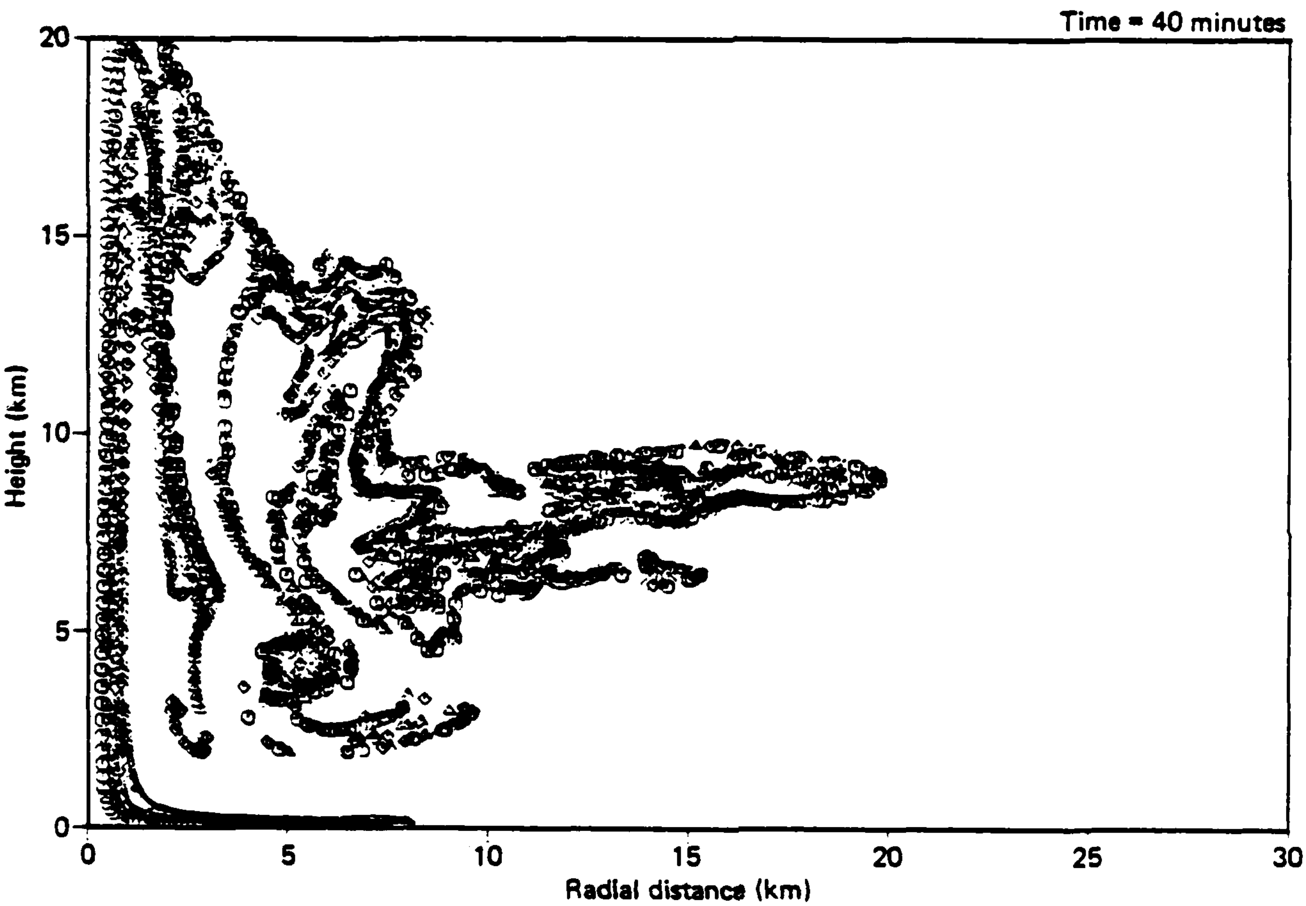

Smoke tracers: 10-km radius area fire; $Q = 2.5$ kW/m^3; $\phi_0 = 0.77$.

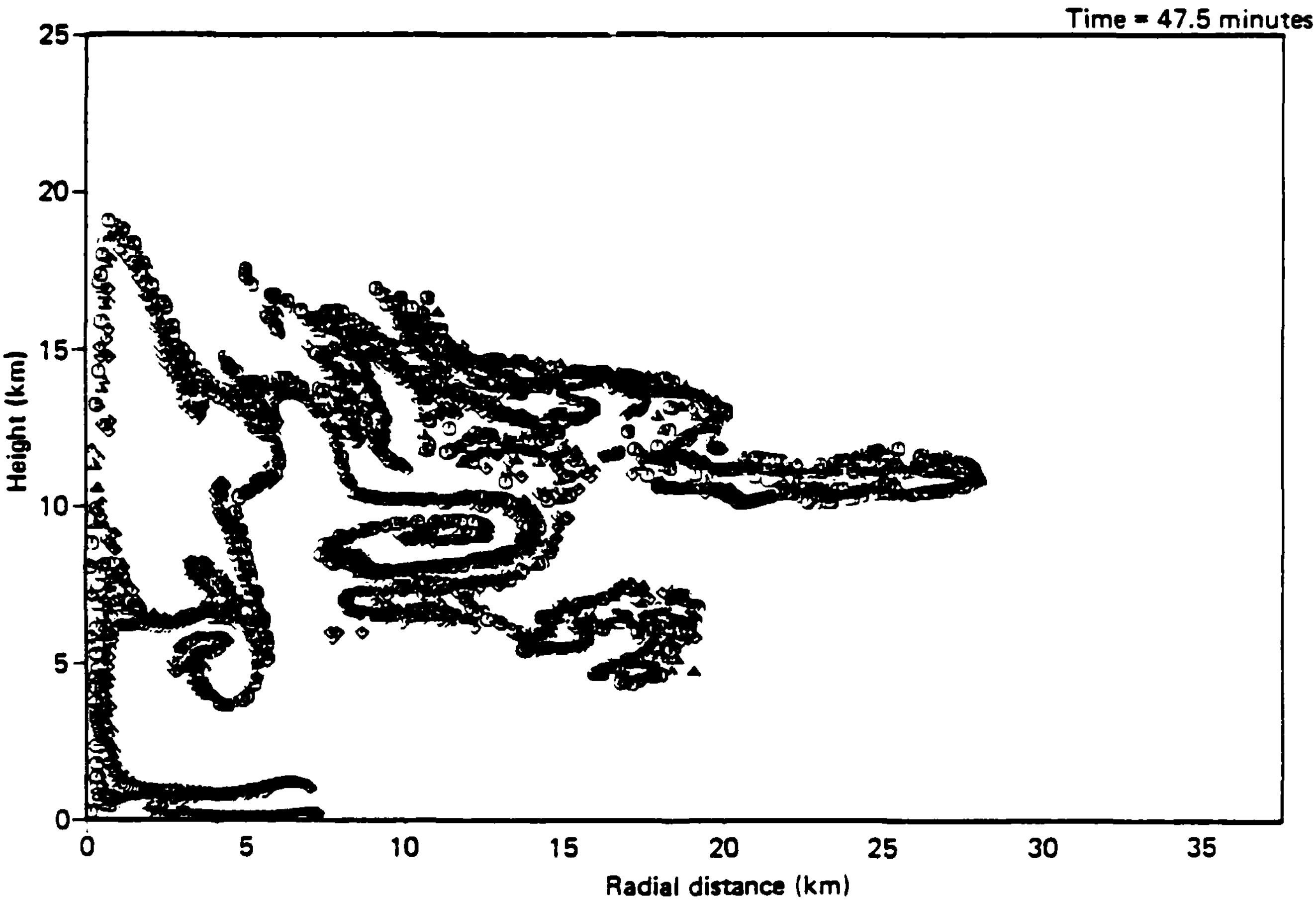

CONCLUSIONS

- ATMOSPHERIC GRADIENTS CONTROL PLUME RISE
- MODERATE ENERGY PLUMES CONTAINED BY TROPOPAUSE
- MOISTURE INFLUENCES SMOKE CLOUD HEIGHT
- BETTER RESOLUTION OF CITY REQUIRED
- NEW HEAT RELEASE MODEL NEEDED
- LOWER HEAT RELEASE SIMULATIONS NEEDED

PSR
EATON

TROPOPAUSE RESPONSE TO LARGE AREA FIRES

DAVID P BACON

SCIENCE APPLICATIONS
INTERNATION CORPORATION

FEBRUARY 26, 1986

PRESENTED AT THE DNA GLOBAL EFFECTS
PROGRAM MEETING AT NASA/AMES

SAIC Science Applications International Corporation

The Terminal Area Simulation System (TASS)

Equations for:	Momentum Pressure Potential Temperature Water Vapor Cloud Water Cloud Ice Rain Snow Hail Smoke (Massless Tracer) Dust (Massive Tracer)
Turbulence:	Smagorinsky - shear - stratification

SAIC Science Applications International Corporation

Parameterizations:

- Rain drop initiation
- Rain drop growth
- Evaporation of rain
- Freezing of supercooled cloud water and rain
- Initiation of cloud ice
- Ice growth
- Cloud ice becomes hail
- Deposition and sublimination of hail and cloud ice
- Hail growth
- Shedding of unfrozen water
- Initiation of snow
- Snow growth
- Melting of hydrometeors

Additional Diagnostics:

- Radar reflectivity
- Hydrometeor concentrations

SAIC Science Applications International Corporation

Boundary Conditions:

Surface - Nonslip velocity
- Continuous thermodynamics
- Time-dependent heat source

Axial - Symmetric

Lateral - Open boundary

Top - Zero vertical velocity
- Other variables continuous

Initial Conditions:

Ambient atmosphere initialized by temperature and dewpoint sounding.

Fireball modelled by a "Thermal Bubble" - a hemispherical region of overtemperature (1 MT Nuclear = 675 KT Thermal)

SAIC. Science Applications International Corporation

WOOD: 8500-9000 BTU/lb

8600 BTU/lb ~ 20 MJ/kg

2 % SMOKE EMISSION FACTOR = 20 g/kg

SMOKE EMISSION = 1 g/MJ

FIRE INTENSITY: UNIFORM OVER 10 km RADIUS

45 min LINEAR RISE
60 min @ 50 kW/m**2
45 min LINEAR DECAY

TOTAL HEAT INPUT ~ 10^17 J
TOTAL SMOKE INPUT ~ 10^11 g

SAIC Science Applications International Corporation

LCH DATA @ 2400Z 4-10-79

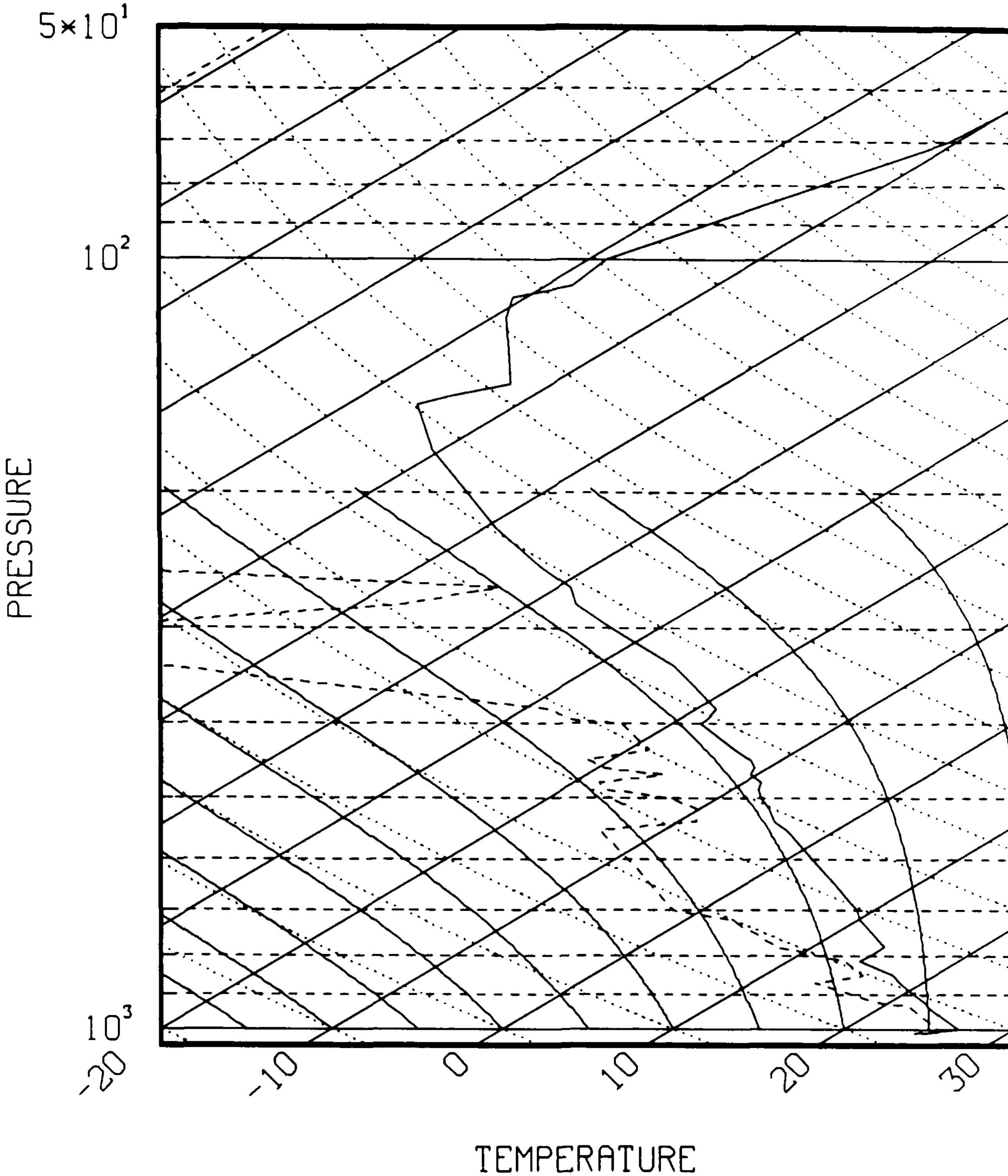

SMK 2.5 HR--50 KW/M**2 @ LCH TIME= 15.1

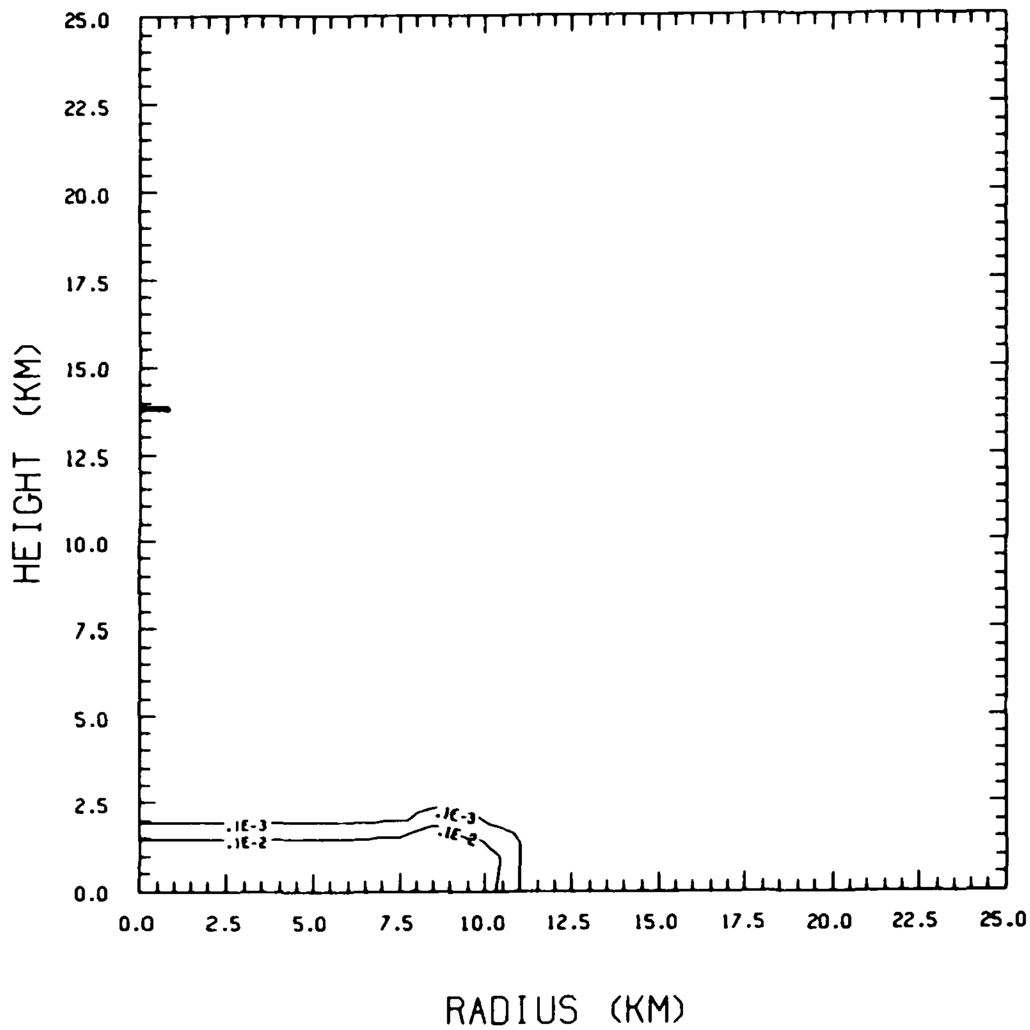

CONTOUR FROM .10000E-03 TO 10.000
(USER'S LEVELS)

SMK 2.5 HR--50 KW/M**2 @ LCH TIME= 45.0

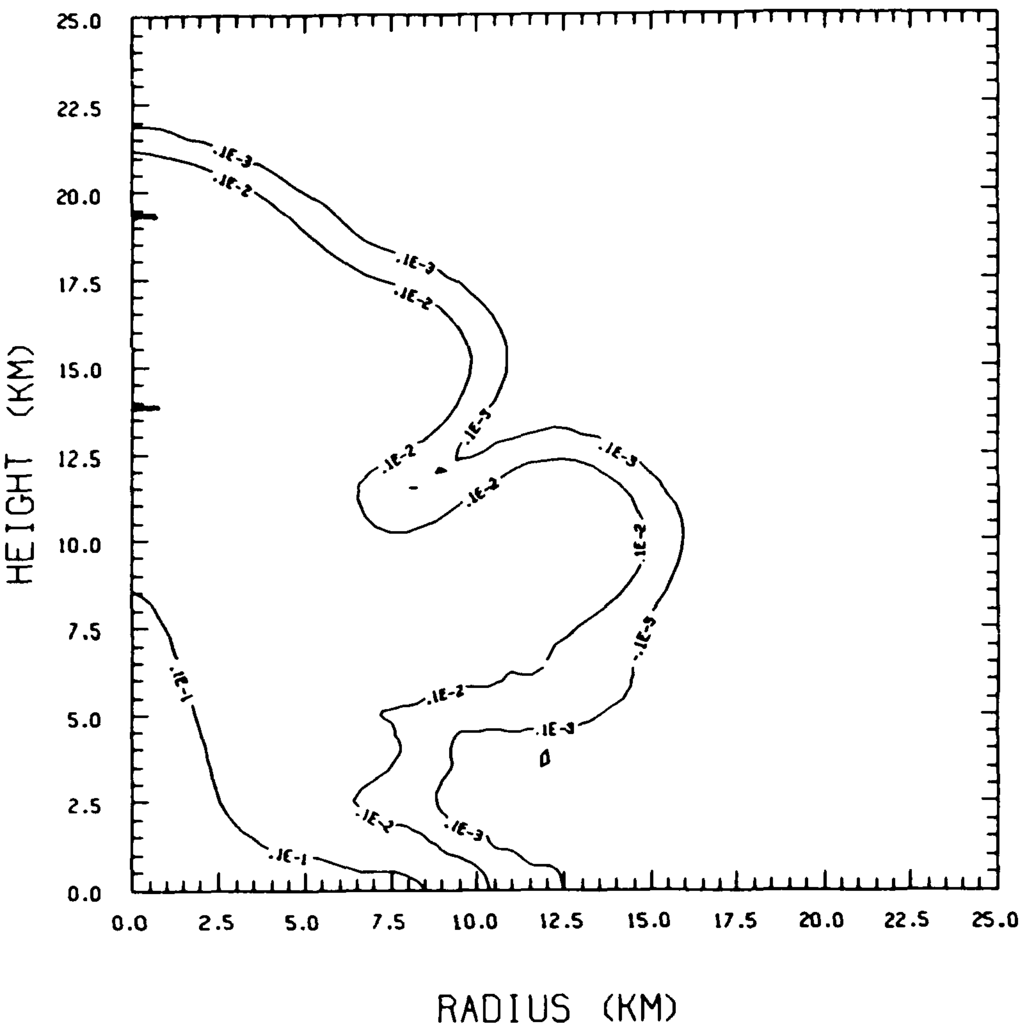

CONTOUR FROM .10000E-03 TO 10.000
(USER'S LEVELS)

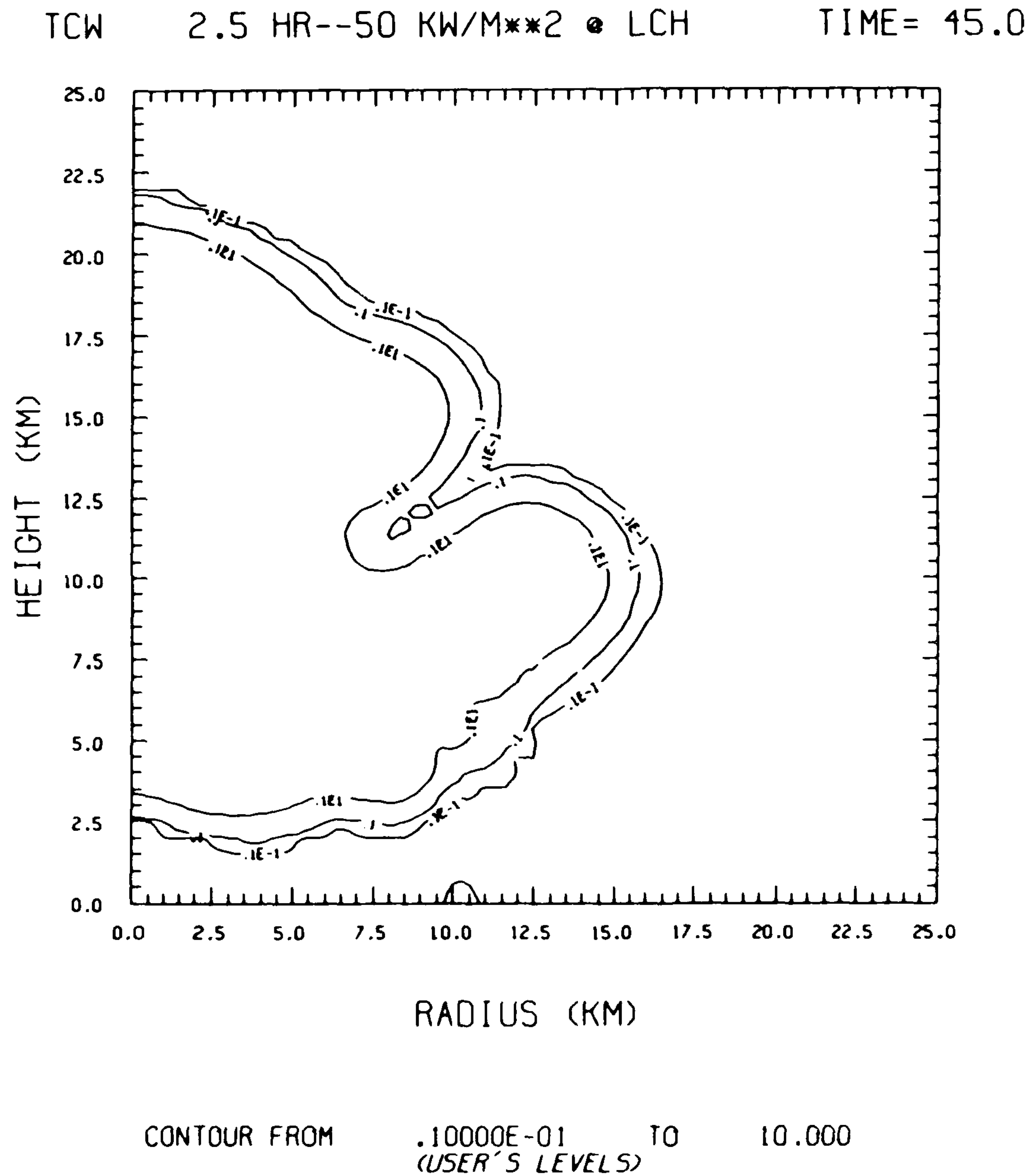
TCW 2.5 HR--50 KW/M**2 @ LCH TIME= 45.0
HEIGHT (KM)
RADIUS (KM)
0.0
2.5
5.0
7.5
10.0
12.5
15.0
17.5
20.0
22.5
25.0
.1E-1
.1
.1E1
CONTOUR FROM .10000E-01 TO 10.000
(USER'S LEVELS)

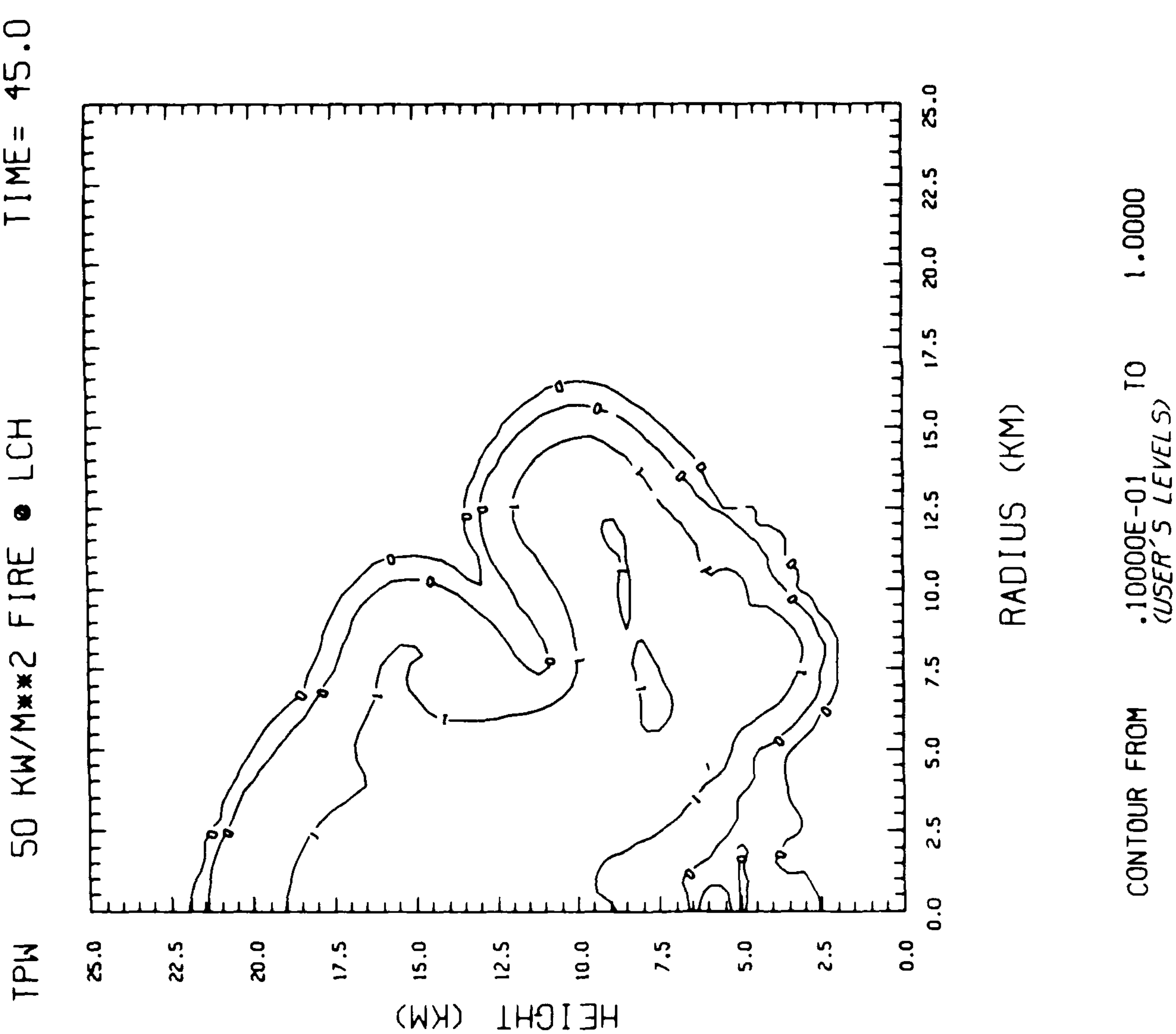
TPW 50 KW/M**2 FIRE @ LCH TIME= 45.0
HEIGHT (KM)
RADIUS (KM)
CONTOUR FROM .10000E-01 TO 1.0000
(USER'S LEVELS)

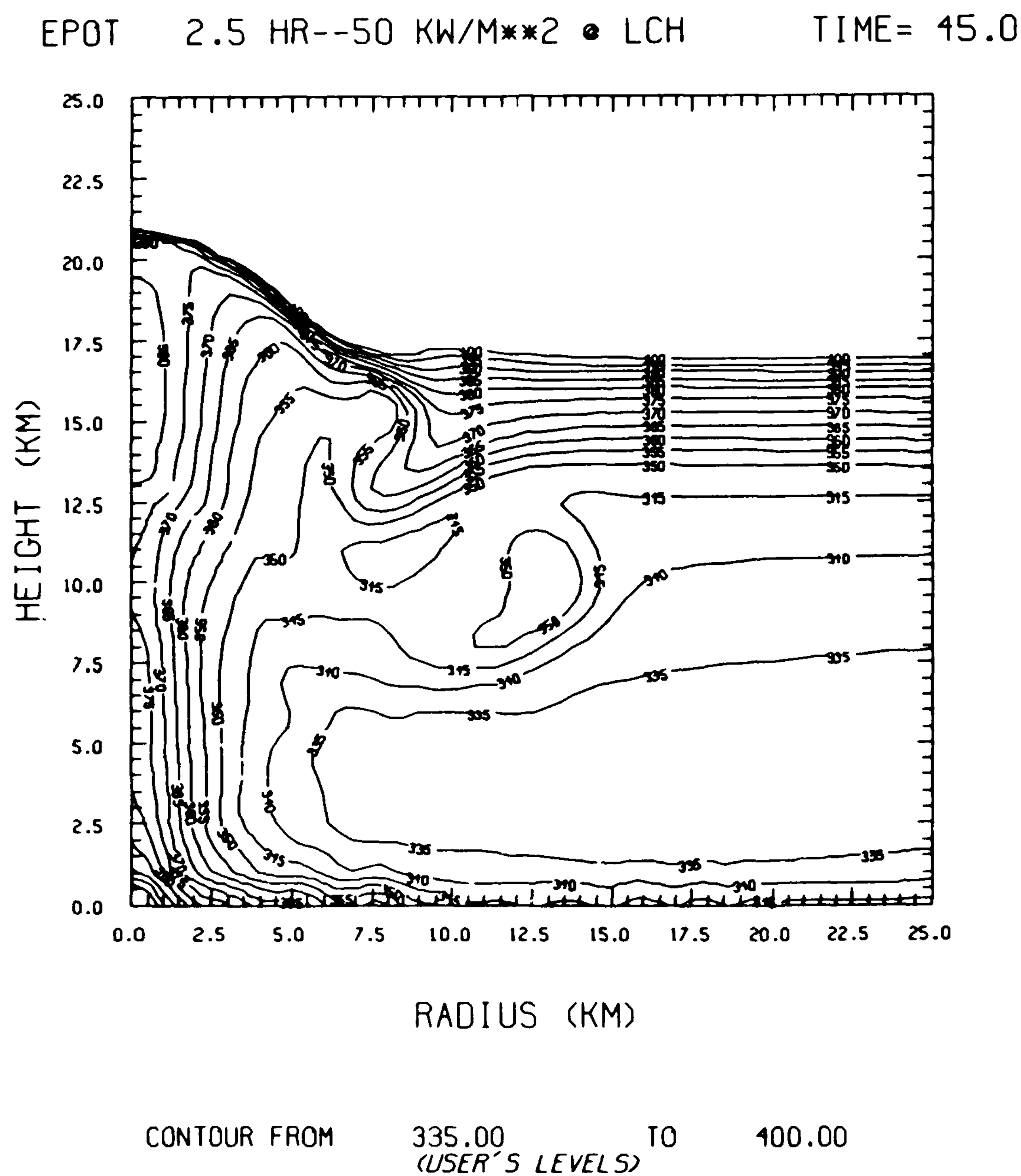

EPOT 2.5 HR--50 KW/M**2 @ LCH TIME= 45.0
HEIGHT (KM)
RADIUS (KM)
0.0
2.5
5.0
7.5
10.0
12.5
15.0
17.5
20.0
22.5
25.0
CONTOUR FROM 335.00 TO 400.00
(USER'S LEVELS)

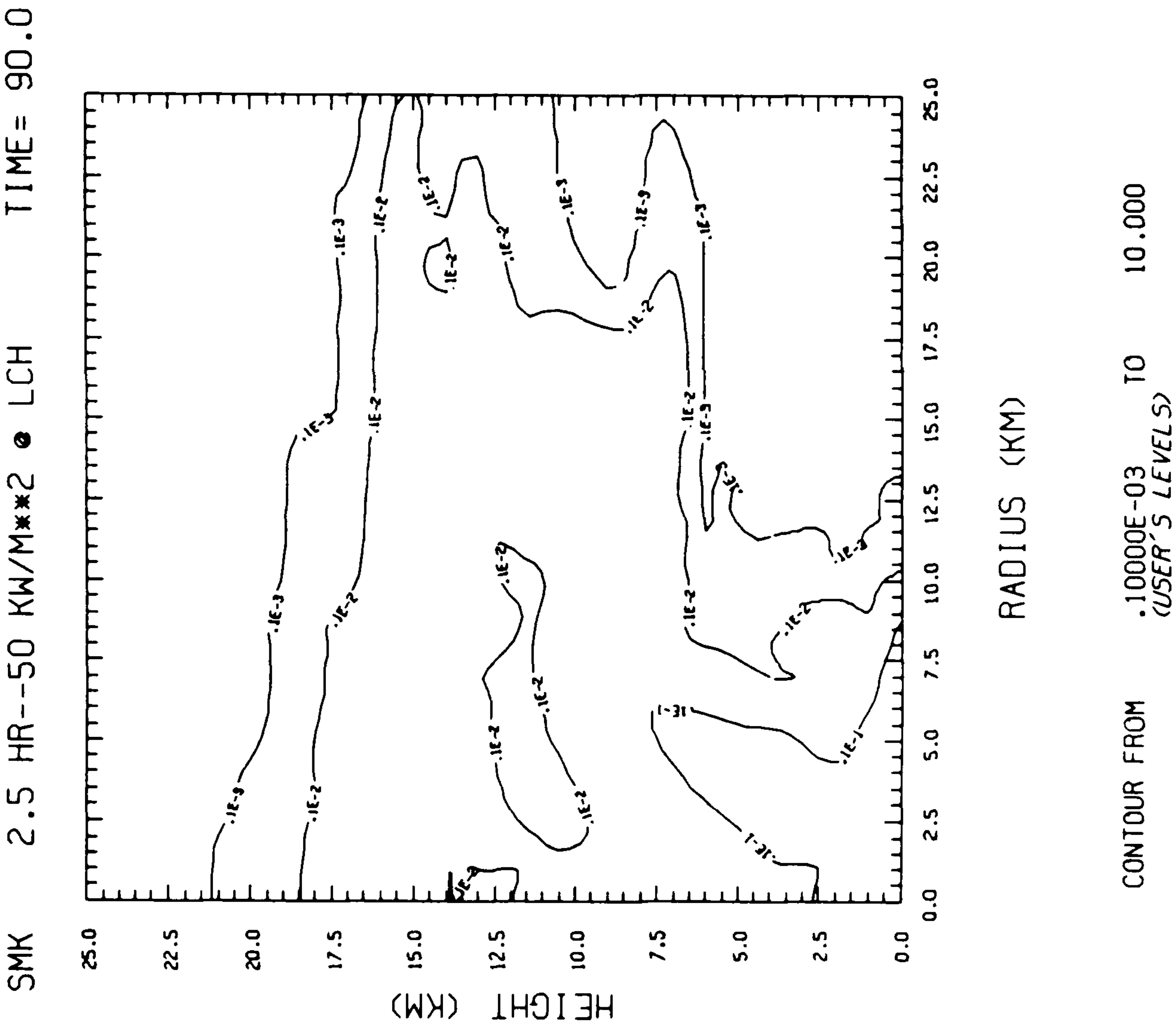
SMK 2.5 HR--50 KW/M**2 @ LCH TIME= 90.0
HEIGHT (KM)
RADIUS (KM)
0.0
2.5
5.0
7.5
10.0
12.5
15.0
17.5
20.0
22.5
25.0
.1E-3
.1E-2
.1E-1
CONTOUR FROM .10000E-03 TO 10.000
(USER'S LEVELS)

TCW 2.5 HR--50 KW/M**2 @ LCH TIME= 90.0

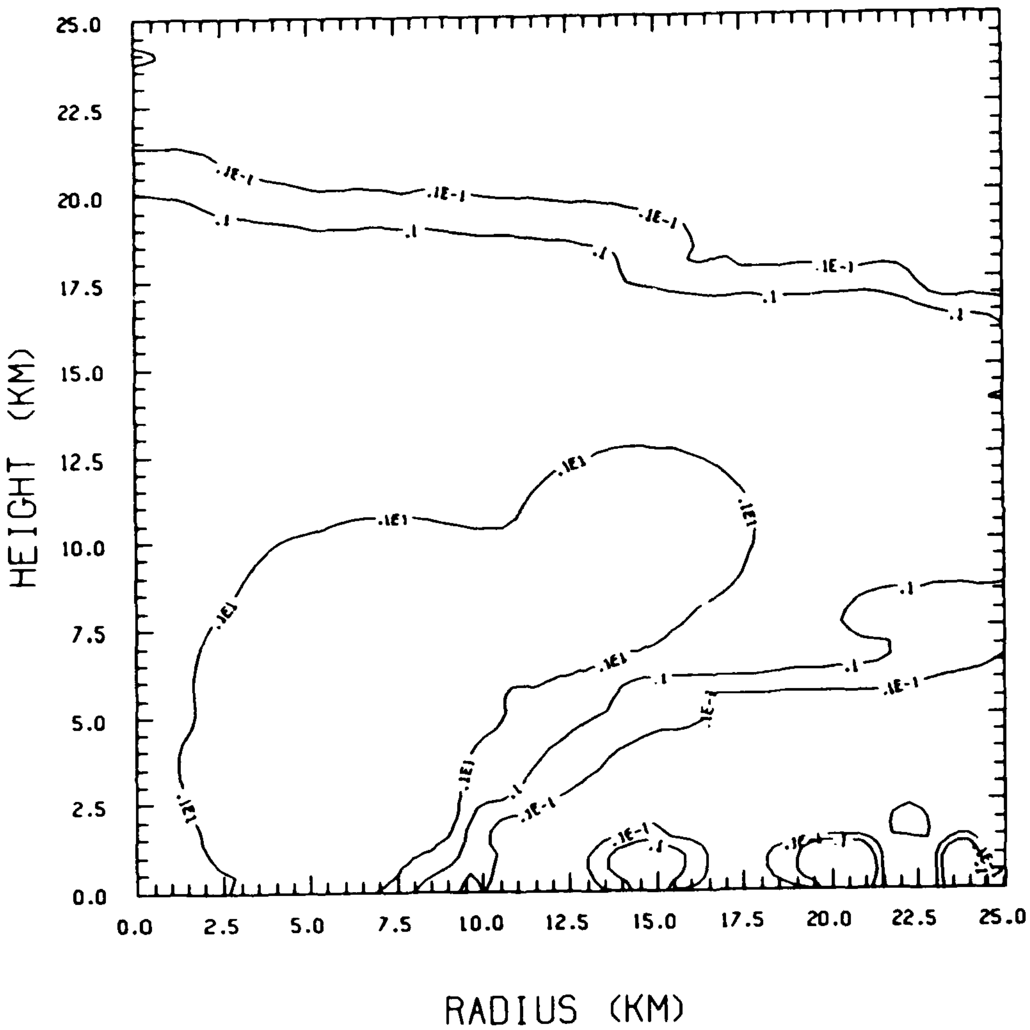

CONTOUR FROM .10000E-01 TO 10.000
(USER'S LEVELS)

TPW 50 KW/M**2 FIRE @ LCH TIME= 90.0

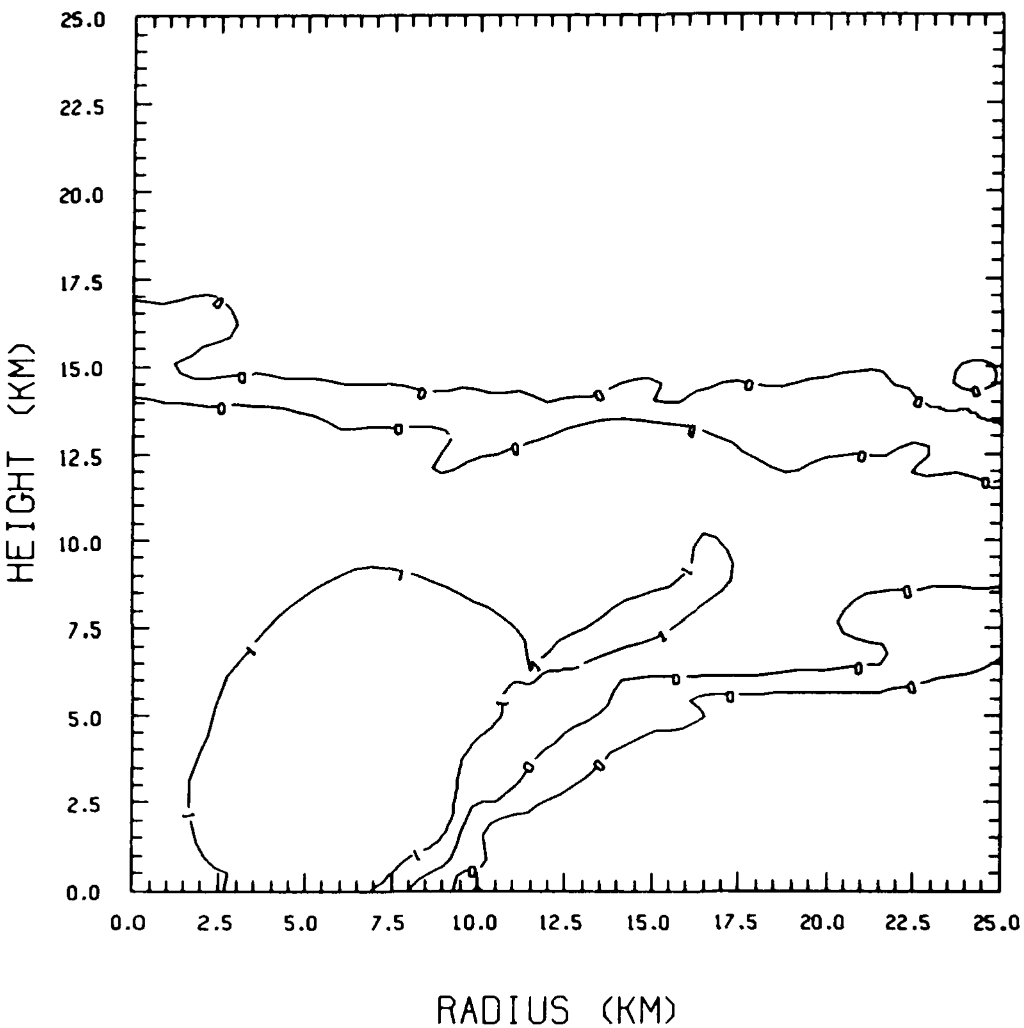

CONTOUR FROM .10000E-01 TO 1.0000
(USER'S LEVELS)

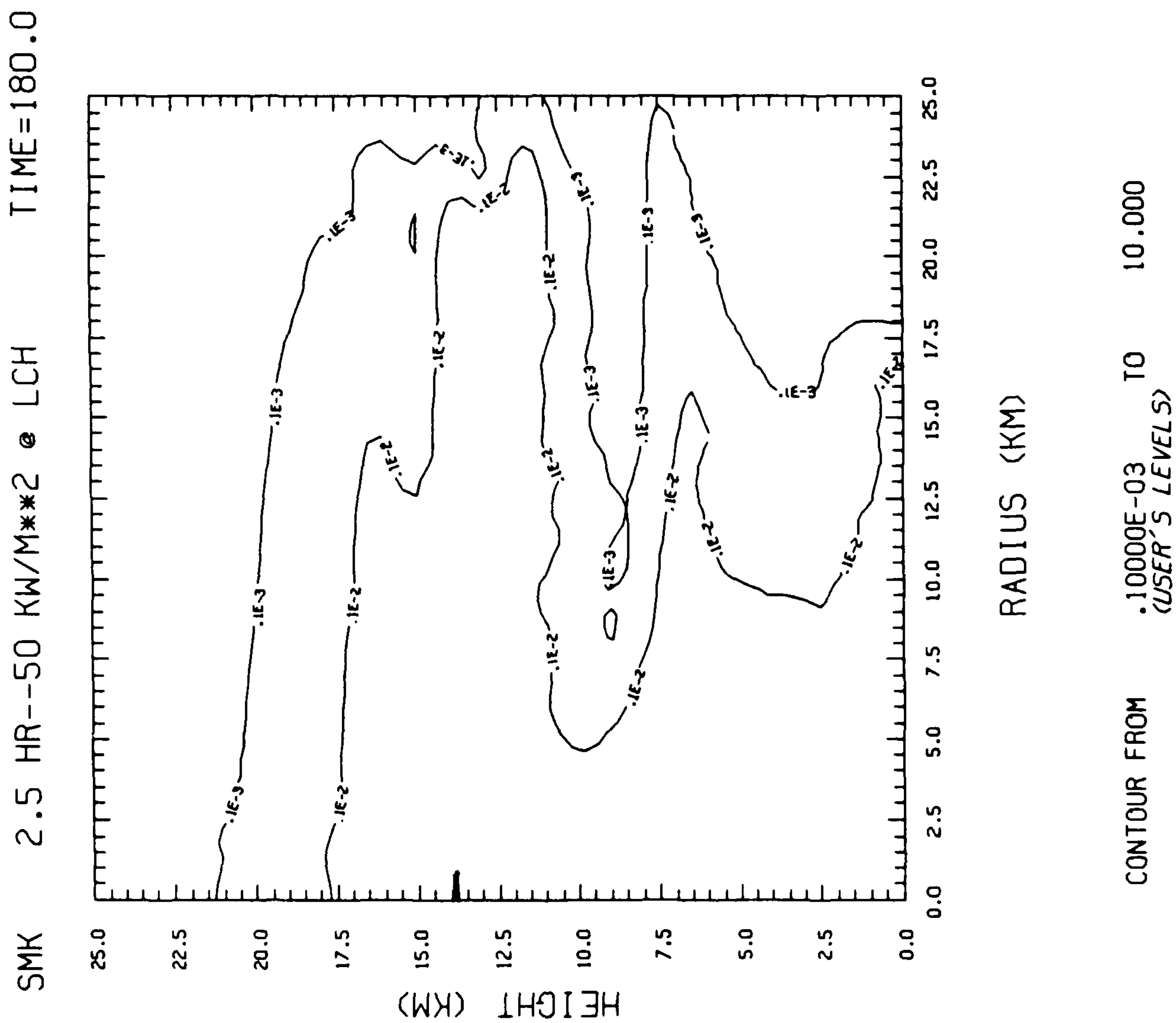
SMK 2.5 HR--50 KW/M**2 @ LCH TIME=180.0
HEIGHT (KM)
25.0 22.5 20.0 17.5 15.0 12.5 10.0 7.5 5.0 2.5 0.0
0.0 2.5 5.0 7.5 10.0 12.5 15.0 17.5 20.0 22.5 25.0
RADIUS (KM)
.1E-3
.1E-2
CONTOUR FROM .10000E-03 TO 10.000
(USER'S LEVELS)

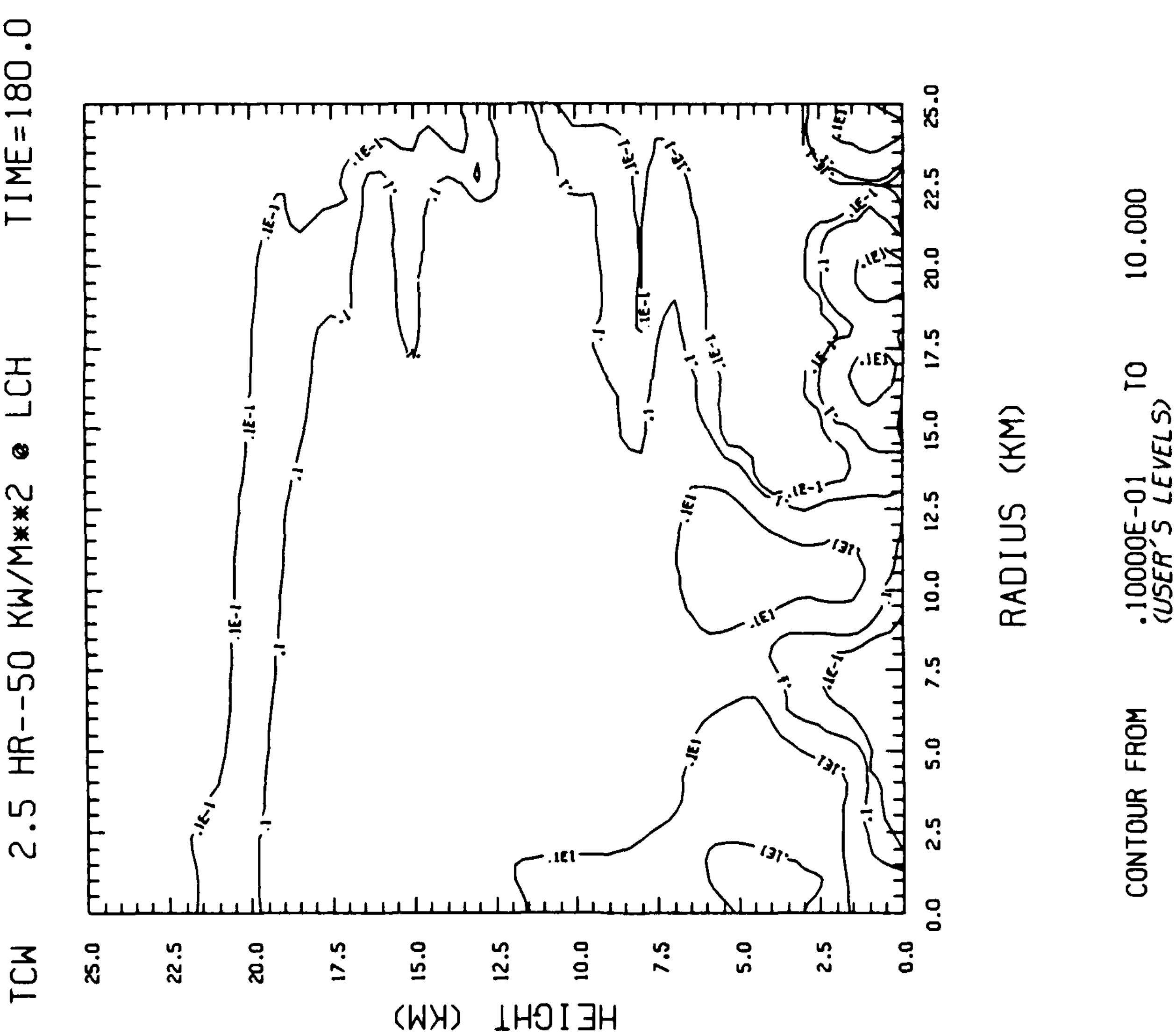
TCW 2.5 HR--50 KW/M**2 @ LCH TIME=180.0
HEIGHT (KM)
25.0
22.5
20.0
17.5
15.0
12.5
10.0
7.5
5.0
2.5
0.0
RADIUS (KM)
CONTOUR FROM .10000E-01 TO 10.000
(USER'S LEVELS)

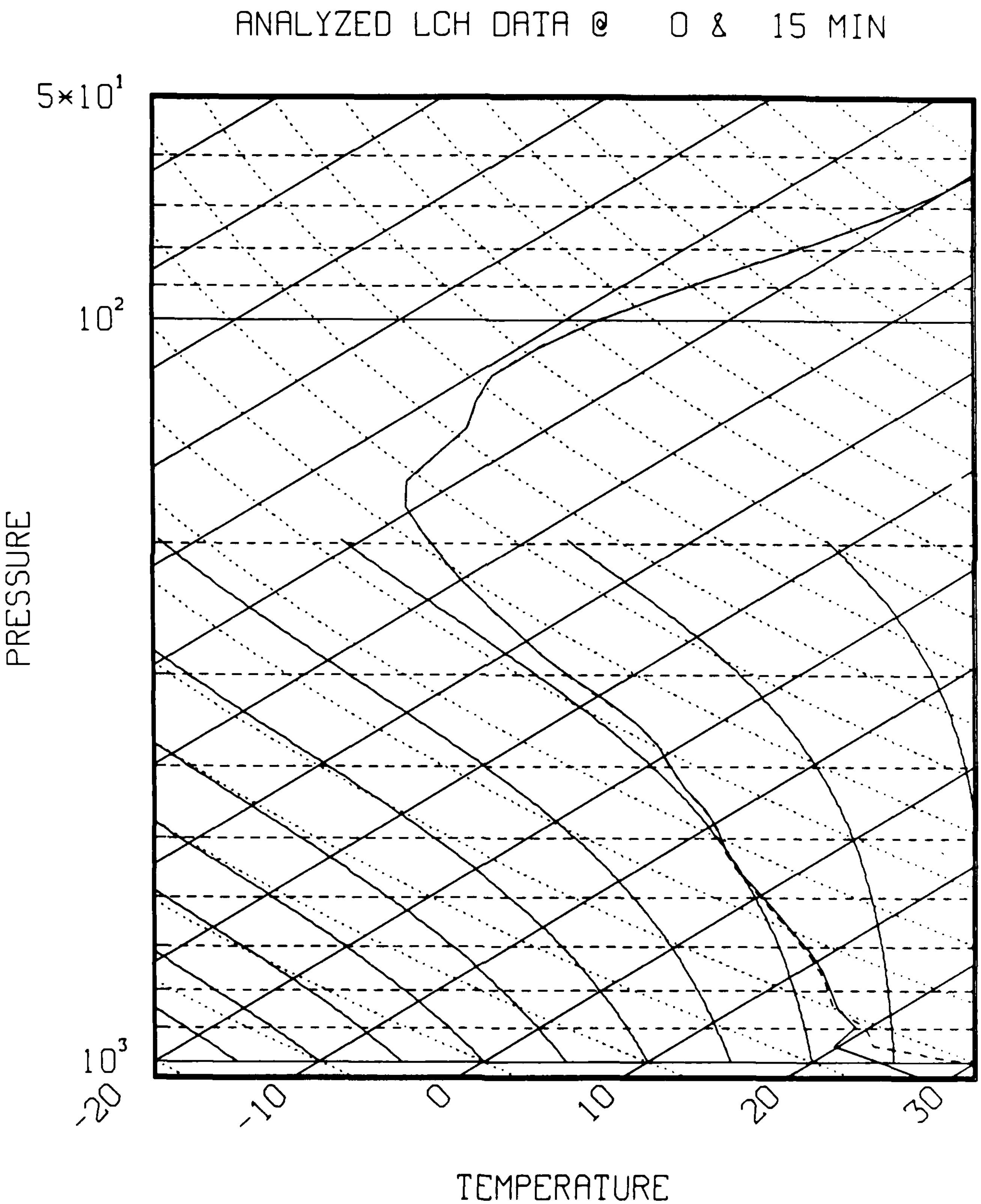

ANALYZED LCH DATA @ 0 & 15 MIN
5×10^1
10^2
10^3
PRESSURE
-20
-10
0
10
20
30
TEMPERATURE

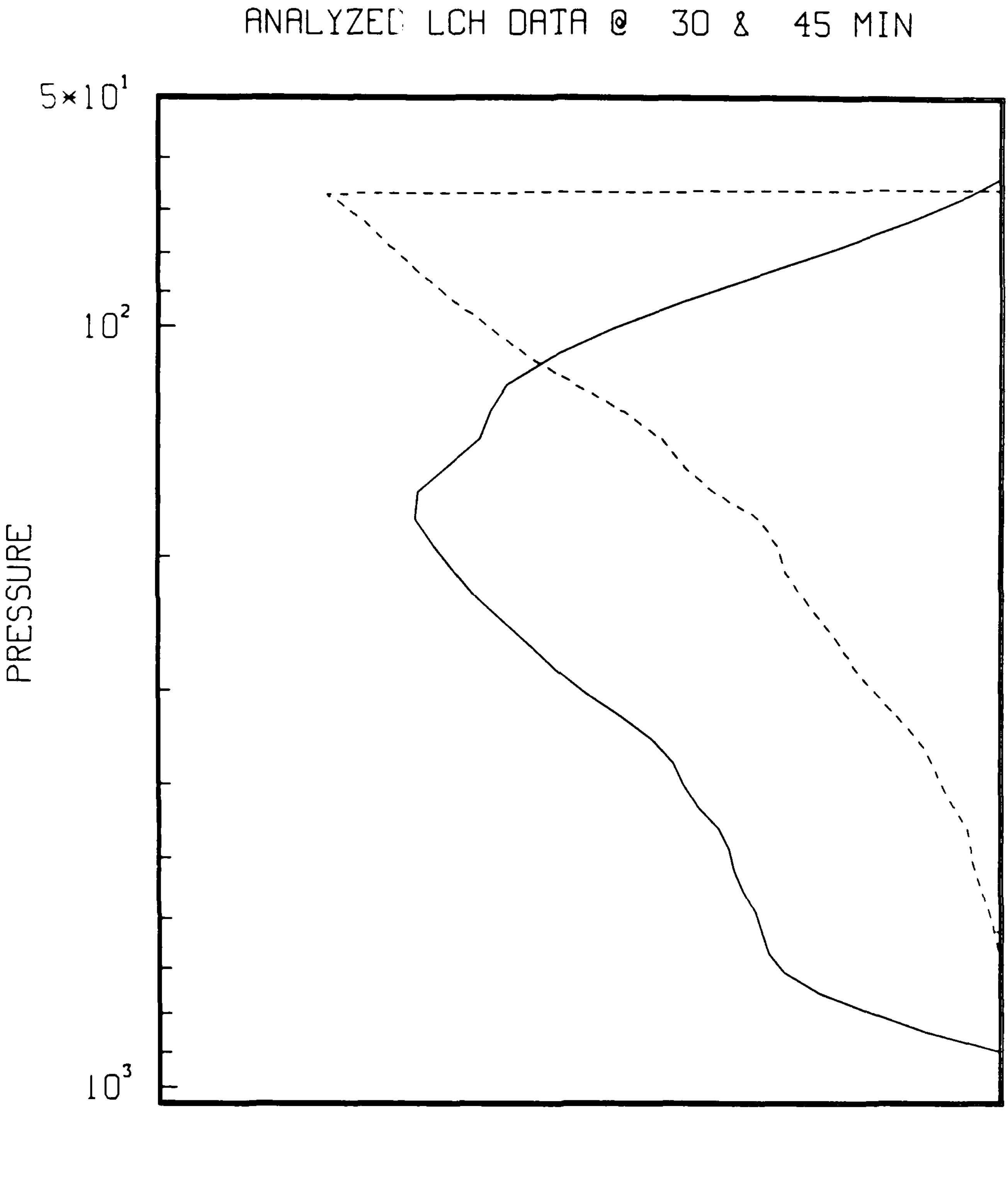
ANALYZED LCH DATA @ 30 & 45 MIN
5×10^1
10^2
10^3
PRESSURE
TEMPERATURE

ANALYZED LCH DATA @ 60 & 90 MIN

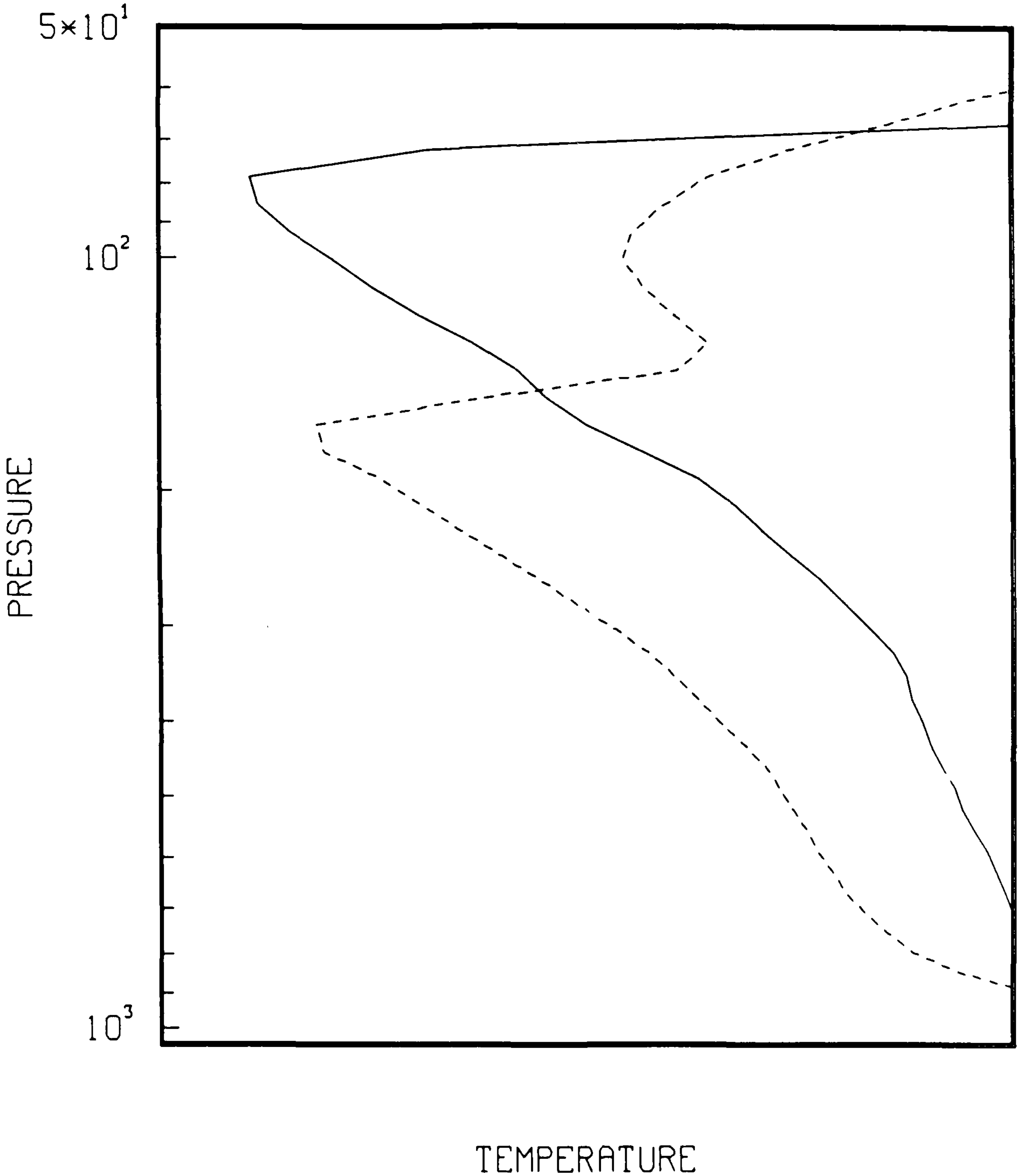

ANALYZED LCH DATA @ 120 & 150 MIN

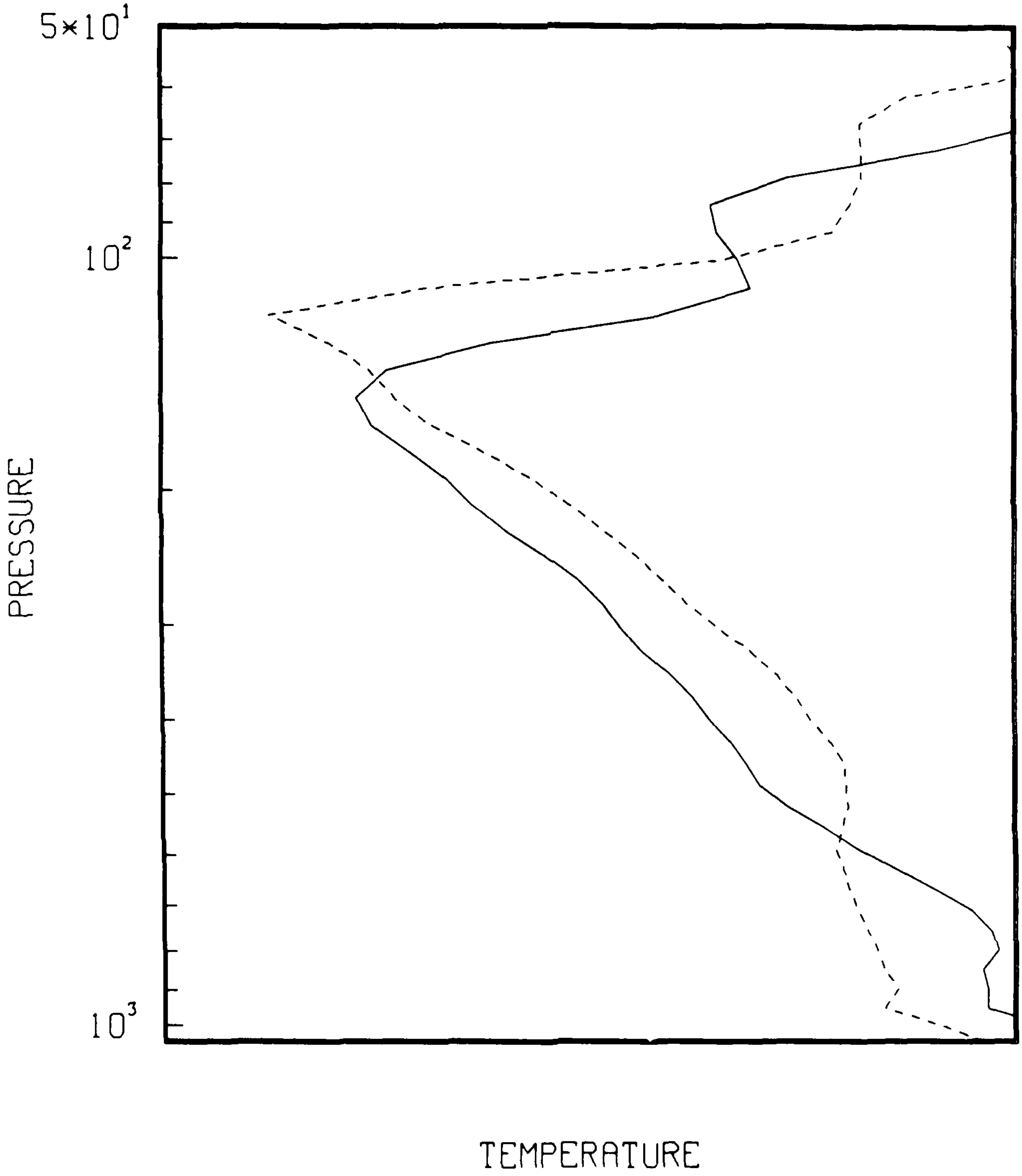

ANALYZED LCH DATA @ 180 MIN

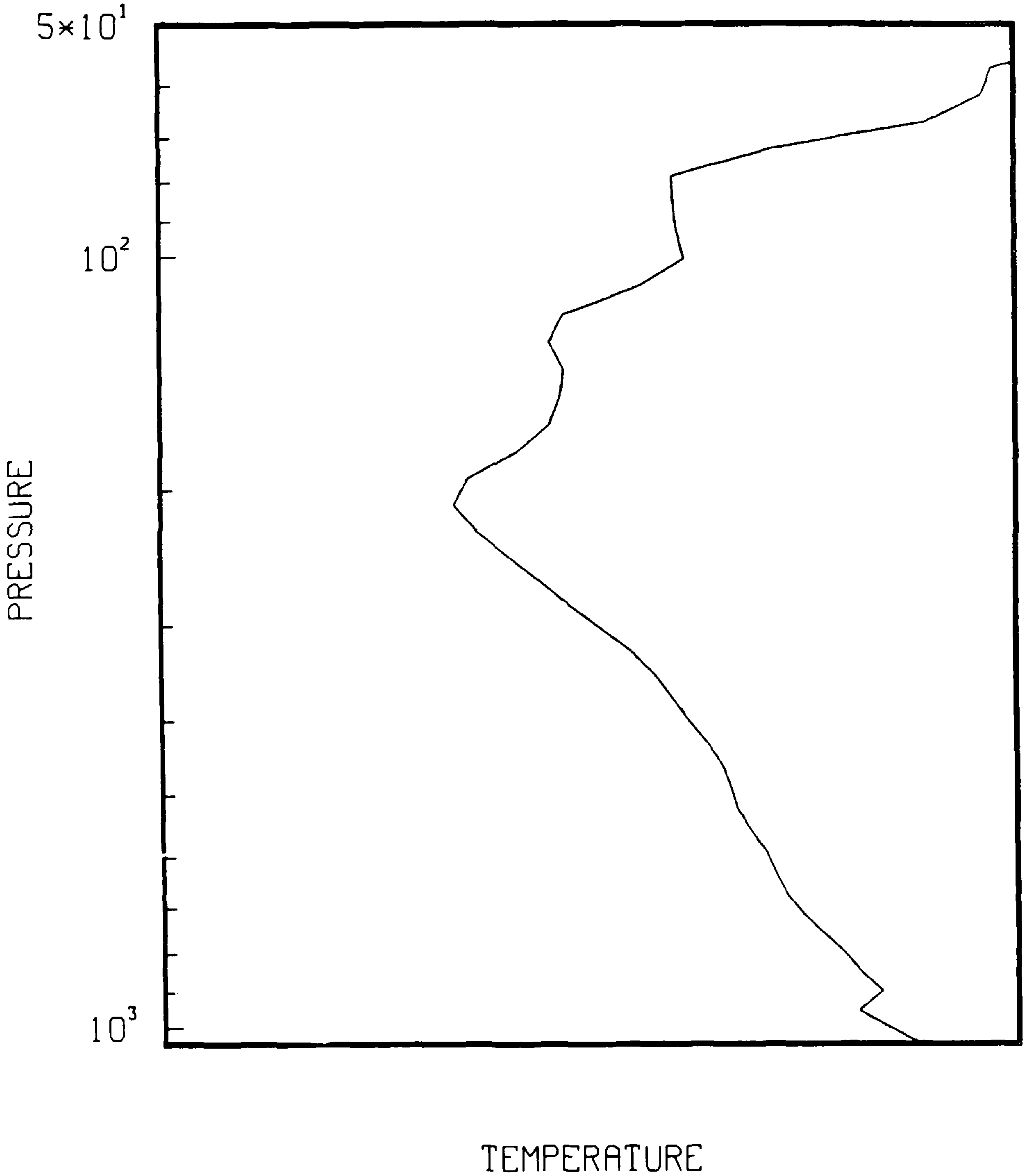

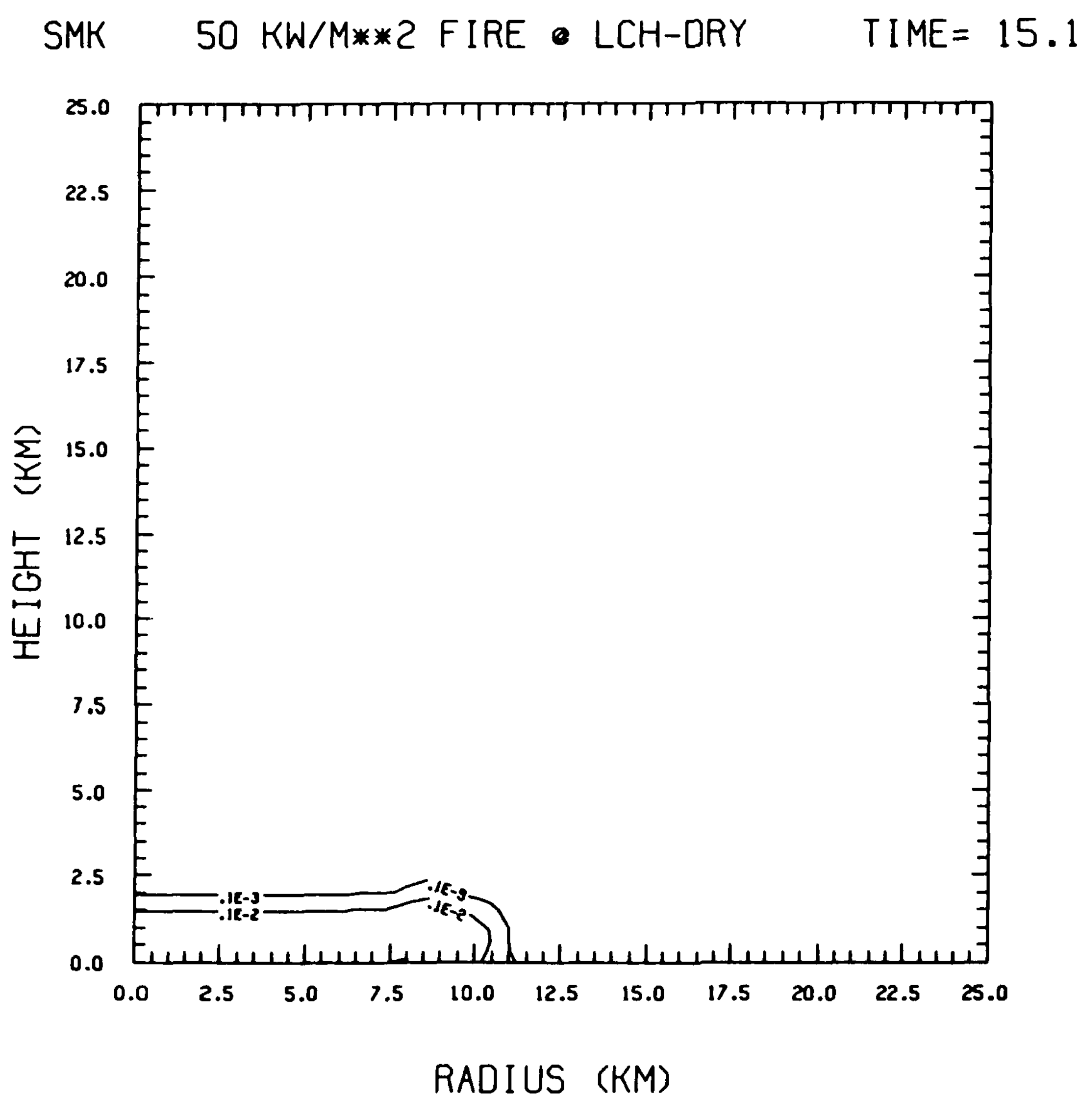

CONTOUR FROM .10000E-03 TO 10.000
(USER'S LEVELS)

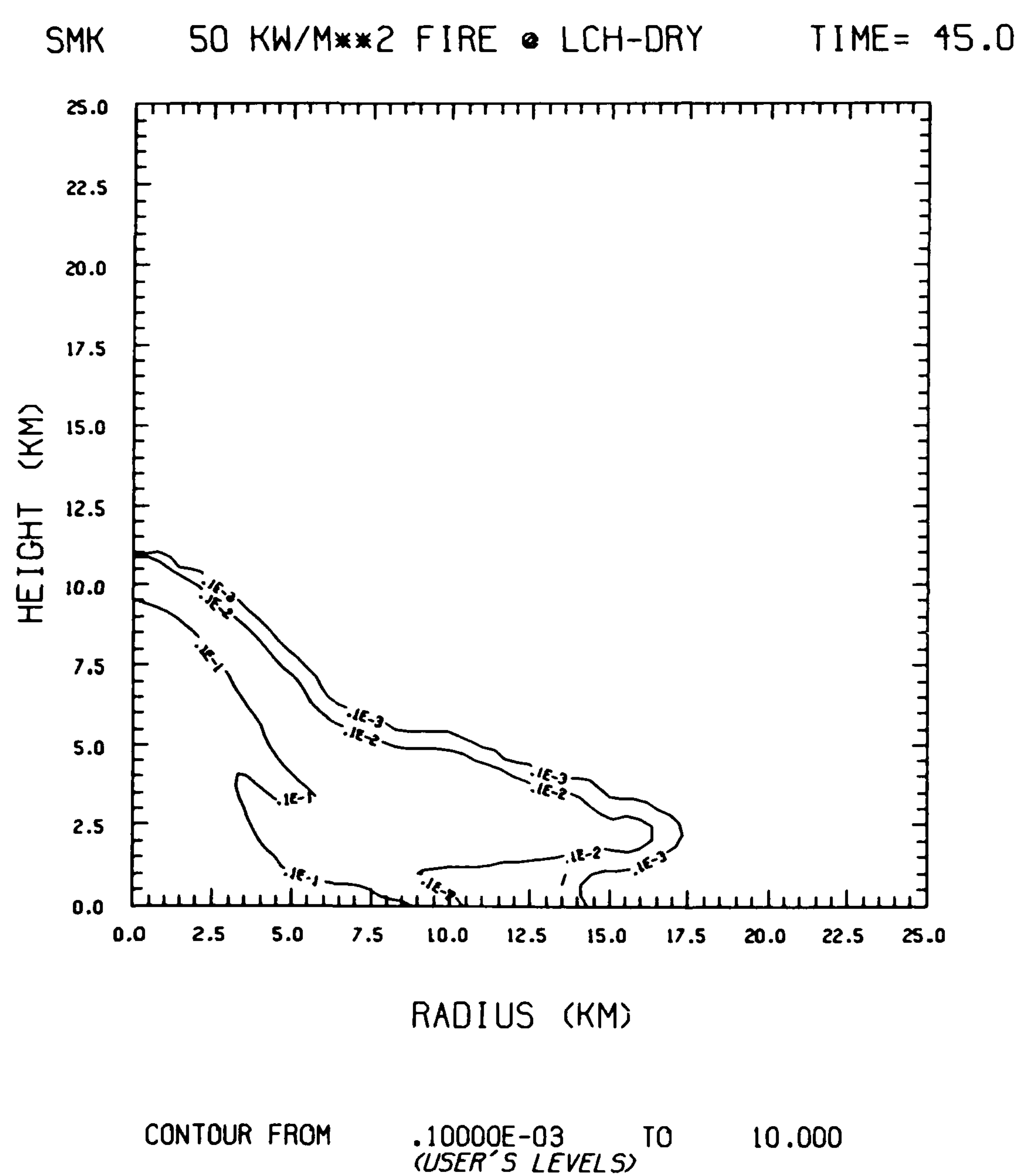

SMK 50 KW/M**2 FIRE @ LCH-DRY TIME= 45.0
HEIGHT (KM)
RADIUS (KM)
0.0
2.5
5.0
7.5
10.0
12.5
15.0
17.5
20.0
22.5
25.0
.1E-3
.1E-2
.1E-1
CONTOUR FROM .10000E-03 TO 10.000
(USER'S LEVELS)

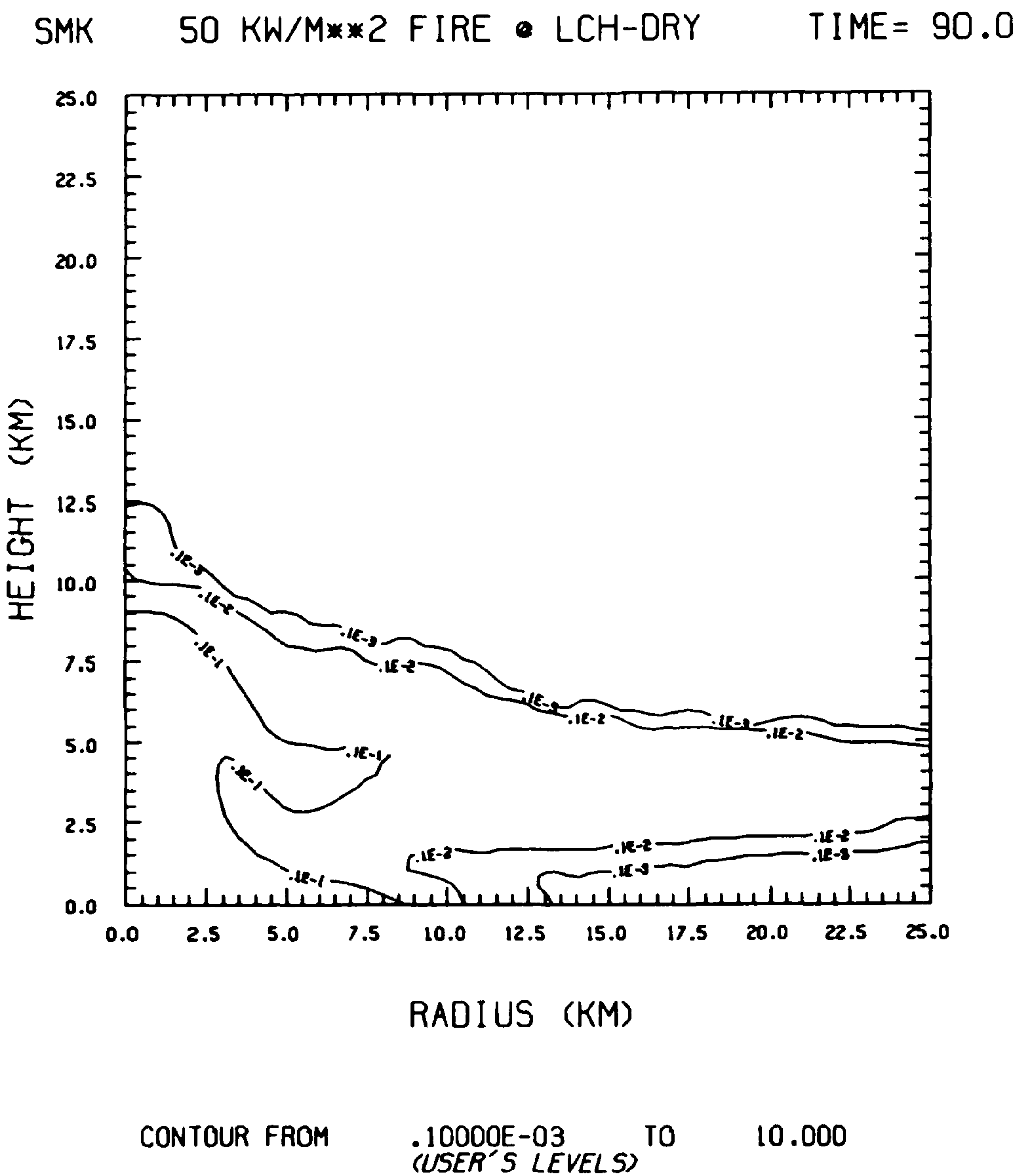
SMK 50 KW/M**2 FIRE @ LCH-DRY TIME= 90.0
HEIGHT (KM)
RADIUS (KM)
0.0
2.5
5.0
7.5
10.0
12.5
15.0
17.5
20.0
22.5
25.0
.1E-3
.1E-2
.1E-1
CONTOUR FROM .10000E-03 TO 10.000
(USER'S LEVELS)

CONCLUSIONS:

- WITHOUT THE PRESENCE OF WATER, THE SMOKE CANNOT STABILIZE AOVE THE TROPOPAUSE.

- WITHN MOISTURE PRESENT, THERE IS O(10^3) TIMES MORE CONDENSATE THAN SMOKE AND O(10^2) TIMES MORE PRECIPITATION. EARLY TIME SCAVENGING MUST BE CONSIDERED.

- SMOKE CAN BE INJECTED INTO THE "STRATOSPHERE", BUT ONLY ALONG WITH WATER WHICH WILL AFFECT ITS RESIDENCE TIME.

SAIC Science Applications International Corporation

NEXT EFFORTS:

- ADD SOUTH DAKOTA SCHOOL OF MINES SCAVENGING MODEL TO TASS.
- ADD DIAGNOSTICS FOR OPTICAL DEPTH AND TOTAL SMOKE ABOVE A GIVEN ALTITUDE v. ALTITUDE.

SAIC Science Applications International Corporation

The Numerical Simulation of Smoke Plume Dynamics in Intense Fires

Michael M. Bradley

Lawrence Livermore National Laboratory

The numerical model

- Two-dimensional
- Time-dependent
- Nonhydrostatic
- Compressible
- Eulerian
- Terrain-following coordinate system
- Cloud and rain parameterization
- Dynamic equations are fully nonlinear
- Flux form of substance transport equations (using fourth-order spatial differencing)

Benchmark Case

- U.S. standard spring–fall atmosphere
- No background wind
- Ambient moisture only – none from fire
- Smoke is passive tracer

Vertical Smoke Distributions After 1 hr

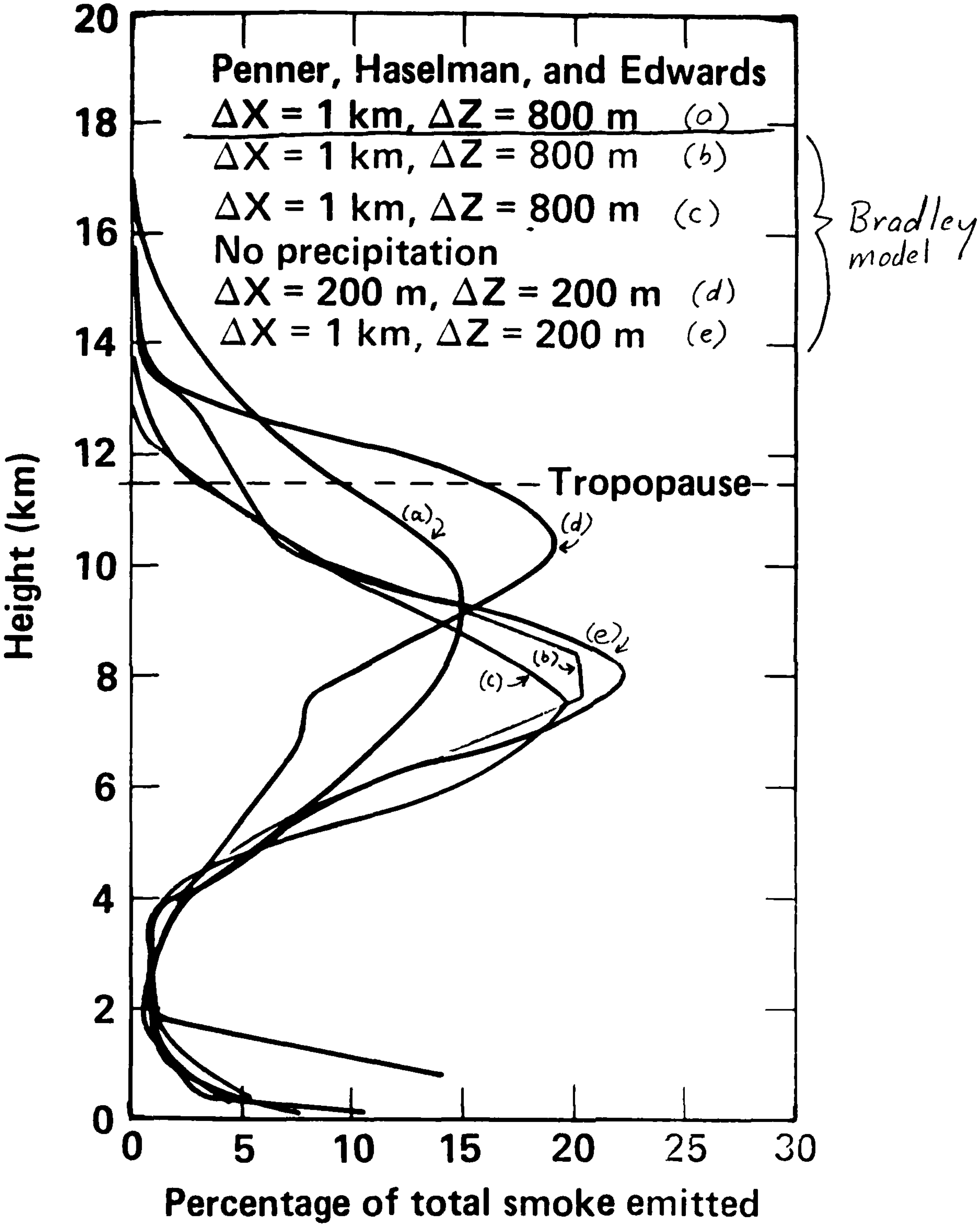

Figure 1 Normalized smoke profiles for intense fire (89 wm^{-2}) with no wind and ambient moisture only.

$\Delta x = \Delta z = 200$ m
time = 1 hr
Bradley model

U.S. Standard spring-fall atmosphere
No ambient wind
Moisture - ambient only
89 KW/m^2 heat source

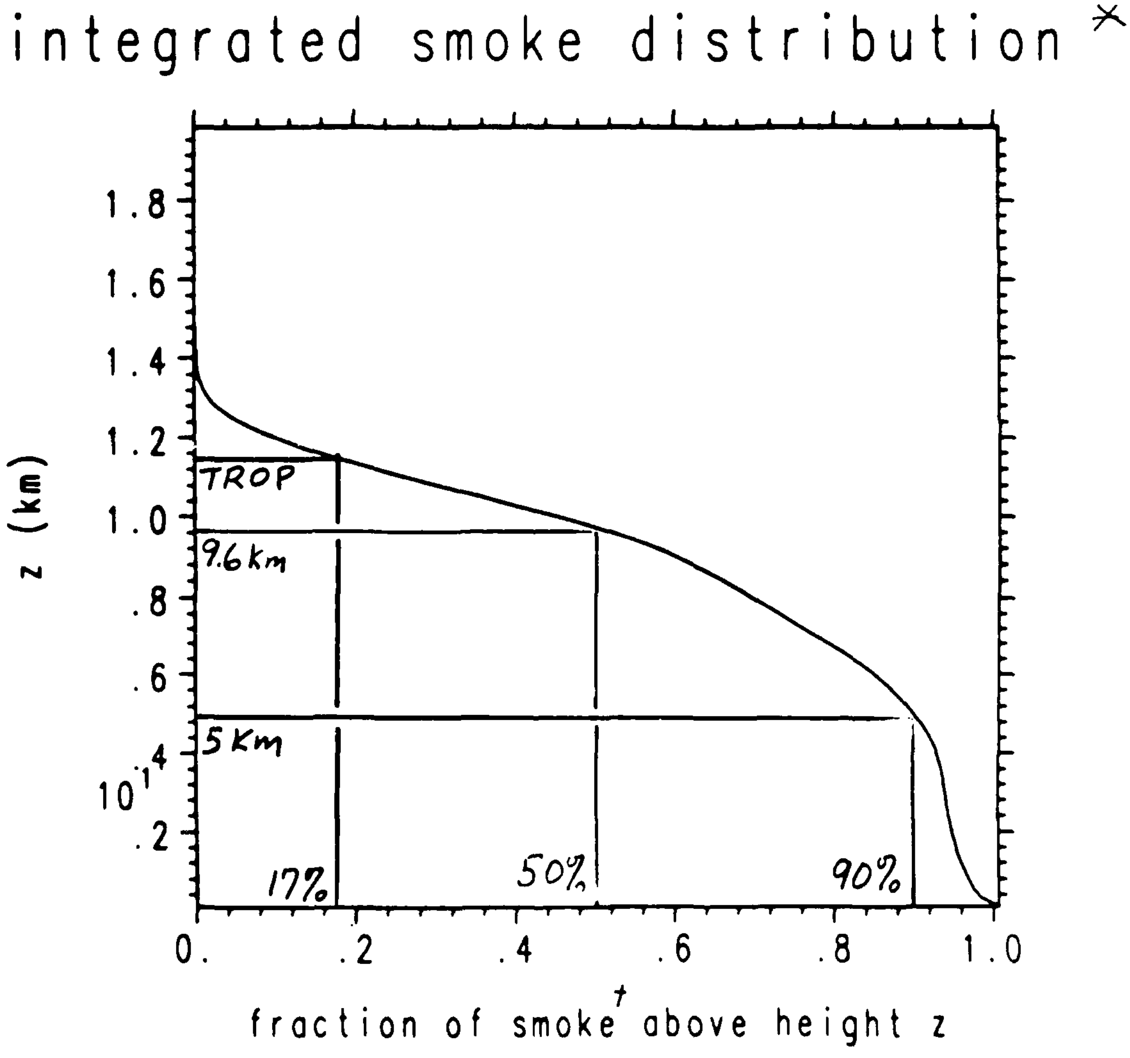

Figure 2

* Top-downward integration of curve (d) on Figure 1.

† Fraction of smoke emitted from source. Conservation is good to within less than ½ %.

A Note on Linearization

Model uses this equation:

$$\partial u/\partial t = -c_p \Theta_m \, \partial\pi/\partial x + \cdots$$

where:

$$\Theta_m = \Theta(1+.61qv)(1-qc-qr-qs)$$

$$\Theta = \bar{\Theta}(z) + \Theta' \qquad qv = \overline{qv}(z) + qv'$$

Some models linearize this to:

$$\partial u/\partial t = -c_p \bar{\Theta}_v \frac{\partial\pi}{\partial x} + \cdots$$

where:

$$\bar{\Theta}_v = \bar{\Theta}(z)(1+.61\overline{qv}(z))$$

At least for the benchmark case, there was no significant difference in the vertical smoke profile using the linearized form.

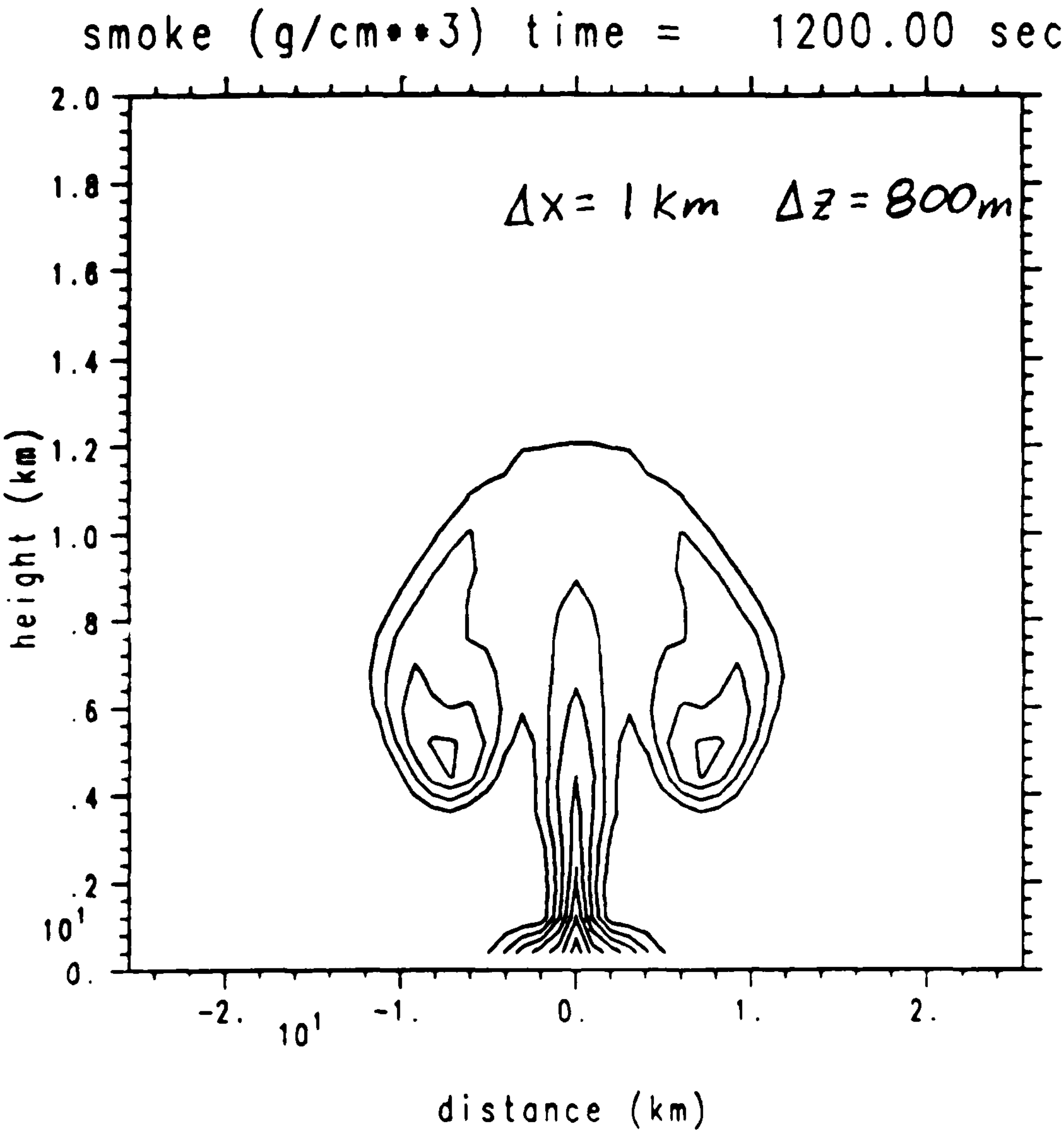

Figure 3. Smoke density contours for low resolution ($\Delta X = 1000m$, $\Delta z = 800m$) simulation. Contour interval is 5×10^{-10} g cm^{-3}. Compare with Figure 4 and curve (b) in Figure 1.

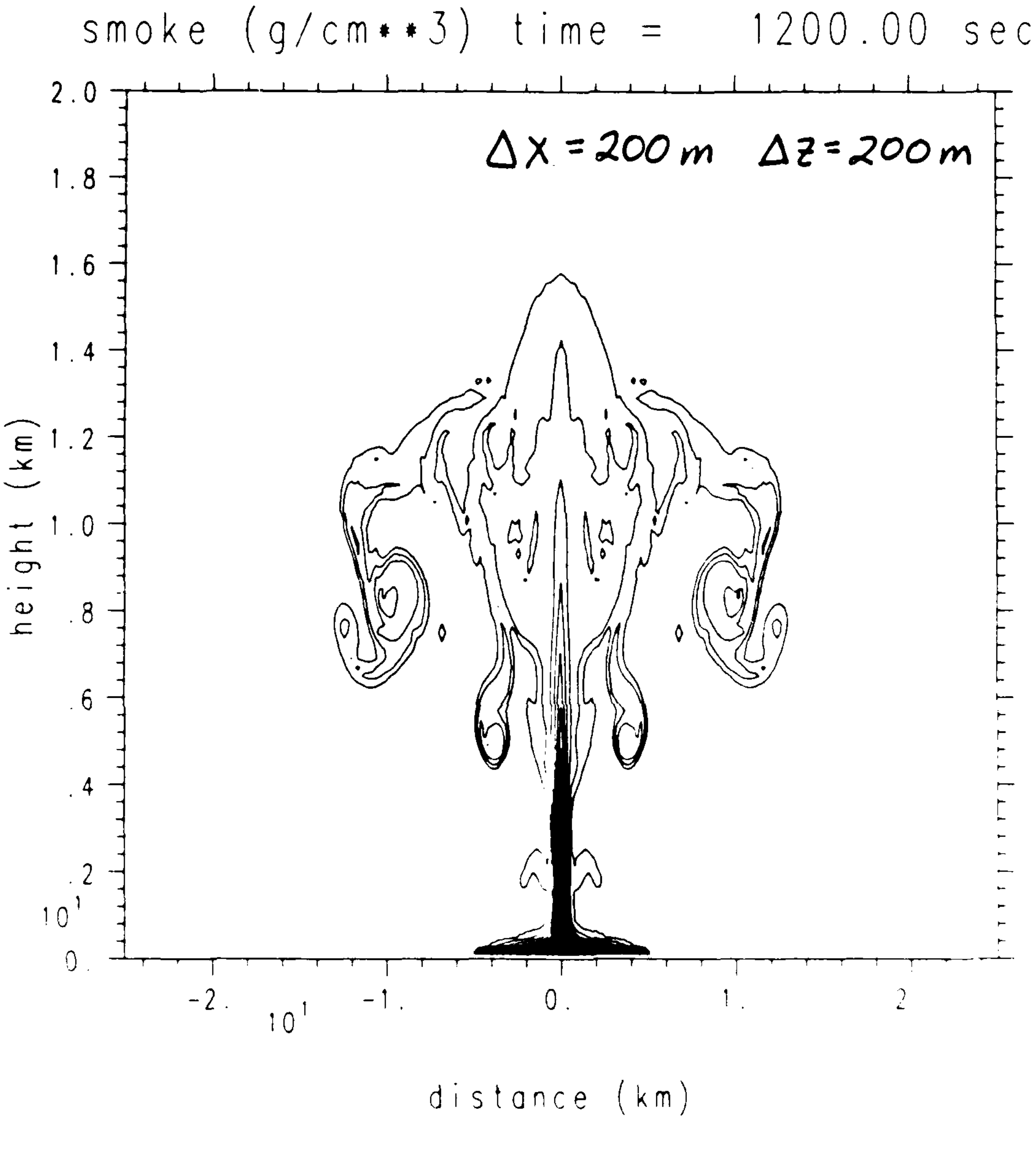

Figure 4. Smoke density contours for high resolution (200m x 200m) simulation. Contour interval is 5×10^{-10} g cm^{-3}. In addition to exhibiting fine structure, the smoke plume rises higher than in the low resolution simulation. Smoke distribution is shown in Figure 1, curve (d) (at 1hr).

Sources of Differences

- Equations
- Numerical methods
- Resolution, especially horizontal
- Turbulence parameterizations
- Atmospheric soundings

Future Research

- Condensation scavenging parameterization
- Interface with sophisticated condensation nucleation model
- Three-dimensional model

SECTION 3

MESOCALE MODELING

REGIONAL-SCALE INTERACTIONS BETWEEN ATMOSPHERIC DYNAMICS AND AEROSOLS

Douglas L. Westphal

The Pennsylvania State Univ.,
Department of Meteorology,
Univ. Park, PA 16802

and

Owen B. Toon

NASA Ames Research Center,
Space Sciences Division,
Moffett Field, CA 94035

NUCLEAR WINTER: MESOSCALE TOPICS

- Vertical lofting of aerosol by the fire and cloud
- Coagulation and wet removal in the convective plume
- Dynamical perturbation by the fire and cloud
- Self-generated bouyancy of soot clouds; cloud formation in bouyant soot clouds; cycling of soot through cloud droplets
- Spread of individual plumes; formation of larger, "GCM-scale" clouds
- Influence of diurnal radiative forcing on the response of the atmosphere
- Influence of geographical location and season on the above items

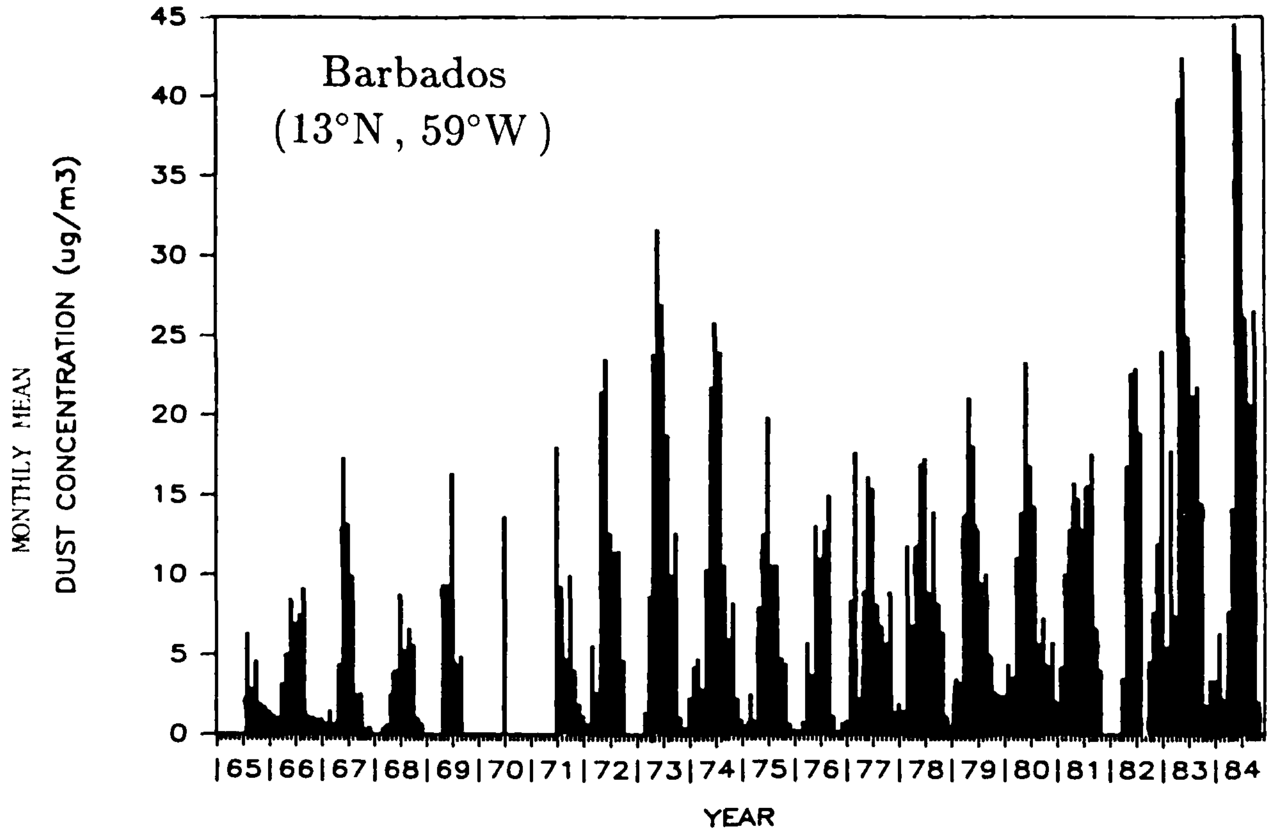

Barbados
(13°N, 59°W)
MONTHLY MEAN
DUST CONCENTRATION (ug/m3)
0
5
10
15
20
25
30
35
40
45
65
66
67
68
69
70
71
72
73
74
75
76
77
78
79
80
81
82
83
84
YEAR

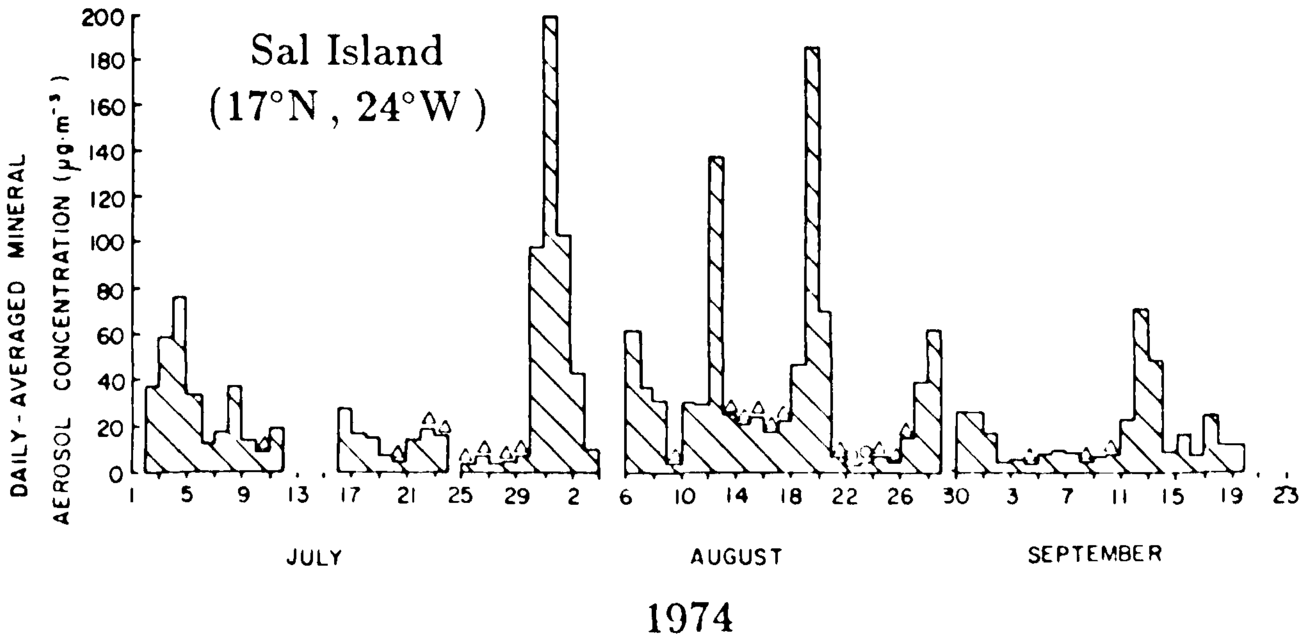

Sal Island
(17°N, 24°W)
DAILY-AVERAGED MINERAL
AEROSOL CONCENTRATION (μg·m⁻³)
0
20
40
60
80
100
120
140
160
180
200
1
5
9
13
17
21
25
29
2
6
10
14
18
22
26
30
3
7
11
15
19
23
JULY
AUGUST
SEPTEMBER
1974

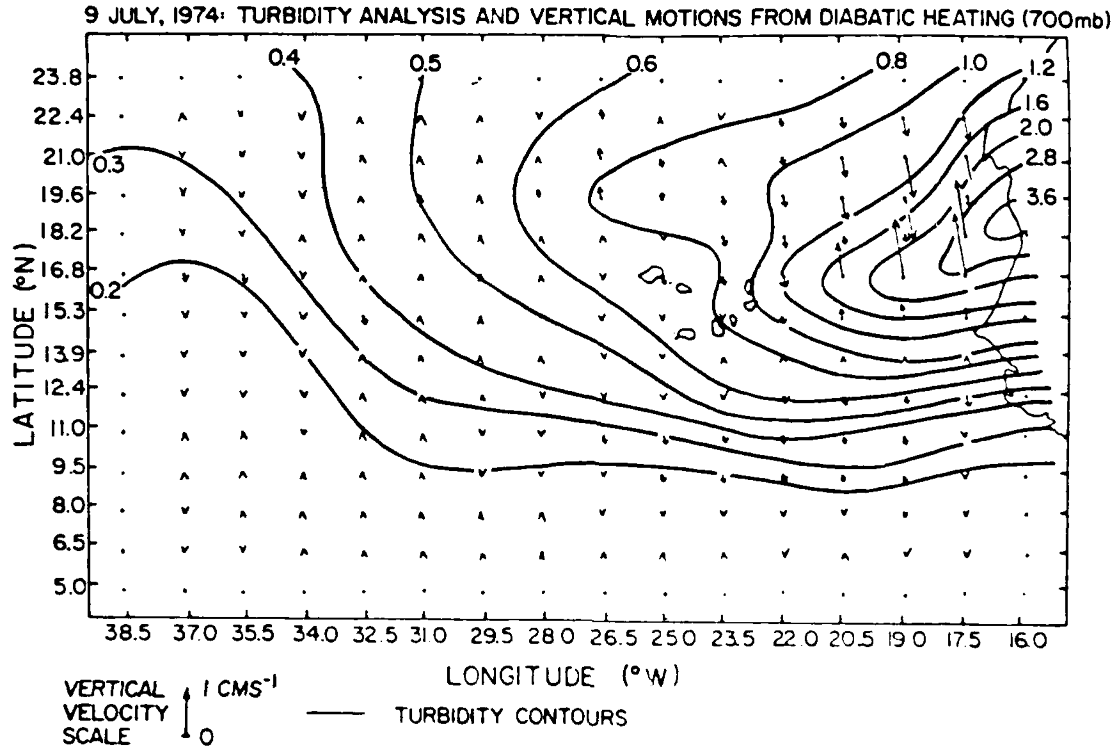

Turbidity isopleths determined from satellite irradiances and diagnosed 700 mb vertical motions associated with radiative heating of dust for 1200 GMT, July 9, 1974 (Karyampudi, 1979).

NUMERICAL MODELS

Atmospheric — Penn State/NCAR Limited-Area Model

- Primitive equations, hydrostatic
- Predicted ground temperature
- Subgrid-scale vertical fluxes
- Precipitation: Large-scale and subgrid-scale (cumulus) precipitation

Aerosol — Ames Research Center's Aerosol Model

- Continuity equation for each size aerosol and each type of aerosol
- Dry and wet removal
- Coagulation
- Condensation
- Surface or gridpoint source, or initial cloud
- Radiation

SCAVENGING PARAMETERIZATION

Scavenging rate Λ in (s^{-1}) is given by

$$\begin{array}{ll} \Lambda = 4.2 \times 10^{-4} E R^{0.79} & R^{0.63} \leq 7000/EH \\ \Lambda = 3R^{0.16}/H & R^{0.63} > 7000/EH \end{array}$$

where:

E is the collection efficiency, 0.83
H the depth of the precipitating cloud (m)
R the rainfall rate $(mm\, hr^{-1})$

- Marshall-Palmer droplet size distribution assumed
- No dependence on aerosol size
- Non-convective rainfall R_n is due to supersaturation in the grid box
- Convective rainfall R_c and the fraction a_p covered by convection are determined by a cumulus cloud parameterization

The total scavenging rate for a grid box is

$$\Lambda = (1 - a_p)\Lambda(R_n) + a_p\Lambda(R_n + R_c)$$

120 hr. simulated 700 mb streamlines (solid), isotachs (dashed, in ms^{-1}), and areas of precipitation (cross-hatched).

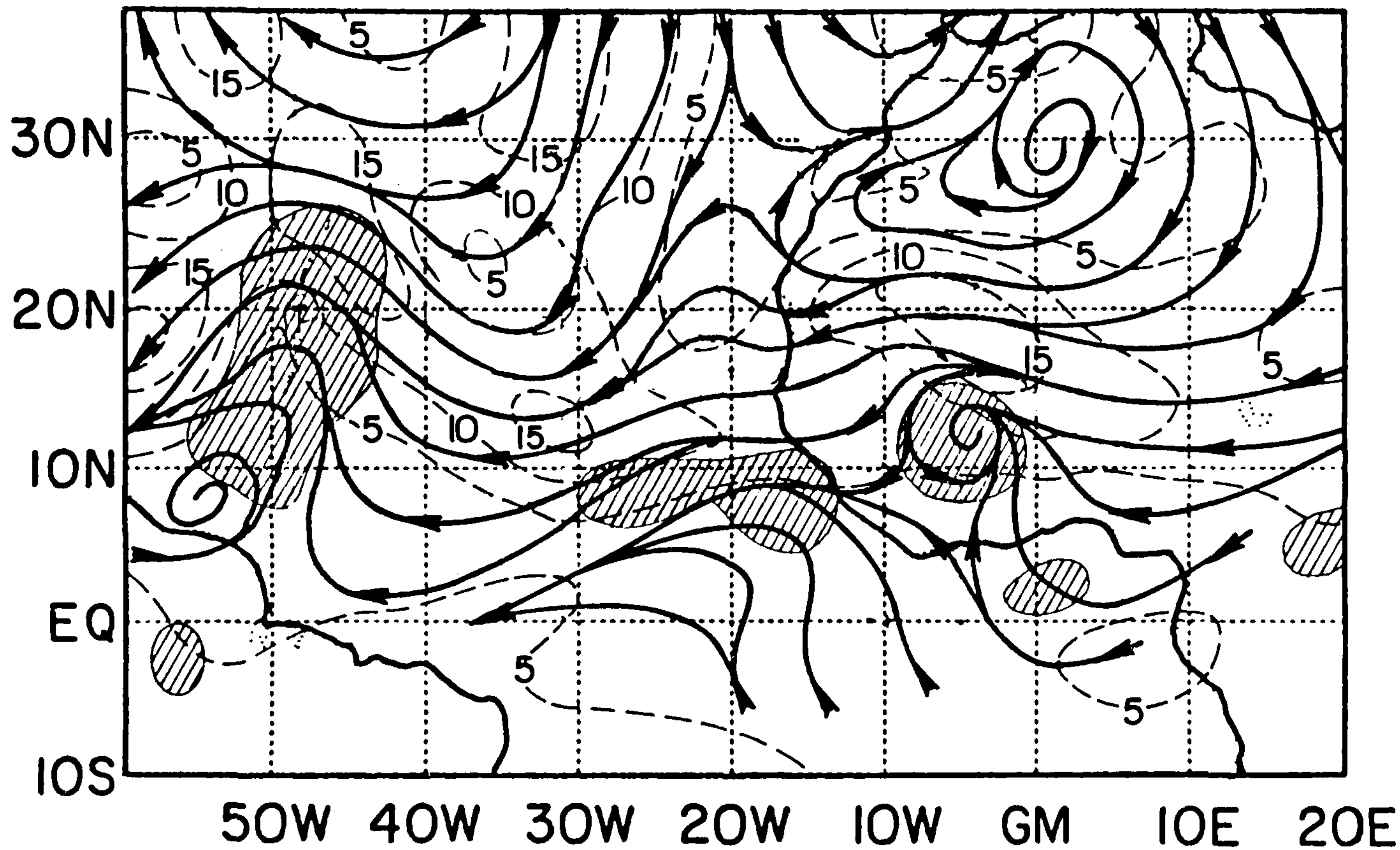

O hr. Optical Depth , 23 Mt

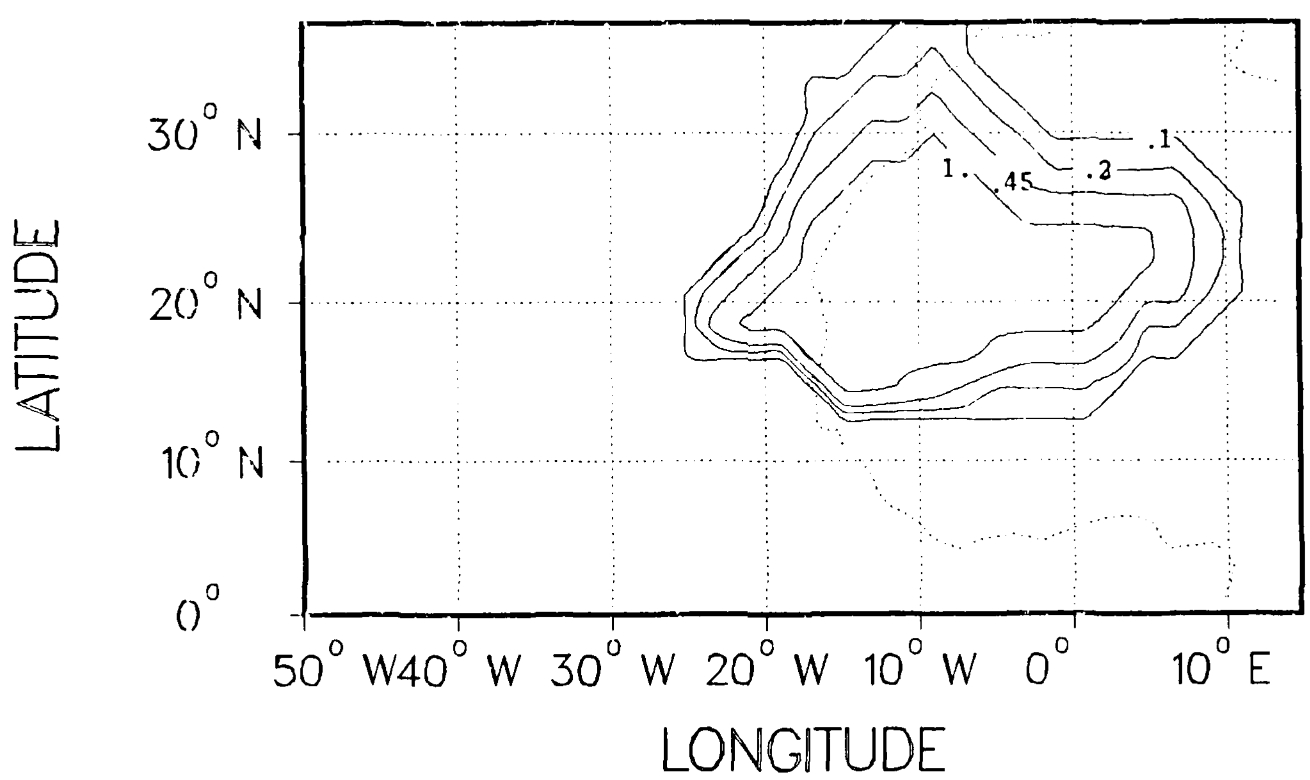

Vertical Profiles of Mass Concentration ($\mu g\, m^{-3}$)

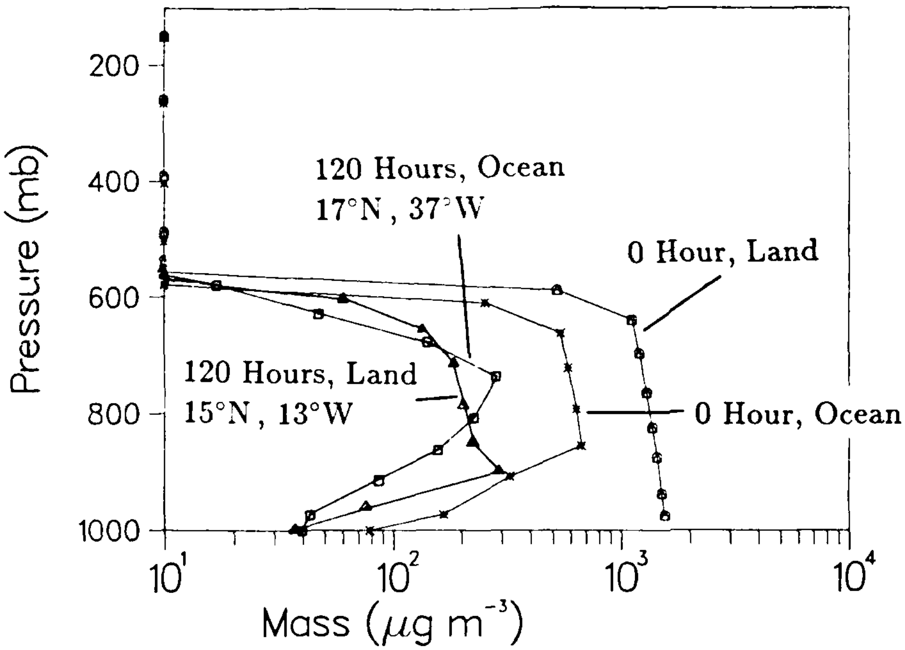

Size Distributions by Volume

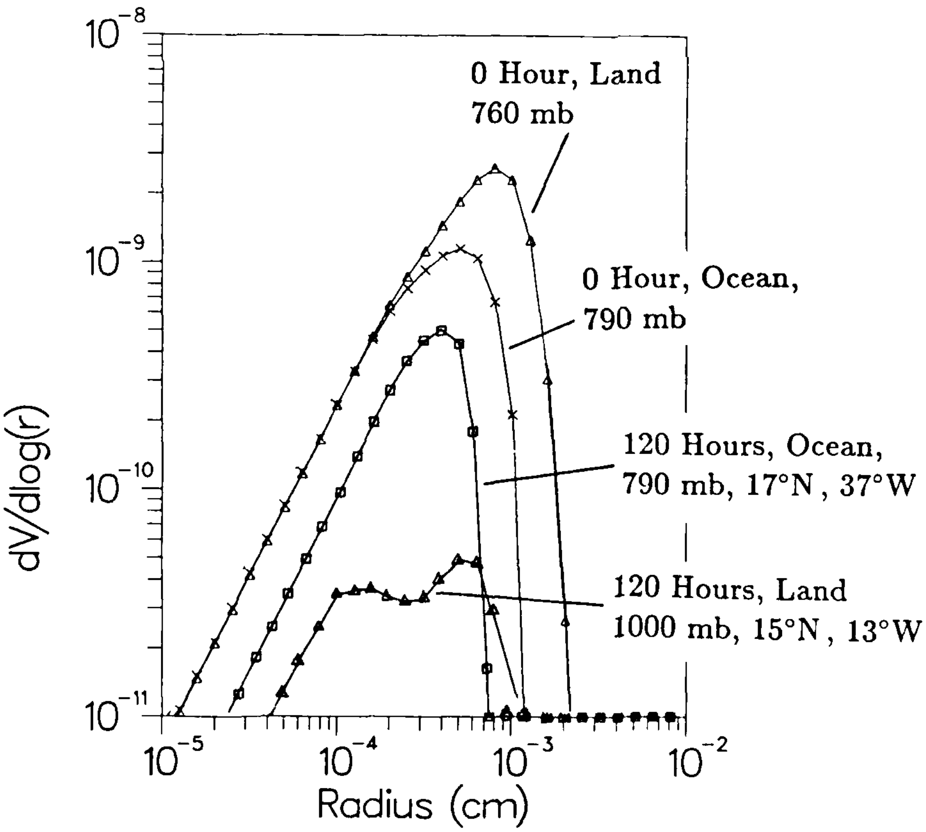

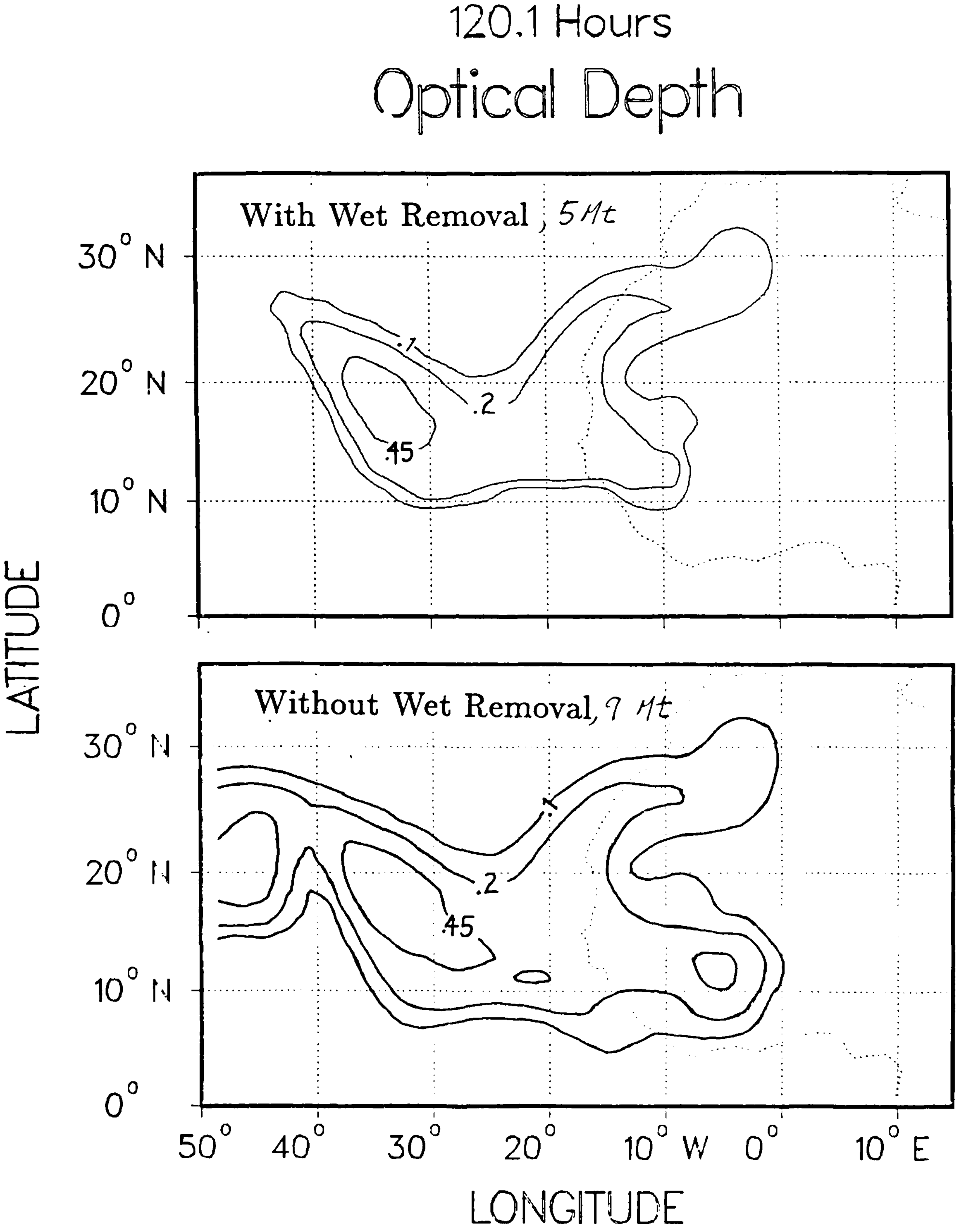
120.1 Hours
Optical Depth
With Wet Removal, 5 Mt
Without Wet Removal, 9 Mt
.1
.2
.45
30° N
20° N
10° N
0°
LATITUDE
50°
40°
30°
20°
10° W
0°
10° E
LONGITUDE

FUTURE WORK

- Include radiative heating in the Saharan dust simulations
- Conduct tests to determine the resolution requirements of soot cloud modeling
- Use a non-hydrostatic model to develop an input dataset of the initial spatial and size distribution of a soot cloud
- Carry out experiments that address the outstanding problems of nuclear winter

Algorithms for Computations of Aerosol Physics and Radiative Transfer

Owen B. Toon
NASA Ames Research Center
Space Sciences Division
Moffett Field, CA 94035

Overview of Ames Program

I Develop Natural Analogs to Nuclear Winter

A. Saharan Dust Storms

B. Volcanic Clouds

II Determine Fuel Loading

III Develop Algorithms for Aerosol Physics

IV Perform Regional Scale Modeling

Algorithms for Aerosol Physics

I Aerosol Microphysics and Transport

II Radiative Transfer in Aerosols

III Interactions Between Aerosols and Clouds

Aerosol Microphysics and Transport

I General Properties

A. In Arbitrary Coordinates So Can Be Used In A Variety of Dynamical Models

B. Description in Preparation

II Transport

A Timesplit So Can Be Used in 1,2,or 3-D Models

B. Finite Elements in Horizontal, Curve Fitting Scheme in Vertical. Exactly Conserve Mass,Have Little Numerical Diffusion,No Negative Numbers, Numerically Efficient

III Microphysics

A. Resolves Size Distribution

B. Includes:Sedimentation, Coagulation,Multiple Aerosol Constituents,Condensational Growth, Gases

$$\frac{\partial C_z}{\partial t} + \nabla_z \cdot C_z V_z + \frac{\partial}{\partial Z}(W_z + V_{fall})\ C_z - \nabla_z\ \rho K_H\ \nabla C_z/\rho$$

$$- \frac{\partial}{\partial Z}\rho K_z \frac{\partial}{\partial Z}(C/\rho) = (P-L) \qquad (2)$$

$$\frac{\partial C}{\partial t} + \frac{\partial UC}{\partial \bar{X}_1} + \frac{\partial VC}{\partial \bar{X}_2} + \frac{\partial}{\partial \bar{X}_3} WC - \frac{\partial}{\partial \bar{X}_1}\rho^* K_1 \frac{\partial}{\partial \bar{X}_1} C/\rho^*$$

$$-\frac{\partial}{\partial \bar{X}_2}\rho^* K_2 \frac{\partial}{\partial \bar{X}_2} C/\rho^* - \frac{\partial}{\partial \bar{X}_3}\rho^* K_3 \frac{\partial}{\partial \bar{X}_3} C/\rho^* = (P-L)\ V_m' H_{m1} H_{m2} \qquad (1)$$

$$\frac{\partial C_z}{\partial t} + \nabla_z \cdot C_z V_z + \frac{\partial}{\partial Z}(W_z + V_{fall})\ C_z - \nabla_z\ \rho K_H\ \nabla C_z/\rho$$

$$- \frac{\partial}{\partial Z}\ \rho K_z\ \frac{\partial}{\partial Z}\ (C/\rho) = (P-L) \qquad (2)$$

$$\frac{\partial C}{\partial t} + \frac{\partial UC}{\partial \bar{X}_1} + \frac{\partial VC}{\partial \bar{X}_2} + \frac{\partial}{\partial \bar{X}_3} WC - \frac{\partial}{\partial \bar{X}_1} \rho^* K_1 \frac{\partial}{\partial \bar{X}_1} C/\rho^*$$

$$\frac{\partial}{\partial \bar{X}_2} \rho^* K_2 \frac{\partial}{\partial \bar{X}_2} C/\rho^* - \frac{\partial}{\partial \bar{X}_3} \rho^*\ K_3 \frac{\partial}{\partial \bar{X}_3} C/\rho^* = (P-L)\ V_m' H_{m1} H_{m2} \qquad (1)$$

TABLE 1

Conversion scaling factors for various coordinate systems

Coordinate Systems	H_{m1}	H_{m2}	H_{m3}	ds_1	ds_2	Vm	ds_3
Spherical Coordinates	$\sin \Phi$	1	a	$d\lambda$	$d\Phi$		
Mercator	$\frac{\cos\phi}{\cos\phi_0}$	$\frac{\cos\phi}{\cos\phi_0}$	1	dx	dy		
Polar Stereographic	$\left(\frac{1+\sin\phi}{2}\right)^{-1}$	$\left(\frac{1+\sin\phi}{2}\right)^{-1}$	1	dx	dy		
Lambert Conformal	$\frac{(1+\sin\phi)\cos\phi_n}{(1+\sin\phi_0)\cos\phi_0}$	$\frac{(1+\sin\phi)\cos\phi_n}{(1+\sin\phi_0)\cos\phi_0}$	1	dx	dy		
Rectangular	1	1	1	dx	dy	1	dz
Pressure						$1/\rho g$	dp
Sigma = $\frac{P-Ptop}{P_{btm}-Ptop} = \frac{P-Ptop}{P^*}$						$P^*/\rho g$	$d\sigma$
Log Pressure $Z = H \ln (P/P_{sfc})$						$^T/To$	dz

$U = Uc/H_{m1}$ $V = Vc/H_{m2}$ $W = ds_{3/dt} + Vfall\ V_m^{-1}$ $C = C_z V_m \cancel{a_1 a_2} H_{m1} H_{m2}$

$Kx_1 = 1/H_{m1}^2 K$ $K_{x2} = 1/H_{m2}^2 K$ $Kx_3 = V_m^{-2} K_z$

$\rho^* = \rho V_m H_{m1} H_{m2}$ $dx_1 = H_{m3} ds_1$ $dx_2 = H_{m3} ds_2$ $dx_3 = ds_3$

Φ = colatitude

ϕ = latitude ϕ_o = latitude at which projection is true

λ = longitude n = constant which can be adjusted to make the projection true at a second latitude ϕ_1

a = radius of Farth

ρ = air density $n = (k(k-1))^{-1}$ $k = \ln\left(\frac{\cos\phi_0}{\cos\phi_1}\right) \div \ln\left(\frac{\tan(\pi/4 - \phi_0/2)}{\tan(\pi/4 - \phi_1/2)}\right)$

g = gravitational acceleration H = Scale height = RTo/g

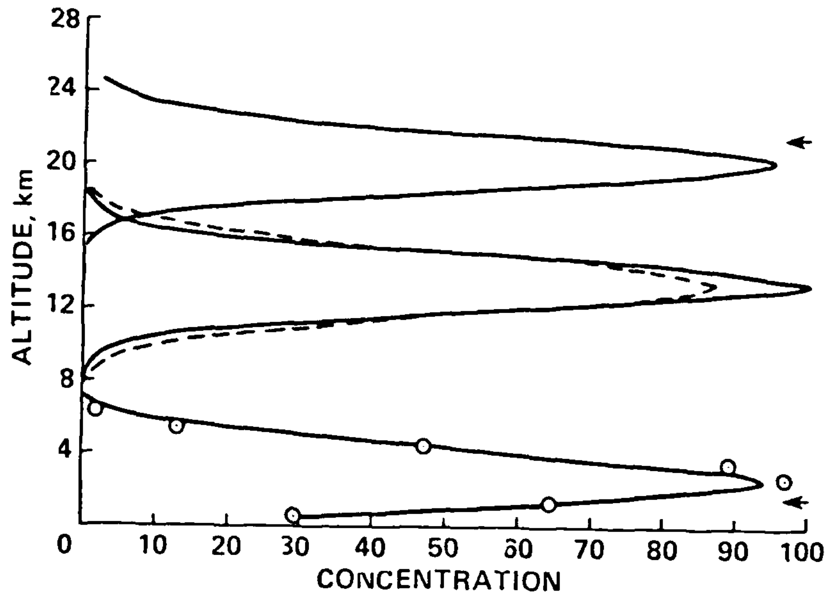

28
24
20
16
12
8
4
0
ALTITUDE, km
10
20
30
40
50
60
70
80
90
100
CONCENTRATION

AD-A185 150 TECHNICAL PAPERS PRESENTED AT THE DEFENSE NUCLEAR AGENCY GLOBAL EFFECTS R..(U) DOD NUCLEAR INFORMATION AND ANALYSIS CENTER SANTA BARBARA CA.. 15 MAY 86 4/4

UNCLASSIFIED DASIAC-TN-86-29-VOL-2 DNA001-82-C-0274 F/G 15/6.4 NL

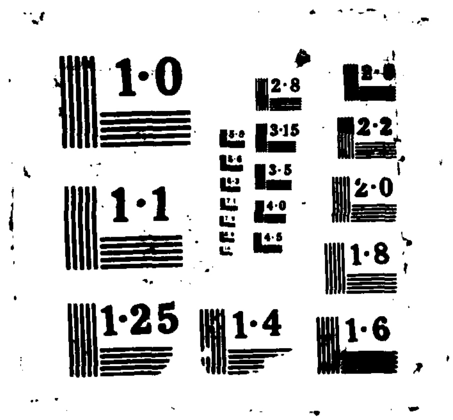
1·0
2·8
3·15
3·5
4·0
4·5
2·2
2·0
1·1
1·8
1·25
1·4
1·6

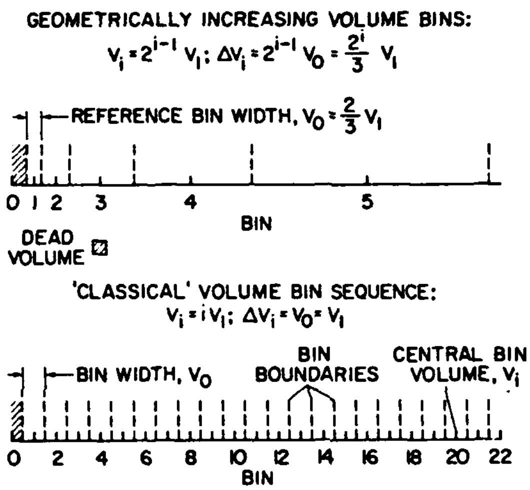

Figure 7.- Aerosol particle volume bin structures for numerical models.

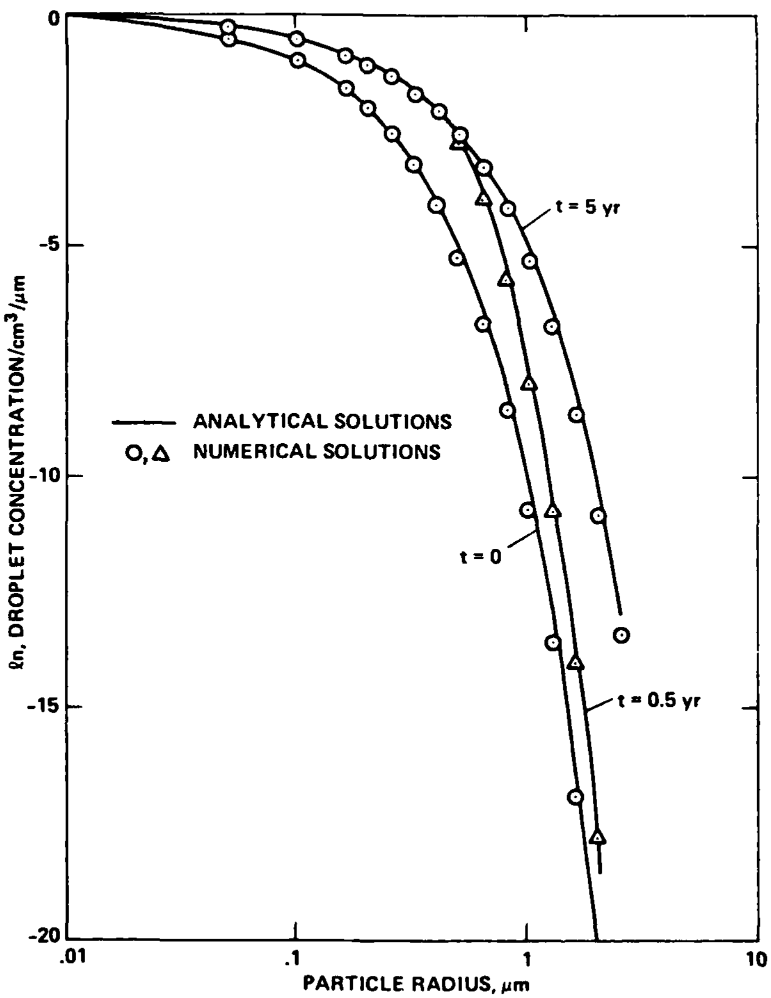

Figure 8.- Aerosol droplet growth. The evolution of a droplet size distribution following a change in the droplet growth rate is shown. Both analytical and numerical solutions are given. The conditions for the calculation are described in the text.

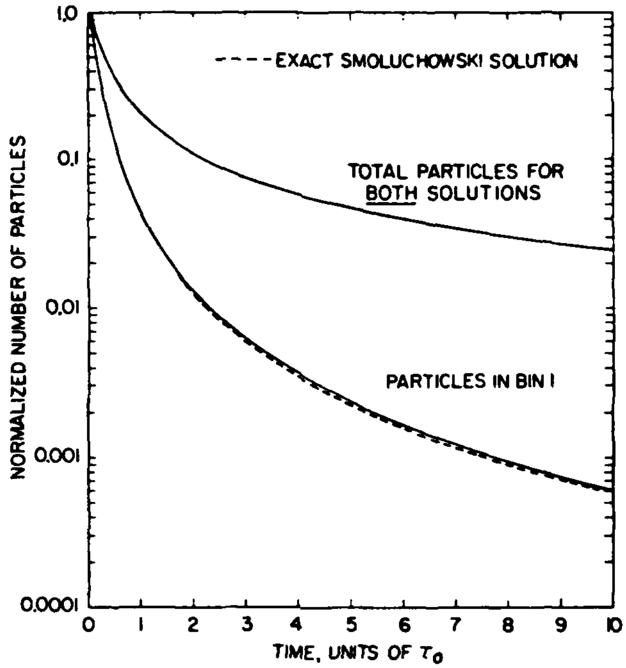

Figure 9.- Aerosol coagulation. Calculated transient decay curves are shown for the number of particles in the smallest model size bin, and for the total number of particles of all sizes, when one particle is initially placed in the smallest model bin. Time is measured relative to the characteristic coagulation time, τ_o. The exact solutions of Smoluchowski are shown for comparison.

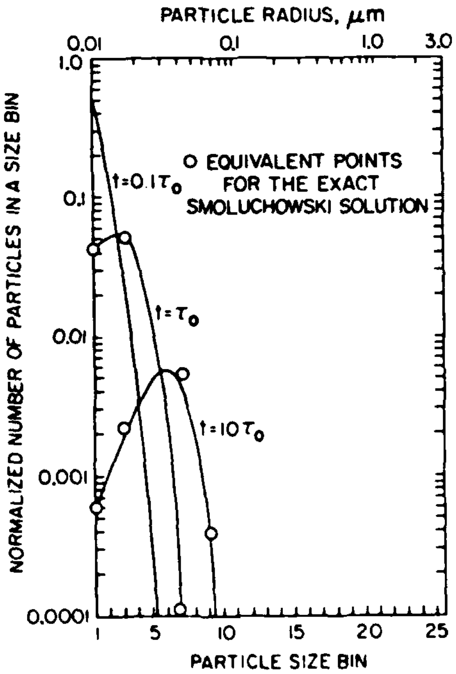

Figure 10.- The development of an aerosol size spectrum by coagulation. The conditions for the calculation are the same as for figure 9.

Radiative Transfer

I Solar Wavelengths

Use Two-Stream Approximation for Scattering with Tridiagonal Solver. Numerically Efficient, Accurate to 10% or Better for Heating Rates.

II Infrared Wavelengths

Use Two Stream Source Function Technique for Scattering. Numerically Efficient, Exact in Limit of No Scattering, 10% Accuracy with Scattering.

III Status

A. Algorithms Developed and Checked for Speed and Accuracy

B. Absorption Coefficients Under Development Based on McClatchey tape.

$$\mu \frac{\partial I_\nu}{\partial \tau}(\tau_\nu, \mu, \phi) = I_\nu(\tau_\nu, \mu, \phi) - S_\nu(\tau_\nu, \mu, \phi) - \frac{\omega_{0\nu}}{4\pi} \int_0^\pi \int_0^{2\pi} P_\nu(\mu, \mu\prime, \phi, \phi\prime) I_\nu(\nu, \mu\prime, \phi\prime) d\mu\prime d\phi\prime. \quad (1)$$

$$\frac{\partial F_n^+}{\partial \tau_n} = \gamma_{1n} F_n^+ - \gamma_{2n} F_n^- - S_{+n} \quad (10)$$

$$\frac{\partial F_n^-}{\partial \tau_n} = \gamma_{2n} F_n^+ - \gamma_{1n} F_n^- - S_{-n} \quad (11)$$

$$F_n^+ = k_{1n} exp(\lambda_n \tau) + \Gamma_n k_{2n} exp(-\lambda_n \tau) + C_n^+(\tau) \quad (18)$$

$$F_n^- = \Gamma_n k_{1n} exp(\lambda_n \tau) + k_{2n} exp(-\lambda_n \tau) + C_n^-(\tau). \quad (19)$$

Mesoscale Modeling of Coastal Flows During Periods of Extended Solar Obscuration

by

Charles R. Molenkamp

Basic Question:

If a layer of smoke obscures the ground, will a temperature difference develop between land and sea that could modify the flow field so that the likelihood of precipitation would be increased?

Preliminary Answer:

Not in the first few days after solar obscuration.

Approach:

Numerical Simulation Using the Colorado State University Mesoscale Model (Pielke, et. al)

- CSU Mesoscale Model

  - Hydrostatic incompressible flow
  - Radiational and surface heat budget
  - Surface flux, planetary boundary, and synoptic layers
  - Vertical diffusion depends on atmospheric stability

Procedure:

Run CSU Mesoscale Model

- 4 hour initialization
- 24 hour normal diurnal cycle starting at dawn (05:18)
- 48 hours with no solar incident radiation

Initial Conditions

- West Coast with 5 m/s synoptic flow from West
- Sounding for the Oregon Coast on 23 Aug 72
- Sea Surface Temperature is 289 K

CSU Mesoscale Model -- Radiation Calculation

- Solar flux absorbed in the atmosphere by water vapor
- Longwave flux divergence includes absorption, emisssion by water vapor and CO_2
- Surface temperature calculated by a heat balance equation
  - incoming solar radiation
  - incoming longwave radiation
  - latent heat flux
  - sensible heat flux
  - soil heat flux
  - outgoing surface longwave radiation

MODIFICATIONS TO THE CSU MESOSCALE MODEL

- CLOUDS
  - When the atmosphere is saturated any excess water vapor is assumed to exist as cloud water (fog)
  - Evaporative heating/cooling changes temperature
- RADIATION (Long Wave)

MODIFICATIONS TO THE CSU MESOSCALE MODEL

- CLOUDS

- RADIATION (Long Wave)

  - New model for clear air long wave radiation
    The new version calculates fluxes at each level
    The old version assumed for each level that the entire atmosphere had the temperature of that level

  - Effect of clouds on long wave radiation
    The upward and downward flux out of each cloudy layer is given by:

$$F_{out} = (1 - \epsilon) F_{in} + \epsilon\sigma T^4$$

where ϵ is the emissivity of the layer
and T is the temperature at the outgoing edge of the layer

2 Runs of the Model

- OLD
  - no clouds
  - old radiation parameterization

- NEW
  - clouds where atmosphere is saturated
  - new radiation parameterization, including the effect of clouds

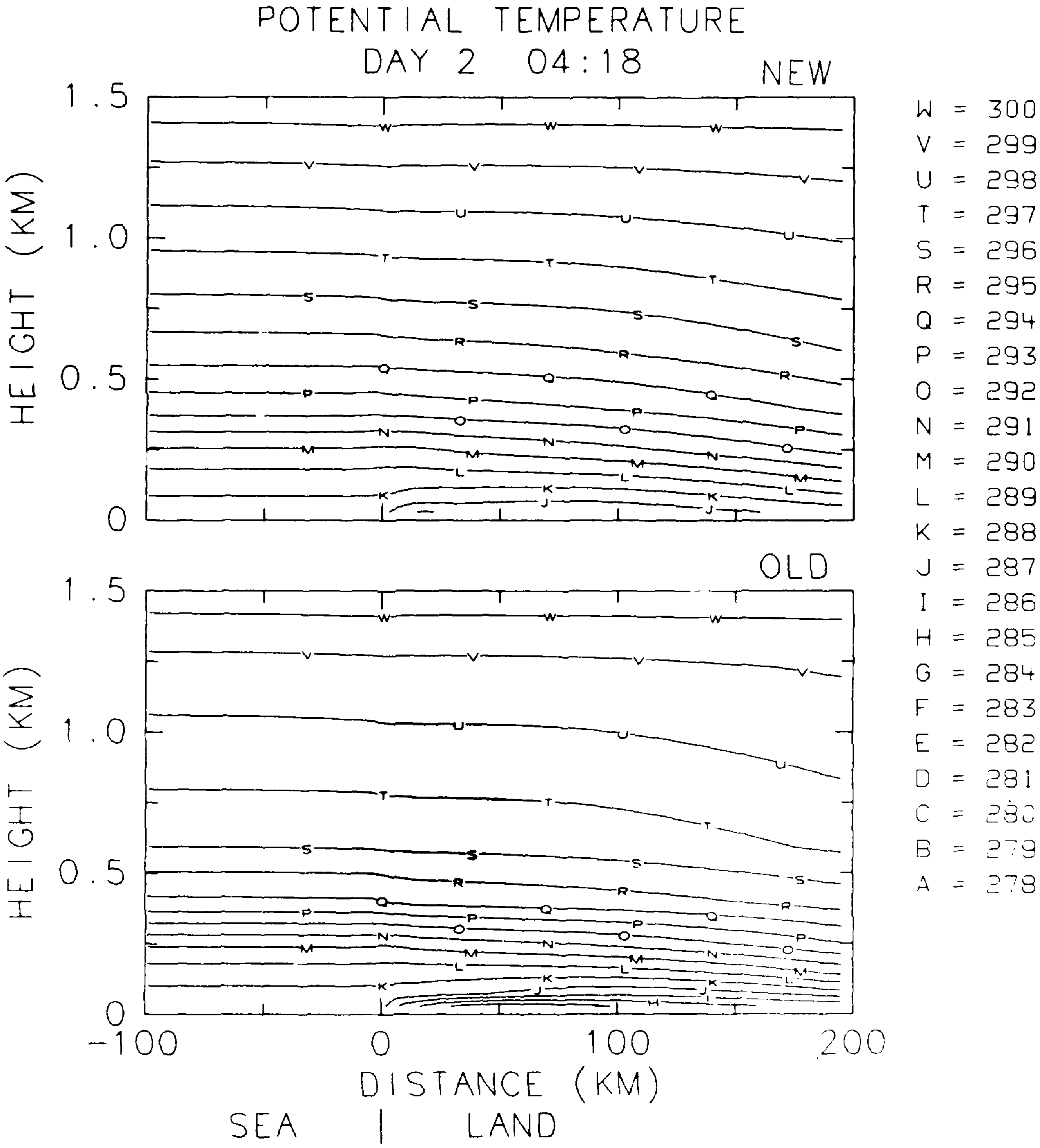

POTENTIAL TEMPERATURE
DAY 2 04:18
NEW
OLD
HEIGHT (KM)
HEIGHT (KM)
1.5
1.0
0.5
0
-100
0
100
200
DISTANCE (KM)
SEA | LAND
W = 300
V = 299
U = 298
T = 297
S = 296
R = 295
Q = 294
P = 293
O = 292
N = 291
M = 290
L = 289
K = 288
J = 287
I = 286
H = 285
G = 284
F = 283
E = 282
D = 281
C = 280
B = 279
A = 278

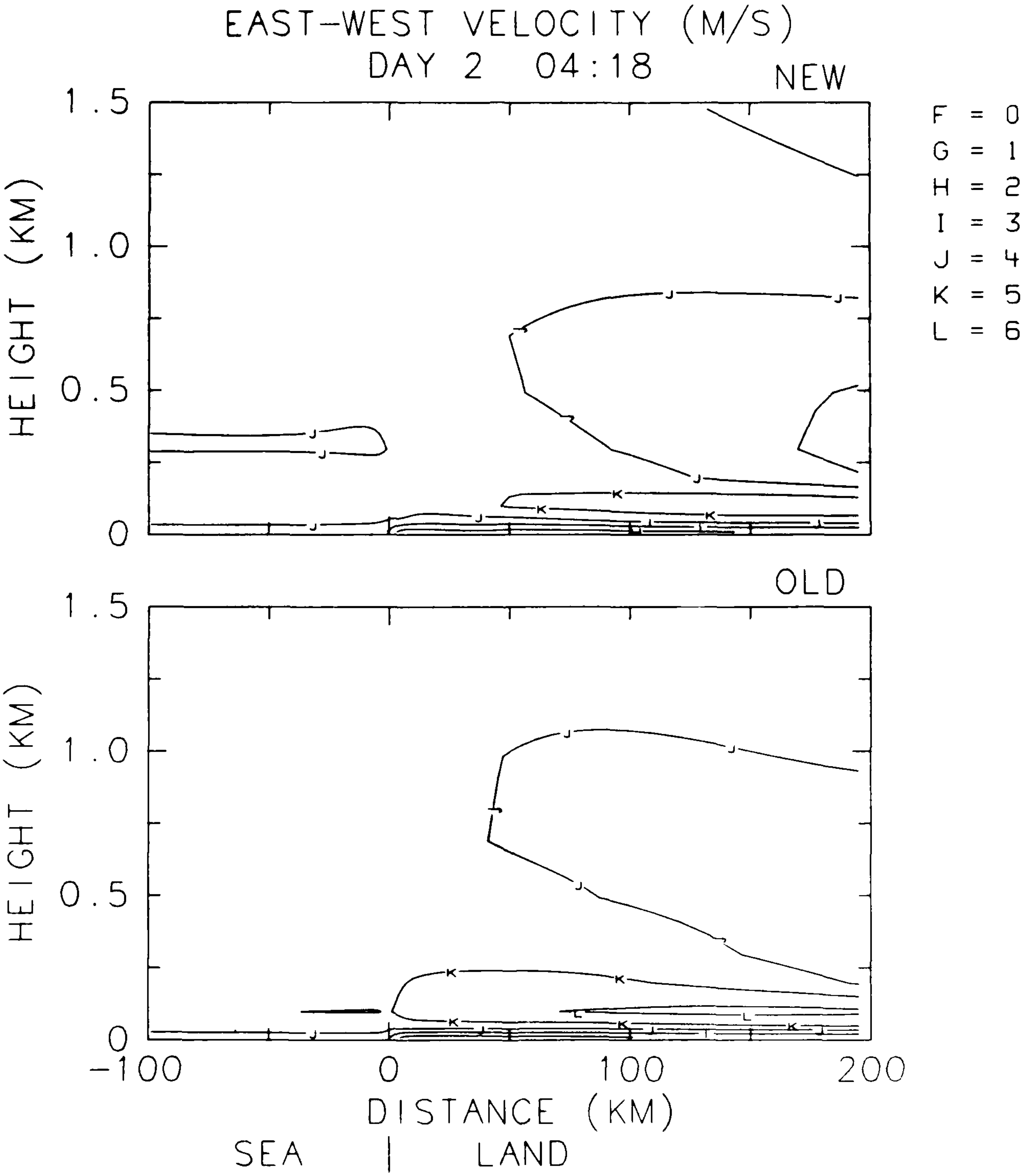
EAST-WEST VELOCITY (M/S)
DAY 2 04:18
NEW
OLD
F = 0
G = 1
H = 2
I = 3
J = 4
K = 5
L = 6
HEIGHT (KM)
1.5
1.0
0.5
0
-100
0
100
200
DISTANCE (KM)
SEA
LAND

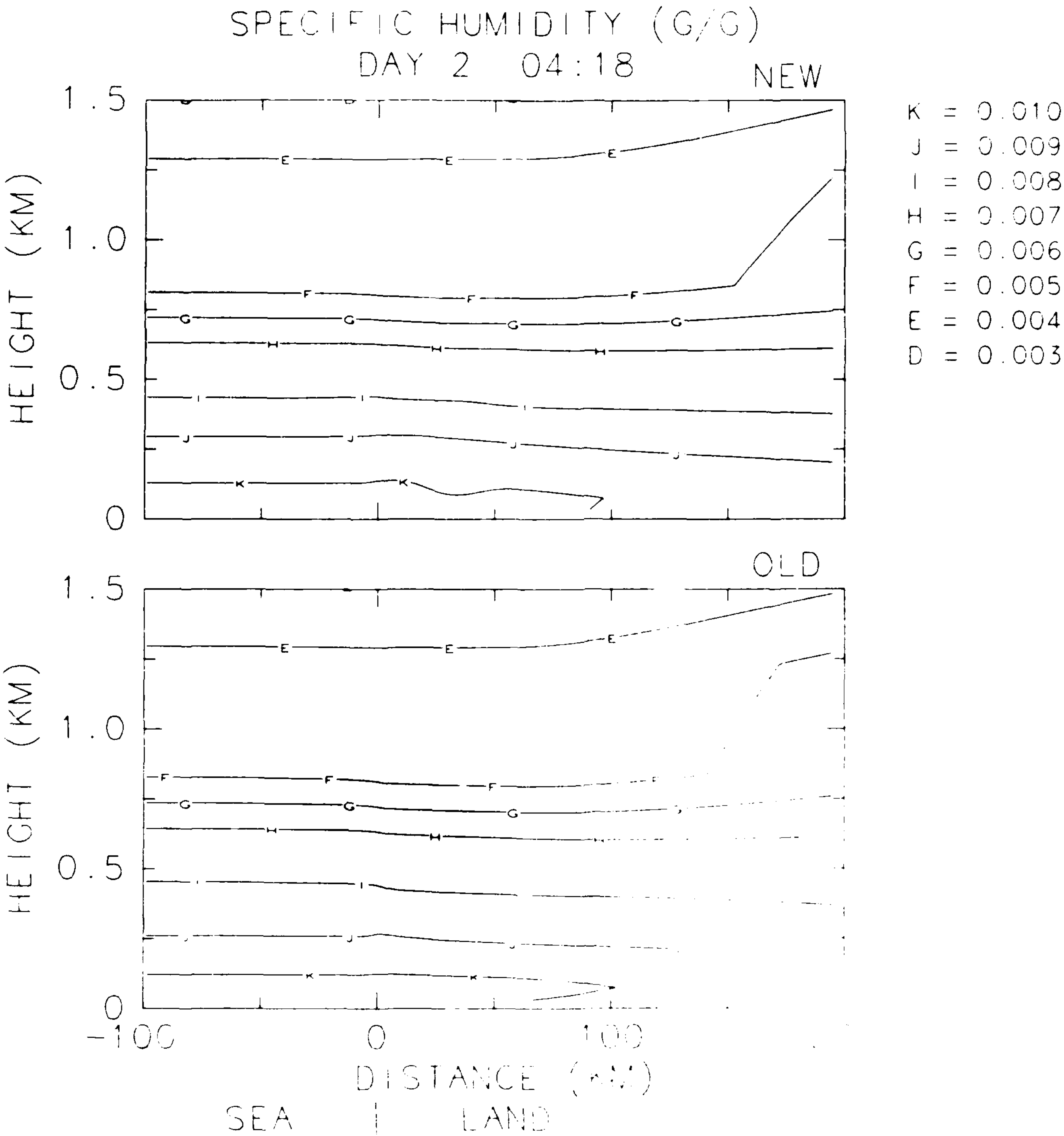

SPECIFIC HUMIDITY (G/G)
DAY 2 04:18
NEW
K = 0.010
J = 0.009
I = 0.008
H = 0.007
G = 0.006
F = 0.005
E = 0.004
D = 0.003
HEIGHT (KM)
OLD
DISTANCE (KM)
SEA
LAND

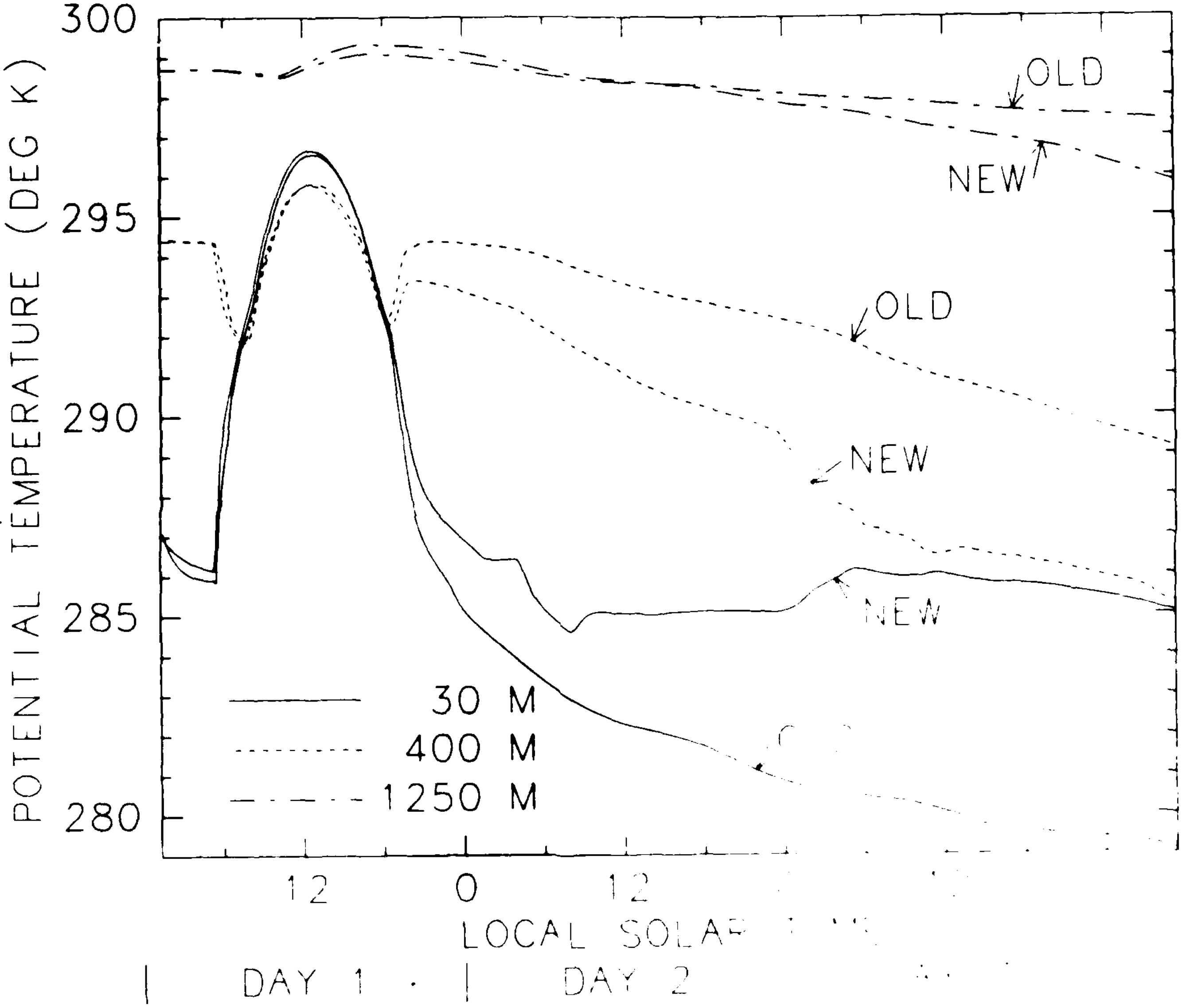

300
295
290
285
280
POTENTIAL TEMPERATURE (DEG K)
OLD
NEW
OLD
NEW
NEW
30 M
400 M
1250 M
12
0
12
LOCAL SOLA
DAY 1
DAY 2

WIND NORMAL TO COASTLINE
AT 27 KM INLAND

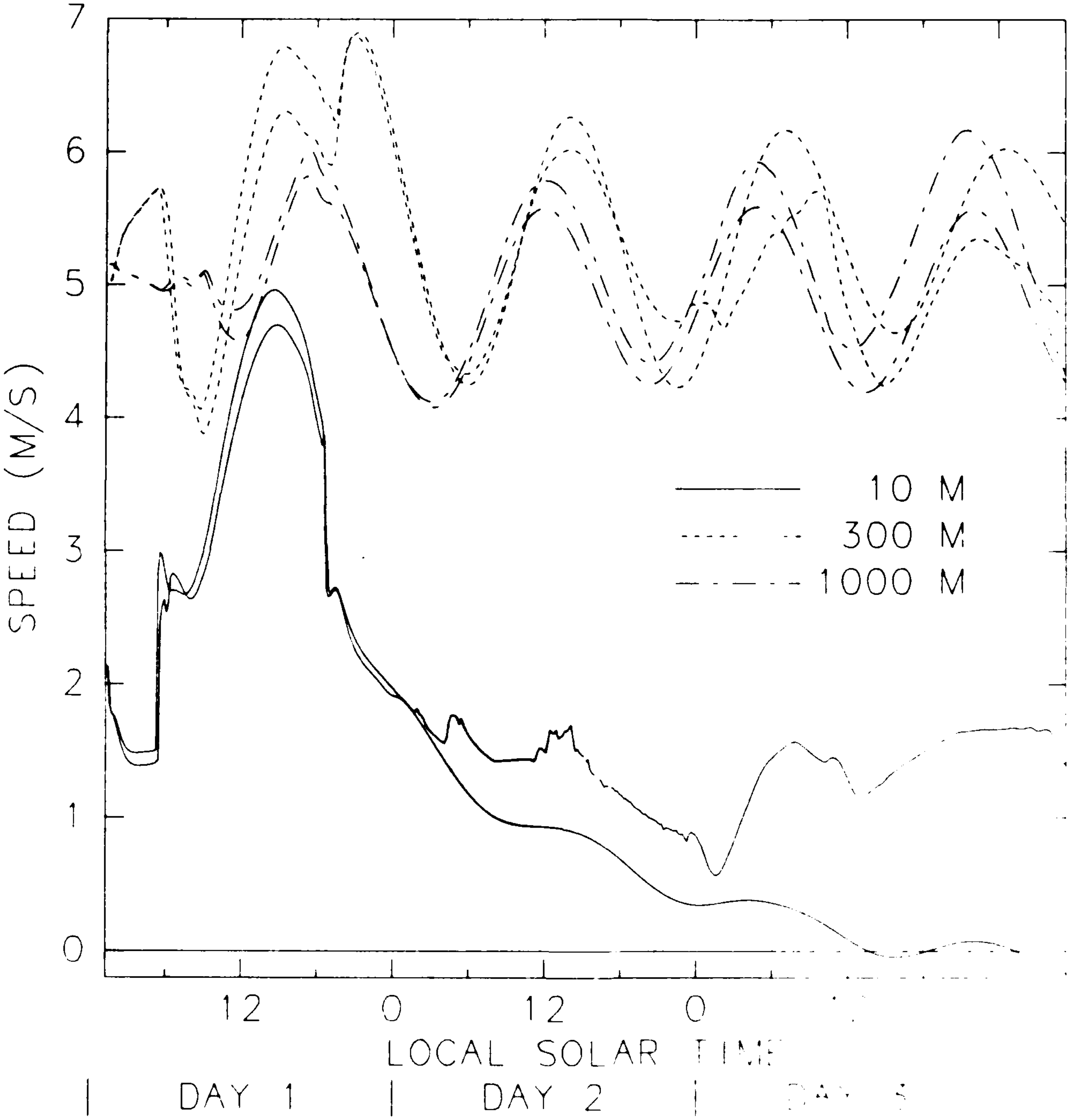

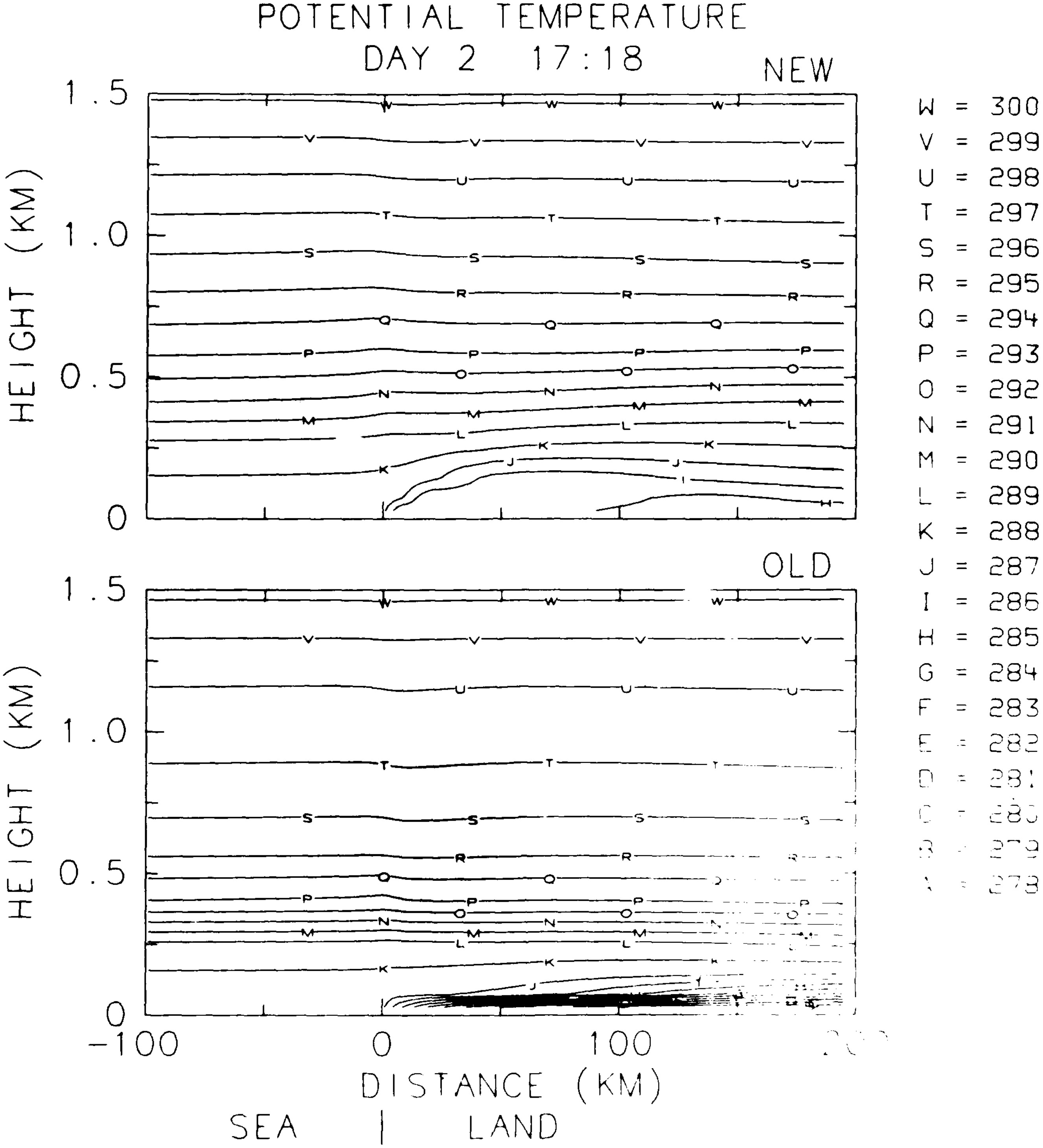
POTENTIAL TEMPERATURE
DAY 2 17:18
NEW
OLD
HEIGHT (KM)
1.5
1.0
0.5
0
-100
0
100
DISTANCE (KM)
SEA | LAND
W = 300
V = 299
U = 298
T = 297
S = 296
R = 295
Q = 294
P = 293
O = 292
N = 291
M = 290
L = 289
K = 288
J = 287
I = 286
H = 285
G = 284
F = 283
E = 282

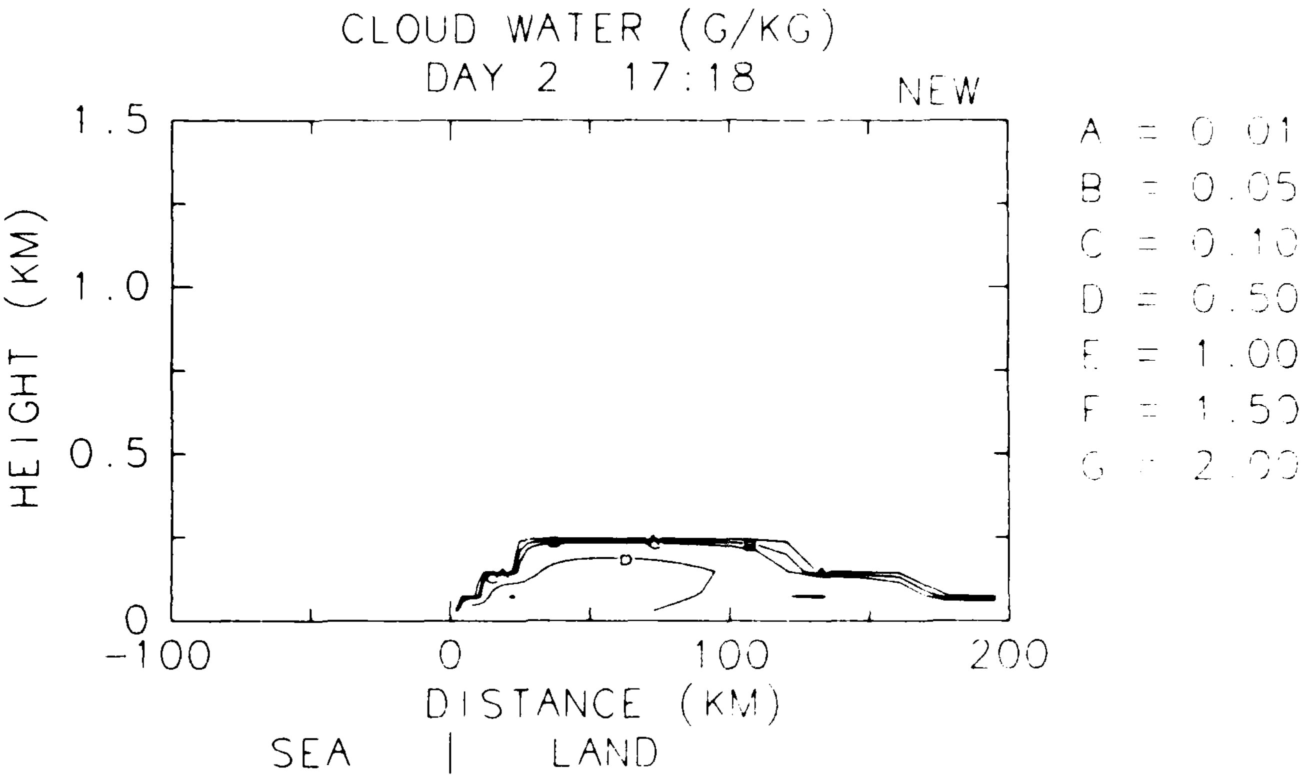

CLOUD WATER (G/KG)
DAY 2 17:18
NEW
1.5
1.0
0.5
0
HEIGHT (KM)
-100
0
100
200
DISTANCE (KM)
SEA | LAND
A = 0.01
B = 0.05
C = 0.10
D = 0.50
E = 1.00
F = 1.50
G = 2.00

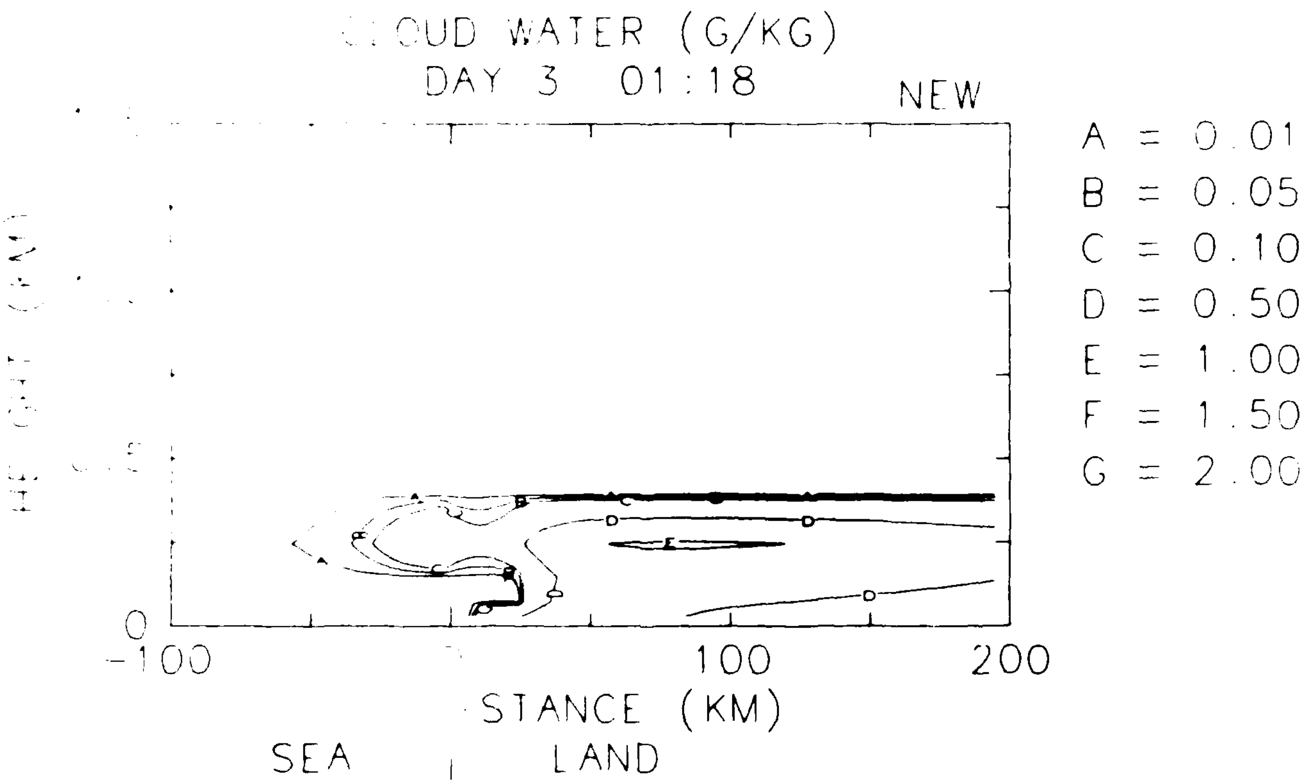
CLOUD WATER (G/KG)
DAY 3 01:18
NEW
A = 0.01
B = 0.05
C = 0.10
D = 0.50
E = 1.00
F = 1.50
G = 2.00
0
-100
100
200
STANCE (KM)
SEA
LAND

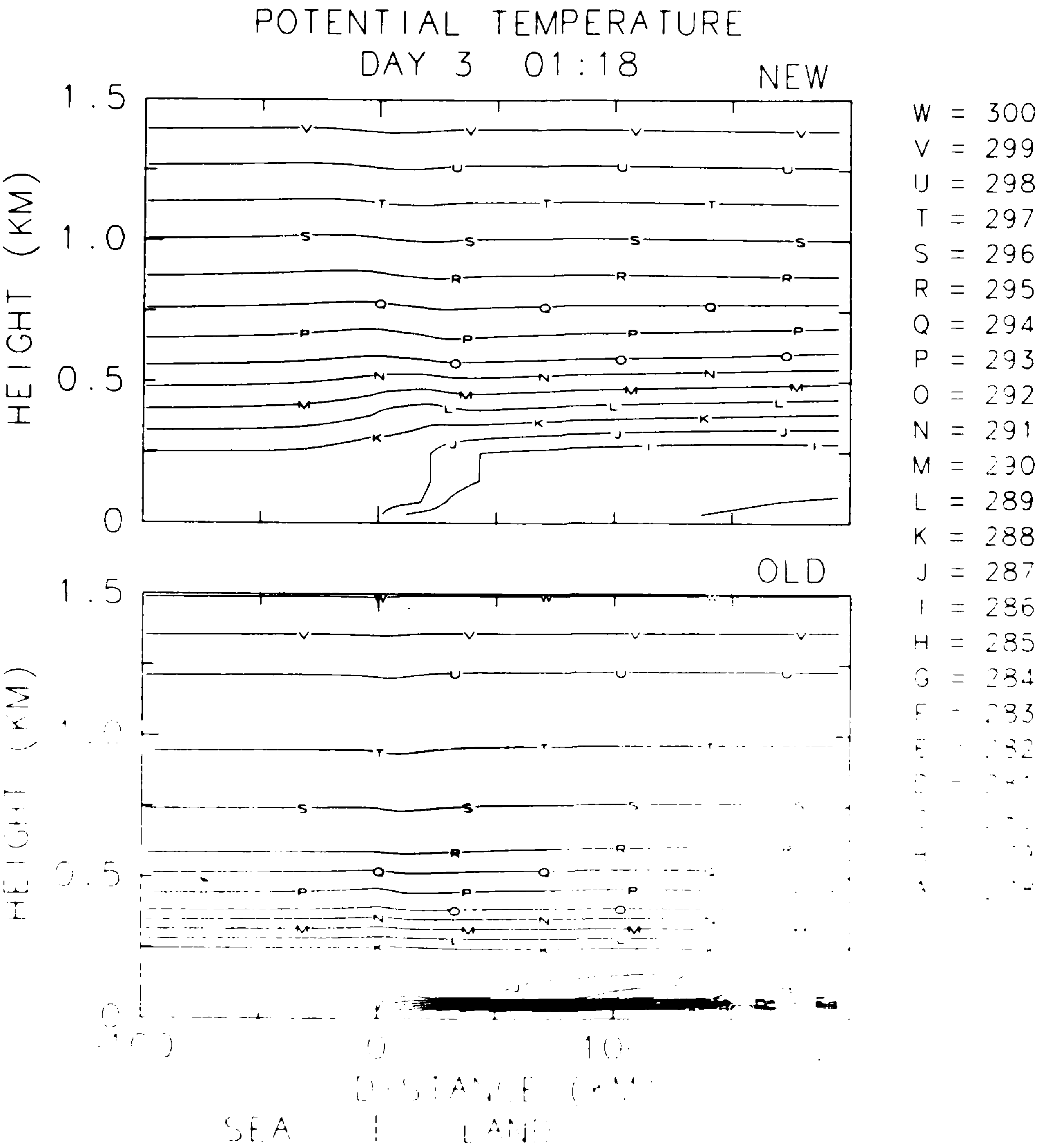
POTENTIAL TEMPERATURE
DAY 3 01:18
NEW
OLD
HEIGHT (KM)
1.5
1.0
0.5
0
W = 300
V = 299
U = 298
T = 297
S = 296
R = 295
Q = 294
P = 293
O = 292
N = 291
M = 290
L = 289
K = 288
J = 287
I = 286
H = 285
G = 284
SEA

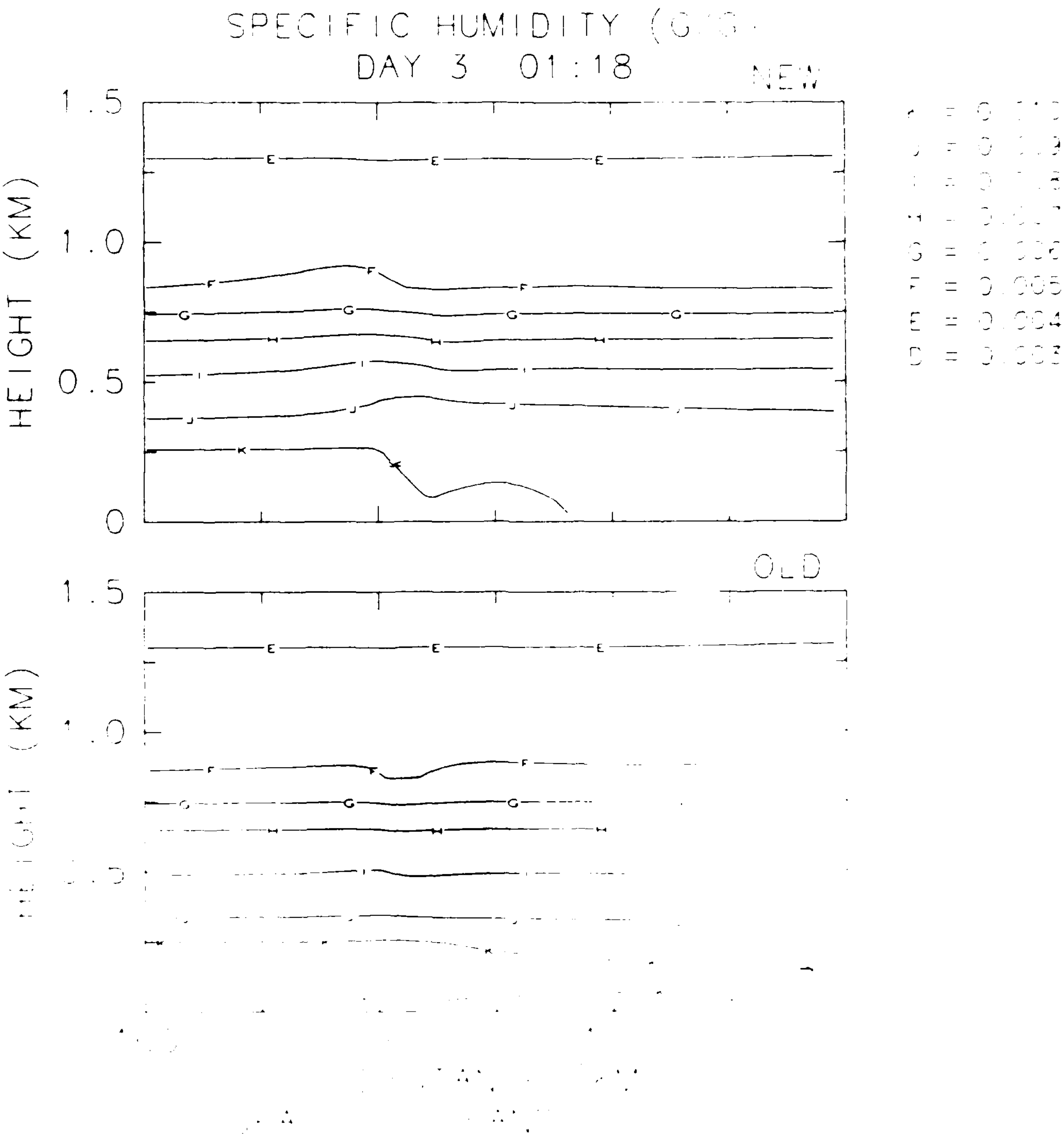
SPECIFIC HUMIDITY (G/G)
DAY 3 01:18
NEW
OLD
HEIGHT (KM)
1.5
1.0
0.5
0
F = 0.005
E = 0.004

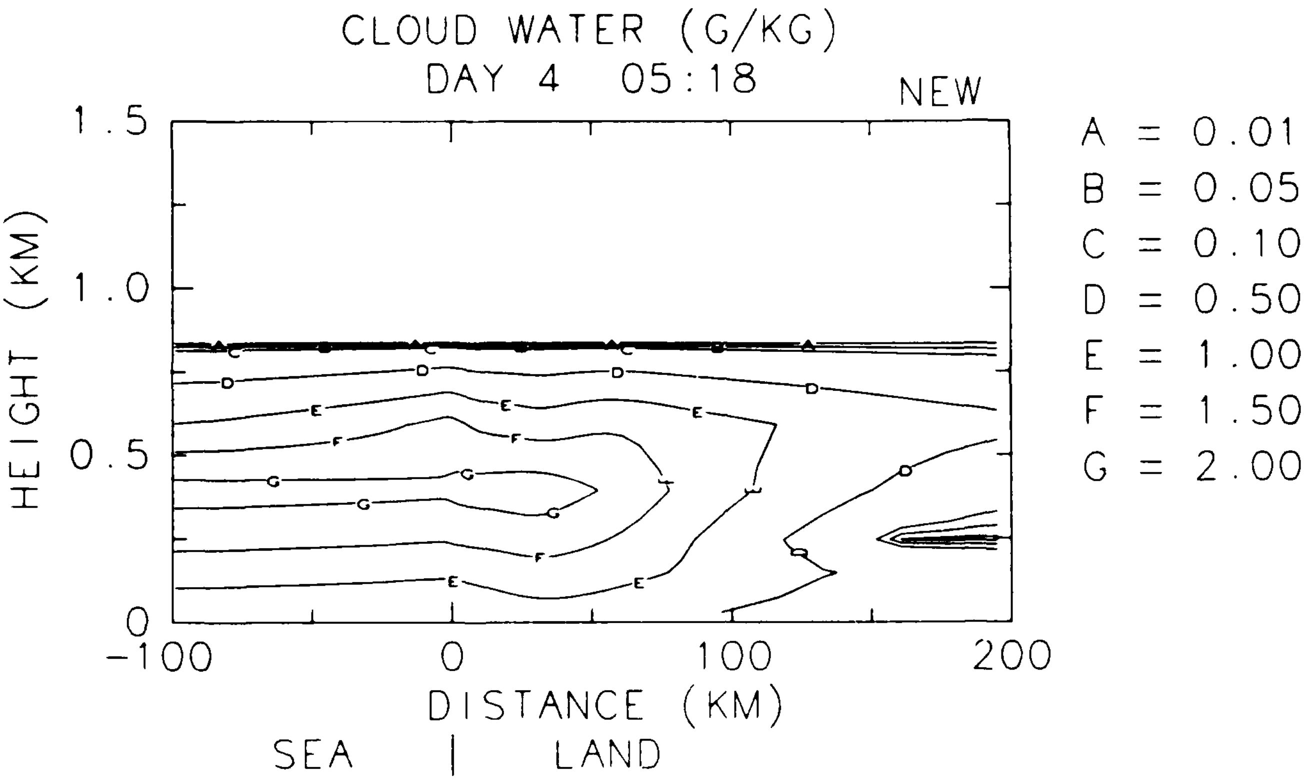

CLOUD WATER (G/KG)
DAY 4 05:18
NEW
1.5
1.0
0.5
0
HEIGHT (KM)
-100
0
100
200
DISTANCE (KM)
SEA | LAND
A = 0.01
B = 0.05
C = 0.10
D = 0.50
E = 1.00
F = 1.50
G = 2.00

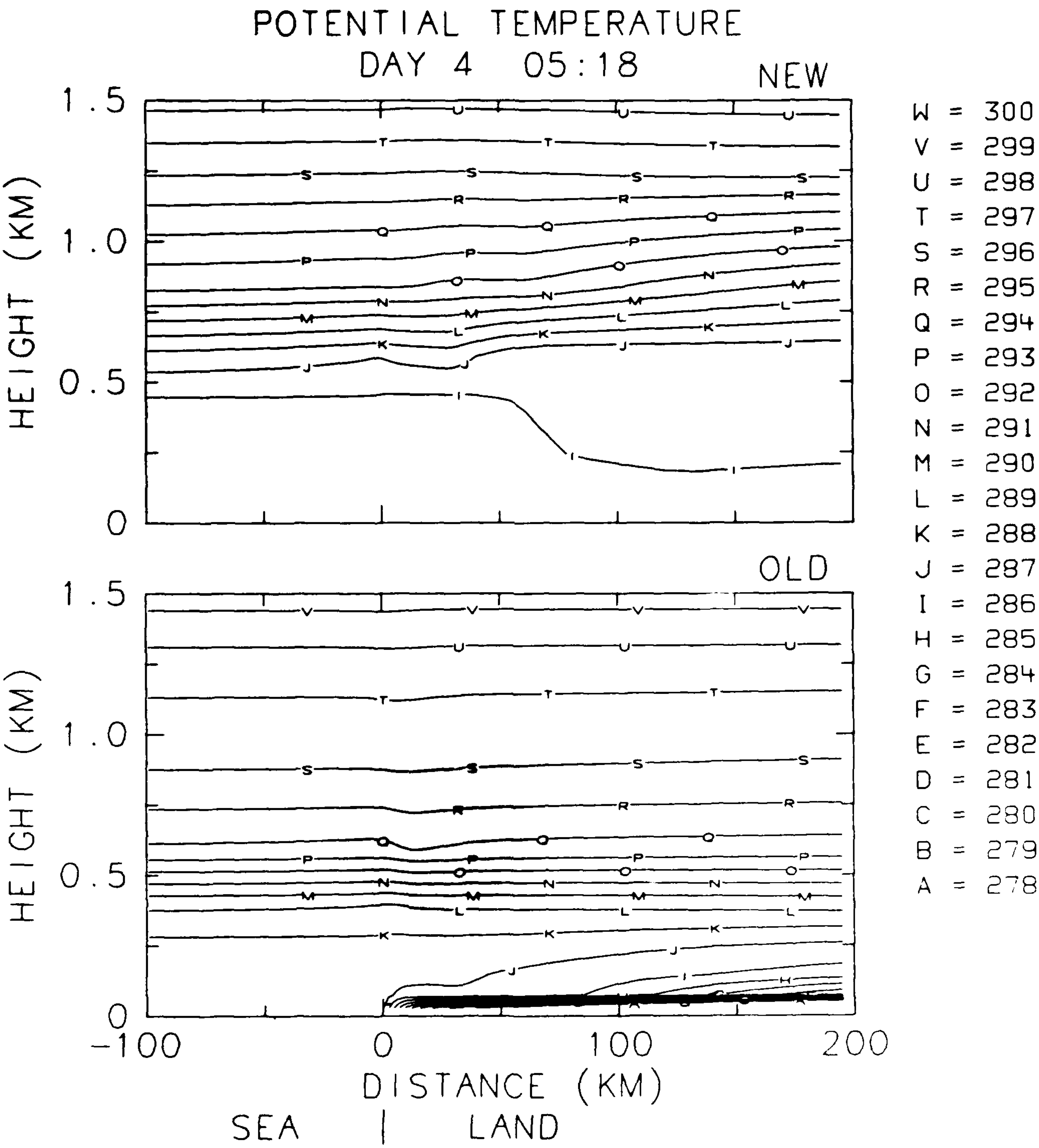
POTENTIAL TEMPERATURE
DAY 4 05:18
NEW
OLD
HEIGHT (KM)
DISTANCE (KM)
SEA | LAND
W = 300
V = 299
U = 298
T = 297
S = 296
R = 295
Q = 294
P = 293
O = 292
N = 291
M = 290
L = 289
K = 288
J = 287
I = 286
H = 285
G = 284
F = 283
E = 282
D = 281
C = 280
B = 279
A = 278

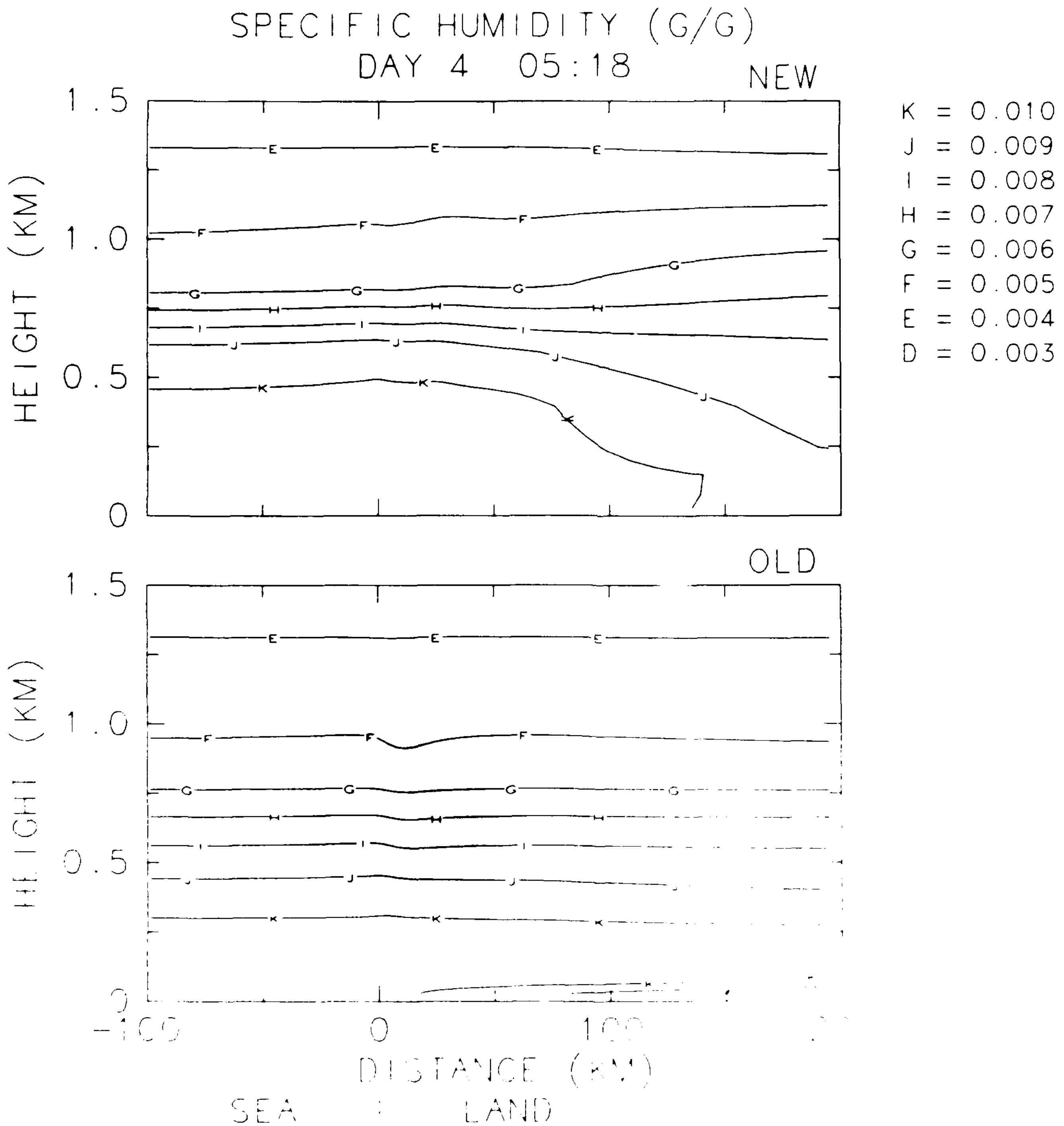

SPECIFIC HUMIDITY (G/G)
DAY 4 05:18
NEW
OLD
K = 0.010
J = 0.009
I = 0.008
H = 0.007
G = 0.006
F = 0.005
E = 0.004
D = 0.003
HEIGHT (KM)
1.5
1.0
0.5
0
DISTANCE (KM)
SEA
LAND

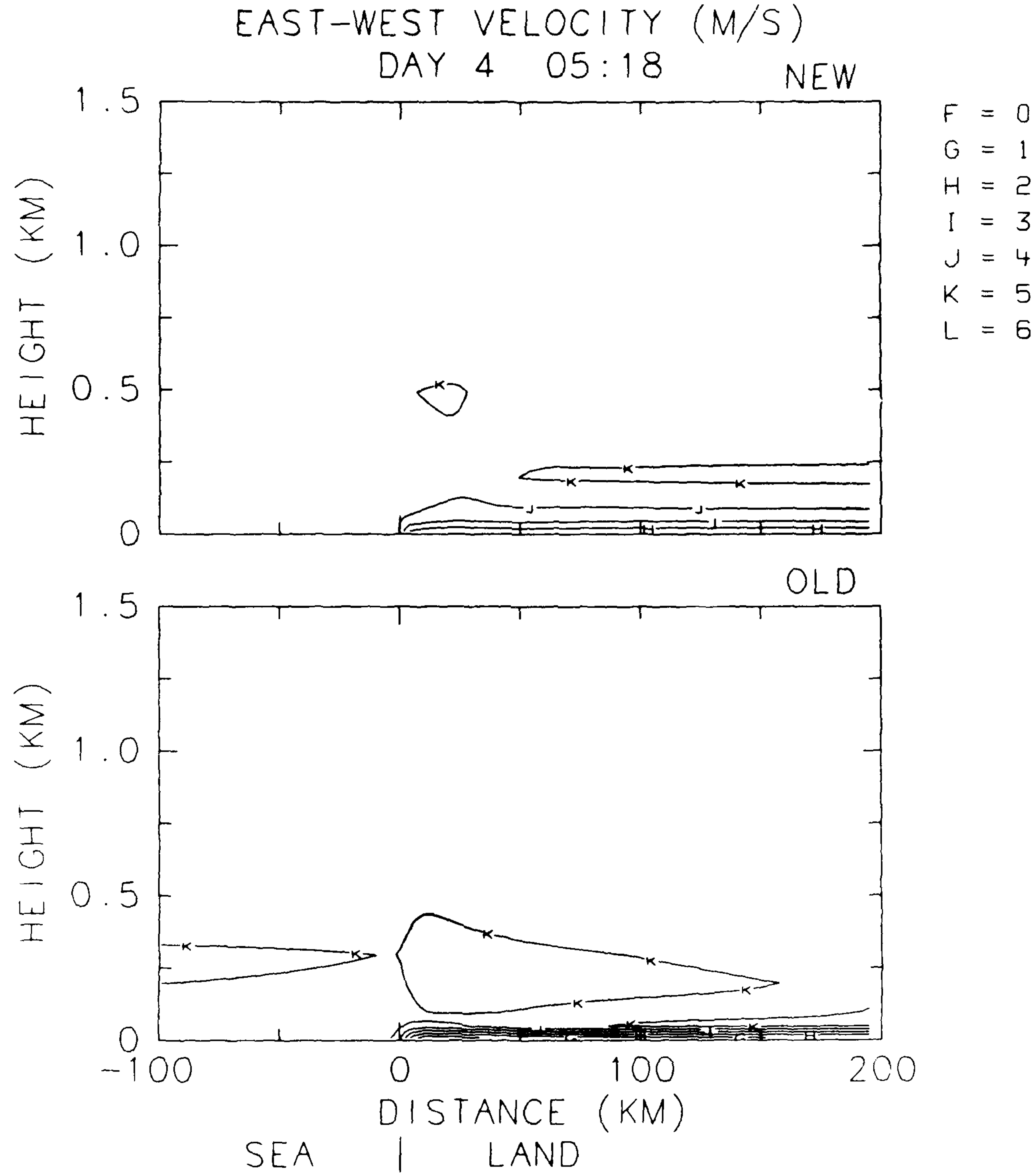

EAST-WEST VELOCITY (M/S)
DAY 4 05:18
NEW
OLD
F = 0
G = 1
H = 2
I = 3
J = 4
K = 5
L = 6
HEIGHT (KM)
DISTANCE (KM)
SEA | LAND

- OLD
  - + Very Cold Layer Forms over Land
  - + Cold Layer is Very Thin
  - + No Significant Perturbation above 200 M
  - + No Significant Vertical Motion

- NEW
  - + Fog Forms over Land at Dawn and Thickens with Time
  - + Fog Forms over Ocean about 20 Hours Later
    - Vertical Mixing of Moisture from Sea
    - Radiative Cooling Aloft
  - + Fog over Land and Sea Up to 800 M in 2 1/2 Days
  - + Fog Eliminates Land/Sea Surface Temperature Contrast
  - + No Significant Vertical Motion

A Numerical Simulation of The Possible Effects of Nucleation Scavenging on Plume Injection

by

Greg Tripoli

Chang Chen

William Cotton

R. A. M. S.

Regional Atmospheric Modeling System

Time dependent P.D.E. for

$\vec{V}$ (u, v, w) (velocity)

p (pressure)

Θ (potential temperature)

$$\left.\begin{array}{l} r_v \\ r_c \\ r_r \\ r_i \\ r_g \\ r_a \end{array}\right\}$$

mixing ratio $\left(\frac{\text{grams water}}{\text{grams air}}\right)$ for vapor, cloud, rain, crystal, graupel, aggregates

Phoretic Scavenging

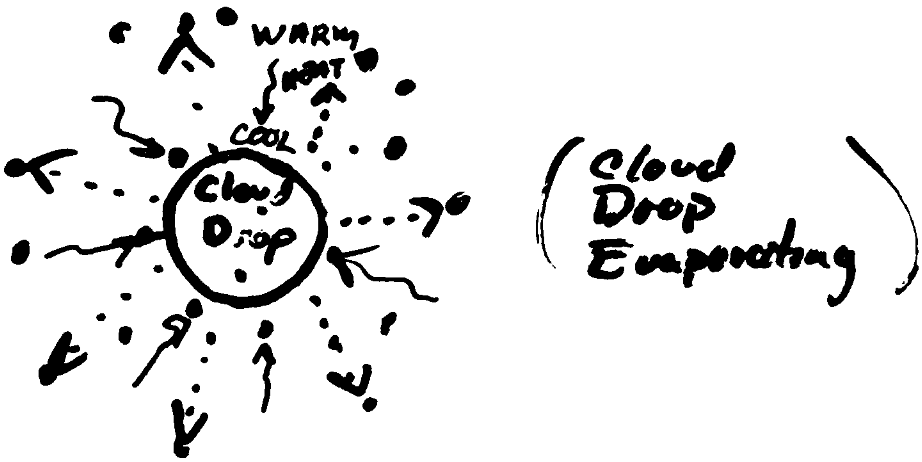

Brownian Scavenging

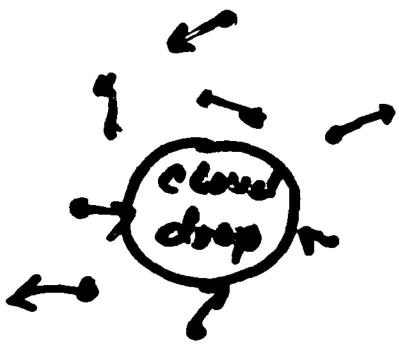

Hydronamic Capture

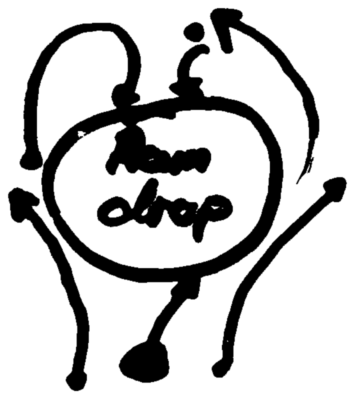

Electric Effects

Nucleation Scavenging

A

B

C

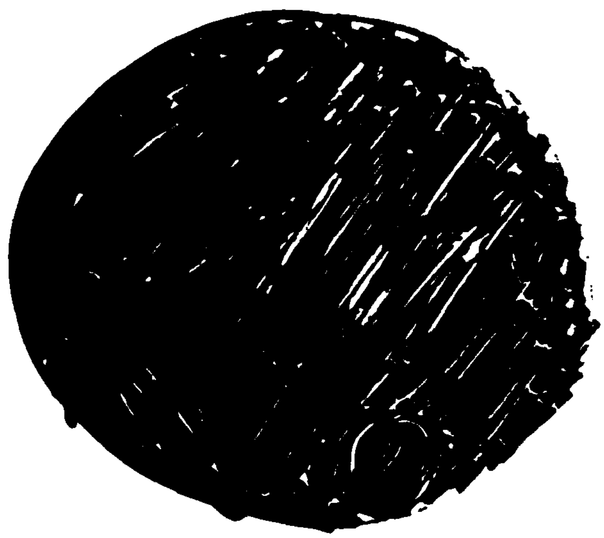

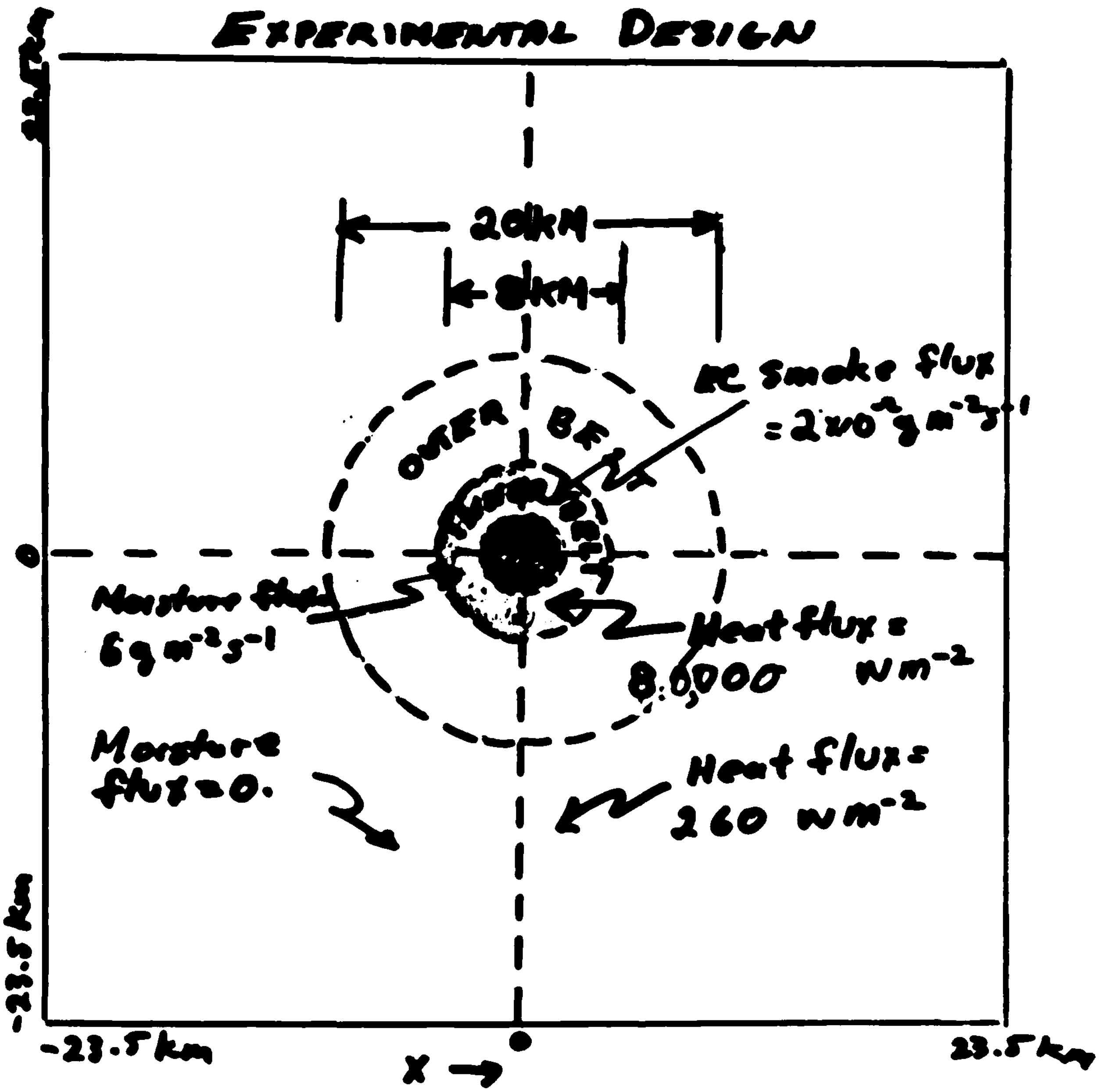

$\Delta X = 1 km$
$\Delta Y = 1 km$
$\Delta Z = .75 km$

EC Produced is
20% of smoke which is
1% of fuel
(Crutzen, et. al, 1984, for wood)

Assumptions:

1. Homogeneous fuel density of 110 kg/m² (10% water content) within inner belt.
2. Neglect fire in outer belt.
3. City center same as inner belt

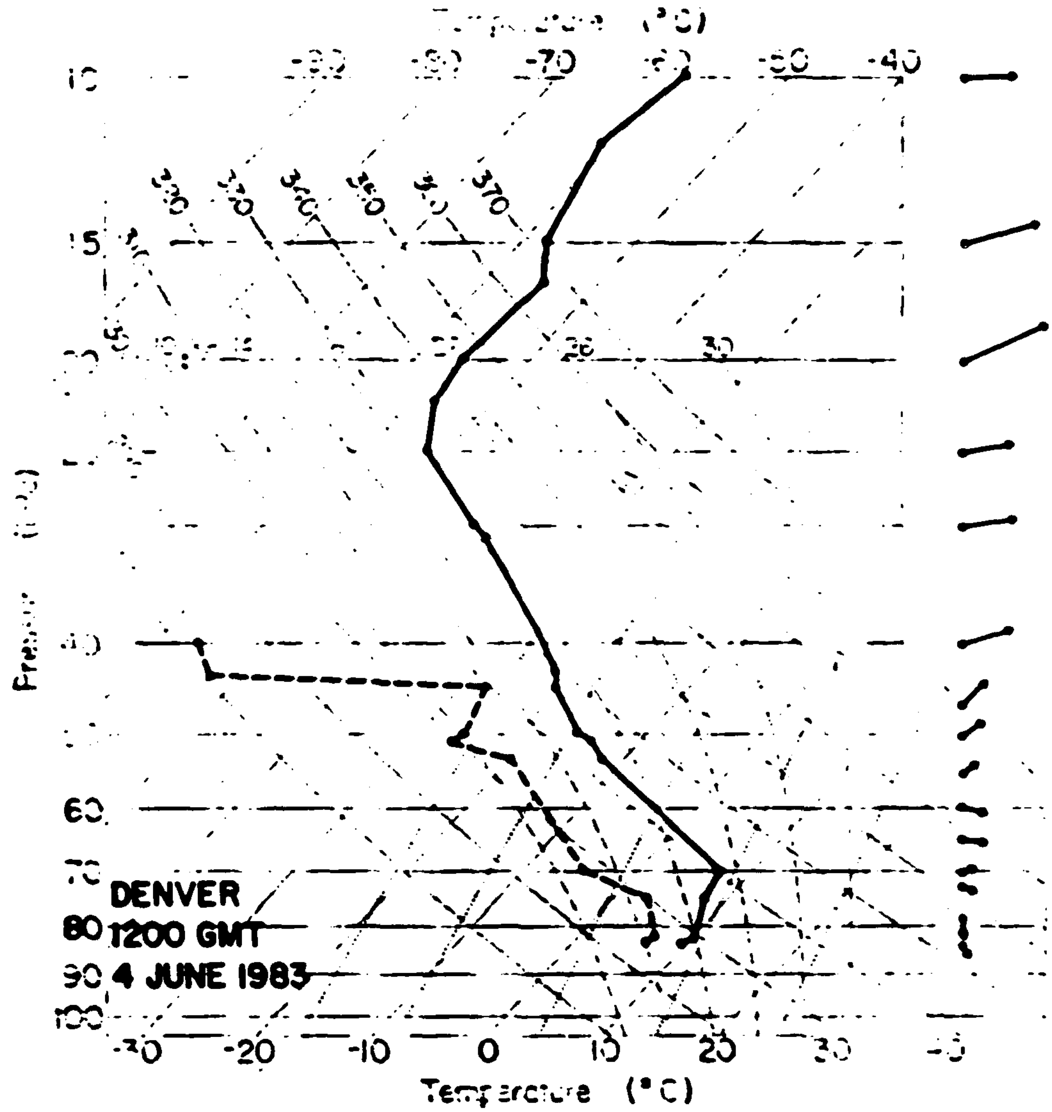
DENVER
1200 GMT
4 JUNE 1983
Temperature (°C)
-70
-40
370
60
80
-20
-10
0
10
20

Figure 3

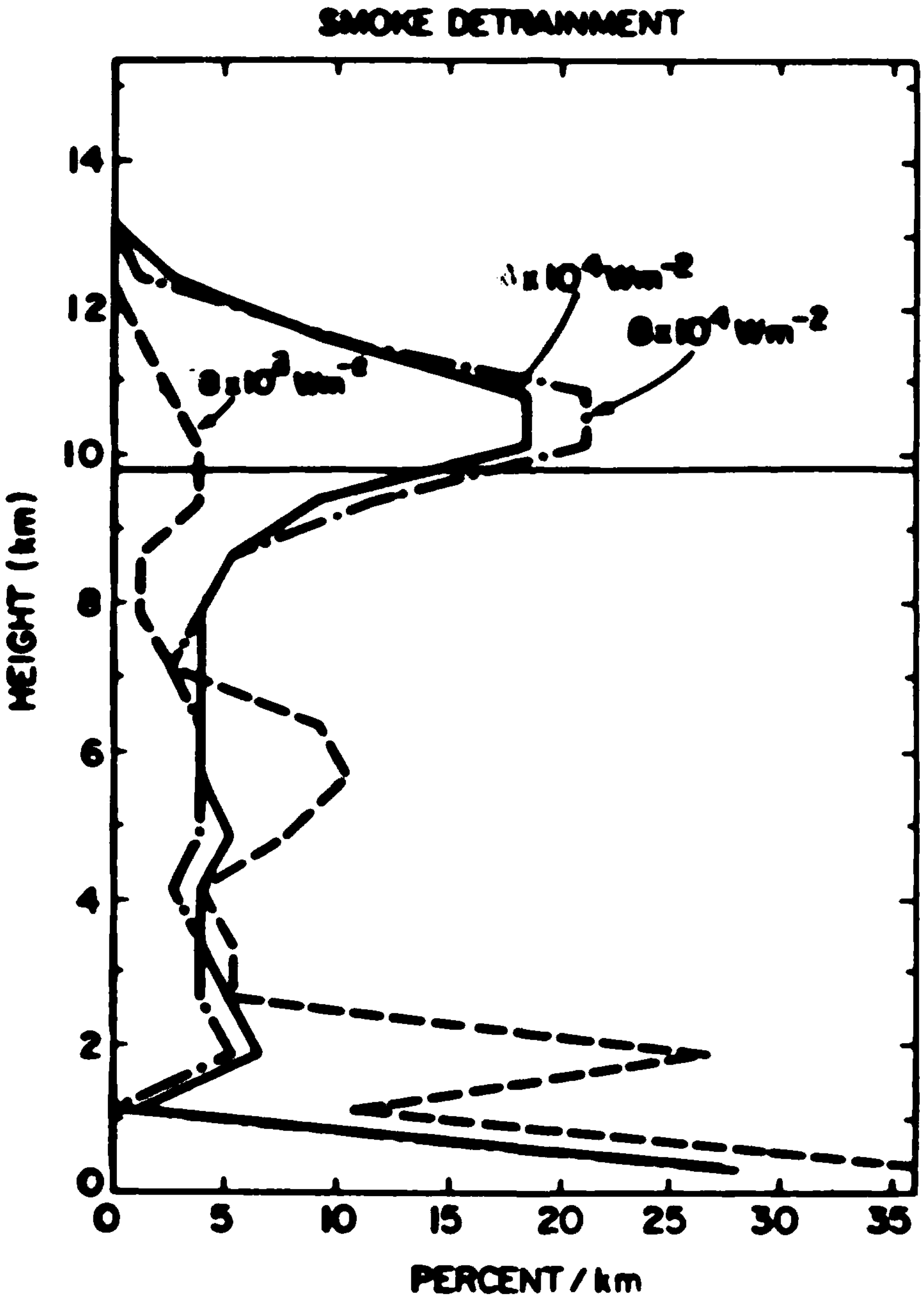
SMOKE DETRAINMENT
HEIGHT (km)
0
2
4
6
8
10
12
14
PERCENT / km
0
5
10
15
20
25
30
35

Figure 4

DESIGN OF EXPERIMENT TO TEST EFFECTIVENESS OF NUCLEATION SCAVENGING

1) Use conservative standard spring/fall atmosphere, wind as Penner _et al_. (1985)

2) Use Penner _et al_. (1985) high intensity case (low intensity case results trivial since deep cloud never forms)

3) Use Cotton (1985) phoretic/Brownian scavenging model.

4) Nucleation scavenging:

$$S_N = \frac{CL_{cr} + C_{ci} + C_{cg} + C_{ca}}{r_c} r_{EC}$$

INHERENT ASSUMPTIONS FOR NUCLEATION SCAVENGING

1) All smoke particles will nucleate.

2) Smoke collected onto precipitation particle will be lost from system, even if precipitation re-evaporates. (We assume many will be combined to make large precipitating smoke particle).

3) Collection efficiency of cloud droplets unity despite smaller size.

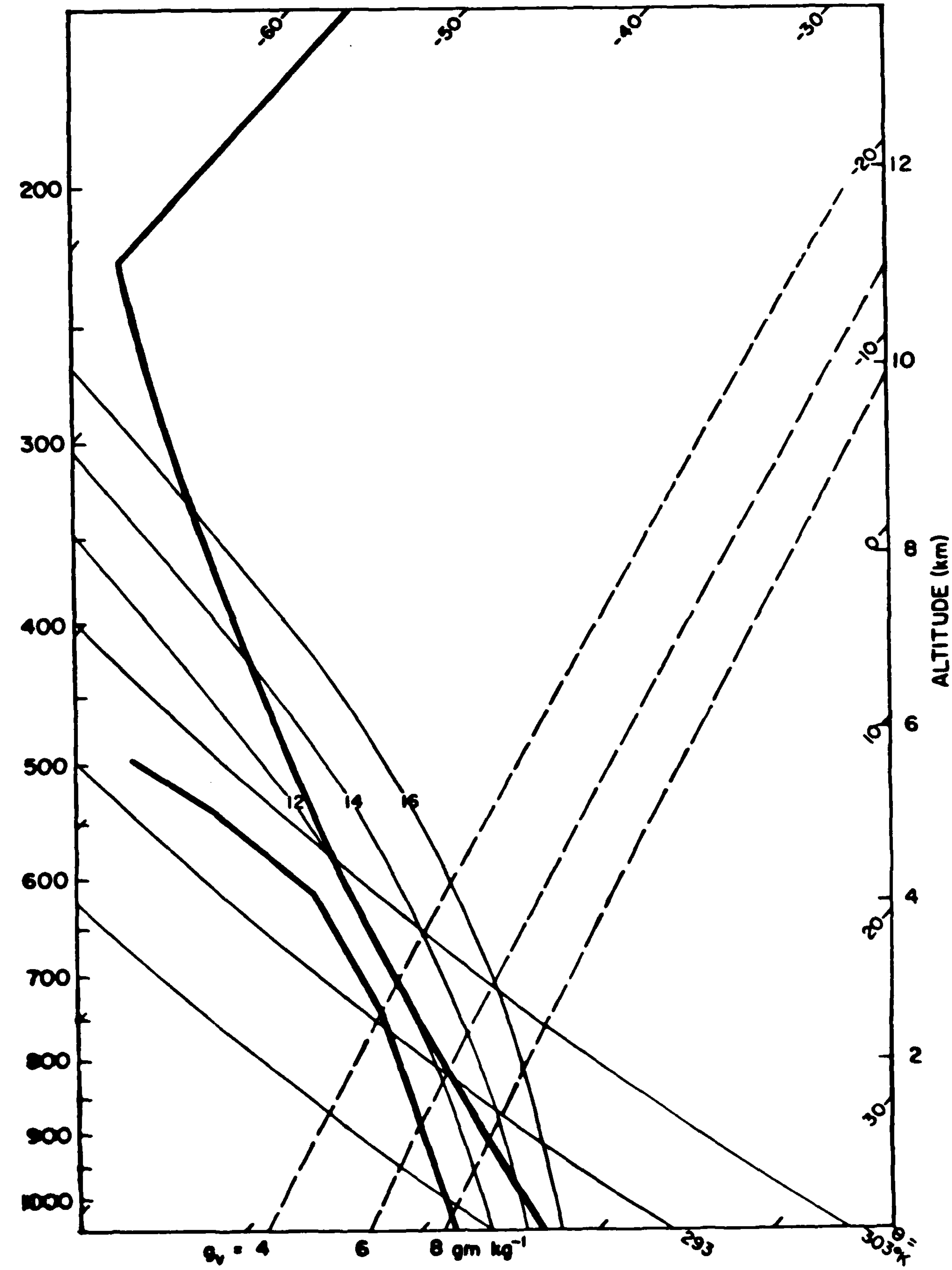
-60
-50
-40
-30
-20
-10
0
10
20
30
200
300
400
500
600
700
800
900
1000
12
14
16
q_v = 4
6
8 gm kg^{-1}
293
303°K
12
10
8
6
4
2
0
ALTITUDE (km)

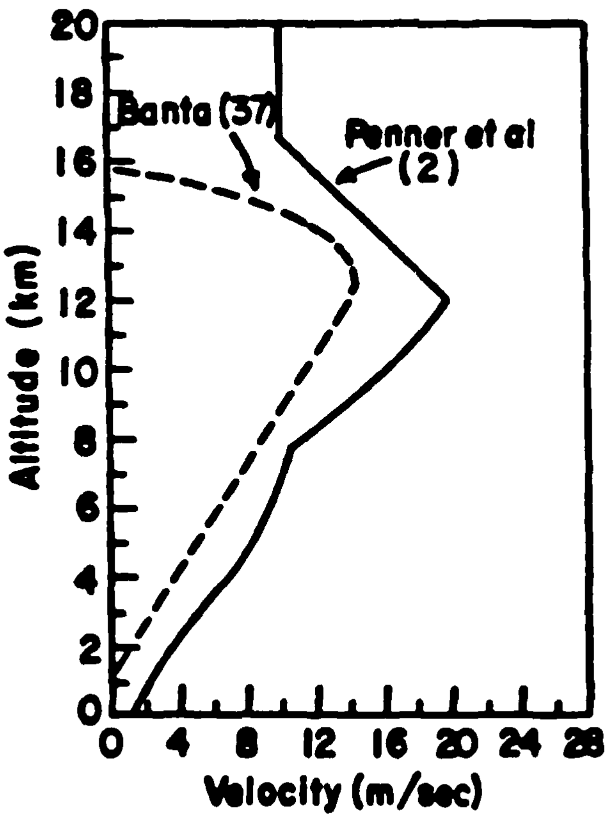
Banta (37)
Penner et al
(2)
Altitude (km)
Velocity (m/sec)
20
18
16
14
12
10
8
6
4
2
0
0
4
8
12
16
20
24
28

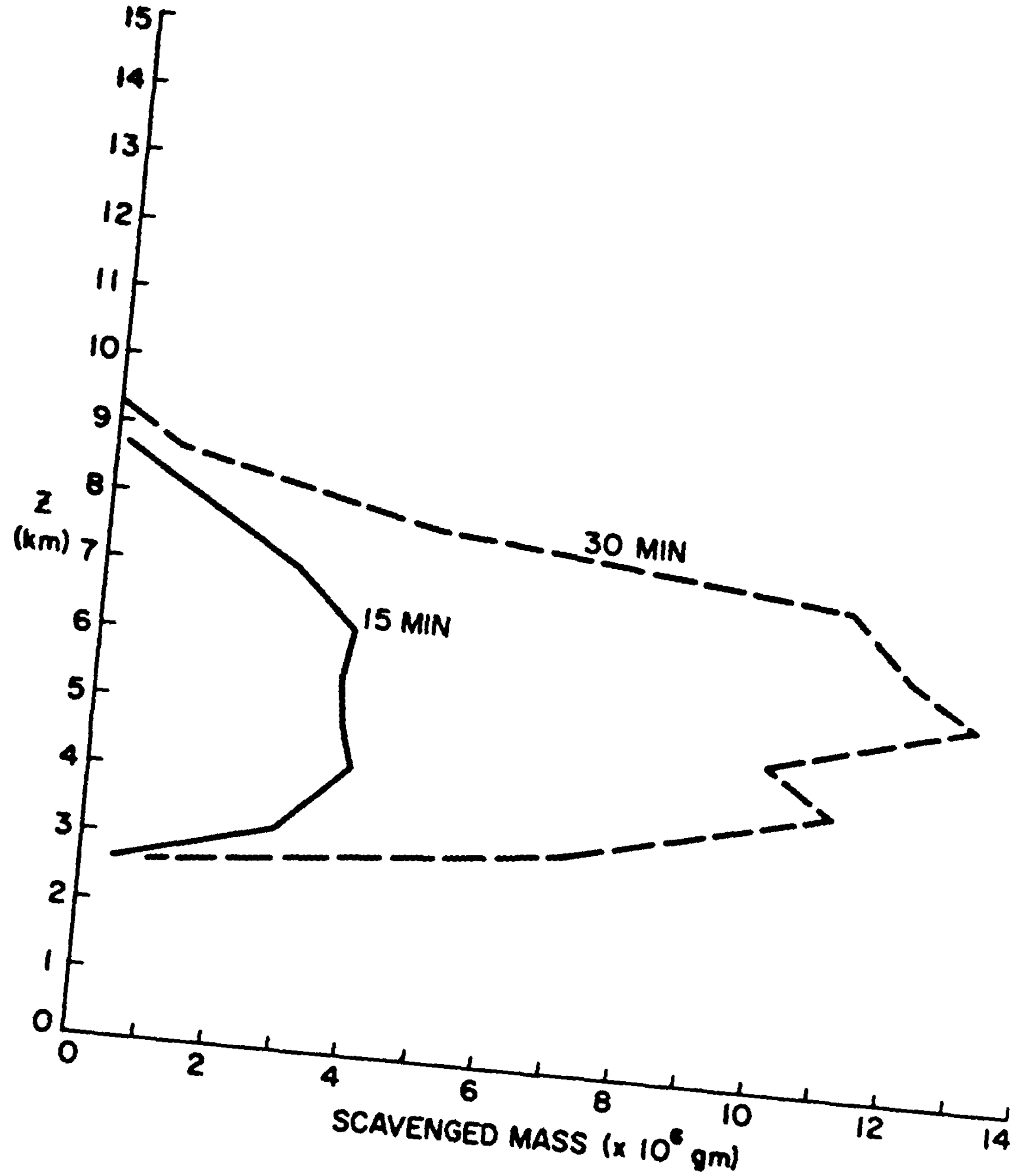

(No Nucleation Scavenging)

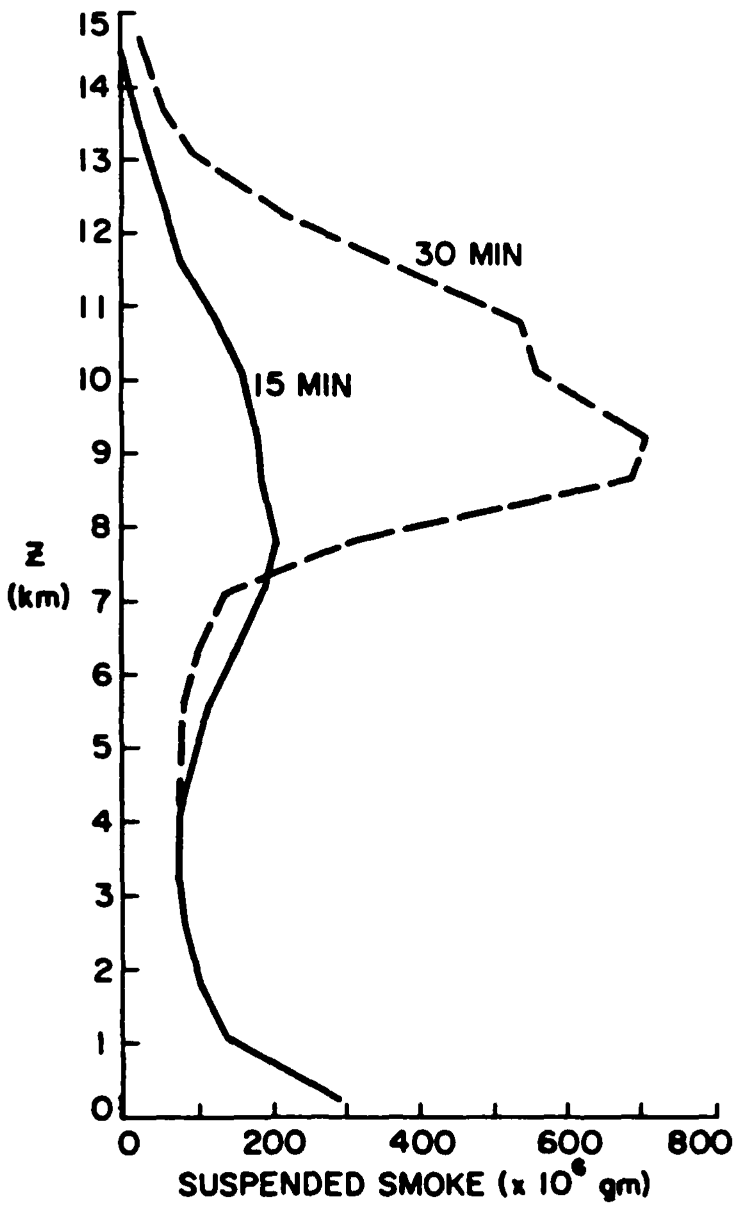

(No Nucleation Scavenging)

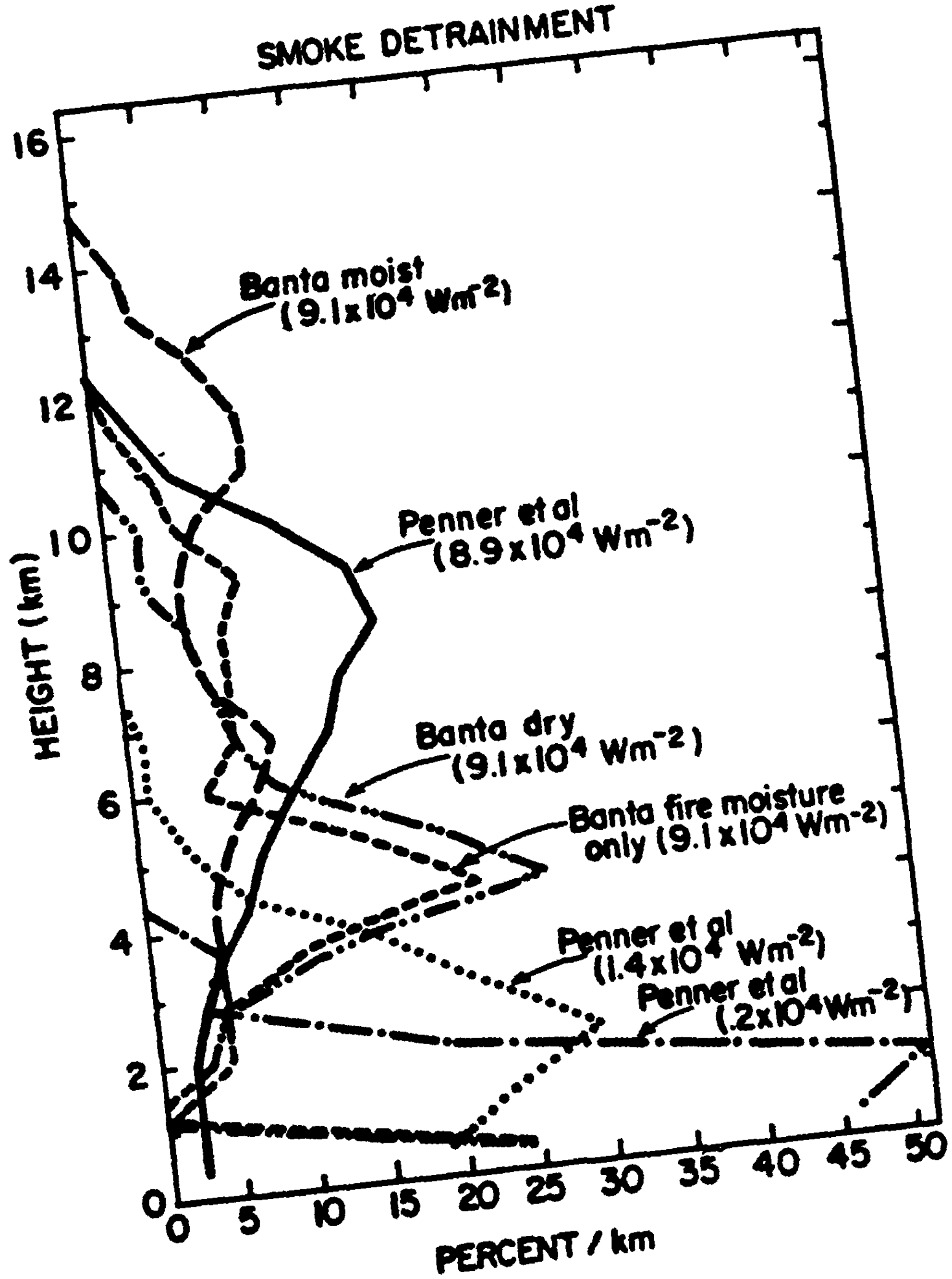

Figure 10

(Results of other investigators)

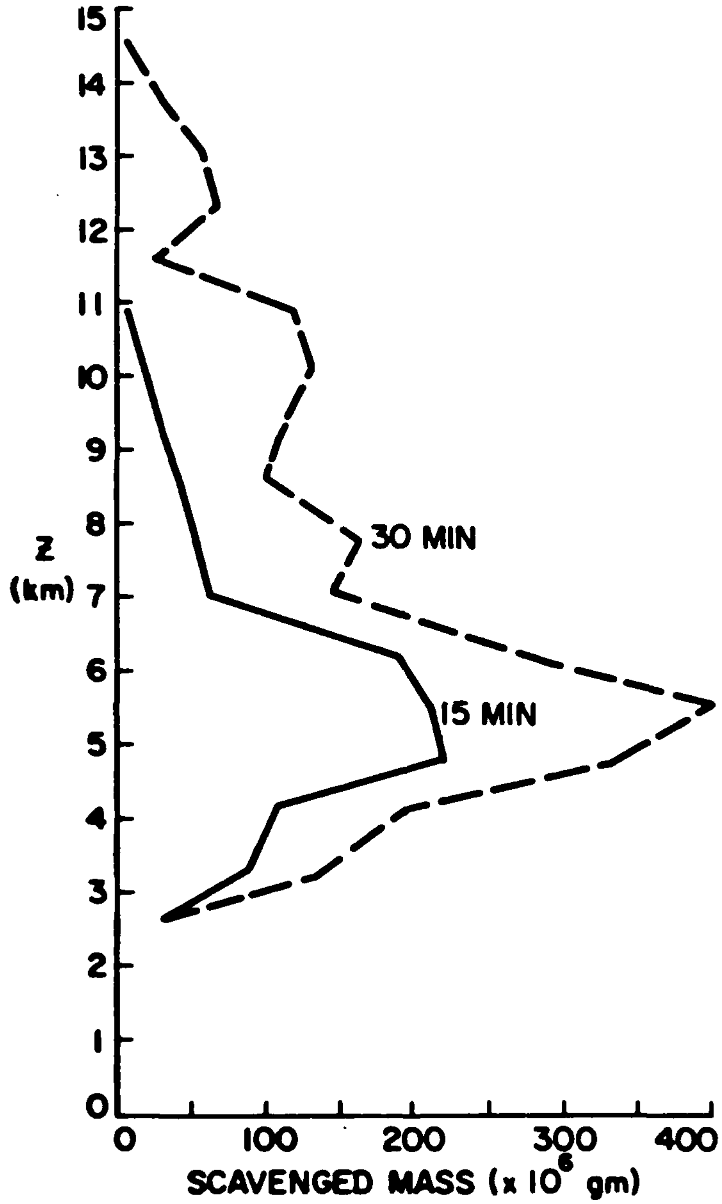

Nucleation Scavenging

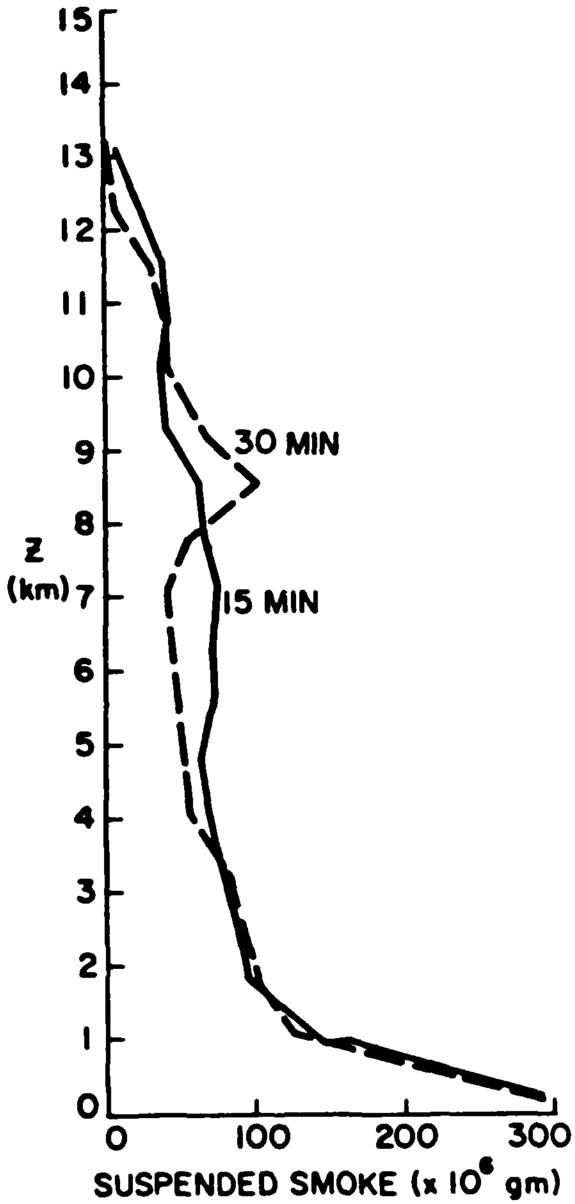

Nucleation Scavenging

CONCLUSIONS ABOUT SCAVENGING

A. Nucleation scavenging might remove up to 80% of smoke if effective.

B. Phoretic scavenging is of minor importance.

C. There are some major uncertainties:

1) How effective is smoke as a cloud condensation nuclei?

2) Will the very large numbers of CCN render the accretion of cloud droplets by precipitation particles ineffective (1 g/kg cloud ~ 1 micron cloud drops).

3) How much larger will the smoke particles captured by precipitation be?

DISTRIBUTION LIST

DEPARTMENT OF DEFENSE

ARMED FORCES RADIOBIOLOGY RSCH INST
ATTN: V BOGO

ASSISTANT TO THE SECRETARY OF DEFENSE
ATOMIC ENERGY
ATTN: COL T HAWKINS

DEFENSE INTELLIGENCE AGENCY
ATTN: N BARON
ATTN: RTS-2B

DEFENSE NUCLEAR AGENCY
ATTN: DFRA
ATTN: DFSP G ULLRICH
ATTN: RAAE K SCHWARTZ
ATTN: RAAE L WITTWER
ATTN: RAAE T WALSH
ATTN: RAEE G BAKER
ATTN: RAEE R WEBB
ATTN: SPAS M FRANKEL
ATTN: TDRP D AUTON
ATTN: TDTD/C CORSETTI
4 CYS ATTN: TITL

DEFENSE TECHNICAL INFORMATION CENTER
12 CYS ATTN: DD

NATIONAL DEFENSE UNIVERSITY
ATTN: G FOSTER MOBIL CONCEPTS DEV CTR

OFFICE OF THE SEC OF DEFENSE
ATTN: LTCOL G BETOURNE
ATTN: R RUFFIN

OFFICE OF THE SECRETARY OF DEFENSE
ATTN: COL A RAMSAY

DEPARTMENT OF THE ARMY

NATIONAL WAR COLLEGE
ATTN: COL S GARDINER
ATTN: H ALMOND

U S ARMY ATMOSPHERIC SCIENCES LAB
ATTN: R SUTHERLAND
ATTN: SLCAS-AR-M MR RUBIO

U S ARMY CORPS OF ENGINEERS
ATTN: DAEN-RDM R GOMEZ
ATTN: DR CHOROMOKOS DAEN-RDM

U S ARMY CORPS OF ENGINEERS
ATTN: L ZIEGLER
ATTN: R BECKER

U S ARMY ENGR WATERWAYS EXPER STATION
ATTN: L LINK

U S ARMY MISSILE INTELLIGENCE AGENCY
ATTN: J GAMBLE

U S ARMY NATICK RSCH DEV & ENGRG CENTER
ATTN: H M EL-BISI

U S ARMY STRATEGIC DEFENSE COMMAND
ATTN: DR J LILLY
ATTN: G EDLIN
ATTN: J VEENEMAN
ATTN: M CAPPS
ATTN: R BRADSHAW

DEPARTMENT OF THE NAVY

CNO EXECUTIVE PANEL
ATTN: CAP L BROOKS

NAVAL RESEARCH LABORATORY
ATTN: R JEK

NAVAL SURFACE WEAPONS CENTER
ATTN: K-44 S MASTERS

DEPARTMENT OF THE AIR FORCE

AF/INYXC
ATTN: LTCOL N BARRY

AIR FORCE GEOPHYSICS LABORATORY
ATTN: D CHISHOLM
ATTN: LS/R MURPHY
ATTN: LSI/H GARDINER
ATTN: LYC/R BANTA
ATTN: LYP H S MUENCH

AIR FORCE INSTITUTE OF TECHNOLOGY/EN
ATTN: AFIT/ENP MAJ S R BERGGREN

AIR FORCE OFFICE OF SCIENTIFIC RSCH
ATTN: D BALL

AIR FORCE OPERATIONAL TEST & EVAL CTR
ATTN: MAJ N RODRIGUES

AIR FORCE SPACE DIVISION
ATTN: YNC CAPT K O'BRYAN

AIR FORCE TECHNICAL APPLICATIONS CTR
ATTN: J MARSHALL

AIR FORCE WEAPONS LABORATORY, NTAAB
ATTN: CAPT LEONG
ATTN: J JANNI
ATTN: J W AUBREY, NTED
ATTN: LT LAHTI
ATTN: LTCOL V BLISS

AIR UNIVERSITY
ATTN: LTCOL F REULE

AIR WEATHER SERVICE, MAC
ATTN: MAJ J SCHLEHER

BALLISTIC MISSILE OFFICE/DAA
ATTN: LT ROTHCHILD
ATTN: MYSP/CAP TOMASZEWSKI

DEPUTY CHIEF OF STAFF/XOX
ATTN: AFXOX

STRATEGIC AIR COMMAND
ATTN: CAP CONNERY

STRATEGIC AIR COMMAND/XPXF
ATTN: T BAZZOLI

DEPARTMENT OF ENERGY

ARGONNE NATIONAL LABORATORY
ATTN: H DRUCKER
ATTN: M WESLEY
ATTN: P BECKERMAN

BROOKHAVEN NATIONAL LABORATORY
ATTN: B MANOWITZ
ATTN: E WEINSTOCK

DEPARTMENT OF ENERGY
ATTN: I NEDDOW
ATTN: T HARRIS

DESERT RESEARCH INSTITUTE
ATTN: J HALLETT
ATTN: J HUDSON

LAWRENCE BERKELEY NATIONAL LAB
ATTN: H ROSEN

UNIVERSITY OF CALIFORNIA
LAWRENCE LIVERMORE NATIONAL LAB
ATTN: C R MOLENKAMP
ATTN: C SHAPIRO
ATTN: F LUTHER
ATTN: G BING
ATTN: G SIMONSON
ATTN: J PENNER
ATTN: J POTTER
ATTN: L-10 A GROSSMAN
ATTN: L-262 A BROYLES
ATTN: L-262 J KNOX
ATTN: L-453 L ANSPAUGH
ATTN: M MACCRACKEN
ATTN: R MALONE
ATTN: R PERRET
ATTN: S GHAN

LOS ALAMOS NATIONAL LABORATORY
ATTN: D SAPPENFIELD
ATTN: E J CHAPYAK
ATTN: E JONES
ATTN: E SYMBALISTY
ATTN: G GLATZMAIER
ATTN: G M SMITH
ATTN: L H AUER
ATTN: L CLOUTMAN
ATTN: P HUGES
ATTN: T YAMATTA

OAK RIDGE NATIONAL LABORATORY
ATTN: D FIELDS

SANDIA NATIONAL LABORATORIES
ATTN: A L JOHNSON
ATTN: B ZAK
ATTN: D DAHLGREN
ATTN: D FORDHAM
ATTN: D WILLIAMS
ATTN: K D BERGERON
ATTN: L TROST
ATTN: M D BENNETT
ATTN: R C BACKSTROM

OTHER GOVERNMENT

CENTRAL INTELLIGENCE AGENCY
ATTN: A WARSHAWSKY
ATTN: R NELSON

DEPARTMENT OF AGRICULTURE
ATTN: D HAINES

DEPARTMENT OF TRANSPORTATION
ATTN: COL M ROESCH

ENVIRONMENTAL PROTECTION AGENCY
ATTN: R COTHERN
ATTN: W E FALLON

FEDERAL EMERGENCY MANAGEMENT AGENCY
ATTN: B W BLANCHARD
ATTN: D BENSON NP-CP-MR
ATTN: D KYBAL
ATTN: J POWERS
ATTN: J RUMBARGER
ATTN: S ALTMAN

GENERAL ACCOUNTING OFFICE
ATTN: A PIERCE
ATTN: P J BOLLEA
ATTN: V BIELECKI

NASA
ATTN: N CRAYBILL
ATTN: W R COFER

NASA
ATTN: R HABERLE
ATTN: O TOON
ATTN: R YOUNG
ATTN: T ACKERMAN

NATIONAL BUREAU OF STANDARDS
ATTN: G MULHOLLAND
ATTN: R LEVINE
ATTN: R REHM
ATTN: R SCHRACK

NATIONAL BUREAU OF STANDARDS
ATTN: H BAUM

NATIONAL CENTER ATMOSPHERIC RESEARCH
ATTN: J KIEHL
ATTN: S SCHNEIDER
ATTN: S THOMPSON
ATTN: V RAMASWAMY

NATIONAL CLIMATE PROGRAM OFFICE
ATTN: A HECHT
ATTN: M YERG

NATIONAL OCEANIC & ATMOSPHERIC ADMIN
ATTN: F FEHSENFELD
ATTN: J DELUISI
ATTN: R DICKINSON
ATTN: R PUESCHEL
ATTN: V DERR

NATIONAL OCEANIC & ATMOSPHERIC ADMIN
ATTN: B HICKS

NATIONAL RESEARCH COUNCIL
ATTN: K BEHR
ATTN: R DEFRIES

NATIONAL SCIENCE FOUNDATION
ATTN: B BEASLEY
ATTN: E BIERLY
ATTN: H VIRJI
ATTN: L HAMATY
ATTN: R SINCLAIR
ATTN: R TAYLOR
ATTN: S KEENY

NUCLEAR REGULATORY COMMISSION
ATTN: R ALEXANDER

OFFICE OF SCIENCE AND TECH POLICY
ATTN: B HEALY
ATTN: COL S WYMAN

OFFICE OF TECHNOLOGY ASSESSMENT
ATTN: R WILLIAMSON

U S ARMS CONTROL & DISARMAMENT AGCY
ATTN: B DOENGES NWC-DPA
ATTN: CDR P JAMISON
ATTN: COL H HERTEL
ATTN: G PITMAN
ATTN: H SCHAEFFER
ATTN: LTCOL S LAWRENCE
ATTN: R GODESKY
ATTN: R HOWES
ATTN: R O'CONNELL NWC-DPA

U S DEPARTMENT OF STATE
ATTN: A CORTE
ATTN: C CLEMENT
ATTN: COL M SEATON
ATTN: S CLEARY
ATTN: T VREBALOVICH

U S GEOLOGICAL SURVEY
ATTN: R DECKER

U S GEOLOGICAL SURVEY
ATTN: E SHOEMAKER

U S HOUSE OF REPRESENTATIVES
ATTN: C BAYER
ATTN: COMMITT ON SCI & TECH J DUGAN

U S HOUSE OF REPRESENTATIVES
ATTN: J FREIWALD
ATTN: M HERBST

US DEPARTMENT AGRICULTURE
ATTN: D WARD

DEPARTMENT OF DEFENSE CONTRACTORS

AERO-CHEN RESEARCH LABS, INC
ATTN: D B OLSON

AERODYNE RESEARCH, INC
ATTN: C KOLB
ATTN: J LURIE

AEROJET ELECTRO-SYSTEMS CO
ATTN: A FYMAT
ATTN: S HAMILTON
ATTN: R PAN

AEROSPACE CORP
ATTN: C RICE
ATTN: L R MARTIN

AEROSPACE CORPORATION
ATTN: G LIGHT

ALLEN RESEARCH CORP
ATTN: R ALLEN

AMERICAN ASSN ADVANCEMENT OF SCIENCE
ATTN: D M BURNS

ANALYTIC SERVICES, INC (ANSER)
ATTN: R BROFFT
ATTN: R ELLINGSON

APPLIED RESEARCH CORP
ATTN: A ENDAL

ASSN. DIST. AMERICAN SCIENTISTS
ATTN: J HUBBARD

AT&T DEFENSIVE SYSTEMS STUDIES
ATTN: R JANOW

ATMOSPHERIC AND ENVIRONMENTAL RES
ATTN: N SZE

AUDIO INTELLIGENCE DEVICES INC
ATTN: H BAUM

AVCO SYSTEMS DIVISION
ATTN: G GRANT

BALL AEROSPACE SYSTEMS DIVISION
ATTN: B CUMMINGS
ATTN: C BRADFORD

BDM CORP
ATTN: D SHAEFFER
ATTN: E L COFFEY
ATTN: J LEECH

BERKELEY RSCH ASSOCIATES, INC
ATTN: S BRECHT

BOEING AEROSPACE COMPANY
ATTN: N GERONTAKIS

BOEING TECHNICAL & MANAGEMENT SVCS, INC
ATTN: G HALL

C. L. CONSULTING SERVICES
ATTN: F FEER

CALIFORNIA RESEARCH & TECHNOLOGY, INC
ATTN: M ROSENBLATT
ATTN: R GAJ
ATTN: S KRUEGER

CALSPAN CORP
ATTN: R MAMBRETTI
ATTN: R MISSERT

CARNEGIE CORPORATION OF NEW YORK
ATTN: D ARSENIAN

CASSIDY AND ASSOCIATES
ATTN: J JACOBSON

CHARLES STARK DRAPER LAB, INC
ATTN: A TETEWSKI

COLORADO STATE UNIVERSITY
ATTN: D KRUEGER
ATTN: W COTTON

COMPUTER SCIENCES CORP
ATTN: G CABLE

DARTSIDE CONSULTING
ATTN: A FORESTER

DELTA RESEARCH
ATTN: L WEINER
ATTN: M RADKE

DYNAMICS TECHNOLOGY, INC
ATTN: D HOVE

ENW INTERNATIONAL, LTD
ATTN: J CANE

EOS TECHNOLOGIES, INC
ATTN: B GABBARD
ATTN: N JENSEN
ATTN: W LELEVIER

FACTORY MUTUAL RESEARCH CORP
ATTN: M A DELICHATSIOS

FEDERATION OF AMERICAN SCIENTISTS
ATTN: J STONE

GENERAL ELECTRIC CO
ATTN: R E SCHMIDT

GENERAL ELECTRIC CO
ATTN: H ROBSON

GENERAL RESEARCH CORP
ATTN: B BENNETT
ATTN: J BALTES

HAROLD ROSENBAUM ASSOCIATES, INC
ATTN: G WEBER

HORIZONS TECHNOLOGY INC
ATTN: A EDWARDS
ATTN: J A MANGO
ATTN: J AMBROSE

HORIZONS TECHNOLOGY, INC
ATTN: R W LOWEN
ATTN: W T KREISS

HUGHES AIRCRAFT
ATTN: E DIVITA

INFORMATION SCIENCE, INC
ATTN: W DUDZIAK

INSTITUTE FOR DEFENSE ANALYSES
ATTN: C CHANDLER
ATTN: E BAUER
ATTN: F ALBINI

JOHNS HOPKINS UNIVERSITY
ATTN: M LENEVSKY
ATTN: R FRISTROM
ATTN: W BERL

KAMAN SCIENCES CORP
ATTN: J RUSH
ATTN: J SCRUGGS

KAMAN SCIENCES CORP
ATTN: P GRIFFIN
ATTN: P TRACY

KAMAN TEMPO
ATTN: B GAMBILL
ATTN: D FOXWELL
ATTN: DASIAC
ATTN: E MARTIN
ATTN: R RUTHERFORD
ATTN: R YOUNG
ATTN: S FIFER
ATTN: W KNAPP

KAMAN TEMPO
ATTN: D ANDERSON
ATTN: DASIAC

LOCKHEED MISSILES & SPACE CO, INC
ATTN: ATTN J HENLEY
ATTN: J GLADIS
ATTN: J PEREZ

LOCKHEED MISSILES & SPACE CO, INC
ATTN: P DOLAN
ATTN: W MORAN

M I T LINCOLN LAB
ATTN: S WEINER

MARTIN MARIETTA DENVER AEROSPACE
ATTN: D HAMPTON

MAXIM TECHNOLOGIES, INC
ATTN: J MARSHALL

MCDONNELL DOUGLAS CORP
ATTN: R C ANDREWS
ATTN: T CRANOR
ATTN: T TRANER

MCDONNELL DOUGLAS CORP
ATTN: A MONA
ATTN: F SAGE
ATTN: G BATUREVICH
ATTN: J GROSSMAN
ATTN: R HALPRIN
ATTN: S JAEGER
ATTN: W YUCKER

MERIDIAN CORP
ATTN: E DANIELS
ATTN: F BAITMAN

MIDWEST RESEARCH INSTITUTE
ATTN: J S KINSEY

MISSION RESEARCH CORP
ATTN: R ARMSTRONG

MISSION RESEARCH CORP
ATTN: C LONGMIRE
ATTN: D ARCHER
ATTN: D KNEPP
ATTN: D SOWLE
ATTN: F FAJEN
ATTN: K R COSNER
ATTN: M SCHEIBE
ATTN: R BIGONI
ATTN: R CHRISTIAN
ATTN: R GOLDFLAM
ATTN: R HENDRICK
ATTN: T OLD
ATTN: W WHITE

MITRE CORPORATION
ATTN: J SAWYER

MRJ INC
ATTN: D FREIWALD

NATIONAL ADVISORY COMMITTEE
ATTN: J ALMAZAN
ATTN: J BISHOP

NATIONAL INST. FOR PUBLIC POLICY
ATTN: K PAYNE

NICHOLS RESEARCH CORP, INC
ATTN: H SMITH
ATTN: J SMITH
ATTN: M FRASER
ATTN: R BYRN

NORTHROP SERVICES INC
ATTN: T OVERTON

ORLANDO TECHNOLOGY INC
ATTN: R SZCZEPANSKI

PACIFIC-SIERRA RESEARCH CORP
ATTN: G ANNO
ATTN: H BRODE, CHAIRMAN SAGE
ATTN: M DORE
ATTN: R SMALL

PALOMAR CORP
ATTN: B GARRETT
ATTN: C FELDBAUM

PHOTOMETRICS, INC
ATTN: I L KOFSKY

PHOTON RESEARCH ASSOCIATES
ATTN: J MYER

PHYSICAL RESEARCH CORP
ATTN: A CECERE

PHYSICAL RESEARCH INC
ATTN: H FITZ

PHYSICAL RESEARCH INC
ATTN: D MATUSKA

PHYSICAL RESEARCH INC
ATTN: A WARSHAWSKY
ATTN: J WANG
ATTN: W SHIH

PHYSICAL RESEARCH INC
ATTN: R JORDANO

PHYSICAL RESEARCH, INC
ATTN: D WESTPHAL
ATTN: D WHITENER
ATTN: H WHEELER
ATTN: R BUFF
ATTN: R DELIBERIS
ATTN: T STEPHENS
ATTN: W C BLACKWELL

PHYSICAL RESEARCH, INC
ATTN: G HARNEY
ATTN: J DEVORE
ATTN: J THOMPSON
ATTN: R STOECKLY
ATTN: W SCHLEUTER

PHYSICAL RESEARCH, INC
ATTN: H SUGIUCHI

POLYTECHNIC OF NEW YORK
ATTN: B J BULKIN
ATTN: G TESORO

PRINCETON UNIVERSITY
ATTN: J MAHLMAN

QUADRI CORP
ATTN: H BURNSWORTH

R & D ASSOCIATES
ATTN: A KUHL
ATTN: F GILMORE
ATTN: G JONES
ATTN: J SANBORN
ATTN: R TURCO

R & D ASSOCIATES
ATTN: B YOON

R J EDWARDS INC
ATTN: R SEITZ

RADIATION RESEARCH ASSOCIATES, INC
ATTN: B CAMPBELL
ATTN: M WELLS

RAND CORP
ATTN: G L DONOHUE
ATTN: P ROMERO

RAND CORP
ATTN: J GERTLER

ROCKWELL INTERNATIONAL CORP
ATTN: S I MARCUS

ROCKWELL INTERNATIONAL CORP
ATTN: J KELLEY

S-CUBED
ATTN: B FREEMAN
ATTN: K D PYATT, JR
ATTN: R LAFRENZ

S-CUBED
ATTN: C NEEDHAM
ATTN: S HIKIDA
ATTN: T CARNEY

SCIENCE APPLICATIONS INC
ATTN: R EDELMAN

SCIENCE APPLICATIONS INTL CORP
ATTN: C HILL

SCIENCE APPLICATIONS INTL CORP
ATTN: D HAMLIN

SCIENCE APPLICATIONS INTL CORP
ATTN: B MORTON
ATTN: B SCOTT
ATTN: D SACHS
ATTN: G T PHILLIPS
ATTN: J BENGSTOM

SCIENCE APPLICATIONS INTL CORP
ATTN: D BACON
ATTN: DR L GOURE
ATTN: F GIESSLER
ATTN: J COCKAYNE

ATTN: J SHANNON
ATTN: J STUART
ATTN: M SHARFF
ATTN: W LAYSON

SCIENCE APPLICATIONS INTL CORP
ATTN: J SONTOWSKI

SCIENCE APPLICATIONS INTL CORP
ATTN: T HARRIS

SCIENTIFIC RESEARCH ASSOC, INC
ATTN: B WEINBERG

SPARTA INC
ATTN: R HARPER

SRI INTERNATIONAL
ATTN: C WITHAM
ATTN: D GOLDEN
ATTN: D MACDONALD
ATTN: D ROBERTS
ATTN: E UTHE
ATTN: G ABRAHAMSON
ATTN: J BACKOVSKY
ATTN: W CHESNUT
ATTN: W JOHNSON

SRI INTERNATIONAL
ATTN: R BRAMHALL
ATTN: R WOOLFOLK
ATTN: W VAIL

STAN MARTIN ASSOCIATES
ATTN: S B MARTIN

STANTON CONSULTING
ATTN: M STANTON

SWETL, INC
ATTN: T Y PALMER

SYSTEM PLANNING CORP
ATTN: J SCOURAS
ATTN: M BIENVENU
ATTN: R SCHEERBAUM

SYSTEMS AND APPLIED SCIENCES CORP
ATTN: M KAPLAN

TECHNOLOGY INTERNATIONAL CORP
ATTN: W BOQUIST

TELEDYNE BROWN ENGINEERING
ATTN: D ORMOND
ATTN: F LEOPARD
ATTN: J FORD

TELEDYNE BROWN ENGINEERING
ATTN: D GUICE

TEXAS ENGR EXPERIMENT STATION
ATTN: W H MARLOW

TOYON RESEARCH CORP
ATTN: C TRUAX
ATTN: J GARBARINO
ATTN: J ISE

TRW
ATTN: H BURNSWORTH
ATTN: J BELING

TRW ELECTRONICS & DEFENSE SECTOR
ATTN: F FENDELL
ATTN: G KIRCHNER
ATTN: G MROZ
ATTN: H CROWDER
ATTN: J FEDELE
ATTN: M BRONSTEIN
ATTN: R BACHARACH
ATTN: S FINK
ATTN: T NGUYEN

TRW ELECTRONICS & DEFENSE SECTOR
ATTN: M HAAS

VISIDYNE, INC
ATTN: H SMITH
ATTN: J CARPENTER

WASHINGTON, UNIVERSITY OF
ATTN: J I KATZ

FOREIGN

AERE ENVIRONMENTAL AND MEDICAL SC
ATTN: S PENKETT

ATOMIC WEAPONS RESEARCH ESTABLISHMENT
ATTN: P F A RICHARDS

ATOMIC WEAPONS RESEARCH ESTABLISHMENT
ATTN: D L JONES
ATTN: D M MOODY

AUSTRALIA EMBASSY
ATTN: DR LOUGH
ATTN: MAJ GEN H J COATES
ATTN: P PROSSER

BRITISH DEFENCE STAFF
ATTN: C FENWICK
ATTN: J CRANIDGE
ATTN: J EDMONDS
ATTN: M NORTON
ATTN: P WEST

CANADIAN FORESTRY SERVICE
ATTN: B STOCKS
ATTN: T LYNHAM

CSIRO
ATTN: I GALBALLY

CSIRO: ATMOSPHERIC RESEARCH
ATTN: A PITTOCK

EMBASSY OF BELGIUM
ATTN: L ARNOULD

ISRAEL EMBASSY
ATTN: N BELKIND

MAX-PLANCK INSTITUTE FOR CHEMISTRY
ATTN: P J CRUTZEN

MINISTRY OF DEFENCE
ATTN: R RIDLEY

NATIONAL DEFENCE HEADQUARTERS
ATTN: H A ROBITALLE

TRINITY COLLEGE
ATTN: F HARE

DIRECTORY OF OTHER

ATMOS. SCIENCES
ATTN: G SISCOE

BROWN UNIVERSITY
ATTN: R K MATTHEWS

BUCKNELL UNIVERSITY
ATTN: O ANDERSON

CALIFORNIA, UNIVERSITY
ATTN: R WILLIAMSON

CALIFORNIA, UNIVERSITY OF
ATTN: L BADASH/DEPT OF HISTORY

COLORADO, UNIVERSITY LIBRARIES
ATTN: J BIRKS
ATTN: R SCHNELL

DREXEL UNUVERSITY
ATTN: J FRIEND

DUKE UNIVERSITY
ATTN: F DELUCIA

GEORGE MASON UNIVERSITY
ATTN: PROF S SINGER
ATTN: R EHRLICH

GEORGE WASHINGTON UNIVERSITY
ATTN: R GOULARD

GEORGIA INST OF TECH
ATTN: E PATTERSON

HARVARD COLLEGE LIBRARY
ATTN: W PRESS

HARVARD UNIVERSITY
ATTN: G CARRIER

HARVARD UNIVERSITY
ATTN: D EARDLEY

IOWA, UNIVERSITY OF
ATTN: HISTORY DEPT/S PYNE

MARYLAND UNIVERSITY OF
ATTN: A ROBOCK DEPT METEOROLOGY
ATTN: A VOGELMANN DEPT METEOROLOGY
ATTN: R ELLINGSON DEPT METEOROLOGY

MIAMI LIBRARY UNIVERSITY OF
ATTN: C CONVEY

MIAMI UNIV LIBRARY
ATTN: J PROSPERO ATMOS SC

NEW YORK STATE UNIVERSITY OF
ATTN: R CESS

OAK RIDGE ASSOCIATED UNIVERSITIES
ATTN: C WHITTLE

PENNSYLVANIA STATE UNIVERSITY
ATTN: D WESTPHAL

SOUTH DAKOTA SCH OF MINES & TECH LIB
ATTN: H ORVILLE

TENNESSEE, UNIVERSITY OF
ATTN: K FOX

UNIVERSITY OF SOUTH FLORIDA
ATTN: S YING

UNIVERSITY OF WASHINGTON
ATTN: C LEOVY
ATTN: L RAOKE
ATTN: P HOBBS

VIRGINIA POLYTECHNIC INST LIB
ATTN: M NADLER

WASHINGTON STATE UNIVERSITY
ATTN: DR A CLARK

WISCONSIN UNIVERSITY OF
ATTN: P WANG

END
11-87
DTIC